Engineering of Saccharomyces cerevisiae for production of resveratrol and its derivatives

Li, Mingji; Nielsen, Jens; Borodina, Irina

Publication date:
2016

Document Version
Publisher's PDF, also known as Version of record

DTU Biosustain
The Novo Nordisk Foundation Center for Biosustainability

Thesis for the degree of doctor of philosophy

Engineering of *Saccharomyces cerevisiae* for production of resveratrol and its derivatives

MINGJI LI

The Novo Nordisk Foundation
Center for Biosustainability

The Novo Nordisk Foundation Center for Biosustainability
Technical University of Denmark
2970 Hørsholm, Denmark

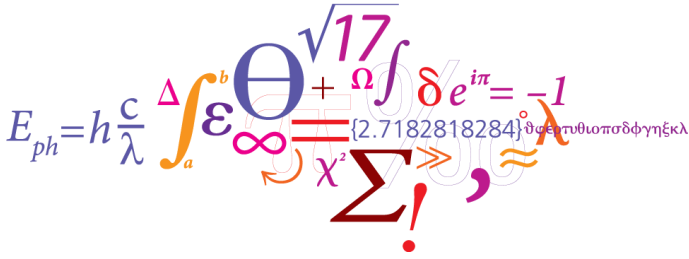

Engineering of *Saccharomyces cerevisiae* for production of resveratrol and its derivatives

MINGJI LI

PhD Thesis

The Novo Nordisk Foundation Center for Biosustainability

Technical University of Denmark

2970 Hørsholm, Denmark

Printed by GraphiCo, Denmark, 2016

PREFACE

This dissertation serves as a partial achievement of the requirement to obtain the doctor degree of philosophy at the PhD School of Technical University of Denmark. This work was mainly done at the Yeast Cell Factories group, The Novo Nordisk Foundation Center for Biosustainability, Technical University of Denmark, Denmark and partly at the Systems and Synthetic Biology group (Sys2Bio), Department of Biology and Biological Engineering, Chalmers University of Technology, Sweden between 2013 and 2016, under supervision of Prof. Jens Nielsen and Dr. Irina Borodina. The work deployed metabolic engineering strategies and synthetic biology techiniques to investigate resveratrol and its derivatives production in *Saccharomyces cerevisiae*. This project was funded by DTU PhD scholarship.

Mingji Li

April 2016

ABSTRACT

Resveratrol is a natural potent antioxidant with multiple beneficial effects on human health and is therefore used in medical, food, and cosmetic areas. In my PhD thesis I describe how I engineered yeast cell factory *Saccharomyces cerevisiae* for production of resveratrol by fermentation of cheap carbon sources. I adopted rational metabolic engineering rational design strategies, synthetic biology techniques and system biology approaches to engineer and analyse yeast cell factories.

There are two biosynthesis pathways of resveratrol, starting from tyrosine or phenylalanine, which in this thesis are defined as the TAL pathway and PAL pathway respectively. For the TAL pathway, I collaborated with Christian Bille Jendresen, Steen Gustav Stahlhut to screen fourteen diverse heterologous tyrosine ammonia lyases (*TAL*s) for their activity in yeast and *E. coli*. I expressed the 14 *TALs* in *S. cerevisiae* and analysed the resulting strains for production of *p*-coumaric acid. Two of the screened TALs, one from *Herpetosiphon aurantiacus* and another from *Flavobacterium johnsoniae*, were highly active and selective, i.e., they did not have a side reaction of converting phenylalanine to cinnamic acid. These results were published in Applied and Environmental Microbiology (Jendresen *et al.*, 2015).

I then constructed the TAL pathway to resveratrol by expressing the two *TAL* genes in combination with 4-coumaryl-CoA ligase (*4CL*) from *Arabidopsis thaliana* and resveratrol synthase (*VST*) from *Vitis vinifera* in *S. cerevisiae*; the best combination resulted in 11.66 ± 0.57 mg l^{-1} and

2.74±0.05 mg l^{-1} resveratrol on minimum medium in the presence or absence of 5 mM tyrosine respectively. In order to improve resveratrol production, I increased the flux towards tyrosine precursor by de-regulating the aromatic amino acids biosynthesis pathway (overexpression of feedback-inhibition resistant versions of $Aro4p^{fbr}$ and $Aro7p^{fbr}$) and the supply of malonyl-CoA precursor by de-regulating acetyl-CoA carboxylase (overexpression of $Acc1p^{S659A,\ S1157A}$) to avoid inactivation by the global regulator Snf1p. The first strategy resulted in 78% improvement of resveratrol titer and the second in 31% improvement. Combining the two strategies further improved resveratrol titer to 6.40±0.03 mg l^{-1}. I hypothesized that the activity of resveratrol biosynthetic enzymes was limiting the flux towards resveratrol. To test this hypothesis I integrated the resveratrol pathway genes into Ty-4 retrotransposon regions, which resulted in integration of up to 8 copies of the pathway genes. Indeed my hypothesis was correct as this strategy boosted the elements was revealed to be the key limiting factor for resveratrol biosynthesis and sharply improved resveratrol production 36-fold and gave 235.57±77.00 mg l^{-1} resveratrol in batch fermentation. I fermented the final strain in controlled fed-batch reactors with glucose or ethanol feed and obtained 415.65 and 531.41 mg l^{-1} of resveratrol respectively. The results were published in Metabolic Engineering (Li *et al.*, 2015).

I also engineered the PAL pathway for resveratrol production by introducing *PAL2* encoding phenylalanine ammonia lyases, *C4H* encoding cinnamate-4-hydroxylase, and *4CL2* from *A. thaliana* and *VST1* from *V.*

vinifera in *S. cerevisiae*. To enhance the activity of C4H, a notorious cytochrome P450 enzyme, I overexpressed NADPH-cytochrome P450 reductase (*ATR2*) from *A. thaliana* and *S. cerevisiae* cytochrome b5 (*CYB5*). Ty-4 element-mediated multiple integration of PAL pathway and overexpression of $ARO4^{fbr}$ and $ARO7^{fbr}$ together with $ACC1^{S659A,\ S1157A}$ resulted in 201.72 ±7.91 mg l^{-1} resveratrol. In order to further improve the precursor supply, I knocked out *ARO10* encoding phenylpyruvate decarboxylase and overexpressed a post-translational unregulated variant of acetyl-CoA synthetase ($ACS1^{L641P}$) from *Salmonella enterica*, which improved resveratrol production to 272.64 ±1.34 mg l^{-1}. Finally, I obtained 811.50 mg l^{-1} and 754.70 mg l^{-1} resveratrol in fed-batch fermentation of the engineered strain using glucose or ethanol feed respectively. I further integrated heterologous methyltransferases into the resveratrol platform strain and hereby demonstrated for the first time *de novo* biosynthesis of two resveratrol derivatives, pinostilbene and pterostilbene, which have better stability and uptake in the human body compared to resveratrol. The manuscript has been submitted.

Key words: resveratrol, tyrosine, phenylalanine, *p*-coumaric acid, natural products, cultured ingredients, biosynthesis, cell factories, metabolic engineering, CRISPR/Cas9, synthetic biology, *Saccharomyces cerevisiae*, fermentation.

DANSK RESUME

Resveratrol er et naturligt og meget potent antioxidant, som har flere gavnlige effekter på menneskers helbred. Derfor bruges resveratrol i vid udstrækning i medicin, fødevarer og kosmetik. I min ph.d.-afhandling beskriver jeg videnskabeligt, hvordan gærceller (*Saccharomyces cerevisiae)* kan genmodificeres til at producere resveratrol ved at fermentere billige kulstof-kilder. Jeg brugte rationel metabolisk genmodificering og rationelle designstrategier, syntetiske biologi-teknologier og en systembiologisk tilgang i designet og i analysen af gærcelle-fabrikkerne.

Resveratrol kan dannes gennem to biosyntetiske veje, som begynder med aminosyren tyrosin eller fenylalanin, og som henholdsvis benævnes TAL og PAL-vejene i denne afhandling. I forhold til TAL-vejen arbejdede jeg sammen med Christian Bille Jendresen og Steen Gustav Stahlhut for at screene 14 forskellige heterologe udgaver af tyrosin ammoniak lyase (*TALs*) for deres aktivitet i gær og *E. coli*. Jeg udtrykte de 14 *TALs* i *S. cerevisiae* og analyserede cellelinjerne for produktion af *p*-cumarsyre (*p*-coumaric acid). To af de screenede TALs – en fra *Herpetosiphon aurantiacus* og en fra *Flavobacterium johnsoniae* – var yderst aktive og selektive i den forstand, at de ikke omdannede fenylalanin til uønsket kanelsyre (cinnamic acid). Disse resultater er blevet publiceret i Applied and Environmental Microbiology (Jendresen *et al.*, 2015).

Efterfølgende designede jeg TAL-vejen til at producere resveratrol via de to *TAL*-gener kombineret med 4-coumaryl-CoA ligase (*4CL*) fra *Arabidopsis thaliana* og resveratrol syntase *(VST)* fra *Vitis vinifera* i *S. cerevisiae*. Den

mest effektive kombination resulterede i 11.66 ±0.57 mg l^{-1} og 2.74 ±0.05 mg l^{-1} resveratrol på minimal medie henholdsvist med eller uden 5 mM tyrosin. For at optimere resveratrol-produktionen modificerede jeg cellerne, så der kom større flux i retning af flere forstadier til tyrosyn. Dette blev gjort ved at deregulere biosyntese-vejen for aromatiske aminosyrer (gennem overekspression af feedback-inhiberings-resistente versioner af $Aro4p^{fbr}$ and $Aro7p^{fbr}$). Desuden forøgede jeg tilførslen af forstadier til malonyl-CoA ved at deregulere acetyl-CoA carboxylase (overexpression af $Acc1p^{S659A, S1157A}$) for at undgå dens inaktivering ved den globale regulator Snf1p. Den første strategi resultetede i 78 % større koncentration af resveratrol, den anden gav en 31 % forbedring. Ved at kombinere de to strategier opnåedes 130% forbedring af resveratrol koncentration (6.40 ±0.03 mg l^{-1} i medie uden tyrosin). Min hypotese var, at aktiviteten af resveratrol biosyntese-enzymerne begrænsede fluxen hen mod resveratrol. For at teste hypotesen integrerede jeg generne fra resveratrol-vejen i Ty-4 retrotransposon-regionerne, hvilket resulterede i integration af op til otte kopier af generne. Det viste sig, at hypotesen stemte overens med virkeligheden, idet denne strageti boostede resveratrol produktionen med en faktor 36 og således gav 235.57 ±77.00 mg l^{-1} i fermenteringssuppen. Jeg fermenterede den endelige cellelinje i kontrollerede fed-batch reaktorer med glukose eller etanol som kulstofskilde, og på denne måde opnåedes en resveratrol-koncentration på henholdsvis 416 mg l^{-1} og 531 mg l^{-1}. Resultaterne blev publiseret i Metabolic Engineering (Li *et al.*, 2015).

Jeg genmodificerede også PAL-vejen for at øge resveratrolproduktionen. Dette gjordes ved at introducere *PAL2*-kodende fenylalanin ammoniak lyase,

C4H (som koder for cinnamate-4-hydroxylase) og *4CL2* fra *A. thaliana* og *VST1* fra *V. vinifera* i *S. cerevisiae*. For at øge aktiviteten af C4H – et almindeligt kendt cytokrom P450 enzym – overudtrykte jeg NADPH-cytokrom P450 reduktase (*ATR2*) fra *A. thaliana* og *S. cerevisiae* cytokrom b5 (*CYB5*). Ty-4 element-medieret fler-integration of PAL vejen og overudtryk af $ARO4^{fbr}$ og $ARO7^{fbr}$ sammen med $ACC1^{S659A, S1157A}$ resulterede i 201.72±7.91 mg l^{-1} resveratrol. For yderligere at forbedre tilførslen af forstadier til resveratrol, lavede jeg et knock-out af *ARO10*, der koder for fenylpyruvat dekarboxylase og overudtrykte en post-translationel, ureguleret variant af acetyl-CoA syntetase ($ACS1^{L641P}$) fra *Salmonella enterica*, hvilket forbedrede resveratrolproduktionen til 272.64±1.34 mg l^{-1}. Til sidst lykkedes det at opnå en koncentration på henholdsvis 811.50 mg l^{-1} og 754.70 mg l^{-1} resveratrol i fed-batch reaktorer med henholdsvis glukose eller ethanol som kulstofskilde. Desuden integrerede jeg heterologe versioner af metyltransferaser ind i resveratrol- platforms-cellelinjerne og på den måde demonstrerede jeg for første gang *de novo* biosyntesen af to afledninger af resveratrol kaldet pinostilben og pterostilben, som har en bedsre stabilitet og optages bedre i menneskekroppen sammenlignet med resveratrol. Dette manuskript er blevet indsendt til publikation.

Nøgleord: resveratrol, tyrosin, fenylalanin, *p*-cumarsyre, naturlige produkter, kultiverede ingredienser, biosyntese, cellefabrikker, metaboliske modificeringer, CRISPR/Cas9, syntetisk biologi, *Saccharomyces cerevisiae*, fermentering.

CONTENTS

LIST OF PUBLICATIONS

I. **M. Li**, I. Borodina. 2014. Application of synthetic biology for production of chemicals in yeast. *FEMS Yeast Research*. 14, 1-5.

II. C. Jendresen, S. Stahlhut, **M. Li**, P. Gaspar, S. Siedler, J. Förster, J. Maury, I. Borodina, A. Nielsen. 2015. Highly Active and Specific Tyrosine Ammonia-Lyases from Diverse Origins Enable Enhanced Production of Aromatic Compounds in Bacteria and *Saccharomyces cerevisiae. Applied and Environmental Microbiology*. 2015, 81(13): 4458-4476.

III. **M. Li**, K. Kildegaard, Y. Chen, A. Rodrigueza, I. Borodina, J. Nielsen. 2015. *De novo* production of resveratrol from glucose or ethanol by engineered *Saccharomyces cerevisiae. Metabolic Engineering*. 2015, 32: 1-11.

IV. **M. Li**, K. Schneider, M. Kristensen, I.Borodina, J. Nielsen. Engineering yeast for high-level production of stilbenoid antioxidants. 2016. *Manuscript, under review.*

Additional work during the PhD study but not included in this thesis

V. A. Rodriguez-Prado, K. Kildegaard, **M. Li**, I. Borodina, J. Nielsen. 2015. Establishment of a yeast platform strain for production of p-coumaric acid through metabolic engineering of aromatic amino acid biosynthesis. *Metabolic Engineering*. 2015, 32: 1-11.

CONTRIBUTION SUMMARY

I. M.L. reviewed the current literatures and drafted the manuscript. M.L.and I.B. edited the manuscript.

II. M.L. participated in design, conducted the experiments, analyzed the data and drafted the manuscript for the yeast part.

III. M.L., I.B. and J.N. conceived the study. M.L., K.R.K. and I.B designed the experiments. M.L. performed most of the experimental work and A.R. performed parts of the experimental work. M.L., Y.C., I.B., and J.N. analyzed the results. M.L., I.B., and J.N. wrote the manuscript.

IV. M.L., I.B. and J.N. conceived of the project and wrote the manuscript. M.L. and I.B. designed the experiments and analyzed the results. M.L. carried out most of the experimental work. M.L. and K.S. designed the fed-batch fermentation. M.L. and M.K. performed LC-MS assay of resveratrol derivatives.

V. M.L. performed parts of the experimental work and assisted in data analysis.

CHAPTER 1 Introduction

1.1 *Saccharomyces cerevisiae* as a yeast cell factory for production of chemicals

The yeast *Saccharomyces cerevisiae* has been used for over 5,000 years for baking and brewing. It was the first eukaryotic organism to be sequenced 20 years ago and has become an established model organism for studying functional genomics of eukaryotes. *S. cerevisiae* is also one of the major industrial microorganisms used for the biosynthesis of biofuels, chemicals and proteins. As an industrial host, *S. cerevisiae* offers many advantages. The yeast grows rapidly with a doubling time of approx. 90 min in rich medium (Bergman, 2001). It can be grown on completely defined medium, which allows the selection of isolates by several nutritional auxotrophic markers. It can also metabolise a variety of carbon sources, including glucose, galactose, raffinose, ethanol, acetate, *etc*. It is tolerant to high concentrations of sugar, to ethanol and to low pH and many organic acids. In contrast to bacteria, the yeast is resistant to phage contamination. Due to the long history of usage for baking and brewing, it has been classified as a Generally Regarded As Safe (GRAS) microorganism by the US Food and Drug Administration. As a GRAS microorganism, it is particularly suitable for producing cultured ingredients for food, cosmetics, and beverages. Thus, *S. cerevisiae* was the first genetically modified organism (GMO) approved for the production of food additives (Walker, 1998) as well as the first GMO to be directly used in beer (Verstrepen *et al.*, 2006). The applications of yeast now extend far beyond the food industry.

1.1.1 Metabolic engineering case studies

As a robust cell factory, *S. cerevisiae* has been used for the production of many chemicals, ranging from bulk chemicals and biofuels to high-value natural products. Several processes that use native or engineered yeast as the host have been commercialised, such as 1st and 2nd generation bioethanol, succinic acid (Reverdia in 2012, BioAmber in 2013), isobutanol (Gevo in 2012 and Dupont in 2013), artemisinin (Amyris in 2013), resveratrol (Evolva in 2014), vanillin (Evolva and International Flavors & Fragrances in 2014), stevia (Evolva and Cargill expected in 2016), *etc*.

Organic acids

Due to excellent tolerance of low pH, yeast strains are preferred to bacteria as hosts for the production of organic acids. The main hurdle in engineering of *S. cerevisiae* for high-level production of bulk chemicals is production of ethanol as a by-product under both anaerobic and aerobic conditions. Under aerobic conditions, ethanol was found to be produced by *S. cerevisiae* in the presence of high glucose concentrations (Crabtree, 1929), which was later named the "Crabtree effect". Pyruvate decarboxylase (*PDC*) is the key enzyme for alcoholic fermentation. Knocking out *PDC* resulted in a decrease of ethanol production and also led to pyruvate accumulation (Flikweert *et al.*, 1997). However, the *PDC*-deficient strain had two problems: 1) it could not grow on high concentrations of glucose and 2) it required supplementation of C_2 compounds, e.g., ethanol or acetate. These problems were overcome by several stages of adaptive laboratory evolution (van Maris *et al.*, 2004). It was shown that the evolved strain had a mutation

in the regulatory gene MTH1 that decreased glucose uptake rate and hence allowed the strain to grow also in media with high glucose concentration (Oud *et al.*, 2012). A recent study showed that evolved *PDC*-deficient strains overexpressed *ACH1*, which lead to production of cytosolic acetyl-CoA and thus eliminated the requirement for supplementation of medium with C_2 compounds (Chen *et al.*, 2015). Evolved *PDC*-deficient strain could produce 135 g l^{-1} pyruvate with a yield of 0.54 g g^{-1} glucose in batch fermentation (van Maris *et al.*, 2004). The *PDC* deletion strategy was also employed to produce other organic acids, such as lactic acid and malic acid. Ishida *et al*. overexpressed bovine L-lactate dehydrogenase *LDH* in a *pdc1* mutant to generate an engineered yeast strain, which could produce up to 122 g l^{-1} L-lactic acid with a yield on glucose of 61% (Ishida *et al.*, 2006)). By overexpressing pyruvate carboxylase (*PYC2*), cytosolic malate dehydrogenase (*MDH3*) and a malate transporter *SpMAE1* from *Schizosaccharomyces pombe* in an evolved *PDC*-deficient strain, Zelle *et al*. produced malic acid (Zelle *et al.*, 2008). The recombinant yeast produced 59 g l^{-1} malate at a yield of 0.42 mol (mol glucose)$^{-1}$. Another way of decreasing Pdcp activity is by limiting the amount of co-factor thiamine. Xu *et al*. applied this strategy for producing fumaric acid in *S. cerevisiae* (Xu *et al.*, 2013). The authors deleted *THI2*, encoding a transcriptional activator of thiamine biosynthesis, and *FUM1*, encoding fumarate hydratase, as well as overexpressed *FUM1*, *PYC* (cytosolic pyruvate carboxylase) and *MDH* (malate dehydrogenase) genes from *Rhizopus oryzae*. Shake flask fermentation of the engineered strain resulted in the accumulation of

5.64 ±0.16 g l^{-1} fumaric acid. Recently several non-native acids have been produced in *S. cerevisiae* by introducing synthetic pathways. Weber *et al*. first synthesised muconic acid in *S. cerevisiae* (Weber *et al.*, 2012) and Curran *et al*. improved the production of muconic acid to 141 mg l^{-1} through a series of modifications (Curran *et al.*, 2013). The production of 3-hydroxypropionic acid has also been achieved in *S. cerevisiae* via synthetic malonyl-CoA and β-alanine routes (Borodina *et al.*, 2015; Chen *et al.*, 2014; Jensen *et al.*, 2014a; Kildegaard *et al.*, 2016)

Biofuels

The budding yeast is inherently tolerant to ethanol and can be engineered to utilise xylose, the second most abundant sugar obtained from cellulosic materials. Therefore, it has been used as a host to produce the next generation biofuels. Bioethanol is one of the most successful scaled-up biofuels produced by engineered yeast. Cellulosic ethanol was commercialised in 2013 by Beta Renewables, a biotechnology company focusing on advanced biofuels and biochemical compounds. The yeast has also been genetically modified to generate advanced biofuels, such as isobutanol and bisabolene. The isobutanol pathway consisting of acetolactase synthase (*alsS*) from *Bacillus subtilis*, ketol-acid reductoisomerase (*ilvC*) from *Escherichia coli*, dihydroxy-acid dehydratase (*ilvD*), 2-keto-acid decarboxylase (*kivD*), and alcohol dehydrogenase (*adhA*) from *Lactococcus lactis* was constructed in an *S. cerevisiae* strain, which overexpressed the activator of ferrous transport (*AFT1*), with deletions of the following genes: aldehyde dehydrogenase (*ALD6*), carbonyl/aldehyde

reductase *TMA29*, glycerol-3-phosphate dehydrogenases (*GPD1* and *GPD2*), and pyruvate decarboxylases (*PDC1*, *PDC5*, and *PDC6*). The engineered yeast produced 18.6 g l^{-1} isobutanol with a yield of 0.33 g g^{-1} on glucose in complex medium (Lies *et al.*, 2012). On the other hand, Avalos *et al*. employed a compartmentalisation strategy by expressing the Ehrlich valine degradation pathway in the mitochondria to increase the local enzyme concentration and the availability of intermediates (Avalos *et al.*, 2013). The engineered strain harbouring the mitochondria-targeted pathway resulted in 0.64 g l^{-1} isobutanol, 0.13 g l^{-1} isopentanol, and 0.11 g l^{-1} 2-methyl-1--butanol. In the other study, Peralta-Yahya *et al*. expressed bisabolene synthases (Ag1) from *Abies grandis* (Peralta-Yahya *et al*., 2011) in a farnesyl diphosphate (FPP)-overproducing platform strain. The FPP platform strain contained the following genetic modifications: overexpression of a truncated HMG-CoA reductase (*tHMGR*), overexpression of FPP synthase (*ERG20*), deletion of the global transcriptional regulator of the sterol pathway (*upc2-1*), and downregulation of squalene synthase (*ERG9*). The engineered strain accumulated nearly 1 g l^{-1} bisabolene in shake flask cultivation.

Natural products

Natural products are high-value chemicals usually extracted from plants. However this process is dependent on the supply of plant material, which can vary depending on the weather, pathogen infections, plant diseases and other environmental factors. Microbial synthesis of natural products avoids these disadvantages and many natural products have been successfully

produced by engineered yeast, such as flavonoids (Trantas *et al.*, 2009), isoprenoids (Kirby and Keasling, 2008), alkaloids (Hawkins and Smolke, 2008), stilbenes (Becker *et al.*, 2003), polyketides (Mutka *et al.*, 2006), *etc*. Biosynthesis of artemisinic acid in *S. cerevisiae* is a milestone of metabolic engineering of natural products in yeast (Ro *et al.*, 2006). Artemisinic acid is the direct precursor of artemisinin, which is an effective anti-malarial drug. Artemisinin is mainly extracted from the plant sweet wormwood *Artemisia annua L*, which is in short supply. Microbial production of artemisinic acid, followed by chemical conversion into artemisinin provides a viable source of the drug. Ro *et al*. identified a key cytochrome P450 monooxygenase (P450) that converts the precursor farnesyl pyrophosphate (FPP) to artemisinic acid (Ro *et al.*, 2006). By engineering the FPP pathway and expressing the novel cytochrome P450 and its partner cytochrome P450 oxidoreductase, more than 115 mg l^{-1} artemisinic acid was obtained. Subsequently, the production of artemisinic acid was improved, reaching a titre of 25 g l^{-1} by expressing newly discovered and more efficient alternative aldehyde dehydrogenase (*ALDH1*) from *Artemisia annua* as well as a putative alcohol dehydrogenase (*ADH1*) (Paddon *et al.*, 2013). Another breakthrough in biosynthesis of natural products in yeast was recently reported by Galanie *et al*. (Galanie *et al.*, 2015). In this study they identified an enzyme which can convert the (*R*)-enantiomer of reticuline to the (*S*)-enantiomer and then built a complete opioid biosynthesis pathway towards hydrocodone, consisting of 23 enzymes from different sources (plants, mammals, bacteria, and yeast itself) in *S. cerevisiae*. Although the

engineered strain accumulated only small amounts of the product (~0.3 μg l^{-1}), the study demonstrated the feasibility of total biosynthesis of opioids through a long complex pathway in *S. cerevisiae*.

Although increasingly more examples of using yeast to produce different chemicals have been published in scientific journals, the strain performance parameters, i.e., titre, rate and yield, are usually several orders of magnitude lower than what is required for industrial-scale production. Developing a strain from the laboratory proof-of-concept level to a high-performing cell factory, suitable for large-scale fermentation, is still a major endeavour, requiring large investment. There is therefore an urgent need for new approaches to enable faster and cheaper strain development.

1.1.2 System biology approaches

With the advent of the big-data age, genomics, transcriptomics, proteomics, metabolomics and even single cellular analyses generate immense amounts of data. Systems biology aims at global understanding of the cellular function and regulation and here the 'omic data availability plays the key role. The expectation is that systems biology will lead to a more efficient data-guided metabolic engineering.

Genomics

The genome of *S. cerevisiae* was completely sequenced in 1996 (Goffeau *et al.*, 1996). Two years later, a website, *Saccharomyces* Genome Database (SGD) (http://www.yeastgenome.org/) was created to provide the genomic information, functions, pathways, and *etc*. of the budding yeast

(Cherry *et al.*, 1998). Subsequently, the single gene-deletion collection, covering 96% of annotated open reading frames (ORFs) of *S. cerevisiae*, was constructed (Giaever *et al.*, 2002). In 2003, the first genome-scale model of yeast was generated by Forster *et al*. by reconstruction of metabolic network in *S. cerevisiae* using available genomic, biochemical, and physiological information (Forster *et al.*, 2003).

Burgard *et al*. introduced OptKnock, the first rational modelling software, to guide gene deletion targets for overproducing targeted products (Burgard *et al.*, 2003). The researchers from the same group further developed the hierarchical computational algorithm OptStrain to identify genetic modifications of gene expressions (over-expressions) and gene disruptions to improve metabolites of interest (Pharkya *et al.*, 2004). Genome-scale model of *S. cerevisiae* has been used to identify gene disruption strategies for desired phenotype improvements by Patil *et al*. (Patil *et al.*, 2005). In this study, they adopted an OptGene algorithm, which uses Evolutionary Algorithms (EAs) and Simulated Annealing (SA) to identify the global optimal solutions. OptGene has been used in several studies for successfully predicting metabolic engineering strategies, e.g., for improving the production of succinic acid (Otero *et al.*, 2013) and vanillin (Brochado *et al.*, 2010).

Transcriptomics

Transcriptome refers to all RNA transcripts in the cell and serves as one of the bridges between genotype and phenotype. Many tools for RNA profiling have been developed. Microarray is one such tool, which uses

DNA probes to detect labelled cDNA molecules that hybridise to the arrays, via fluorescent scans with a laser (Schena *et al.*, 1995). Although there are some biases to the early microarrays, such as low reliable data given by different companies (Tan *et al.*, 2003), low reproducibility between different research groups (Irizarry *et al.*, 2005), and instability induced by ozone (Fare *et al.*, 2003), the modern microarray technology has greatly improved after decades development and has been successfully applied in yeast (Clark *et al.*, 2002). The comparison of microarrays with the recently introduced sequencing-based methods demonstrated good correlation and validity of microarray data (Malone and Oliver, 2011). RNA-sequencing (RNA-Seq) has revolutionized the transcriptome profiling, making it cheaper faster and more accurate (Wang *et al.*, 2009). In this approach, the RNA pools are first reverse-transcribed to generate a cDNA library and then adaptors are attached to the cDNA fragments. The cDNA segments are then sequenced by using high-throughput sequencing technologies, such as Illumina IG (Nagalakshmi *et al.*, 2008), Applied Biosystems SOLiD (Ondov *et al.*, 2008), or Roche 454 Life Science (Vera *et al.*, 2008). The reads resulting from these sequencing technologies can be either aligned to the known transcripts or de novo assembled to generate a genome-scale transcription map and expression level of each gene without reference genomic information. The advantages of RNA-seq methods include high reproducibility, smaller RNA amounts, little or no background signal, high accuracy of quantifying expression levels, and the capacity to detect transcripts without a known genomic sequence (Wang *et al.*, 2009). RNA-

seq analysis has been applied in numerous studies on metabolic engineering of yeast. E.g., one study systematically investigated the xylose utilisation via three different pathways (Feng and Zhao, 2013). In this study, the authors identified three transcription factors for xylose metabolism regulation and nine transcription factors responsible for host dependence regulation. Their findings offered possible metabolic engineering targets for improving the production of cellulosic ethanol in yeast. RNA-seq has also been used to analyse the transcriptional responses after being subjected to genetic perturbations for the identification of precise targets for gene expression or repression (Kim *et al.*, 2015).

Proteomics

Proteomics aims to quantify and comprehensively characterise all the proteins present in a cell. Compared with nucleic acid-based genomics and transcriptomics, proteomics methods are more demanding in terms of the required instrumentation and personnel expertise. Two-dimensional gel electrophoresis (2DE) played an important role in the early stage of the development of proteomic analyses. Briefly, proteins are first separated on a polyacrylamide gel with a stabilised pH gradient according to their pI using isoelectric focusing and subsequently resolved on SDS-PAGE gel according to their molecular mass. The spots are identified using MS and the map is created. The following analyses are carried out under the same conditions in order to obtain the alignment to the original 2DE map. 2DE had many disadvantages, such as low reproducibility, poor sensitivity in detecting proteins with extreme pH values or molecular mass, and inability to identify

low abundant and hydrophobic proteins (Chandramouli and Qian, 2009). Due to the rapid developments in mass spectrometry (MS), the LC-MS has taken over 2DEs for proteomics analysis. The MS-based techniques separate the ionised proteins loaded in the mobile-phase according to their mass to charge ratio. The accuracy, high throughput, and robustness of MS make it a widely used technique to globally profile proteome with or without combination with many other technologies. To study the molecular mechanism involved in tolerance to inhibitors during adaption, Lin *et al*. deployed an ^{18}*O-labeling-aided shotgun comparative proteome analysis to study* S. cerevisiae subjected to furfural (Lin *et al.*, 2009). Their findings of the response of yeast to furfural may assist in development of yeast strains tolerant to furfural, which is present in biomass hydrolyzates. By combining proteome analysis with phenotype, genotype and transcriptome data, Husnik *et al*. found no apparent difference between the first metabolically engineered yeast strain ML01 to be commercialised by the wine industry and the parental industrial wine yeast (Husnik *et al.*, 2006). By integrating quantitative proteomics with DNA microarrays and databases of known physical interactions, Ideker *et al*. suggested that about 15 of the 289 detected proteins are regulated post-transcriptionally in response to galactose utilisation (Ideker *et al.*, 2001). In addition to protein abundance, post-translational modifications and protein interactors, protein conformational changes can also be probed directly on a large scale by coupling limited proteolysis with a targeted proteomics workflow. Applying this method, Feng *et al*. evaluated the structural features of more than 1,000

yeast proteins in their biological matrices simultaneously and observed that about 300 proteins changed their conformation when altering nutrients (Feng *et al.*, 2014).

The essence of metabolic engineering is to change the fluxes inside the cell in such a way that the major part of carbon is redirected towards the product of interest. Therefore, measurements of the intracellular fluxes and metabolite concentrations are very useful tools to evaluate the state of the cell and to decide on the next metabolic engineering steps.

Metabolomics

Metabolomics aims to identify and quantify extracellular or intracellular metabolites. Targeted metabolomics aims at quantitating a portion of selected representative compounds in the key pathways. It is useful for evaluating metabolic changes perturbed by genetic modifications or a given environment (Wei *et al.*, 2010). In comparison, non-targeted metabolomics, which is a holistic method, focuses on global non-biased analysis of all of the small molecule metabolites in one biological system under specific conditions (Naz *et al.*, 2014). Because the majority of the intracellular metabolites have very high conversion rates, the cells must be quenched instantly if one wants to obtain a snapshot picture of the metabolite concentration at a given time-point. Several quenching methods suitable for *S. cerevisiae* have been reported (Canelas *et al.*, 2008; Dunn and Winder, 2011; Song *et al.*, 2015). The application of Mass Spectrometry (MS) in metabolomics to analyse cellular metabolites has drastically expanded due to its accessibility and versatility in the last two decades (Villas-Boas *et al.*,

2005). Hasunuma *et al*. demonstrated that metabolomics is a powerful tool to identify targets for metabolic engineering (Hasunuma *et al.*, 2011). In this study, they discovered that acetic acid decreases the flux through the pentose phosphate pathway, which is needed for xylose uptake. Zampar *et al*. investigated the collected dynamic and quantitative 'omics data during the diauxic shift in *S. cerevisiae* to study how metabolism from glycolytic to gluconeogenic operation changes in eukaryotic cells (Zampar *et al.*, 2013). Based on their analysis, the authors found the key activities responsible for the diauxic shift and identified the transcription factors associated with the observed changes in protein abundances. The genetic perturbations even at a single-cell level can be examined using mass spectrometry-based metabolomics. By employing this method, Ibanez *et al*. observed correlations between metabolites from the glycolytic pathway and ATP/ADP ratio changes at the single-cell level (Ibanez *et al.*, 2013).

1.1.3 Synthetic biology techniques

Global understanding of the microbial metabolism by the 'omics analysis provides potential targets for rational metabolic engineering. In order to implement the designed targets, synthetic biology tools for rapid and precise genetic manipulation are needed. Fortunately, *S. cerevisiae* has excellent DNA transformation efficiency and high inherent homologous recombination efficiency (Petes *et al.*, 1991), which ease the genetic manipulations. Since the yeast was sequenced in 1996, the genetic toolbox has been under continuous development and the last few years in particular have brought significant progress in this area.

Promoters

Regulating the expression level of genes is an important engineering tool, hence a library of well-characterised promoters, terminators, and UPRs is needed. Jeppsson *et al*. synthesised an artificial promoter library consisting of 37 constructs, the strength of which covered a range of three orders of magnitude between the strongest and the weakest ones in *S. cerevisiae* (Jeppsson *et al.*, 2003). Alper *et al.* generated a p*TEF1* (translation and elongation factor 1) mutated promoter library using an error-prone PCR strategy (Alper *et al.*, 2005). In this study, they characterised the mutant promoter library at single-cell-level via measuring GFP fluorescence using flow cytometry and at the transcriptional level by quantifying relative mRNA levels of *GFP* using RT-PCR. The final functional promoter library had 22 members with a phenotype strength spanning a 196-fold range and with a mean value of 29% between adjacent members, which thereby allowed for precise quantitative control of gene expression *in vivo* by choosing the corresponding promoter. Partow *et al*. made a comparison and evaluation of seven different constitute promoters (p*TEF1*, p*ADH1*, p*TPI1*, p*HXT7*, p*TDH3*, p*PGK1* and p*PYK1*) in *S. cerevisiae* (Partow *et al*., 2010) in controlled bioreactors. Two of the tested promoters (p*TEF1* and p*PGK1*) showed relatively constant activities at different glucose concentrations, while the activity of the other promoters was affected by glucose concentration. Peng *et al*. additionally compared several promoters on different carbon substrates and their activity across the diauxic shift (Peng *et al.*, 2015). These promoters included glycolytic

promoters (p*PGK1*, p*TDH3*, p*ENO2*, p*ADH1*, and p*TPI1*), translational elongation factor promoters (p*TEF1*, p*TEF2* and p*YEF3*), galactose metabolic promoters (p*GAL10*/p*GAL1*), ribosomal protein promoters (p*RPL3*, p*RPL15A*, p*RPL4* and p*RPL8B*), chaperone promoters (p*SSA1* and p*SSB1*), the copper-inducible p*CUP1* promoter, low-glucose-inducible promoters (p*TPS1*, p*HXT7*, p*ADH2* and p*CYC1*), and the p*PDA1* promoter. In order to reduce endogenous cellular interactions and avoid homologous recombination, Redden *et al*. created a series of non-homologous, purely synthetic, minimal yeast promoters (Redden and Alper, 2015). By assembling short core elements with different UAS elements of 10 bp in length, they constructed the shortest fungal promoters of 116 bp with high levels of both inducible and constitutive expression. This methodology of promoter engineering has great potential for metabolic engineering applications.

Terminators

In addition to promoters, terminators also play an important role in gene expression by influencing the 3′-end processing of mRNA, mRNA stability, and translational efficiency. Yamanishi *et al*. comprehensively evaluated the activity of 5,302 terminators from *S. cerevisiae* and observed a 70-fold range variation in terminators activity (Yamanishi *et al.*, 2013). The finding indicated that some degradation mechanisms and regulators may exist in the yeast and the terminator region can affect gene expression by determining mRNA abundance. Subsequently, the researchers from the same group tested the activity of the top five strong terminator regions when pairing

with different promoters or reporters under different growth conditions in several yeast strains (Ito *et al.*, 2013). Their results indicate that the activities of all five terminator regions were stronger than that of *PGK1* terminator, the commonly used terminator, in all investigated conditions and therefore provide alternatives when engineering yeast cell factories. On the other hand, Curran *et al*. described a set of short (35−70 bp) synthetic terminators in *S. cerevisiae* (Curran *et al.*, 2015). The strongest terminators showed 3.7-fold higher expression and 4.4-fold higher transcription relative to the commonly used *CYC1* terminator. These synthetic terminators together with their previously designed artificial minimal promoters offer very useful toolboxes when designing metabolic pathways for chemicals production in *S. cerevisiae.*

RNA tools

One can also control gene expression at the post-transcriptional level. RNA interference (RNAi) is a technique for post-transcriptional silencing genes of interest. In the process, the enzyme Dicer encoding the ribonuclease III (RNaseIII) endonuclease successively cuts long double-stranded RNA (dsRNA) into small interfering RNAs (siRNAs) of ~21 nt; the siRNAs are then bound to Argonaute (Ago) and subsequently guide Ago to identify and cleave the target transcripts (Tomari and Zamore, 2005). However, *S. cerevisiae* lost the RNA silencing pathway (Dicer and Argonaute) during evolution (Nakayashiki *et al.*, 2006). Introducing Dicer and Argonaute from *Saccharomyces castellii* proved to restore the RNA silencing machinery in *S. cerevisiae* (Drinnenberg *et al.*, 2009). The RNA

interference (RNAi)-assisted genome evolution method (RAGE) was developed to accumulate multiplex beneficial genetic modifications in an evolving yeast genome (Si *et al.*, 2015). By three rounds of RAGE, the authors obtained a strain with substantially improved acetic acid tolerance and identified three targets that conferred the improved phenotype. RAGE can greatly accelerate the identification of desired traits by rapid and iterative genome-wide screening.

CRISPR/Cas9 system

The application of the Clustered Regularly Interspaced Short Palindromic Repeats (CRISPR) and CRISPR-associated (Cas) systems in genome editing is a landmark in the development of genetic tools. Recently, the CRISPR/Cas9 system has been successfully adopted in a wide range of species from bacteria, yeast to plants and mammalian cells (Sander and Joung, 2014). The CRISPR/Cas9 system was first introduced into *S. cerevisiae* by DiCarlo *et al*. in 2013 (DiCarlo *et al.*, 2013). Specifically, the DNA target sequence next to the proto-spacer adjacent motif (PAM) site is identified and matched with the 20 nt single-stranded guide RNA; the Cas9 nuclease then binds to the target sequence and generates a double-stranded break (DSB); homologous recombination occurs between the DNA adjacent to the DSB and the double-stranded oligos (dsOligos) or larger DNA fragments. This allows introducing gene knock-outs, promoter replacements, protein mutations, expression cassettes, *etc*. The CRISPR/Cas9 system can be used to screen out negative transformants by generating the lethal DSB without recombination, thus allowing for high efficient, multiple and

simultaneous, and seamless knock-out or knock-in events. Jakociunas *et al*. applied the CRISPR/Cas9 system in *S. cerevisiae* and targeted up to 5 different genomic loci at the same time with high efficiency by using only 90-bp long dsOligos (Jakociunas *et al.*, 2015a). Later, gene insertions and gene deletions were achieved simultaneously in a single transformation by application CRISPR/Cass9 system in laboratory and industrial *S. cerevisiae* strains (Jakociunas *et al.*, 2015b; Stovicek *et al.*, 2015b).

Vectors

A set of vectors named EasyClone was designed for *S. cerevisiae* to simultaneously integrate multiple genes into the genome (Jensen *et al.*, 2014b). This expression system consist of a backbone with a replication origin from bacteria which allows for plasmid amplification in *E. coli*, a USER cloning cassette used for insertion of standardised biobricks, two terminators in opposite directions flanking the USER cloning site, an auxotrophic selection marker flanked by LoxP sites, and two 'UP' stream and 'DOWN' stream targeting sequences which are homologous to specific integration sites on the genome. The integrative plasmid can be linearised at the USER cassette, and assembled with the genes of interest and promoters by USER cloning (Uracil-Specific Excision Reagent) method. The EasyClone vectors allow the integration of up to 6 genes into 3 different loci in a single transformation event, when using triple selection. The markers can be easily removed by CreA recombinase-mediated loop-out and the strain can be further engineered. Subsequently, Stovicek *et al*. replaced the auxotrophic markers with six synthetic dominant markers obtaining

EasyClone 2.0 vectors, which allow engineering of industrial strains without auxotrophies (Stovicek *et al.*, 2015a). A vector set EasyCloneMulti was developed for integrating multiple copies of expression cassettes into retrotransposon element (Maury *et al.*, 2016). The genome sequencing results reveal that many Ty elements are distributed through the chromosomes of *S. cerevisiae* (Goffeau *et al.*, 1996). High copy number of integrations onto Ty elements through a single transformation with a high efficiency has been reported (Lee and Da Silva, 1997; Parekh *et al.*, 1996; Wang *et al.*, 1996). Maury *et al*. created a set of integrative vectors that targets Ty retrotransposons tagged with different auxotrophic marker degradation and has been successfully applied in our study to improve resveratrol production (Li *et al.*, 2015).

1.2 Microbial production of resveratrol

1.2.1 Discovery

Resveratrol (3,4',5-trihydroxystilbene) is a polyphenolic compound with antioxidant activity. It was isolated by Takaoka from a poisonous medicinal plant *Veratrum album* in 1939 (Takaoka, 1939). Resveratrol was later found in extracts of the roots of Japanese knotweed, *Polygonum cuspidatum*, which is a Chinese herbal medicine and now the main source for commercial resveratrol (Nonomura *et al.*, 1963). Subsequently, it was also isolated from grape *Vitis vinifera* and has been characterised as a phytoalexin, because it was produced in response to fungal infection or exposure to ultraviolet light (Langcake and Pryce, 1976). Red wine was then found to be rich in resveratrol (Siemann and Creasy, 1992). This fact was hypothesised to explain the French paradox, namely low rate of coronary heart diseases among French in spite of the high-fat diet (Renaud and de Lorgeril, 1992). Resveratrol also occurs in more than other 70 plant species, covering 32 genera, of which most are edible, including peanuts, berries, cocoa, *etc*. (Aggarwal *et al.*, 2004; Fan *et al.*, 2010; Harikumar and Aggarwal, 2008; Nikolova, 2007). It is believed that red wine, grape, Japanese knotweed and peanuts are the most abundant natural sources of resveratrol (Pervaiz and Holme, 2009; Shakibaei *et al.*, 2009).

1.2.2 Isomers

Resveratrol exists in two forms, *cis*-resveratrol and *trans*-resveratrol (Fig. 1.2.1), which differ in the confirmation of the double bond between the

two phenolic rings. The two isoforms of resveratrol can be discriminated by different UV spectrum (288 nm for the *cis* isomer and 308 nm for the *trans* isomer) (Trela and Waterhouse, 1996). The *trans*-resveratrol is the major and more stable natural form. However, the *trans*-resveratrol is unstable under exposure to UV light and would undergo *cis*-isomerization (Camont *et al.*, 2009). In the absence of light, the *trans*-form can remain stable for several months if it is kept from high pH environment (Trela and Waterhouse, 1996).

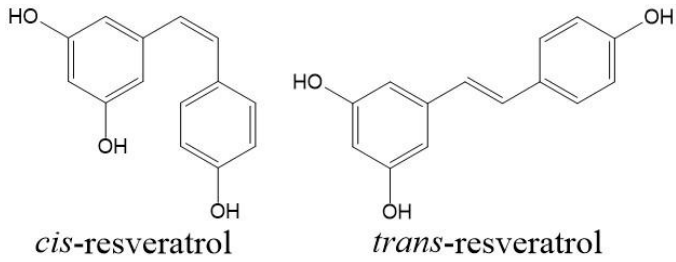

Fig 1.2.1 Structures of two resveratrol isoforms.

1.2.3 Medical research

Despite resveratrol being discovered in 1939, it did not get much attention until the late 1990s (Fig. 1.2.2), when the biological effects of the *Polygonum*-extracted stilbene on lipid metabolism in the liver of mice and rats were uncovered (Arichi *et al.*, 1982; Kimura *et al.*, 1983). Thereafter, many therapeutic effects of resveratrol have been reported. The International Conference on Resveratrol and Health was set up in 2010 and formulated a set of recommendations in relation to human consumption (Vang, 2013).

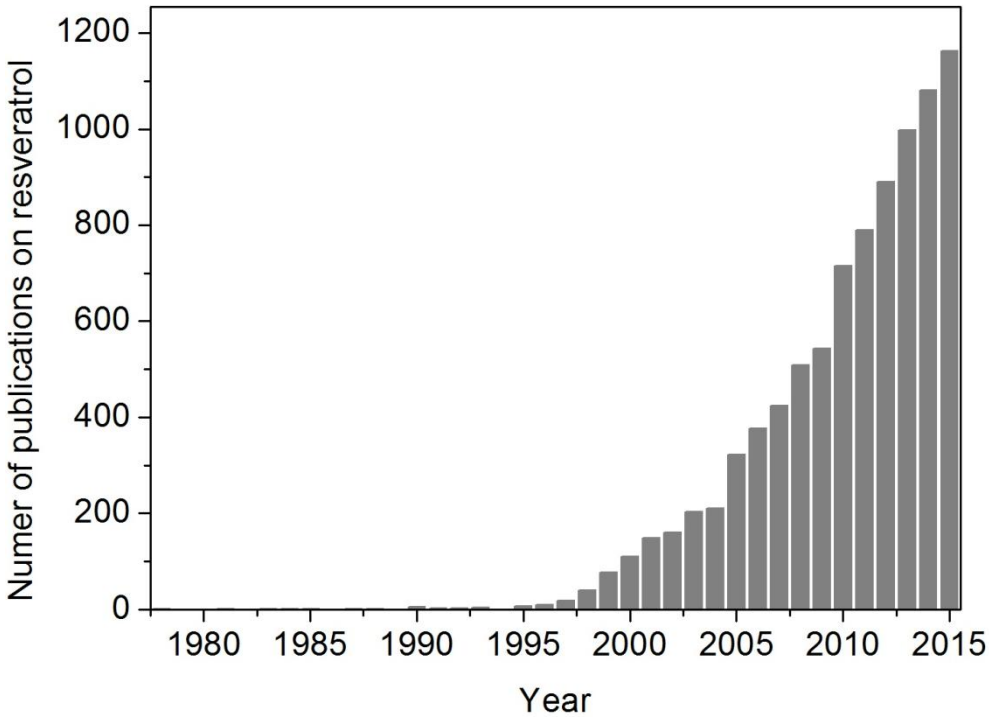

Fig 1.2.2 Increasing number of scientific publications on resveratrol.[1]

Antioxidant

Resveratrol can function as an antioxidant by forming stable radicals through resonance structure of aromatic groups (King *et al.*, 2006). Oxidative stress, which refers to the accumulation of reactive oxygen species (ROS) generated during cellular metabolism, can result in cellular damage by oxidative modification of DNA, protein, and lipids (Arthur *et al.*, 2008). DNA damage resulting from ROS can lead to mutagenesis,

[1] The number of publications was obtained by searching term "resveratrol" in title/abstract for each year from 1978 to 2015 on PubMed (http://www.ncbi.nlm.nih.gov/pubmed/).

oncogenesis and aging. Resveratrol showed the free radical scavenging activity to protect DNA against oxidation-induced damage (Burkhardt *et al.*, 2001; Kumar *et al.*, 2007). The oxidation of low-density lipoprotein (LDL) is strongly associated with the development of coronary heart disease (Holvoet, 2004). It was reported that resveratrol can inhibit LDL oxidation *in vitro* by chelating copper and directly scavenging free radicals (Frankel *et al.*, 1993). *In vivo* assay also revealed that resveratrol can reduce lipid peroxidation and increase plasma antioxidant capacity in rats (Sengottuvelan *et al.*, 2006; Wenzel *et al.*, 2005). In addition, resveratrol was shown to protect proteins against ROS oxidation (Olas *et al.*, 2006; Olas *et al.*, 2004).

Cardiovascular

The potential effect of resveratrol in red wine on the French Paradox inspired people to study resveratrol effects on cardiovascular activity. One of the notable cardioprotective mechanisms of resveratrol is the inhibition on platelet aggregation, which is used to seal damaged blood vessels to stop bleeding when wounded (King *et al.*, 2006). Excessive platelet aggregation can lead to pathogenesis of cardiovascular disease. Both *in vivo* and *in vitro* assays support resveratrol having inhibitory effect on platelet aggregation (Olas *et al.*, 2008; Wang *et al.*, 2002). There is also evidence that resveratrol can up-regulate endothelial nitric oxide synthase (eNOS), which can improve nitric oxide (NO)-mediated vasodilation and accelerate blood flow (Gresele *et al.*, 2008; Wallerath *et al.*, 2002). Additional explanations of the protective impacts of resveratrol on cardiovascular system through inhibiting LDL oxidation or anti-proliferation were also reported (Kovanen

and Pentikainen, 2003; Laden and Porter, 2001; Mizutani *et al.*, 2000; Zou *et al.*, 2000).

Anti-tumour

Cancer is a major challenge to human health worldwide with 8.2 million deaths due to cancer in 2012 (Torre *et al.*, 2015). Many studies have been dedicated to finding the causes for cancer and ways to decrease the risk of the disease. The studies of resveratrol on anticancer activity have dramatically increased since 1997, when Jang *et al*. published the chemopreventive activity of resveratrol in the three major stages of carcinogenesis, tumour initiation, promotion, and progression (Jang *et al.*, 1997). It suggested that multiple mechanisms may contribute to the anti-proliferative activity of resveratrol, including the arrest of the cell cycle (Castello and Tessitore, 2005; Joe *et al.*, 2002), the induction of apoptosis through activating p53 (Demoulin *et al.*, 2015; Ding and Adrian, 2002), and suppressing the nuclear factor-κB (Ivanov *et al.*, 2008), activator protein-1 (Kim *et al.*, 2012) and cyclooxygenase-2 (Lee *et al.*, 2012).

An additional explanation is that resveratrol is firstly metabolised to piceatanol by the cytochrome P450 1B1 (CYP1B1) enzyme in biological system; and it is piceatanol that plays the anti-tumour effect (Potter *et al.*, 2002). Many *in vivo* studies clearly and strongly support a chemopreventive effect of resveratrol in the development of cancer and therefore many clinical trials of resveratrol are underway (Baur and Sinclair, 2006).

Anti-aging

A new application area for resveratrol was opened in the early 2000s with the discovery that resveratrol is able to mimic caloric restriction effects and extend the lifespan of yeast (Howitz *et al.*, 2003), worms (Viswanathan *et al.*, 2005), flies (Bauer *et al.*, 2004), and rodents (Baur *et al.*, 2006) through activation of the sirtuin pathways. Sirtuins are silent information regulator proteins, which belong to conserved NAD^+-dependent deacetylases (class III histone deacetylases) and overexpression of sirtuins can result in extension of lifespan (Tissenbaum and Guarente, 2001). Many studies suggested that human sirtuin 1 (SIRT1) was activated indirectly by resveratrol (Borra *et al.*, 2005; Kaeberlein *et al.*, 2005; Pacholec *et al.*, 2010). One potential target of resveratrol is AMP-activated protein kinase (AMPK), which has been shown to activate SIRT1 and thus indicates a possible mechanism for the indirect activation of SIRT1 by resveratrol (Canto *et al.*, 2009). AMPK acts as a regulator of global metabolism to increase NAD^+ levels and activate Sirt1p (Canto *et al.*, 2009). It has been suggested that high concentrations of resveratrol can increase the AMP/ATP (Carling *et al.*, 1987) or ADP/ATP ratio (Xiao *et al.*, 2011) to indirectly activate AMPK (Hawley *et al.*, 2010) and therefore increase the lifespan of *Caenorhabditis elegans* (Apfeld *et al.*, 2004). However, there is no strong evidence whether resveratrol can have an anti-aging effect on humans and the lifespan extension effect on other organisms is disputed as well.

Besides, resveratrol has been reported to possess many other therapeutic activities, such as anti-inflammatory, neuroprotective, *etc*. activity

(Fernandez-Mar *et al.*, 2012). These potential health benefits partially depend on the absorption and the bioavailability of resveratrol (King *et al.*, 2006). Although the absorption of resveratrol has been shown to be efficient following oral administration, the bioavailability of resveratrol is low, which limits its application in humans (Cottart *et al.*, 2010; Patel *et al.*, 2011). The other issue is the low solubility of resveratrol in water, which is only 0.05 g l^{-1}. Consequently, additional information and more clinic trials on resveratrol are needed to release these constrains.

1.2.4 Biosynthesis pathway of resveratrol

Resveratrol is derived from the phenylpropanoid pathway, which exists in all higher plants and serves as the source of a wide range of phenolic compounds, such as flavonoids, lignins, and coumarins. There are two pathways to synthesise resveratrol either from tyrosine or from phenylalanine (Fig. 1.2.3), which are defined as TAL pathway and PAL pathway respectively in the thesis.

The first step of PAL pathway is deamination of phenylalanine catalysed by phenylalanine ammonia lyase (*PAL*) to generate cinnamic acid. The product of PAL, cinnamic acid, is then converted to *p*-coumaric acid by cinnamate-4-hydroxylase (*C4H*). C4H is a P450 enzyme, which usually requires cytochrome P450 reductase (*CPR*) to function. Alternatively, *p*-coumaric acid can be obtained by one-step deamination from tyrosine catalysed by tyrosine ammonia lyase (*TAL*). The 4-coumaroyl-CoA ligase (*4CL*) then attaches coenzyme A to *p*-coumaric acid to generate 4-coumaroyl-CoA. Three molecules of malonyl-CoA are then condensed to

one molecule of 4-coumaroyl-CoA by resveratrol synthase (*STS*) to result in one molecule of resveratrol.

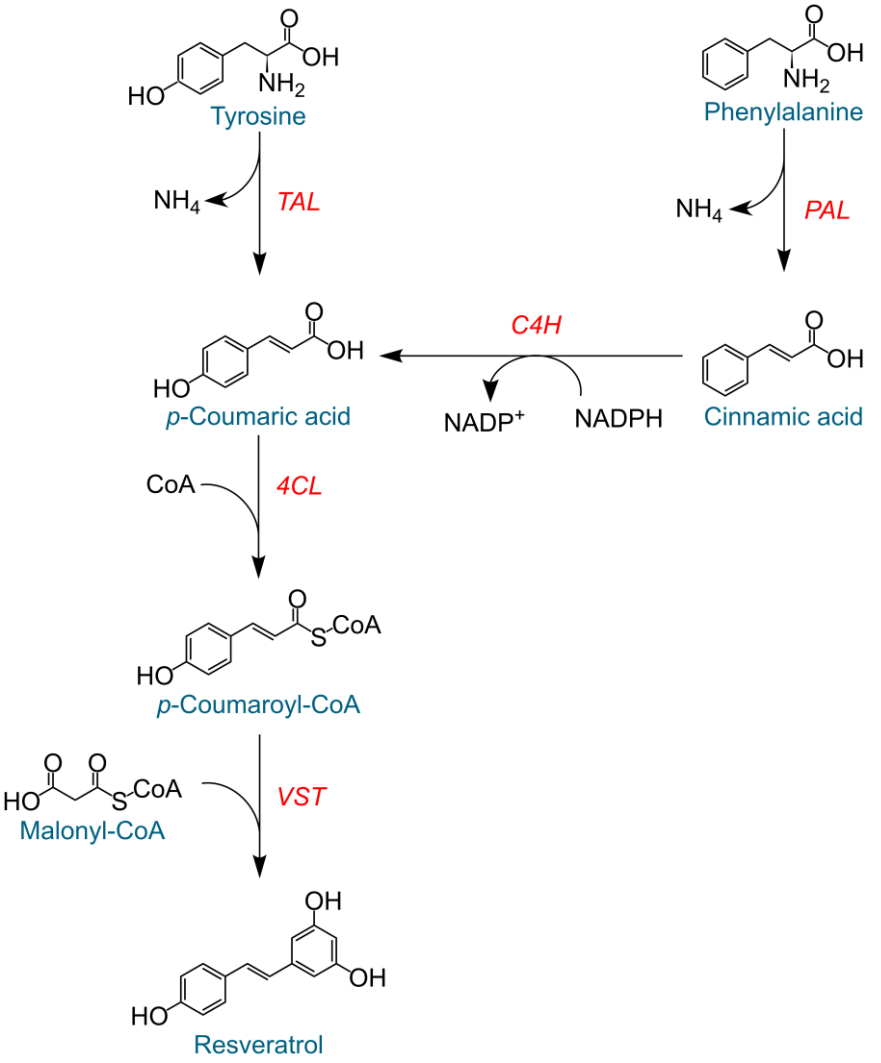

Fig. 1.2.3 Biosynthesis pathway of resveratrol. *PAL*, phenylalanine ammonia lyase; *C4H*, cinnamate-4-hydroxylase; *CPR*, cytochrome P450 reductase; *TAL*, tyrosine ammonia lyase; *4CL*, 4-coumaroyl-CoA ligase; *VST*, resveratrol synthase.

1.2.5 Metabolic engineering of microorganisms for resveratrol production

Resveratrol can be obtained by plant extraction, chemical synthesis, and microbial production. Resveratrol produced biologically either in plants or in recombinant microorganisms is mainly *trans*-resveratrol. The plant-derived resveratrol is usually extracted from the most abundant natural sources, such as grapes and Japanese knotweed *P. cuspidatum*. However, there are several disadvantages: 1) the supply of the plant resources is unstable due to geographic diversity; 2) plant farming is susceptible to environmental factors, such as weather and climate change, pest invasion, and disease infection; 3) the extraction process is very complicated, which lowers the resveratrol extraction efficiency (Karacabey and Mazza, 2008); 4) the purity is low and ranges widely, with some preparations containing as low as 50% of the active ingredient and additionally containing emodin, which has a laxative effect (Srinivas *et al.*, 2007); and 5) it is not environmentally friendly. Chemical synthesis of resveratrol has been extensively studied and the yield of chemical synthesis is relatively high. However, except for the well-known environmental drawback, the challenges of resveratrol production *via* chemical synthesis also lie in: 1) the fact that it usually requires multiple steps and harsh conditions, such as high temperature, polluting metal catalysts (Fan *et al.*, 2010); 2) it is easily contaminated by many unwanted by-products (Mei *et al.*, 2015); and 3) it may lack stereoselectivity, which leads to a mixture of *trans*- and *cis*-isomers (Fan *et al.*, 2010). In comparison, the mentioned disadvantages by

plant extraction and chemical synthesis of resveratrol can be averted by microbial biosynthesis. Many engineered microorganisms have been employed for resveratrol production.

S. cerevisiae

The first proof-of-concept microbial production of resveratrol was reported by Becker *et al*. in 2003 (Becker *et al.*, 2003). The authors expressed *4CL216* from a hybrid poplar (*Populus trichocarpa*×*Populus deltoids*) and *VST1* from *Vitis vinifera* in *S. cerevisiae* FY23. The recombinant strain accumulated 1.45 μg l^{-1} resveratrol in the form of piceid, resveratrol glucoside, when the recombinant yeast culture was fed 10 mg l^{-1} *p*-coumaric acid. Later on, Beekwilder *et al*. integrated the two genes, *4CL2* from *Nicotiana tabacum cv.* Samsun and *STS* from *V. vinifera*, into the genome of *S. cerevisiae* CEN.PK113-3B, which resulted in 5.8 mg l^{-1} non-glycosylated resveratrol from 820.8 mg l^{-1} *p*-coumaric acid on YNB medium (Beekwilder *et al.*, 2006). When *4CL1* from *Arabidopsis thaliana* and *STS* from *Arachis hypogaea* were introduced into *S. cerevisiae* W303-1A, 3.1 mg l^{-1} resveratrol was obtained from 15.3 mg l^{-1} *p*-coumaric acid on YPED medium (Shin *et al.*, 2011). Instead, Sydor *et al.* used one industrial yeast strain isolated from Brazilian sugar cane plantation (Barra Grande) to express *4CL1* from *A. thaliana* and *STS* from *V. vinifera*. When growing the resulting strain on YEPD medium and feeding it with 15 mM *p*-coumaric acid (2.46 g l^{-1}), they obtained 391 mg l^{-1} resveratrol (Sydor *et al.*, 2010a). This was the highest production of resveratrol reported in yeast prior to our study.

Zhang *et al.* adopted a fusion strategy to channel substrates from 4CL to VTS, which were from *A. thaliana* and *V. vinifera*, respectively, in yeast *S. cerevisiae* WAT11 (Zhang *et al.*, 2006b). Although the yeast can only accumulate 0.65 mg l^{-1} resveratrol on medium with 12 mg l^{-1} *p*-coumaric acid, when they fused 4CL and STS with a Gly-Ser-Gly linker, the yield was 15-fold higher than the expression of individual enzymes. Surprisingly, 9.8% of the total production was found to be *cis*-resveratrol. Subsequently, the structure of the unnatural fusion protein 4-coumaroyl-coA ligase::stilbene synthase (4CL::STS) was characterised and its kinetic parameters were compared with that of each enzyme (Wang *et al.*, 2011b). The results showed that no structural or functional properties of *At*4CL1 and *Vv*VST in the fusion protein were significantly changed. Although the fusion protein had a slightly higher catalytic efficiency over each enzyme, it was likely that the increased resveratrol production resulted from localization of the active sites in close proximity. Instead, they generated scaffolds to recruit 4CL and STS for increasing resveratrol production and this resulted in 5-fold improvement of resveratrol production to 6.7 mg l^{-1} over the strain without scaffolds (Wang and Yu, 2012). Therefore, their strategies provide an alternative design for metabolic engineering to improve catalytic efficiency. In addition, they found 6.0 mg l^{-1} resveratrol from extraction of fresh yeast cell pallets, which means that a transporter was needed to pump resveratrol out of the cells (Zhang *et al.*, 2006b). To address this problem, the same group introduced an *E. coli* transporter *araE* and obtained 3.1 mg l^{-1} resveratrol, which was 2.44-fold improvement over

the control strain (Wang *et al.*, 2011a). They attempted to express tyrosine ammonia lyase (*TAL*) from *Rhodobacter sphaeroides* in the yeast host, but failed due to problems with expression (Zhang *et al.*, 2006b). In a later study, they used a codon-optimized *TAL* gene and produced 1.90 mg l^{-1} resveratrol from 12 mg l^{-1} tyrosine on synthetic defined drop-out medium (Wang *et al.*, 2011a). Notably, 1.06 mg l^{-1} resveratrol was accumulated in the medium even without tyrosine supplementation; the authors attributed this to the tyrosine contained in the medium.

Alternatively to TAL, Shin *et al*. introduced *PAL* from *Rhodosporidium toruloides*, cinnamic acid 4-hydroxylase (*C4H*) and *4CL* both from *A. thaliana*, and *STS* from *A. hypogaea* into *S. cerevisiae* W303-1A (Shin *et al.*, 2012). Due to the catalysing activity of PAL from *R. toruloides* on both tyrosine and phenylalanine (Jiang *et al.*, 2005), the engineered strain could produce 3.4 mg l^{-1} resveratrol on complex medium. To increase the pool of malonyl-CoA, they swapped the ACC1 promoter with a stronger galactose-inducible GAL1 promoter, which resulted in 2-fold increase of *ACC1* transcriptional level and 1.3-fold increase of the resveratrol production to 4.3 mg l^{-1}. A further improvement of 1.7-fold resveratrol production (5.8 mg l^{-1}) was achieved when 12 mM tyrosine was added. The other study tried to produce resveratrol from phenylalanine by introducing PAL from Populus hybrid (*Populus trichocarpa* × *P. deltoids*), C4H and 4CL from *G. max* and STS from *V. vinifera* cv. Soultanina in *S. cerevisiae* YPH499. In order to increase the activity of C4H, they expressed NADPH-cytochrome P450 reductase (CPR) from the same source as PAL. The final strain only

accumulated 0.29 mg l^{-1} resveratrol from 10 mM phenylalanine (Trantas *et al.*, 2009).

Vos *et al*. investigated the effect of specific growth rate on the physiology and productivity of the engineered yeast resveratrol-producing strains, which were engineered by Katz *et al*. (Katz *et al.*, 2011), in aerobic, glucose-limited chemostat cultivation (Vos *et al.*, 2015). Stoichiometric analysis revealed that *de novo* production of resveratrol was strongly correlated with the growth rate due to requirement of high amount energy (13 moles of ATP per mole resveratrol) and involvement of key precursors, which were growth rate-dependent, for resveratrol synthesis. Introduction of resveratrol biosynthesis pathway into *S. cerevisiae* resulted in apparent transcriptional differences in the genes involved in precursor biosynthesis, such as *TKL1*, *ARO7* and *ARO9*. This highlighted the need for uncoupling growth and resveratrol production for industrial application.

E. coli

The widely-used host, *E. coli*, was employed to produce resveratrol. Watts *et al*. expressed *4CL1* from *A. thaliana* and *STS* from *A. hypogaea* in *E. coli* strain BW27784 and obtained 104.5±4.4 mg l^{-1} resveratrol on mineral medium supplemented with 1 mM *p*-coumaric acid (164.16 mg l^{-1}) (Watts *et al.*, 2006). On the other hand, when *4CL2* from *N. tabacum cv.* Samsun and *STS* from *V. vinifera* were introduced into *E. coli* BL21, the recombinant strain resulted in 16 mg l^{-1} resveratrol during the fermentation on complex 2×YT medium with 5 mM *p*-coumaric acid (820.8 mg l^{-1}) (Beekwilder *et al.*, 2006). The highest accumulation of resveratrol achieved

in *E. coli* reported so far was 2.3 g l^{-1} (Lim *et al.*, 2011). In this study, they screened seven resveratrol synthases from *V. vinifera* (*Vv*STS), *Polygonum cuspidatum* (*Pcu*1STS and *Pcu*3STS), *Psilotum nudum* (*Pn*STS), *Pinus massoniana* (*Pm*STS), *Pinus strobes* (*Ps*STS), and *Pinus densiflora* (*Pd*STS) via bioinformatics and homology modelling. The *in vitro* assay revealed an inhibition effect of acetyl-CoA on STS; the *k*cat/*Km* of *Ah*STS and *Vv*STS were significantly higher than that of STS from the other organisms. The *in vivo* assay of the screened STS showed *Vv*STS as the best candidate for resveratrol production when paring with *At*4CL from *A. thaliana*, which resulted in 1.38±0.18 g l^{-1} resveratrol on M9 medium from 2.46 g l^{-1} *p*-coumaric acid in BW27784. They further improved resveratrol production to 2.3 g l^{-1} from by additionally supplementing cerulenin to limit carbon lost from malonyl-CoA to fatty acids biosynthesis pathway. Wu *et al*. also reported resveratrol production from tyrosine in *E. coli* JM109 (Wu *et al.*, 2013). They deployed a multivariate modular strategy by putting *TAL* from *R. glutinis*, *4CL* from *Petroselinum crispum* and *STS* from *V. vinifera* together with malonate assimilation pathway from *Rhizobium trifolii* (matB malonyl-CoA synthetase and matC malonate carrier protein) to increase the supply of malonyl-CoA as distinct modules. The optimum strain resulted in 35.02 mg l^{-1} of resveratrol from 3 mM tyrosine (543.57 mg l^{-1}) on MOPS medium. Afonso *et al*. investigated the physiological states and plasmid segregation stability of the *E. coli* strain BW27784 expressing *4CL1* from *A. thaliana* and *STS* from *A. hypogaea* on low copy and high copy number plasmids, respectively (Afonso *et al.*, 2015). They concluded that culture

conditions, cellular viability, and the concentration of *p*-coumaric acid had impact on resveratrol accumulation. Specifically, I) culture conditions, for example, temperatures over 35℃ led to resveratrol degradation (Chung *et al.*, 2006) and inappropriate pH (<6.5 or >7.0) resulted in reduction of resveratrol by affecting cell growth; II) cellular viability affected resveratrol production by altering physiological states; and III) high concentration of *p*-coumaric acid could result in decrease of cellular viability, such as the reduction of cell number by damaging cell membranes, and the disruption of cellular functions via binding to the bacterial genomic DNA (Lou *et al.*, 2012) and consequently affected resveratrol volumetric yields.

Other microorganisms

Shi *et al*. isolated and identified 21 resveratrol-producing microorganisms out of 65 endophytes from Merlot wine grapes (*V. vinifera* L. cv. Merlot), wild Vitis (*Vitis quinquangularis* Rehd.), and Japanese knotweed (*P. cuspidatum* Siebold & Zucc.) (Shi *et al.*, 2012). Among these isolates, *Alternaria* sp. MG1 isolated from cob of Merlot gave constitutive, the most stable, and the highest resveratrol production after three subcultures. Later on, they investigated the effects of bioconversion conditions on resveratrol production (Zhang *et al.*, 2013a). Under the optimal conditions (a resting time of 21.3 h with the innoculum of 12.16% (wet cell weight in 100 mL medium) in 0.2 mM phosphate buffer together with 0.1 g/L $MgSO_4$, 0.2 g/L $CaSO_4$, and 4.66 mM phenylalanine at pH 6.5), the strain accumulated 1.376 μg l^{-1} resveratrol. They further identified the resveratrol biosynthesis pathway consisting of PAL, C4H and 4CL by

analysing and tracking the related enzymes (Zhang *et al.*, 2013b). Due to the concentration of piceid (resveratrol-3-O-β-glucoside) being higher than that of resveratrol in plants but its bioavailability is relatively much lower, Wang *et al*. used *Aspergillus oryzae* to ferment *P. cuspidatum* for bioconversion of piceid to resveratrol with the highest yield of resveratrol 1.35% (Wang *et al.*, 2007). Park *et al.* expressed 4-coumarate/cinnamate:coenzyme A ligase (ScCCL) from *Streptomyces coelicolor* and codon optimised STS from *A. hypogaea* in *Streptomyces venezuelae* DHS2001 (Park *et al.*, 2009). The recombinant strain resulted in 0.4 mg l^{-1} resveratrol from 1.2 mM *p*-coumaric acid (196.99 mg l^{-1}).

Resveratrol derivatives

The beneficial effects of resveratrol are constrained by its instability, which results from its sensitivity to light, oxygen and harsh pH conditions and therefore leads to a reduction of the bioavailability and bioactivity (Walle *et al.*, 2004). One way to solve this problem is to use more stable resveratrol derivatives, such as *O*-methyl ethers pinostilbene and pterostilbene. Pinostilbene is a mono-methyl ester of resveratrol, while pterostilbene is dimethylester of resveratrol. Many studies have shown that pinostilbene and pterostilbene have equal or even better bioactivities than resveratrol (Chao *et al.*, 2010; Fulda, 2010; Rimando *et al.*, 2002). In addition, the substitution of hydroxyl group by methoxy group increases the hydrophobicity and thus improves oral absorption and cellular uptake ((Kapetanovic *et al.*, 2011; Remsberg *et al.*, 2008).

Consequently, metabolic engineering of microorganisms for production of resveratrol derivatives is of great interest. Katsuyama *et al*. cloned the pinosylvin methyltransferase (PMT) homologue from *Oryza sativa* in a resveratrol-producing platform *E. coli* strain (the strain overexpressed *PAL* from *R. rubra*, *4CL* from *Lithospermum erythrorhizon*, *STS* from *A. hypogaea*, and *ACC* from *Corynebacterium glutamicum*), which resulted in 18 pinostilbene and 5.8 mg l^{-1} pterostilbene from 540 mg l^{-1} tyrosine (Katsuyama *et al.*, 2007). In 2013, resveratrol *O*-methyltransferases (*ROMT*) from *Vitis riparia* and *Sorghum bicolor* were evaluated in *E. coli* (Jeong *et al.*, 2014). This study suggested that *SbROMT* was mainly in charge of mono-methylation but not di-methylation of resveratrol: 34 mg l^{-1} pinostilbene and only 0.16 mg l^{-1} pterostilbene were obtained from 1 mM resveratrol (228.24 mg l^{-1}). In contrast, only a small amount of both methylated resveratrol derivatives were generated by *VrROMT*. Wang *et al.* investigated *ROMT* from *V. vinifera* and reported that this variant specifically catalysed the methylation of resveratrol into pterostilbene in both *E. coli* and *S. cerevisiae* (Wang *et al.*, 2015). The engineered *E. coli* and *S. cerevisiae* could produce 50 mg l^{-1} and 2.2 mg l^{-1} pterostilbene respectively from *p*-coumaric acid by expressing the fusion protein 4CL::STS and VvROMT.

Table 1.1 summary of resveratrol production in microbes

Microorganism	Genes and sources	Medium and substrate	Resveratrol production	Reference
S. cerevisiae FY23	*4CL216* (*P. trichocarpa*×*P. deltoids*) and *VST1* (*V. vinifera*)	SCDL medium 10 mg l^{-1} *p*-coumaric acid	1.45μg l^{-1}	(Becker *et al.*, 2003)
S. cerevisiae CEN.PK113-3B	*4CL2* (*N. tabacum cv.* Samsun) and *STS* (*V. vinifera*)	YNB medium 820.8 mg l^{-1} *p*-coumaric acid	5.8 mg l^{-1}	(Beekwilder *et al.*, 2006)
S. cerevisiae W303-1A	*4CL1* (*A. thaliana*) and *STS* (*A. hypogaea*)	YPED medium 15.3 mg l^{-1} *p*-coumaric acid	3.1 mg l^{-1}	(Shin *et al.*, 2011)
S. cerevisiae isolated from Barra Grande	*4CL1* (*A. thaliana*) and *STS* (*V. vinifera*)	YEPD medium 2,460 mg l^{-1} *p*-coumaric acid	391 mg l^{-1}	(Sydor *et al.*, 2010a)
S. cerevisiae EC1118	*4CL1* (*A. thaliana*) and *STS* (*V. vinifera*)	wine broth 164 mg l^{-1} *p*-coumaric acid	8.25 mg l^{-1}	(Sun *et al*., 2015)
S. cerevisiae WAT11	*4CL* (*A. thaliana*) and *STS* (*V. vinifera*) in the form of *4CL*::*STS* fusion	SD medium 12 mg l^{-1} *p*-coumaric acid	0.65 mg l^{-1}	(Zhang *et al*., 2006b)
S. cerevisiae WAT11	*4CL* (*A. thaliana*) and *STS* (*V. vinifera*) attached to the scaffolds	SD medium 64 mg l^{-1} *p*-coumaric acid	14.4 mg l^{-1}	(Wang and Yu, 2012)
S. cerevisiae	TAL (*R. sphaeroides*), 4CL (*A.*	SD medium	1.90 mg l^{-1}	(Wang *et al.*, 2011a)

WAT11	*thaliana*) and VST1 (*V. vinifera*)	12 mg l^{-1} tyrosine		
S. cerevisiae W303-1A	*PAL* (*R. toruloides*), *C4H* (*A. thaliana*), *4CL* (*A. thaliana*), *STS* (*A. hypogaea*) and p*GAL1*::p*ACC1-ACC1*	YP medium 12 mM tyrosine	5.8 mg l^{-1}	(Shin *et al.*, 2012)
S. cerevisiae YPH499	*PAL* (*P. trichocarpa* × *P. deltoids*), *C4H* (*G. max*), *4CL* (*G. max*), *STS* (*V. vinifera* cv. Soultanina) and *CPR* (*P. trichocarpa* × *P. deltoids*)	CM medium 10 mM phenylalanine on	0.29 mg l^{-1}	(Trantas *et al.*, 2009)
E. coli strain BW27784	*4CL1* (*A. thaliana*) and *STS* (*A. hypogaea*)	Mineral medium 164 mg l^{-1} *p*-coumaric acid	104.5±4.4 mg l^{-1}	(Watts *et al.*, 2006)
E. coli BL21	*4CL2* (*N. tabacum cv.* Samsun) and *STS* (*V. vinifera*)	2×YT medium 820.8 mg l^{-1} *p*-coumaric acid	16 mg l^{-1}	(Beekwilder *et al.*, 2006)
E. coli BW27784	*4CL* (*A. thaliana*) and *STS* (*V. vinifera*)	M9 medium 2.46 g l^{-1} *p*-coumaric acid	2.3 g l^{-1}	(Lim *et al.*, 2011)
E. coli JM109	*TAL* (*R. glutinis*), *4CL* (*P. crispum*), *STS* (*V. vinifera*), *matB* (*Rhizobium. trifolii*) and *matC* (*Rhizobium. trifolii*)	MOPS medium 543.57 mg l^{-1} tyrosine	35.02 mg l^{-1}	(Wu *et al.*, 2013)

CHAPTER 2 Application of synthetic biology for production of chemicals in yeast *Saccharomyces cerevisiae.*

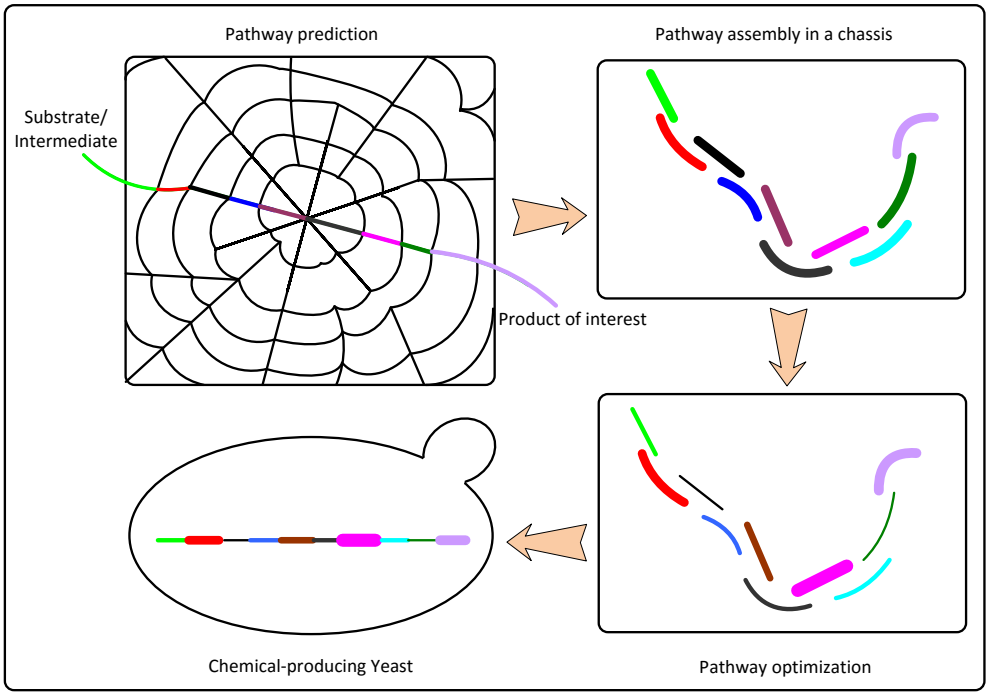

Synthetic biology and metabolic engineering enable generation of novel cell factories that efficiently convert renewable feedstocks into biofuels, bulk and fine chemicals, thus creating the basis for biosustainable economy independent on fossil resources. This review describes synthetic biology applications for design, assembly and optimization of non-native biochemical pathways in yeast *S. cerevisiae.*

FEMS Yeast Research, 15, 2015, 1–12

doi: 10.1111/1567-1364.12213
Minireview

MINIREVIEW

Application of synthetic biology for production of chemicals in yeast *Saccharomyces cerevisiae*

Mingji Li and Irina Borodina*

The Novo Nordisk Foundation Center for Biosustainability, Technical University of Denmark, Hørsholm, Denmark

*Corresponding author. Irina Borodina, The Novo Nordisk Foundation Center for Biosustainability, Technical University of Denmark, Kogle allé 6, 2970 Hørsholm, Denmark, Tel.: +45 4525 8020; Fax: +45 4525 8001; E-mail: irbo@biosustain.dtu.dk
Editor. Hal Alper

ABSTRACT

Synthetic biology and metabolic engineering enable generation of novel cell factories that efficiently convert renewable feedstocks into biofuels, bulk, and fine chemicals, thus creating the basis for biosustainable economy independent on fossil resources. While over a hundred proof-of-concept chemicals have been made in yeast, only a very small fraction of those has reached commercial-scale production so far. The limiting factor is the high research cost associated with the development of a robust cell factory that can produce the desired chemical at high titer, rate, and yield. Synthetic biology has the potential to bring down this cost by improving our ability to predictably engineer biological systems. This review highlights synthetic biology applications for design, assembly, and optimization of non-native biochemical pathways in baker's yeast *Saccharomyces cerevisiae*. We describe computational tools for the prediction of biochemical pathways, molecular biology methods for assembly of DNA parts into pathways, and for introducing the pathways into the host, and finally approaches for optimizing performance of the introduced pathways.

Key words: synthetic biology; yeast; chemicals; *S. cerevisiae*; metabolic engineering

INTRODUCTION

Biological production of chemicals from CO_2, biomass, waste streams, and other renewable feedstocks using cell factories presents an alternative to chemical synthesis from fossil resources. The advantages are reduced (or even negative) carbon dioxide emissions, independence on oil and gas supply, and possibility to make novel products or products that are not readily available from native sources. In some cases, reduced costs can be obtained as well.

Over the past 20 years, chemicals for different applications have been produced in metabolically engineered yeast, ranging from fuels to bulk chemicals to pharmaceutical and nutraceutical ingredients (Fig. 1). Since the production of the first non-native chemicals in yeast, such as lactic acid (Dequin and Barre 1994) or xylitol (Hallborn *et al.*, 1991), which required a single heterologous enzyme each, the advances in synthetic biology have now enabled assembly of multienzyme pathways for production of amorphadiene (Westfall *et al.*, 2012), indolylglucosinolate (Mikkelsen *et al.*, 2012), plant alkaloid (Fossati *et al.*, 2014), and other compounds. Moreover, the pathways are no longer limited to the naturally occurring pathways in other organisms, but can also be synthetic *de novo* pathways composed of natural or engineered enzymes that do not occur together in nature (Yim *et al.*, 2011; Borodina *et al.*, 2013).

The road from proof-of-concept compound production to the market is, however, still very resource intensive (Van Dien 2013), hampering the introduction of new commercial fermentation-based processes. The hurdle is engineering of the suitable cell factory that can produce the product at high titer, rate, and yield in large-scale fermentation setup. In the early 1990s, metabolic engineering emerged as a research field, dealing with directed improvement of cell factories. The flux quantification and metabolic network analysis methods developed in this field have been instrumental in creating novel cell

Received: 13 May 2014; **Accepted:** 15 September 2014

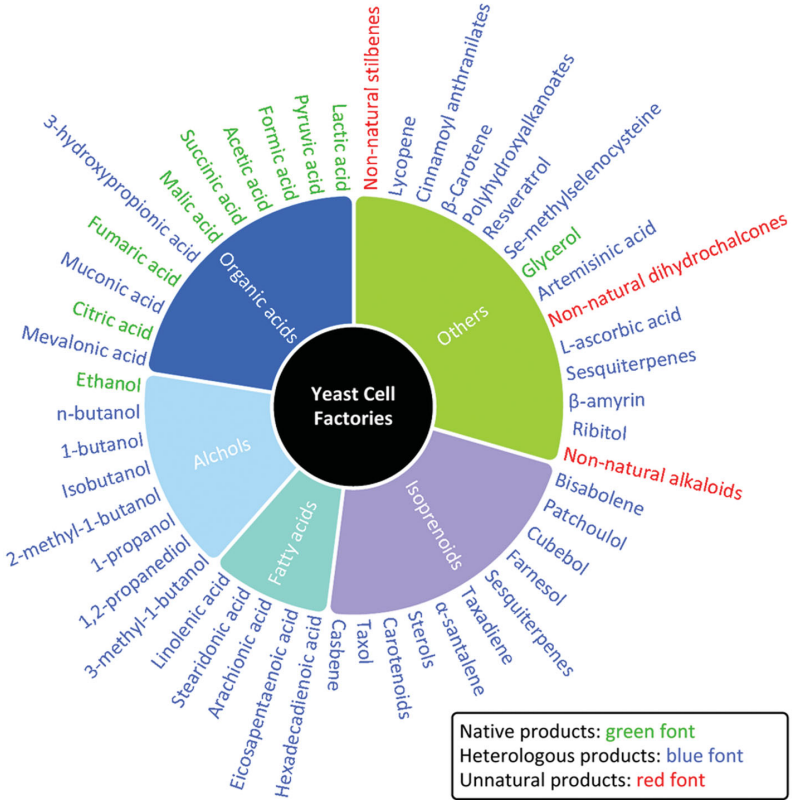

Figure 1. Examples of native, heterologous, and unnatural chemicals that have been produced in yeast.

factories for industrial biotechnology. In contrast to metabolic engineering, which has a well-defined practical objective, the synthetic biology has a more fundamental scientific focus. It is broadly defined as 'the design and construction of new biological systems (e.g. genetic control systems, metabolic pathways, chromosomes, cells) that do not exist in nature through the assembly of well-characterized, standardized, reusable components' (Nielsen *et al.*, 2014). The applications of synthetic biology, as excellently demonstrated in International Genetically Engineered Machine (iGEM) student competitions, are very diverse, spanning from medicine to environment to food, etc. For the industrial biotechnology applications, the two disciplines are very synergistic, where metabolic engineering defines the direction, in which the biochemical networks need to be manipulated, and the synthetic biology provides the tools to accomplish this task. Synthetic biology is expected to improve the design of the cell factories by generating well-characterized chassis (platform strains) and biological parts (BioBricks), which can be rapidly assembled into an organism with the desired properties, for example, producing a specific chemical at high titer, rate, and yield. BioBricks are typically DNA fragments, encoding enzymes, localization signals, transcription, and translation control elements, etc. Platform strains can be plug-and-play strains suitable for industrial fermentation and amenable for genetic manipulation; they can be tailor-made for resistance to inhibitors, for increased supply of a specific precursor or co-factor, for tolerance to specific fermentation conditions (e.g. low pH), or possess other required features. In this review, we will focus on baker's yeast *S. cerevisiae*, which is an attractive host cell for biorefinery applications for several reasons: The strain is robust in large-scale fermentations, it can grow on cheap media, consisting only of carbon source, salts, and vitamins, the residual cell mass can be used for animal feed in some countries in cases when the chemical product is non-toxic, fermentation can be carried out at low pH, which reduces the risk of bacterial contamination and gives less waste in production of organic acids, and genetic manipulation tools are well established. The main disadvantage of *S. cerevisiae* is its inability to utilize alternative carbon sources abundant in the biomass hydrolyzates, such as xylose and arabinose; however, this feature can be genetically engineered. A number of *S. cerevisiae* strains have been already developed for commercial production of non-native chemicals by fermentation, such as artemisic acid (Paddon and Keasling 2014), isobutanol (Urano *et al.*, 2012), and resveratrol (Katz *et al.*, 2012).

The challenges associated with cell factory development are (1) discovery or synthesis of a biochemical pathway toward the desired chemical, (2) efficient and rapid assembly of this pathway in the host, (3) optimization of enzymatic activity and expression levels of individual enzymes in the pathway, and (4) optimization of the host cell for efficient supply of precursors, co-factors, and energy for the process. Here, we review application of synthetic biology for the production of chemicals in yeast from three aspects: computational pathway design, pathway assembly, and pathway optimization. We will not touch upon the host cell optimization, which is the traditional realm of the metabolic engineering discipline. The interested reader

can be referred to the recent reviews on the subject (Chen and Nielsen 2013; Tippmann *et al.*, 2013; Van Dien 2013; Borodina and Nielsen 2014).

COMPUTATIONAL TOOLS FOR PATHWAY DESIGN

The first step in designing a cell factory for the production of a specific chemical is defining the biochemical reactions that can generate the desired compound from the typical intermediates of the native cellular metabolism. For the natural products, the known pathway can be simply moved from the original organism to the host, although it will not necessarily be an optimal solution. However, most of the biosynthetic pathways leading toward the known 226 000 natural products listed in the dictionary of natural products have not been fully characterized so far (Seyedsayamdost and Clardy 2014). Besides, there are no inherent metabolic pathways for many chemicals, which are currently derived chemically and do not otherwise occur in nature. An example is 1,4-butanediol, for which a *de novo* synthesis route was reconstructed (Yim *et al.*, 2011). Therefore, for pathway design, computational tools can be very helpful, as they provide a comprehensive set of possible biochemical routes and can also evaluate feasibility of various pathways based on thermodynamic and other considerations. In this section, we review some computation tools that can be helpful in the design of biochemical pathways (Table 1).

The most traditional pathway prediction algorithms are based on mining of the known enzymatic reactions and pathways (reference-based frameworks). Reference-based frameworks are inherently limited to the known enzymatic reactions. An algorithm 'From Metabolite to Meta-bolite' (FMM) predicts possible pathways between two chosen metabolites based on the reactions in KEGG database (Chou *et al.*, 2009). Chatsurachai *et al.* searched BRENDA and KEGG databases for heterologous reactions that can connect non-native metabolites to the genome-scale metabolic networks of several industrially important hosts (Chatsurachai *et al.*, 2012). They found that fewer than 33 heterologous reactions are needed to link 3154 non-native metabolites to the metabolic network of *Saccharomyces cerevisiae* and that 67% of these non-native metabolites, including 1,3-propanediol, isoprene, α-farnesene, and poly-β-hydroxybutyrate, can be generated from glucose as the sole carbon source according to the flux balance analysis. An online tool Metabolic Tinker helps to identify thermodynamically feasible routes between two chosen metabolites using a heuristic search in reaction networks generated from CHEBI and RHEA databases (McClymont and Soyer 2013). Metabolic Tinker was used to predict feasible routes from acetoacetyl-CoA to isopentenyl diphosphate, a precursor of isoprenoid compounds. In addition to the native mevalonate route, the algorithm identified an additional thermodynamically favorable pathway via S-adenosyl-L-homocysteine, which, however, has not been experimentally tested. Considering that thermodynamics also has an influence on the reaction kinetics via the flux–force relationship, a quantitative methodology eQuilibrator was proposed to analyze pathways thermodynamic profiles and to find the limiting steps (Noor *et al.*, 2014). Taking into account physiological properties, including pH, ionic strength, metabolite concentration ranges, and cofactor concentration, the authors applied their framework to the central metabolic pathways and found that malate dehydrogenase activity and substrate-level phosphorylation constrain the tricarboxylic acid cycle and Embden–Meyerhof–Parnas fluxes, respectively.

Other algorithms allow *de novo* pathway reconstruction by hypothesizing intermediate metabolites or enzymes that can connect the source and target metabolites. Biochemical Network Integrated Computational Explorer (BNICE) is a tool developed for identifying novel metabolites and reactions on the basis of generalized reaction rules of the Enzyme Commission classification system (Hatzimanikatis *et al.*, 2005). BNICE also evaluates thermodynamic feasibility of the predicted pathways. By recruiting this algorithm, a novel pathway for biodegradation of 1,2,4-trichlorobenzene (Finley *et al.*, 2010), nine novel biosynthetic pathways from pyruvate to 1-butanol (Wu *et al.*, 2011), and three novel biosynthesis pathways to 3-hydroxypropanoate (Henry *et al.*, 2010) were predicted, all of them, however, remain to be experimentally verified. Another algorithm, Reverse Pathway Engineering (RPE), combines chemoinformatics with bioinformatics analysis; it was used to predict the pathways for formation of flavor compound from leucine in lactic acid bacteria (Liu *et al.*, 2014). Based on functional groups transfer, Genomatica's proprietary SimPheny Biopathway Predictor algorithm was successfully used to identify multiple pathways toward 1,4-butanediol from inherent metabolic intermediates in *E. coli* without being restricted by the known enzymes (Yim *et al.*, 2011). Another method uses molecular signatures, which encode the changes in atom bonding environments, where the reaction is taking place. The method identifies the candidate pathways and ranks them according to thermodynamic feasibility, host compatibility, compounds toxicity, and overall nominal flux based on genome-scale modeling (Carbonell *et al.*, 2011, 2014). The method was validated by predicting the pathway toward taxol production in yeast. Jean-Loup Faulon's research group also proposed an automatic pipeline Retropath for the design of synthetic metabolic circuits (Carbonell *et al.*, 2013).

While pathway prediction algorithms can suggest an unnatural enzyme that should catalyze a specific reaction, developing such an enzyme may be quite an endeavor. Structure-based enzyme design is so far at an early development stage (Laskowski *et al.*, 2005; Lopez *et al.*, 2007; Verma *et al.*, 2012), so while specificity for reducing co-factors can be altered with a rather high success rate, it is much more difficult to modulate substrate specificity and allosteric regulation, and it is particularly difficult to create a specific new enzymatic function (Röthlisberger *et al.*, 2008). Nevertheless, pathway prediction algorithms are valuable tools for a synthetic biologist as they facilitate design of unusual nonintuitive *de novo* biosynthetic pathways as well as help to prioritize strain construction efforts by ranking the possible pathways.

PATHWAY ASSEMBLY

Parts

Biosynthesis of non-native chemicals often requires multiple-step pathways containing enzyme-coding genes and control elements, such as promoters, terminators, sensors, and other parts (BioBricks). In the future, the whole DNA constructs will likely be made synthetically from scratch; however, so far, the price of DNA synthesis is still prohibitory to make large constructs on a routine basis, and hence, it is more conventional to synthesize or PCR-amplify smaller BioBricks (<10 kb) and assemble them into an operational pathway. Usage of codon-shuffled synthetic BioBricks may help to erase native cryptic regulatory elements, such as alternative translation initiation sites,

Table 1. Computational tools for prediction of biochemical pathways.

Software	Software availability	Description	References
FFM	Web interface at http://fmm.mbc.nctu.edu.tw/index.php	From Metabolite to Metabolite (FMM) reconstructs pathways between start and end metabolites based on KEGG information. Nice visualization and integration with information from other databases (UniProt, GenBank and dbPTM databases)	Chou *et al.* (2009)
Chatsurachai *et al.*	Python script available at http://www-shimizu.ist.osaka-u.ac.jp/pathway˙search.zip	The algorithm searches BRENDA and KEGG databases to identify heterologous reactions that connect non-native metabolites to the metabolic network of the host	Chatsurachai *et al.* (2012)
Metabolic Tinker	Web interface at http://osslab.lifesci.warwick.ac.uk/Tinker˙Download.aspx. Source code in Java can be downloaded and run on a personal computer or adapted	Metabolic Tinker predicts thermodynamically feasible routes between source and target compounds using reaction databases CHEBI and RHEA.	McClymont and Soyer (2013)
eQuilibrator	Web interface at http://equilibrator.weizmann.ac.il/	eQuilibrator estimates thermodynamic parameters for an enzymatic reaction under the defined conditions (pH, ionic strength, reactant, and product concentrations)	Noor *et al.* (2014)
BNICE	N/A	Biochemical Network Integrated Computational Explorer (BNICE) is a framework for identification and thermodynamic assessment of possible pathways for the degradation or production of a given compound	Hatzimanikatis *et al.* (2005)
Reverse Pathway Engineering (RPE)	N/A	The algorithm predicts the 'missing links' between compounds of interest and their possible metabolic precursors by combining chemoinformatics and bioinformatics.	Liu *et al.* (2014)
Retropath	Webserver, accessible for registered users at http://www.issb.genopole.fr/˜faulon/retropath.php	The algorithm uses molecular signatures to predict and rank possible biochemical pathways. Predicts compatibility with host genes and toxicity prediction	Carbonell *et al.* (2013)

transcription factor binding sites, and others. Standardization of the DNA parts will greatly facilitate the construction process. Currently, the modular approach for pathway assembly is hampered by the lack of well-characterized control elements as promoters and 5′UTRs, which behave predictably in the given strains and under given conditions (Mutalik *et al.*, 2013). A number of parts repositories have been established, such as iGEM Registry of Standard Biological Parts (http://parts.igem.org), the 'Standard European Vector Architecture' (SEVA) database (Silva-Rocha *et al.*, 2013), AddGene (www.addgene.org), and others. All the above-mentioned repositories have physical collections of parts, which can be

obtained under licenses or material transfer agreements. Considering the legal issues and restrictions of use associated with materials transfer, it is often more expedient and convenient to synthesize the constructs, particularly in cases where their commercial application is envisaged. To promote the sharing of BioBricks, establishment of an open-source policy would be advantageous. Moreover, there is a need for a central database for the collection of information on characterization and performance of BioBricks, which will require a major community effort (Way *et al.*, 2014). To match the requirements of the complex designs and the high-throughput cloning by automation, the *in silico* constructs design and sequence analysis of the resulting constructs need to be automated as well. A freely available Web-based software J5 was developed in Keasling's laboratory (Hillson *et al.*, 2012; http://j5.jbei.org). The program facilitates cloning designs for DNA BioBricks assembly and supports several cloning methods. Other free software tools include RAVEN (Appleton *et al.*, 2014; http://www.ravencad.org), GENOCAD (Cai *et al.*, 2010; http://www.genocad.org), TINKERCELL (Chandran *et al.*, 2009; http://www.tinkercell.com), and others. Synthetic Biology Open Language (SBOL) was proposed as an open-source community standard, which can be used for electronic exchange of designs, also across the different software environments (http://www.sbolstandard.org/). Computer-aided design saves researchers' time and reduces human errors.

DNA ASSEMBLY

In spite of the lack of the standardized BioBricks, there is no deficiency in BioBricks assembly methods. An immense variety of synthetic biology tools have been developed over the past years, improving flexibility, speed, and precision of cloning. The classical restriction-ligation-based cloning has been largely replaced with restriction-free *in vitro* techniques, such as Gibson isothermal assembly, in-fusion, uracil-specific excision reaction (USER) cloning, circular polymerase extension cloning (CPEC), ligase cycling reaction (LCR), modular cloning system (MoClo), *in vivo* homologous recombination (also known as gap repair), and other techniques (Fig. 2). While all the methods listed above allow

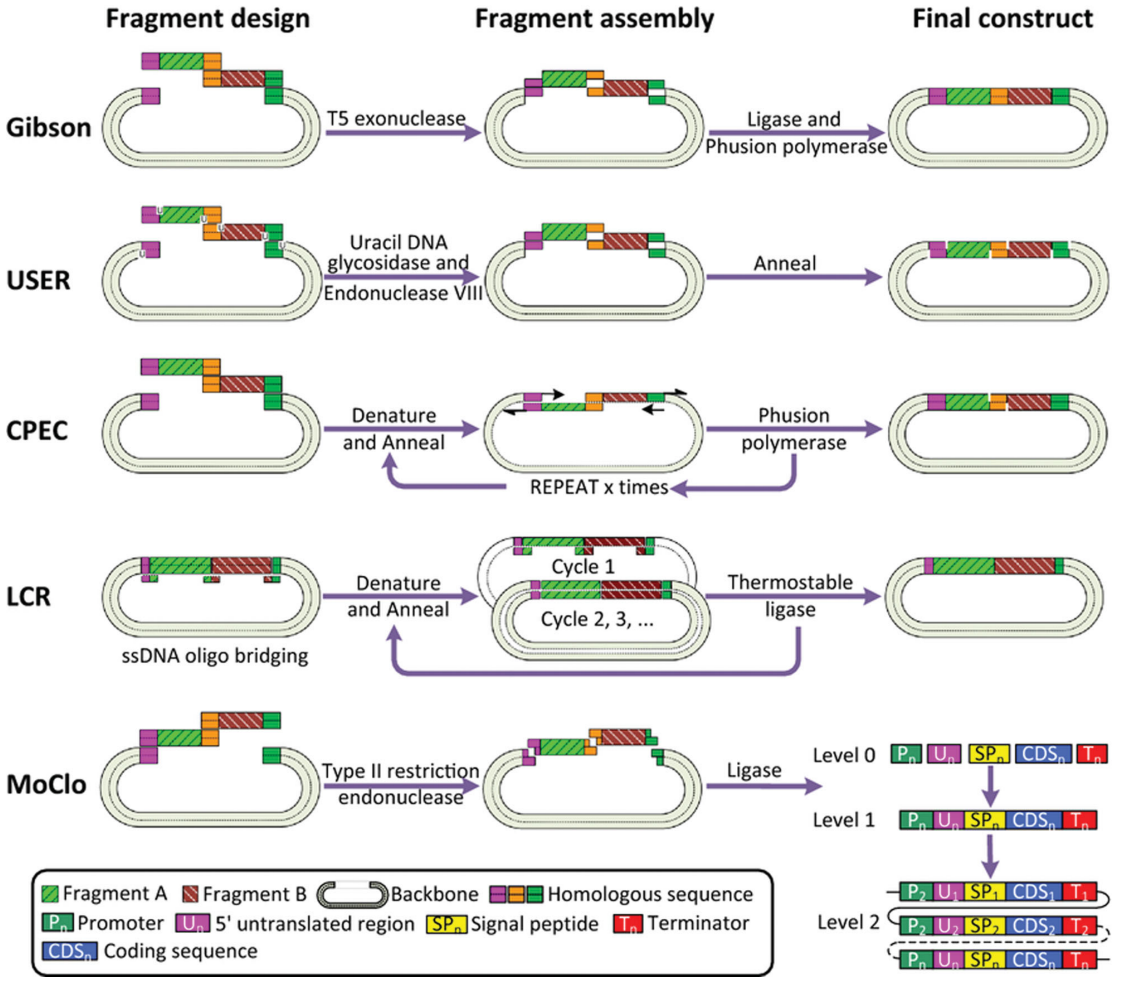

Figure 2. Examples of DNA assembly methods. DNA parts can be assembled using a variety of techniques, which require different designs of the overhangs on DNA parts and different enzymes and procedures for assembly.

Table 2. Technical specifications of several DNA assembly methods.

Assembly methods	Fragment overhangs	Typical number of fragments for assembly	Demonstrated size of assembled construct (kb)	Efficiency	References
Gibson	40 bp overlaps	c. 4	900	90% (for 3 fragments)	Gibson *et al.* (2009)
In-fusion	>15 bp overlaps	2–3	c. 5	>60% (for 2 fragments) <40% (for 3 fragments)	Sleight *et al.* (2010)
USER	7–12 bp overlaps, must contain one dU at the base	3–7	c. 8	>90% (for up to 7 fragments)	Jensen *et al.* (2014) *Lund et al.* (2014)
CPEC	15–25 bp overlaps	>4	c. 8	95–100%	Quan and Tian (2009)
MoClo	4 bp overlaps and recognition site for type IIS restriction enzyme	c. 10	33 (in three rounds)	>90%	Engler *et al.* (2009) *Weber et al.* (2011)
LCR	Fragments must be 5′-phosphorylated, 60- to 90-bp-long bridging oligos are also needed	>10	20	>90% (up to 6 fragments) c. 75% (12 fragments)	de Kok *et al.* (2014)
In vivo recombination in *S. cerevisiae*	>40 bp overlaps	>10	>20	>90% (up to 6 fragments) c. 75% (12 fragments)	de Kok *et al.* (2014)

directional seamless cloning of the DNA fragments, they differ in the number of fragments and size of construct that can be assembled with high fidelity (Table 2); moreover, the methods require different design of DNA parts. If a research laboratory strives for standardization and reuse of parts within and across multiple research projects, then adhering to one specific DNA assembly method saves more money and effort. Here, we will briefly describe the specifics of the most common methods.

Gibson method allows the assembly of 3–4 fragments with 90% efficiency via c. 40-bp-long overlapping sequences (Gibson *et al.*, 2009). The reaction is carried out at 50 °C for 15 min and requires a mix of three enzymes: T5 exonuclease to create single-stranded 3′-overhangs that facilitate the annealing of complementary fragment ends, Phusion DNA polymerase to fill in the gaps within the annealed fragments, and finally Taq DNA ligase to seal the nicks. Using proof-reading DNA polymerase minimizes the risk of errors introduced during assembly. All the enzymes are commercially available; a ready-to-use mix is distributed by New England Biolabs. The method was used to synthesize the first complete artificial bacterial genome, namely synthetic 583-kb genome of *M. genitalium* (Gibson *et al.*, 2010). Gibson method is particularly well suited for assembly of large constructs; however, its performance decreases for larger number of fragments, that is, the efficiency for six fragments was about 25% (de Kok *et al.*, 2014).

In-fusion method uses a proprietary exonuclease from Clontech. The assembly efficiencies for three fragments using 15 bp overlaps were below 40% in the study by Sleight *et al.* (2010).

Uracil-specific excision reaction (USER) allows assembly of multiple DNA fragments via short overhangs of 7–12 nucleotides (Nour-Eldin *et al.*, 2006). Each overhang must contain one deoxyuridine (dU) nucleotide instead of deoxythymidine (dT) nucleotide. The DNA is treated by uracil DNA glycosidase and DNA glycosylase-lyase endo VIII (the mix of the two enzymes is commercially available as USER™ from New England Biolabs). This process releases the sequence upstream from the dU's and thus generates sticky ends, which mediate correct annealing of the fragments. The one-tube assembly reaction takes about an hour. Due to the overhang size of 7–12 bp, the assembled DNA vectors can be directly transformed into competent *E. coli* cells without prior ligation. The DNA fragments for USER assembly are typically generated by PCR amplification with dU-containing primers using a high-fidelity DNA polymerase that is tolerant to dU-containing primers, for example, PhuX7 (Nørholm 2010). USER assembly is convenient for assembly of 2–7 DNA fragments, where efficiency can be as high as 90% (Lund *et al.*, 2014).

Circular polymerase extension cloning (CPEC) uses repeated cycles of denaturation–annealing–extension by DNA polymerase to fuse multiple fragments (Quan and Tian 2009). For fusing two fragments, one cycle is sufficient, taking <5 min, while for fusing multiple fragments 5–25 cycles may be needed depending on the number of fragments. The method has a high efficiency of 95% for up to four fragments assembly (Quan and Tian 2009). The efficiency, however, was below 50% for assembly of over four fragments (de Kok *et al.*, 2014). The advantage of this method is the low cost as it does not require other enzymes than DNA polymerase. The disadvantage of CPEC method is the risk of introducing mutations during the DNA extension.

Modular cloning system (MoClo) (Weber *et al.*, 2011), based on type IIS restriction endonuclease, allows assembly of multiple fragments in successive cloning steps. The underlying principle, also known as Golden Gate cloning, is based on the ability of type II restriction enzymes to cleave outside of their recognition sites; thus, the recognition sites themselves can be removed in the cleavage process, leaving small sticky ends of 4 bp. The single-tube reaction contains a type II restriction endonuclease and ligase; the reaction takes about 5–6 h. The cloning efficiency for up to 10 fragments was about 90% (Engler *et al.*, 2009). An advantage of Golden Gate cloning is that the DNA for assembly is provided as untreated plasmids rather than DNA fragments

generated by PCR or other means. These both simplifies the procedure and reduces the risk of errors due to DNA manipulation. Another advantage of the method is that due to the high efficiency of the assembly, it can be used to generate large shuffled libraries of constructs, when multiple DNA templates are added to the mix. Finally, by alternating the type IIS enzyme and selectable markers, multiple hierarchical assembly rounds can be carried out to assemble basic modules (level 0) into transcription units (level 1) and further into multigene constructs (level 2) and so on. The assembly of a 33-kb-long multigene construct in three successive cloning steps has been demonstrated (Weber *et al.*, 2011).

Ligase cycling reaction (LCR) enables scarless assembly of multiple fragments by employing single-stranded bridging oligos (de Kok *et al.*, 2014). The reaction uses repeated cycles of denaturation, annealing, and ligation with thermostable ligase. The single-stranded DNA bridging oligos guide the correct annealing of fragments. The DNA fragments must be 5′-phosphorylated, which adds some extra cost on their generation either by PCR amplification with 5′-phosphorylated primers or by enzymatic treatment. The total one-tube LCR assembly procedure takes about 1 h. The optimized method was demonstrated to efficiently connect up to 20 DNA parts into 20-kb-long constructs with 60–100% precision. The LCR could connect 12 fragments of the mevalonate pathway with over 75% clones being correct. The authors benchmarked LCR method with Gibson, CPEC, and *in vivo* assembly in yeast, where Gibson and CPEC had <50% correct clones for assembly of over four fragments, while efficiency of *in vivo* assembly was comparable to LCR.

DNA fragments can be directly recombined *in vivo* in *S. cerevisiae* thanks to its efficient DNA repair machinery. Recombination requires overlaps of more than 30–40 bp, where the precision of assembly increases with the size of the overlapping sequences. The resulting DNA constructs can either replicate in yeast cells as independent elements (episomal plasmids or yeast artificial chromosomes) or can be inserted into the genome. The replicating plasmids can be shuffled into *E. coli*, where they can be propagated for sequencing and then transformed into a producing yeast strain. The efficiency of assembly by *in vivo* recombination is similar to LCR (de Kok *et al.*, 2014). Some examples on using *in vivo* recombination for direct engineering of *S. cerevisiae* strains are given in the section below.

DNA INTRODUCTION INTO HOST

A wide variety of vectors have been developed for the introduction of recombinant DNA into *S. cerevisiae* (Krivoruchko *et al.*, 2011). Here, we will just briefly mention the most recent developments and give a few application examples. The episomally replicating vectors suffer from lower stability than chromosomally integrated constructs; they were also shown to have heterogeneous expression within population (Jensen *et al.*, 2014); therefore, methods for chromosomal integration have received much attention recently. Thanks to the efficient homologous recombination machinery of *S. cerevisiae*, the DNA constructs can be efficiently targeted to specific chromosomal regions via homologous sequences of 60–500 bp length. The target regions can be (1) functional elements, such as open reading frames targeted for deletion, promoters targeted for exchange or others, (2) unique well-characterized chromosomal regions resulting in consistent expression levels of the introduced DNA, and (3) multiple elements scattered through the genome, such as rDNA, transposon repeats, and δ-sites, resulting in multiple integration events. The efficiency of integration by homologous recombination can be enhanced by introducing a double-strand break on the target region of the chromosome using highly specific endonucleases, for example, mitochondrial homing endonuclease I-SceI (Kuijpers *et al.*, 2013a), or using CRISPR-Cas9 system (DiCarlo *et al.*, 2013) (Fig. 3).

A set of integrative vectors has been developed for stable high-level expression of introduced genes in *S. cerevisiae* and was applied for reconstructing a seven-step pathway toward an indolylglucosinolate, an anticancer compound from crucifix plants (Mikkelsen *et al.*, 2012). Further development of the vectors resulted in EasyClone vector set, which allows simultaneous stable integration of multiple genes into the genome of *S. cerevisiae*, with the option of marker recycling, thus facilitating the iterative strain construction cycles (Jensen *et al.*, 2014). EasyClone was successfully used to introduce a synthetic *de novo* pathway for the biosynthesis of 3-hydroxypropionic acid in *S. cerevisiae* via β-alanine intermediate (Borodina *et al.*, submitted). *In vivo* recombination, where DNA was introduced into multiple δ-sites in the genome, was used for the reconstruction of pathways for xylose assimilation and for the biosynthesis of zeaxanthin and aureothin with the assembly efficiency of 10–70% (Shao *et al.*, 2009; Shao and Zhao 2013). Jack Pronk's group

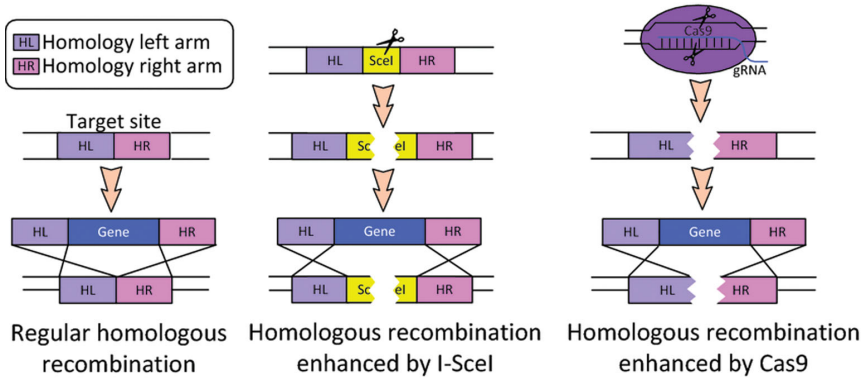

Figure 3. Methods for enhancing DNA integration via homologous recombination in *Saccharomyces cerevisiae*. A double-stranded linear DNA fragment is integrated into *S. cerevisiae* genome via sequences homologous to the target site (left); integration efficiency is improved due to the double-strand break at the target site, generated by I-SceI endonuclease (middle) or CRISPR-Cas9 system (right).

used 60-bp synthetic overhangs to assemble the glycolytic pathway in *S. cerevisiae* (Kuijpers *et al.*, 2013b). Introduction of double-strand break in the yeast chromosome using meganuclease I-SceI improved the efficiency of integration of the construct into the chromosome from 5% to 95% (Kuijpers *et al.*, 2013a). Reiterative recombination method is based on repeated yeast transformations, where a construct is introduced into a specific place on the chromosome along with a marker in the first transformation round, and in the next transformation round, the marker is replaced with a new construct carrying another marker, and so on (Wingler and Cornish 2011). The integration is facilitated by digestion with SceI endonuclease. The authors demonstrated the utility of the method by reconstructing a 3-step lycopene pathway.

PATHWAY OPTIMIZATION

A variety of methods can be used to boost the flux through the engineered pathway (Fig. 4). Balancing expression of the individual enzyme-coding genes may reduce accumulation of intermediates, which can inhibit certain enzymes or exhibit cellular toxicity. It also allows reducing the metabolic load on the host. Other methods bring enzymes in close proximity, to obtain a metabolic channeling effect, where the product of one reaction is directly passed over to the next enzyme to serve as a substrate for the next reaction. Protein engineering is important as well to modulate co-factor or substrate specificity, remove allosteric inhibition effects, increase thermostability, and improve other properties.

More effort has been put into pathway optimization for utilization of D-xylose, the second most abundant renewable sugar in nature, which is, however, not naturally utilized by many yeast *spp*. Kim *et al.* (2013) generated a library of about 8000 variants with different promoter combinations upstream the xylose-pathway genes; the strains showed a wide range of performance, where, for example, xylitol yield varied from 0.01 to 0.22 g g^{-1} xylose. Moreover, different promoter combinations were optimal for the growth of different strains on various substrates. Customized optimization of metabolic pathways by combinatorial transcriptional engineering (COMPACTER) was

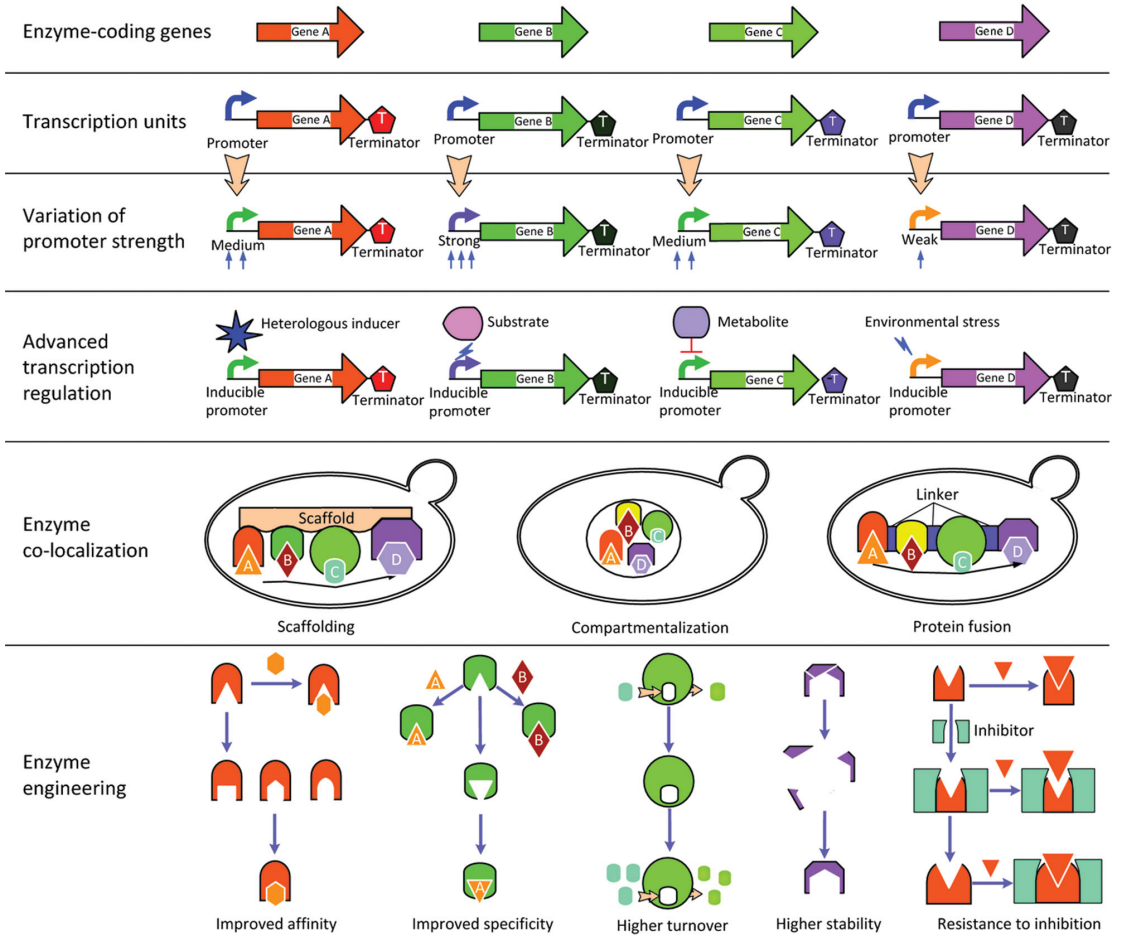

Figure 4. Approaches for optimization of synthetic pathways. A number of variants of enzyme-coding genes are assembled into transcriptional units and pathways and introduced into the host. The expression levels of individual genes can be balanced using constitutive promoters of different strengths or regulated promoters. Enzymes can be brought into proximity by fusion, scaffolding, or expression in specific cellular compartments. Enzyme properties can be improved by protein engineering.

proposed by Du *et al.* (2012) for rapid optimization of heterologous pathways in different genetic backgrounds. As a demonstration, three native constitutive promoters were subjected to nucleotide analog mutagenesis to obtain promoter mutants of varying strengths. The xylose utilization genes were placed under control of these promoters in various combinations, and the resulting strains were assessed for growth on xylose. The optimized xylose utilizing pathways displayed a high xylose consumption rate of 0.4 and 0.92 g L^{-1} h^{-1} in laboratory and industrial yeast strains, respectively. The same approach was applied for a cellobiose utilizing pathway, resulting in cellobiose consumption rates of 1.54 and 2.18 g L^{-1} h^{-1} in laboratory and industrial strains, respectively (Du *et al.*, 2012).

For the multienzyme pathways, it can be an advantage to bring enzymes in proximity either by compartmentalization, fusion or scaffolding. This would prevent the losses in the transportation due to diffusion, degradation, competing pathways, avert toxicity caused by intermediates, and increase turnover rates due to the higher local substrate concentrations (Zhang 2011). Several examples on expressing chemical-producing pathways in specific cellular compartments have been published. Isobutanol production in yeast was improved 2.6-fold by overexpressing the pathway in mitochondria instead of cytosol (Avalos *et al.*, 2013). Similarly, production of valencene and amorphadiene were improved 8- and 20-fold, respectively, when heterologous FDP synthase and sesquiterpene synthase were targeted to mitochondrion (Farhi *et al.*, 2011).

Zhang *et al.* constructed a fusion protein of 4-coumarate-CoA ligase (4CL) and stilbene synthase (STS). A 14-fold resveratrol improvement was observed for the fusion protein 4CL::STS over co-expression of 4CL and STS in *S. cerevisiae* (Zhang *et al.*, 2006). Different fusions of farnesyl diphosphate synthase of yeast and patchoulol synthase from *Pogostemon cablin* were studied in *S. cerevisiae*, which resulted in twofold increase of patchoulol production (Albertsen *et al.*, 2011). Another example of improving chemicals production via fusion strategy is the coupling of farnesyl diphosphate synthase with amorphadiene synthase of *Artemisia annua*, which improved amorphadiene production fourfold over the control (Baadhe *et al.*, 2013).

Scaffolding of enzymes on proteins or RNA structures is another way of enhancing substrate channeling. Dueber *et al.* constructed scaffolds of three protein–protein interaction domains (mouse SH3 and PDZ domains and rat GBD) to optimize the mevalonate biosynthetic pathway in *E. coli*. Three pathway genes were fused to interaction ligands on their C-terminal via flexible nine-residue glycine–serine linkers. Different versions of scaffolds carrying varying ratios of the interaction domains were tested, and the optimal scaffold resulted in 77-fold increase of mevalonate titer in comparison with the nonscaffolded pathway (Dueber *et al.*, 2009). Scaffolding strategy was also adopted in resveratrol production in *S. cerevisiae*, resulting in a 5.0-fold increase over the nonscaffolded control and a 2.7-fold higher production than that of the fusion strategy (Wang and Yu 2012). There have been so far no examples of scaffolding on RNA structures in yeast. In bacteria, a 2-dimensional RNA scaffold was shown to increase hydrogen production by up to 48-fold (Delebecque *et al.*, 2011).

The functional properties of the native enzymes may be improved via protein engineering. The most successful approaches for protein engineering combine computational methods with directed evolution. Computational tools guide the design of the mutant library for the subsequent screening, thus improving the success rate of the directed evolution. The interested reader is referred to a comprehensive review on computer-aided protein-directed evolution (Verma *et al.*, 2012). In the context of yeast engineering for production of chemicals, protein engineering has been used to improve stability of the proteins, change co-factor specificity, remove feedback inhibition, and improve catalytic activity. A truncated form of malate dehydrogenase, which is less susceptible to glucose-induced proteolysis (Minard and McAlister-Henn 1992), was applied for malic acid production (Winkler *et al.*, 2007). The co-factor specificity of xylose reductase has been modulated to avoid redox imbalance under xylose assimilation via xylose reductase–xylitol dehydrogenase pathway. Liang *et al.* used an iterative active site-saturation mutagenesis strategy in *S. cerevisiae* to obtain xylose reductase from *Pichia stipitis* with increased affinity toward NADH instead of NADPH (Liang *et al.*, 2007). Similarly, an error-prone PCR strategy was adopted to mutate the co-factor binding site of xylose reductase, which resulted in 10-fold hig-her V_{max} and increased ethanol titer 40-fold (Runquist *et al.*, 2010). For xylose assimilation via xylose isomerase route, the low activity of heterologous xylose isomerase is a common problem. The strains evolved by adaptation on xylose medium were shown to accumulate up to 32 copies of xylose isomerase gene presumably to compensate for the low activity of the enzyme (Zhou *et al.*, 2012). By applying three rounds of xylose isomerase mutagenesis, followed by selection for growth on xylose, the enzymatic activity of xylose isomerase was improved by 77% and aerobic growth on xylose increased 61-fold (Lee *et al.*, 2012). Removal of feedback inhibition effects in the aromatic amino acids biosynthesis pathway enabled the production of the flavonoid intermediate naringenin in *S. cerevisiae* (Koopman *et al.*, 2012).

Enzyme engineering techniques are thus likely to significantly advance synthetic biology and metabolic engineering of cell factories.

PERSPECTIVES

According to the report of NEST High-Level Expert Group, synthetic biology will enable design of biological systems in a rational and systematic way (Serrano *et al.*, 2005). Established about 15 years ago (Way *et al.*, 2014), synthetic biology has already delivered some impressive results, but also revealed serious obstacles that need to be overcome should it live up to the high expectations. The complexity, variability, and epigenetics of biological systems undermine the predictability of the computer-aided cell designs; the biological parts have limited orthogonality, that is, their behavior varies significantly in different genetic backgrounds (Kwok 2010). Synthesis of novel non-natural enzymes and regulatory elements is hindered by our lack of understanding of protein structural–functional relationship. There are two main philosophies for approaching these complex problems. On the one hand, a minimalistic cell approach aims to reduce the biological complexity by designing minimal cells consisting of well-defined minimal sets of parts. One synthetic chromosome has already been reconstructed in the project on creating a designer *S. cerevisiae* cell Sc2.0, which will enable easier genome manipulation as, for example, genome scrambling (Annaluru *et al.*, 2014). On the other hand, the systems biology approach strives to understand the complexity and function of the existing biological systems (Barrett *et al.*, 2006).

The urgent need for novel bio-based processes provides the stimulus and test beds for the technology development. In the current cell factory development programs, an integrated approach, combining synthetic biology, metabolic engineering, and systems biology, is being implemented. The approach

is based on iterative design–build–test–analyze (DBTA) cycles, where multiple cell factory variants are built and screened in high-throughput fashion, after which the promising candidates are characterized in greater details using systems-level analysis and the generated knowledge is used for the computer-aided design of the next generation of the cell factories. As the knowledge is accumulated, the number of iterations needed to obtain the wanted design will decrease and this will result in drastic reduction of the cost of development of cell factories, providing new solutions for production of food, chemicals, and medicine.

ACKNOWLEDGEMENTS

This work was funded by the Novo Nordisk Foundation. The authors would like to thank Dr. Markus J. Herrgård and Prof. Jens Nielsen for discussions and comments on the manuscript. The authors declare no commercial or financial conflict of interest.

Conflict of interest statement. None declared.

REFERENCES

Albertsen L, Chen Y, Bach LS, Rattleff S, Maury J, Brix S, Nielsen J, Mortensen UH Diversion of flux toward sesquiterpene production in *Saccharomyces cerevisiae* by fusion of host and heterologous enzymes. *Appl Environ Microbiol* 2011;**77**: 1033–40.

Annaluru N, Muller H, Mitchell LA, *et al*. Total synthesis of a functional designer eukaryotic chromosome. *Science* 2014;**344**:55–8.

Appleton E, Tao J, Haddock T, Densmore D Interactive assembly algorithms for molecular cloning. *Nat Methods* 2014;**11**:657–62.

Avalos JL, Fink GR, Stephanopoulos G Compartmentalization of metabolic pathways in yeast mitochondria improves the production of branched-chain alcohols. *Nat Biotechnol* 2013;**31**:335–41.

Baadhe RR, Mekala NK, Parcha SR, Prameela Devi Y Combination of *ERG9* repression and enzyme fusion technology for improved production of amorphadiene in *Saccharomyces cerevisiae*. *J Anal Methods Chem* 2013;**2013**:140469.

Barrett CL, Kim TY, Kim HU, Palsson BØ, Lee SY Systems biology as a foundation for genome-scale synthetic biology. *Curr Opin Biotechnol* 2006;**17**:488–92.

Borodina I, Nielsen J Advances in metabolic engineering of yeast *Saccharomyces cerevisiae* for production of chemicals. *Biotechnol J* 2014;**9**:609–20.

Borodina I, Kildegaard KR, Öberg F, Förster J Genetically Engineered Yeast 2013 Patent Application WO 2014/057036.

Cai Y, Wilson ML, Peccoud J GenoCAD for iGEM: a grammatical approach to the design of standard-compliant constructs. *Nucleic Acids Res* 2010;**38**:2637–44.

Carbonell P, Planson A-G, Fichera D, Faulon J-L A retrosynthetic biology approach to metabolic pathway design for therapeutic production. *BMC Syst Biol* 2011;**5**:122.

Carbonell P, Parutto P, Baudier C, Junot C, Faulon J-L Retropath: automated pipeline for embedded metabolic circuits. *ACS Synth Biol* 2013;**3**:565–77.

Carbonell P, Parutto P, Herisson J, Pandit SB, Faulon J-L XTMS: pathway design in an eXTended metabolic space. *Nucleic Acids Res* 2014;**42**:W389–94.

Chandran D, Bergmann FT, Sauro HM TinkerCell: modular CAD tool for synthetic biology. *J Biol Eng* 2009;**3**:19.

Chatsurachai S, Furusawa C, Shimizu H An *in silico* platform for the design of heterologous pathways in nonnative metabolite production. *BMC Bioinformatics* 2012;**13**:93.

Chen Y, Nielsen J Advances in metabolic pathway and strain engineering paving the way for sustainable production of chemical building blocks. *Curr Opin Biotechnol* 2013;**24**: 965–72.

Chou CH, Chang WC, Chiu CM, Huang CC, Huang HD FMM: a web server for metabolic pathway reconstruction and comparative analysis. *Nucleic Acids Res* 2009;**37**: 129–34.

de Kok SD, Stanton LH, Slaby T, *et al*. Rapid and reliable DNA assembly via ligase cycling reaction. *ACS Synth Biol* 2014;**3**:97–106.

Delebecque CJ, Lindner AB, Silver PA, Aldaye FA Organization of intracellular reactions with rationally designed RNA assemblies. *Science* 2011;**333**:470–4.

Dequin S, Barre P Mixed lactic acid-alcoholic fermentation by *Saccharomyces cerevisiae* expressing the *Lactobacillus casei* L(+)-LDH. *Biotechnology (NY)* 1994;**12**:173–7.

DiCarlo JE, Norville JE, Mali P, Rios X, Aach J, Church GM Genome engineering in *Saccharomyces cerevisiae* using CRISPR-Cas systems. *Nucleic Acids Res* 2013;**41**:4336–43.

Du J, Yuan Y, Si T, Lian J, Zhao H Customized optimization of metabolic pathways by combinatorial transcriptional engineering. *Nucleic Acids Res* 2012;**40**:e142.

Dueber JE, Wu GC, Malmirchegini GR, Moon TS, Petzold CJ, Ullal AV, Prather KL, Keasling JD Synthetic protein scaffolds provide modular control over metabolic flux. *Nat Biotechnol* 2009;**27**:753–9.

Engler C, Gruetzner R, Kandzia R, Marillonnet S Golden gate shuffling: a one-pot DNA shuffling method based on type IIs restriction enzymes. *PLoSOne* 2009;**4**:e5553.

Farhi M, Marhevka E, Masci T, Marcos E, Eyal Y, Ovadis M, Abeliovich H, Vainstein A Harnessing yeast subcellular compartments for the production of plant terpenoids. *Metab Eng* 2011;**13**:474–81.

Finley SD, Broadbelt LJ, Hatzimanikatis V *In silico* feasibility of novel biodegradation pathways for 1,2,4-trichlorobenzene. *BMC Syst Biol* 2010;**4**:7.

Fossati E, Ekins A, Narcross L, Zhu Y, Falgueyret J-P, Beaudoin GAW, Facchini PJ, Martin VJJ Reconstitution of a 10-gene pathway for synthesis of the plant alkaloid dihydrosanguinarine in *Saccharomyces cerevisiae*. *Nat Commun* 2014;**5**:3283.

Gibson DG, Young L, Chuang R-Y, Venter JC, Hutchison CA, Smith HO Enzymatic assembly of DNA molecules up to several hundred kilobases. *Nat Methods* 2009;**6**:343–5.

Gibson DG, Glass JI, Lartigue C, *et al*. Creation of a bacterial cell controlled by a chemically synthesized genome. *Science* 2010;**329**:52–6.

Hallborn J, Walfridsson M, Airaksinen U, Ojamo H, Hahn-Hägerdal B, Penttilä M, Keräsnen S Xylitol production by recombinant *Saccharomyces cerevisiae*. *Biotechnology (NY)* 1991;**9**:1090–5.

Hatzimanikatis V, Li C, Ionita JA, Henry CS, Jankowski MD, Broadbelt LJ Exploring the diversity of complex metabolic networks. *Bioinformatics* 2005;**21**:1603–9.

Henry CS, Broadbelt LJ, Hatzimanikatis V Discovery and analysis of novel metabolic pathways for the biosynthesis of industrial chemicals: 3-hydroxypropanoate. *Biotechnol Bioeng* 2010;**106**:462–73.

Hillson NJ, Rosengarten RD, Keasling JD j5 DNA assembly design automation software. *ACS Synth Biol* 2012;**1**:14–21.

Jensen NB, Strucko T, Kildegaard KR, David F, Maury J, Mortensen UH, Forster J, Nielsen J, Borodina I EasyClone: method for iterative chromosomal integration of multiple genes in *Saccharomyces cerevisiae*. *FEMS Yeast Res* 2014;**14**:238–248.

Katz M, Smits HP, Foerster J, Nielsen JB *Metabolically engineered cells for the production of resveratrol or an oligomeric or glycosidically-bound derivative thereof* 2012 Patent EP 1856251 B1.

Kim B, Du J, Eriksen DT, Zhao H Combinatorial design of a highly efficient xylose-utilizing pathway in *Saccharomyces cerevisiae* for the production of cellulosic biofuels. *Appl Environ Microbiol* 2013;**79**:931–941.

Koopman F, Beekwilder J, Crimi B, van Houwelingen A, Hall RD, Bosch D, van Maris AJ, Pronk JT, Daran J-M *De novo* production of the flavonoid naringenin in engineered *Saccharomyces cerevisiae*. *Microb Cell Fact* 2012;**11**:155.

Krivoruchko A, Siewers V, Nielsen J Opportunities for yeast metabolic engineering: lessons from synthetic biology. *Biotechnol J* 2011;**6**:262–276.

Kuijpers NGA, Chroumpi S, Vos T, Solis-Escalante D, Bosman L, Pronk JT, Daran J-M, Daran-Lapujade P One-step assembly and targeted integration of multigene constructs assisted by the I-SceI meganuclease in *Saccharomyces cerevisiae*. *FEMS Yeast Res* 2013a;**13**:769–81.

Kuijpers NG, Solis-Escalante D, Bosman L, van den Broek M, Pronk JT, Daran J-M, Daran-Lapujade P A versatile, efficient strategy for assembly of multi-fragment expression vectors in *Saccharomyces cerevisiae* using 60 bp synthetic recombination sequences. *Microb Cell Fact* 2013b;**12**:47.

Kwok R Five hard truths for synthetic biology. *Nat News* 2010;**463**:288–90.

Laskowski RA, Watson JD, Thornton JM ProFunc: a server for predicting protein function from 3D structure. *Nucleic Acids Res* 2005;**33**:W89–93.

Lee S-M, Jellison T, Alper HS Directed evolution of xylose isomerase for improved xylose catabolism and fermentation in the yeast *Saccharomyces cerevisiae*. *Appl Environ Microbiol* 2012;**78**:5708–16.

Liang L, Zhang J, Lin Z Altering coenzyme specificity of *Pichia stipitis* xylose reductase by the semi-rational approach CASTing. *Microb Cell Fact* 2007;**6**:36.

Liu M, Bienfait B, Sacher O, Gasteiger J, Siezen RJ, Nauta A, Geurts JMW Combining chemoinformatics with bioinformatics: *in silico* prediction of bacterial flavor-forming pathways by a chemical systems biology approach "reverse pathway engineering". *PLoS ONE* 2014;**9**:e84769.

Lopez G, Valencia A, Tress ML *firestar*-prediction of functionally important residues using structural templates and alignment reliability. *Nucleic Acids Res* 2007;**35**:W573–7.

Lund AM, Kildegaard HF, Petersen MBP, Rank J, Hansen BG, Andersen MR, Mortensen UH A versatile system for USER cloning-based assembly of expression vectors for mammalian cell engineering. *PLoS ONE* 2014;**9**:e96693.

McClymont K, Soyer OS Metabolic tinker: an online tool for guiding the design of synthetic metabolic pathways. *Nucleic Acids Res* 2013;**41**:e113.

Mikkelsen MD, Buron LD, Salomonsen B, Olsen CE, Hansen BG, Mortensen UH, Halkier BA Microbial production of indolylglucosinolate through engineering of a multi-gene pathway in a versatile yeast expression platform. *Metab Eng* 2012;**14**:104–11.

Minard KI, McAlister-Henn L Glucose-induced degradation of the MDH2 isozyme of malate dehydrogenase in yeast. *J Biol Chem* 1992;**267**:17458–64.

Mutalik VK, Guimaraes JC, Cambray G, *et al.* Quantitative estimation of activity and quality for collections of functional genetic elements. *Nat Methods* 2013;**10**:347–53.

Nielsen J, Fussenegger M, Keasling J, Lee SY, Liao JC, Prather K, Palsson B Engineering synergy in biotechnology. *Nat Chem Biol* 2014;**10**:319–22.

Noor E, Bar-Even A, Flamholz A, Reznik E, Liebermeister W, Milo R Pathway thermodynamics highlights kinetic obstacles in central metabolism. *PLoS Comput Biol* 2014;**10**:e1003483.

Nørholm MH A mutant Pfu DNA polymerase designed for advanced uracil-excision DNA engineering. *BMC Biotechnol* 2010;**10**:21.

Nour-Eldin HH, Hansen BG, Nørholm MH, Jensen JK, Halkier BA Advancing uracil-excision based cloning towards an ideal technique for cloning PCR fragments. *Nucleic Acids Res* 2006;**34**:e122.

Paddon CJ, Keasling JD Semi-synthetic artemisinin: a model for the use of synthetic biology in pharmaceutical development. *Nat Rev Microbiol* 2014;**12**:355–67.

Quan J, Tian J Circular polymerase extension cloning of complex gene libraries and pathways. *PLoS ONE* 2009;**4**:e6441.

Röthlisberger D, Khersonsky O, Wollacott AM, *et al.* Kemp elimination catalysts by computational enzyme design. *Nature* 2008;**453**:190–5.

Runquist D, Hahn-Hagerdal B, Bettiga M Increased ethanol productivity in xylose-utilizing *Saccharomyces cerevisiae* via a randomly mutagenized xylose reductase. *Appl Environ Microbiol* 2010;**76**:7796–802.

Serrano L, Vancompernolle K, Ball P, *et al.* EUR 21796 – Synthetic Biology – Applying Engineering to Biology. *Report of a NEST High-Level Expert Group* 2005 Luxembourg European Communities 38.

Seyedsayamdost MR, Clardy J Natural products and synthetic biology. *ACS Synth Biol* 2014 10.1021/sb400025p.

Shao Z, Zhao H Construction and engineering of large biochemical pathways via DNA assembler. *Methods Mol Biol* 2013;**1073**:85–106.

Shao Z, Zhao H, Zhao H DNA assembler, an *in vivo* genetic method for rapid construction of biochemical pathways. *Nucleic Acids Res* 2009;**37**:e16.

Silva-Rocha R, Martinez-Garcia E, Calles B, *et al.* The Standard European Vector Architecture (SEVA): a coherent platform for the analysis and deployment of complex prokaryotic phenotypes. *Nucleic Acids Res* 2013;**41**:D666–75.

Sleight SC, Bartley BA, Lieviant JA, Sauro HM In-fusion BioBrick assembly and re-engineering. *Nucleic Acids Res* 2010;**38**:2624–36.

Tippmann S, Chen Y, Siewers V, Nielsen J From flavors and pharmaceuticals to advanced biofuels: production of isoprenoids in *Saccharomyces cerevisiae*. *Biotechnol J* 2013;**8**:1435–44.

Urano J, Dundon Asleson C, Meinhold P, Feldman R, Aristidou A, Hawkins A, Buelter T, Peters M, Lies D, Porter-Scheinman S *Cytosolic isobutanol pathway localization for the production of isobutanol* 2012 Patent US 8232089 B2.

Van Dien S From the first drop to the first truckload: commercialization of microbial processes for renewable chemicals. *Curr Opin Biotechnol* 2013;**24**:1061–8.

Verma R, Schwaneberg U, Roccatano D Computer-aided protein directed evolution: a review of web servers, databases and other computational tools for protein engineering. *Comput Struct Biotechnol J* 2012;**2**:e201209008.

Wang Y, Yu O Synthetic scaffolds increased resveratrol biosynthesis in engineered yeast cells. *J Biotechnol* 2012;**157**:258–60.

Way JC, Collins JJ, Keasling JD, Silver PA Integrating biological redesign: where synthetic biology came from and where it needs to go. *Cell* 2014;**157**:151–61.

Weber E, Engler C, Gruetzner R, Werner S, Marillonnet S A modular cloning system for standardized assembly of multigene constructs. *PLoS ONE* 2011;**6**:e16765.

Westfall PJ, Pitera DJ, Lenihan JR, *et al.* Production of amorphadiene in yeast, and its conversion to dihydroartemisinic acid, precursor to the antimalarial agent artemisinin. *P Natl Acad Sci USA* 2012;**109**:E111–8.

Wingler LM, Cornish VW Reiterative recombination for the *in vivo* assembly of libraries of multigene pathways. *P Natl Acad Sci USA* 2011;**108**:15135–40.

Winkler A, De Hulster A, Van Dijken J, Pronk J *Malic acid production in recombinant yeast* 2007 Patent WO/2007/061590.

Wu D, Wang Q, Assary RS, Broadbelt LJ, Krilov G A computational approach to design and evaluate enzymatic reaction pathways: application to 1-butanol production from pyruvate. *J Chem Inf Model* 2011;**51**:1634–47.

Yim H, Haselbeck R, Niu W, *et al.* Metabolic engineering of *Escherichia coli* for direct production of 1,4-butanediol. *Nat Chem Biol* 2011;**7**:445–52.

Zhang YH Substrate channeling and enzyme complexes for biotechnological applications. *Biotechnol Adv* 2011;**29**:715–25.

Zhang Y, Li S-Z, Li J, Pan X, Cahoon RE, Jaworski JG, Wang X, Jez JM, Chen F, Yu O Using unnatural protein fusions to engineer resveratrol biosynthesis in yeast and mammalian cells. *J Am Chem Soc* 2006;**128**:13030–1.

Zhou H, Cheng J-S, Wang BL, Fink GR, Stephanopoulos G Xylose isomerase overexpression along with engineering of the pentose phosphate pathway and evolutionary engineering enable rapid xylose utilization and ethanol production by *Saccharomyces cerevisiae*. *Metab Eng* 2012;**14**:611–22.

CHAPTER 3 Screening tyrosine ammonia lyase for *p*-coumaric acid production

Introduction

p-Coumaric acid serves as one of the commonly used precursors to synthesise numerous plant secondary aromatic compounds of biotechnological interest. It can either be derived from tyrosine by deamination with tyrosine ammonia lyase (TAL) or from phenylalanine by deamination with phenylalanine ammonia lyase (PAL) and subsequent hydroxylation of the resulting cinnamic acid by a P450 enzyme cinnamate 4-hydroxylase (C4H). Due to the involvement of a P450 enzyme, which is often difficult to express, in the phenylalanine route, TALs may be preferred alternative to produce *p*-coumaric acid and its derivatives in microorganisms. However, a lack of highly active and specific TALs has been the limiting step in metabolic engineering. We therefore screened 14 sequences based on synteny information and sequence divergence (Jendresen *et al.*, 2015) to find out enzymes that can high actively and specifically convert tyrosine to *p*-coumaric acid. *In vivo* assay showed that enzymes from *Herpetosiphon aurantiacus* and *Flavobacterium johnsoniae* were good candidates for production of *p*-coumaric acid in *Saccharomyces cerevisiae*.

Materials and methods

Strains and plasmids

All the cloning work including biobricks and plasmids construction was done in the *Escherichia coli* strain DH5α. The primers, biobricks, and plasmids used in this study are summarised in Table 3.1, 3.2 and 3.3

respectively. The *E. coli* transformants were screened on Luria-Bertani (LB) plates containing 100 mg mL^{-1} ampicillin (LB-amp). The plasmid-containing *E. coli* were propagated in liquid LB-amp medium at 37 ℃ for plasmid purification.

Table 3.1. List of primers used in the study

Name	Sequence (5' to 3')
*RmXAL*_fw	AGTGCAGGU AAAACAATGGCACCGAGCGTTGATAGC
*RmXAL*_rv	CGTGCGAU TTAGGCCATCATTTTAAC
*S-BagA*_fw	AGTGCAGGUAAAACAATGAAAATTGATGGTCGTGGTCTGACCAT TAGCCAGACCG
*S-BagA*_rv	CGTGCGAU TTACAGATTACCGCCTGC
*RsTAL*_fw	AGTGCAGGUAAAACAATGAGCCCTCCGAAACCGGCAGTTGAACTGG
*RsTAL*_ rv	CGTGCGAU TTAAACCGGACTCTGTTG
*SeSam8*_fw	AGTGCAGGU AAAACAATGACCCAGGTTGTTGAACGTCAGG
*SeSam8*_ rv	CGTGCGAU TTAGCCAAAATCTTTACC
*SrXAL*_fw	AGTGCAGGU AAAACAATGAGCACCCCGAGCGCA
*SrXAL*_ rv	CGTGCGAU TTATGCGGTCGGAGGGGT
*R_XAL*_fw	AGTGCAGGU AAAACAATGCGTAGCGAACAGCTGACC
*R_XAL*_ rv	CGTGCGAU TTAGGCCAGCAGTTCAAT
*PpPAL*_fw	AGTGCAGGU AAAACAATGCACGATGATAACACCAGCCCG
*PpPAL*_ rv	CGTGCGAU TTAACAGCTTGCGCGTGC
*LbTAL*_fw	AGTGCAGGUAAAACAATGCCTCGTTTTTGTCCGAGCATGTATCTGC
*LbTAL*_ rv	CGTGCGAU TTAATCGTTCGGGGTCAT
*L_XAL*_fw	AGTGCAGGU AAAACAATGACCCTGACCCCGACCG
*L_XAL*_ rv	CGTGCGAU TTAGTTAAAGCTGCTAAT
*IlTAL*_fw	AGTGCAGGU AAAACAATGACCACCTCCATTATTGCATTTGG
*IlTAL*_ rv	CGTGCGAU TTATGCCGGTTCTTGATA
*HaTAL1*_fw	AGTGCAGGU AAAACAATGAGCACCACCCTGATTCTG
*HaTAL1*_ rv	CGTGCGAU TTAGCGAAACAGAATAAT
*FjTAL*_fw	AGTGCAGGU AAAACAATGAACACCATCAACGAATATCTGAGC
*FjTAL*_ rv	CGTGCGAU TTAATTGTTAATCAGGTG
*DdPAL*_fw	AGTGCAGGU AAAACAATGATCGAAACCAACCACAAA
*DdPAL*_ rv	CGTGCGAU TTACAGGTTCAGGTTAAT
*BlPAL*_fw	AGTGCAGGU AAAACAATGAGCCAGGTTGCACTGTTTG
*BlPAL*_ rv	CGTGCGAU TTAATCATTCACATTCTG
ColPCR_fw	CCTGCAGGACTAGTGCTGAG
XI-5_D_rv	CCCAAAAGCAATCCAGGAAAAACC

Note: Underlined sequences represent overhangs used in USER cloning.

The TAL genes were integrated into the XI-5 site of genome of *S. cerevisiae* CEN.PK102-5B (MATa *ura*3-52 *his*3Δ1 *leu*2-3/112 *MAL*2-8^{c} *SUC*2) (Entian and Kötter, 2007b) to generate strains from STC0 to STC14. All the yeast strains used in this study are listed in Table 3.4. Yeast cells were grown on synthetic complete (SC) dropout media lacking histidine for selection of transformants with DNA integrations. The correct integrations were checked by colony PCR using primers ColPCR_DW_fw and XI-5_D_rv.

Table 3.2. List of biobricks used in the study.

Biobrick	Source	Template	Forward primer	Reverse primer
BB0369	*RmXAL* from *Rhodotorula mucilaginosa* (*Rhodotorula rubra*)	pCBJ217	*RmXAL*_fw	*RmXAL*_rv
BB0370	*S-BagA* from *Streptomyces*	pCBJ216	*S-BagA*_fw	*S-BagA*_rv
BB0371	*RsTAL* from *Rhodobacter sphaeroides*	pCBJ215	*RsTAL*_fw	*RsTAL*_ rv
BB0372	*SeSam8* from *Saccharothrix espanaensis*	pCBJ218	*SeSam8*_fw	*SeSam8*_ rv
BB0373	*SrXAL* from *Salinibacter ruber*	pCBJ225	*SrXAL*_fw	*SrXAL*_ rv
BB0374	*R_XAL* from *Rheinheimera*	pCBJ220	*R_XAL*_fw	*R_XAL*_ rv
BB0375	*PpPAL* from *Physcomitrella patens* subsp. *patens*	pCBJ221	*PpPAL*_fw	*PpPAL*_ rv
BB0376	*LbTAL* from *Leptospira biflexa* serovar patoc	pCBJ222	*LbTAL*_fw	*LbTAL*_ rv
BB0377	*L_XAL* from *Leptolyngbya*	pCBJ226	*L_XAL*_fw	*L_XAL*_ rv
BB0378	*IlTAL* from *Idiomarina loihiensis*	pCBJ223	*IlTAL*_fw	*IlTAL*_ rv
BB0379	*HaTAL1* from *Herpetosiphon aurantiacus*	pCBJ227	*HaTAL1*_fw	*HaTAL1*_ rv
BB0380	*FjTAL* from *Flavobacterium johnsoniae*	pCBJ228	*FjTAL*_fw	*FjTAL*_ rv
BB0381	*DdPAL* from *Dictyostelium discoideum*	pCBJ224	*DdPAL*_fw	*DdPAL*_ rv
BB0382	*BlPAL* from *Brevibacillus laterosporus*	pCBJ219	*BlPAL*_fw	*BlPAL*_ rv

Table 3.3. List of plasmids used in the study

Plasmid	Parent plasmid	Properties	Reference
pCDFDuet			Novagen
pCBJ215	pCDFDuet	pCDFDuet MCS2::*RsTAL*, Sp^r	(Jendresen *et al.*, 2015)
pCBJ216	pCDFDuet	pCDFDuet MCS2::*S_BagA*, Sp^r	(Jendresen *et al.*, 2015)
pCBJ217	pCDFDuet	pCDFDuet MCS2::*RmXAL*, Sp^r	(Jendresen *et al.*, 2015)
pCBJ218	pCDFDuet	pCDFDuet MCS2::*SeSam8*, Sp^r	(Jendresen *et al.*, 2015)
pCBJ219	pCDFDuet	pCDFDuet MCS2::*BlPAL*, Sp^r	(Jendresen *et al.*, 2015)
pCBJ220	pCDFDuet	pCDFDuet MCS2::*R_XAL*, Sp^r	(Jendresen *et al.*, 2015)
pCBJ221	pCDFDuet	pCDFDuet MCS2::*PpPAL*, Sp^r	(Jendresen *et al.*, 2015)
pCBJ222	pCDFDuet	pCDFDuet MCS2::*LbTAL*, Sp^r	(Jendresen *et al.*, 2015)
pCBJ223	pCDFDuet	pCDFDuet MCS2::*IlTAL*, Sp^r	(Jendresen *et al.*, 2015)
pCBJ224	pCDFDuet	pCDFDuet MCS2::*DdPAL*, Sp^r	(Jendresen *et al.*, 2015)
pCBJ225	pCDFDuet	pCDFDuet MCS2::*SrXAL*, Sp^r	(Jendresen *et al.*, 2015)
pCBJ226	pCDFDuet	pCDFDuet MCS2::*L_XAL*, Sp^r	(Jendresen *et al.*, 2015)
pCBJ227	pCDFDuet	pCDFDuet MCS2::*HaTAL1*, Sp^r	(Jendresen *et al.*, 2015)
pCBJ228	pCDFDuet	pCDFDuet MCS2::*FjTAL*, Sp^r	(Jendresen *et al.*, 2015)
pCfB391		Integrative plasmid, XI-5-LoxP, *SpHIS5*	(Jensen *et al.*, 2014b)
pCfB860	pCfB391	Integrative plasmid, XI-5, LoxP, BB371 (<-*RsTAL*), BB008 (pTEF1<-), *SpHIS5*	This study
pCfB861	pCfB391	Integrative plasmid, XI-5, LoxP, BB370 (<-*S-BagA*), BB008 (pTEF1<-), *SpHIS5*	This study
pCfB862	pCfB391	Integrative plasmid, XI-5, LoxP, BB369 (<-*RmXAL*), BB008 (pTEF1<-), *SpHIS5*	This study
pCfB863	pCfB391	Integrative plasmid, XI-5, LoxP, BB372 (<-*SeSam8*), BB008 (pTEF1<-), *SpHIS5*	This study
pCfB864	pCfB391	Integrative plasmid, XI-5, LoxP, BB382 (<-*BlPAL*), BB008 (pTEF1<-), *SpHIS5*	This study
pCfB865	pCfB391	Integrative plasmid, XI-5, LoxP, BB374 (<-*R_XAL*), BB008 (pTEF1<-), *SpHIS5*	This study
pCfB866	pCfB391	Integrative plasmid, XI-5, LoxP, BB375 (<-*PpPAL*), BB008 (pTEF1<-), *SpHIS5*	This study
pCfB867	pCfB391	Integrative plasmid, XI-5, LoxP, BB376 (<-*LbTAL*), BB008 (pTEF1<-), *SpHIS5*	This study
pCfB868	pCfB391	Integrative plasmid, XI-5, LoxP, BB378 (<-*IlTAL*), BB008 (pTEF1<-), *SpHIS5*	This study
pCfB869	pCfB391	Integrative plasmid, XI-5, LoxP, BB381 (<-*DdPAL*), BB008 (pTEF1<-), *SpHIS5*	This study

pCfB870	pCfB391	Integrative plasmid, XI-5, LoxP, BB373 (<-*SrXAL*), BB008 (pTEF1<-), *SpHIS5*	This study
pCfB871	pCfB391	Integrative plasmid, XI-5, LoxP, BB377 (<-*L_XAL*), BB008 (pTEF1<-), *SpHIS5*	This study
pCfB872	pCfB391	Integrative plasmid, XI-5, LoxP, BB379 (<-*HaTAL1*), BB008 (pTEF1<-), *SpHIS5*	This study
pCfB873	pCfB391	Integrative plasmid, XI-5, LoxP, BB0380 *FjTAL*), BB008 (pTEF1<-), *SpHIS5*	This study

Note: Sp^r, spectinomycin resistance.

Table 3.4. List of yeast strains used in the study.

Strain	**Genotype**	**Reference**
CEN.PK1 02-5B	MAT*a ura3-52 his3Δ1 leu2-3/112 MAL2-8^c SUC2*	(Entian and Kötter, 2007b)
STC1	CEN.PK102-5B, XI-5::P_{TEF1}->*RsTAL-SpHIS5*, leu-, ura-	This study
STC2	CEN.PK102-5B, XI-5::P_{TEF1}->*S-BagA-SpHIS5*, leu-, ura-	This study
STC3	CEN.PK102-5B, XI-5::P_{TEF1}->*RmXAL-SpHIS5*, leu-, ura-	This study
STC4	CEN.PK102-5B, XI-5::P_{TEF1}->*SeSam8-SpHIS5*, leu-, ura-	This study
STC5	CEN.PK102-5B, XI-5::P_{TEF1}->*BlPAL-SpHIS5*, leu-, ura-	This study
STC6	CEN.PK102-5B, XI-5::P_{TEF1}->*R_XAL-SpHIS5*, leu-, ura-	This study
STC7	CEN.PK102-5B, XI-5::P_{TEF1}->*PpPAL-SpHIS5*, leu-, ura-	This study
STC8	CEN.PK102-5B, XI-5::P_{TEF1}->*LbTAL-SpHIS5*, leu-, ura-	This study
STC9	CEN.PK102-5B, XI-5::P_{TEF1}->*IlTAL-SpHIS5*, leu-, ura-	This study
STC10	CEN.PK102-5B, XI-5::P_{TEF1}->*DdPAL-SpHIS5*, leu-, ura-	This study
STC11	CEN.PK102-5B, XI-5::P_{TEF1}->*SrXAL-SpHIS5*, leu-, ura-	This study
STC12	CEN.PK102-5B, XI-5::P_{TEF1}->*L_XAL-SpHIS5*, leu-, ura-	This study
STC13	CEN.PK102-5B, XI-5::P_{TEF1}->*HaTAL1-SpHIS5*, leu-, ura-	This study
STC14	CEN.PK102-5B, XI-5::P_{TEF1}->*FjTAL-SpHIS5*, leu-, ura-	This study

p-Coumaric acid and cinnamic acid production in yeast strains

The engineered strains were routinely grown in 0.5 ml SC medium lacking histidine at 30 ℃ with 250 rpm agitation for 24 h in 96-deep-well plates. Then, 50 µl of the pre-culture was inoculated into 0.5 ml mineral medium (Jensen *et al.*, 2014b) with 2% glucose, which was supplemented with 76 mg l^{-1} uracil, 380 mg l^{-1} leucine, and with either 10 mM tyrosine or

phenylalanine. The mineral medium (pH 6.0) was composed of 20 g l^{-1} glucose, 5 g l^{-1} $(NH_4)_2SO_4$, 3 g l^{-1} KH_2PO_4, 0.5 g l^{-1} $MgSO_4 \cdot 7H_2O$, 2 ml l^{-1} trace metals solution, and 1 ml l^{-1} vitamin solution (Li *et al.*, 2015). Yeast cultures were cultivated at 30 ℃ and 250 rpm for 72 h. For the time course experiment, 100 µl of the pre-culture was used to inoculated into 3 ml FIT medium with 76 mg l^{-1} uracil, 380 mg l^{-1} leucine, and 10 mM tyrosine in a 24-deep-well plates and the cultures were grown at 30 ℃ and 250 rpm for 90 h. Samples for HPLC were taken at the end point for the 96-well-plate cultivations and at regular intervals for the time course experiment. The samples were mixed with the equal volume of absolute ethanol. After centrifugation at 2,272 g for 30 min, the supernatants were collected for HPLC analysis. The OD_{600} of the yeast cultures was measured in a microtiter plate reader BioTek Synergy MX (BioTek) after cultures had been diluted 2 to 20 times.

Analytical methods

The production of *p*-coumaric acid and cinnamic acid were quantified by HPLC (Thermo) equipped with a Discovery HS F5 150 mm 2.1 mm column (particle size 3 mm). Two solvents, 10 mM ammonium formate (pH 3.0) and acetonitrile, were used as the eluents at a flow rate of 1.5 ml min^{-1} in a gradient method to analyse the samples. The absorbance of *p*-coumaric acid at 333 nm and of cinnamic acid at 277 nm was measured by a UV detector. Concentrations were calculated from the standard curves, using pure standards, that were purchased from Sigma-Aldrich.

Results and discussion

Production of *p*-coumaric acid in *Saccharomyces cerevisiae*

Fourteen *TAL* genes (Table 2.2) were cloned under control of a strong promoter pTEF1 and integrated into the genome of *S. cerevisiae*. The resulting strains were grown in mineral medium with addition of tyrosine to analyse the activity of different TALs. Ten out of the fourteen strains expressing different TALs lead to *p*-coumaric acid production within the range of 1 to 95 mg l^{-1}. The strains carrying *RmXAL*, *HaTAL1* and *FjTAL* gave significantly higher production of *p*-coumaric acid than the others (Fig. 2.1). Specifically, *RmXAL* resulted in 91.14±9.16 mg l^{-1} *p*-coumaric acid

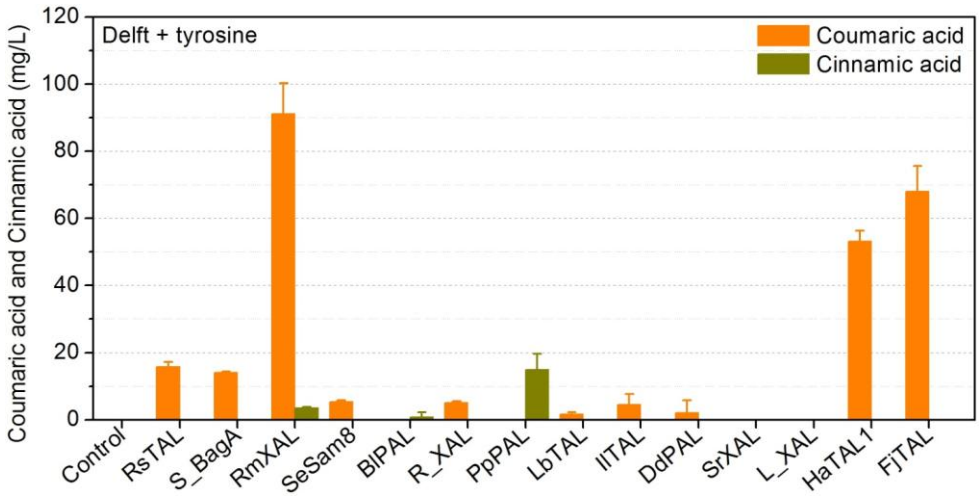

Fig. 3.1 Production of *p*-coumaric acid in *S. cerevisiae* expressing aromatic amino acid ammonia-lyases on mineral medium with 2% glucose and 10 mM tyrosine. The strains were grown at 30 ℃ in 96-deep-well plates for 72 h. As control we used a *S. cerevisiae* strain with an empty vector. The displayed average values and standard deviations were calculated from three biological replicates.

and performed better than *HaTAL1* and *FjTAL*, which gave 53.10±3.17 mg l^{-1} and 68.03±7.49 mg l^{-1} respectively. Interestingly, production of cinnamic acid was observed when *RmXAL*, *BlPAL*, and *PpPAL* were expressed, both with supplementation of phenylalanine and without. The strains expressing *PpPAL* and *RmXAL* could produce up to 14.90±4.71 and 3.48±0.30 mg l^{-1} of cinnamic acid respectively, and the strain expressing *BlPAL* could only give trace amounts of cinnamic acid. Cinnamic acid production indicates that RmXAL, BlPAL, and DdPAL have PAL activities.

Specificity of TALs

Considering that many enzymes were known to have both TAL and PAL activities (Parkhurst and Hodgins, 1971; Rosler *et al.*, 1997; Sawada *et al.*, 1973; Watanabe *et al.*, 1992) as we observed in some of the selected TAL enzymes, we then analysed the specificity of TAL by cultivating the fourteen TAL-expressing strains in the presence of phenylalanine. In accordance with the results described in the previous section, BlPAL and PpPAL showed PAL activity. However, PpPAL resulted in lower cinnamic acid production in the presence of phenylalanine than tyrosine. On the other hand, RmXAL gave no cinnamic acid production when phenylalanine was added to the minimum medium. The phenomena might be explained by the inhibition effect of phenylalanine on the PAL activity. In contrast, IlTAL, which did not show PAL activity when tyrosine was supplemented, resulted in the highest production of cinnamic acid (40.14±7.02 mg l^{-1}). Notably, even without addition of tyrosine, HaTAL1 and FjTAL could still produce 24.65±1.25 and 15.50±1.04 mg l^{-1} *p*-coumaric acid respectively. It indicates

that the two enzymes are good candidates for *p*-coumaric acid production from glucose. No *p*-coumaric acid or cinnamic acid was detected for the remaining enzymes in defined medium. Among the TALs, BlPAL and PpPAL were the only two enzymes which exclusively had a PAL activity.

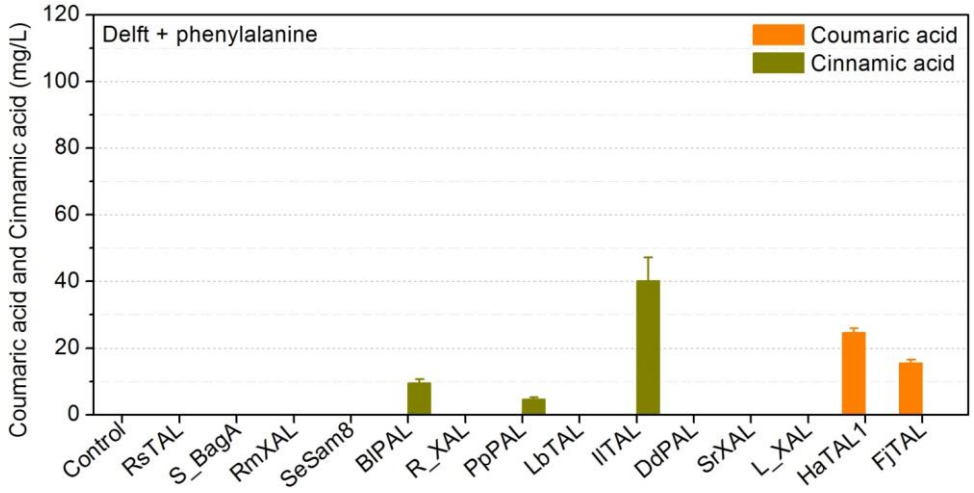

Fig. 3.2 Production of *p*-coumaric acid in *S. cerevisiae* expressing aromatic amino acid ammonia-lyases on minimal medium with 2% glucose and 10 mM phenylalanine. The strains were grown at 30 ℃ in 96-deep well plates for 72 h. As control we used a *S. cerevisiae* strain with an empty vector. The displayed average values and standard deviations were calculated from three biological replicates.

Time course of *p*-coumaric production

Five strains carrying five TALs, including RsTAL, S_BagA, RmXAL, HaTAL1 and FjTAL, were selected for the time course cultivation to investigate the dynamic change of *p*-coumaric acid production with the consumption of tyrosine in feed-in-time (FIT) medium. No apparent growth differences in the five strains were observed (Fig. 2.3 A). Although *p*-

coumaric acid production by the five strains was different, the tyrosine consumption rates were similar (Fig. 2.3 B), which indicates that not all tyrosine was converted to *p*-coumaric acid. RmXAL gave the highest productivity of *p*-coumaric acid in the presence of tyrosine and led to 144.64±4.62 mg l^{-1}, but the production stopped after tyrosine was depleted. In comparison, the other four TALs continued producing *p*-coumaric acid after tyrosine depletion. Rs_TAL and S_BagA resulted in the final *p*-coumaric acid titers of 73-82 mg l^{-1}. HaTAL1 and FjTAL gave the highest titres of around 270 mg l^{-1}.

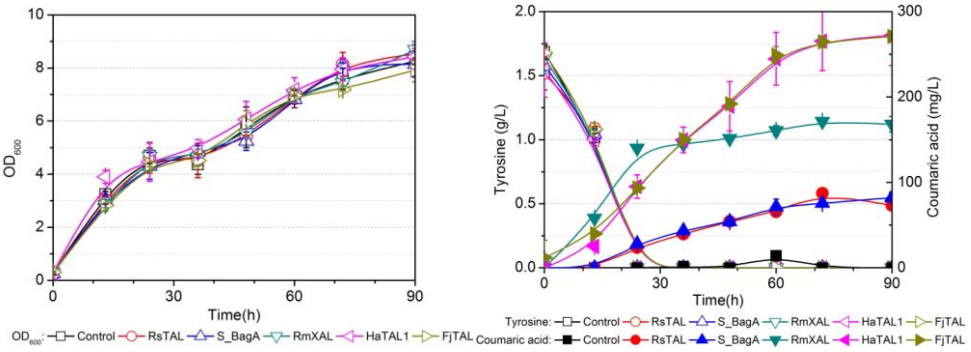

Fig. 2.3 Time course cultivation of the strains expressing *RsTAL*, *S_BagA*, *RmXAL*, *HaTAL1* and *FjTAL* genes on FIT medium with 2% glucose and 10 mM tyrosine. (A) Growth measured by OD_{600}. (B) Production of *p*-coumaric acid. The strains were grown at 30 ℃ in 24-deep well plates for 90 h. As control we used a *S. cerevisiae* strain with an empty vector. The displayed average values and standard deviations were calculated from three biological replicates.

Contents lists available at ScienceDirect

Metabolic Engineering

journal homepage: www.elsevier.com/locate/ymben

CHAPTER 4

De novo production of resveratrol from glucose or ethanol by engineered *Saccharomyces cerevisiae*

Mingji Li [a], Kanchana R. Kildegaard [a], Yun Chen [b,c], Angelica Rodriguez [a], Irina Borodina [a,*], Jens Nielsen [a,b,c,**]

[a] The Novo Nordisk Foundation Center for Biosustainability, Technical University of Denmark, 2970 Hørsholm, Denmark
[b] Department of Biology and Biological Engineering, Chalmers University of Technology, SE-41296 Gothenburg, Sweden
[c] The Novo Nordisk Foundation Center for Biosustainability, Chalmers University of Technology, SE-41296 Gothenburg, Sweden

ARTICLE INFO

Article history:
Received 19 May 2015
Received in revised form
25 July 2015
Accepted 25 August 2015
Available online 4 September 2015

Keywords:
Resveratrol
Tyrosine
Metabolic engineering
Saccharomyces cerevisiae

ABSTRACT

Resveratrol is a natural antioxidant compound, used as food supplement and cosmetic ingredient. Microbial production of resveratrol has until now been achieved by supplementation of expensive substrates, *p*-coumaric acid or aromatic amino acids. Here we engineered the yeast *Saccharomyces cerevisiae* to produce resveratrol directly from glucose or ethanol via tyrosine intermediate. First we introduced the biosynthetic pathway, consisting of tyrosine ammonia-lyase from *Herpetosiphon aurantiacus*, 4-coumaryl-CoA ligase from *Arabidopsis thaliana* and resveratrol synthase from *Vitis vinifera*, and obtained 2.73 ± 0.05 mg L^{-1} resveratrol from glucose. Then we over-expressed feedback-insensitive alleles of *ARO*4 encoding 3-deoxy-D-arabino-heptulosonate-7-phosphate and *ARO*7 encoding chorismate mutase, resulting in production of 4.85 ± 0.31 mg L^{-1} resveratrol from glucose as the sole carbon source. Next we improved the supply of the precursor malonyl-CoA by over-expressing a post-translational de-regulated version of the acetyl-CoA carboxylase encoding gene *ACC*1; this strategy further increased resveratrol production to 6.39 ± 0.03 mg L^{-1}. Subsequently, we improved the strain by performing multiple-integration of pathway genes resulting in resveratrol production of 235.57 ± 7.00 mg L^{-1}. Finally, fed-batch fermentation of the final strain with glucose or ethanol as carbon source resulted in a resveratrol titer of 415.65 and 531.41 mg L^{-1}, respectively.

1. Introduction

Resveratrol (trans-3,5,4′-trihydroxystilbene) is a natural polyphenolic compound from the stilbene family. In plants, resveratrol plays a role as a defense compound against pathogens infection and injury. It occurs naturally in several higher plants, e.g. grapes, peanuts, blueberries, and knotweed (Mei et al., 2015). In preclinical tests resveratrol has shown a wide range of beneficial properties, i.e., antitumor, anti-inflammatory, antidiabetic, antithrombotic, and antiaging properties (Jeandet et al., 2012; Mei et al., 2015). The evidence of resveratrol effects on human health is however so far inconclusive, due to the limited number of clinical trials and small cohort sizes (Poulsen et al., 2013). Nevertheless, resveratrol has attracted much attention from pharmaceutical, food and cosmetic industries. Resveratrol is sold as over-the-counter nutritional supplement; it is included in some cosmetics products, energy drinks, and other products. The demand for resveratrol is expected to further increase in the future. The commercial resveratrol on the market is predominantly extracted from the Japanese knotweed *Polygonum cuspidatum* (Mei et al., 2015). The preparations range widely in purity; some can contain as low as 50% of the active ingredient. The unpurified knotweed extracts, however, additionally contain emodin which has a laxative effect (Srinivas et al., 2007). Thus, there is market demand for lower cost and high purity resveratrol.

One promising solution is biotechnological production of resveratrol by fermentation of genetically engineered microbes (Borodina and Nielsen, 2014). A number of studies have been published on microbial production of resveratrol. In all the studies, the production exclusively relied on using complex medium or supplementing the minimal medium with resveratrol precursors, *p*-coumaric acid, tyrosine or phenylalanine, which are expensive for industrial applications. The first study on recombinant resveratrol production described feeding *p*-coumaric acid to *Saccharomyces cerevisiae*, which expressed

* Corresponding author.
** Corresponding author at: The Novo Nordisk Foundation Center for Biosustainability, Technical University of Denmark, 2970 Hørsholm, Denmark.
E-mail addresses: irbo@biosustain.dtu.dk (I. Borodina), nielsenj@chalmers.se (J. Nielsen).

http://dx.doi.org/10.1016/j.ymben.2015.08.007
1096-7176/

4-coumaryl-CoA ligase (4CL) and resveratrol synthase (VST1) (Becker et al., 2003). Deamination of tyrosine or phenylalanine, catalyzed by tyrosine/phenylalanine ammonia lyase (TAL/PAL), is the first step of resveratrol biosynthesis pathway in plants. Transcription and enzyme activity of PAL is reduced by its product, *trans*-cinnamic acid (Blount et al., 2000; Bolwell et al., 1988), which means that efficient conversion of *trans*-cinnamic acid into *p*-coumaric acid is required to avoid the accumulation of toxic intermediate. The hydroxylation of *trans*-cinnamic acid into *p*-coumaric acid is catalyzed by cinnamic acid hydroxylase (C4H), a P450 enzyme, which requires cytochrome P450 reductase for efficient electron transfer. Trantas et al. expressed phenylalanine ammonia-lyase (PAL), cinnamate-4-hydroxylase (C4H), and cytochrome P450 reductase (CPR) in addition to 4CL and VST1 to produce resveratrol from phenylalanine (Trantas et al., 2009). In the biosynthesis of *p*-coumaric acid-derived compounds via phenylalanine, C4H was reported as the rate-limiting step (Trantas et al., 2009; Yan et al., 2005). A reduction of the *C4H* transcriptional level was observed to result in an 8-fold decrease of *PAL* and 2.5-fold decrease of *4CL* activities in tobacco (Kumar et al., 2012). Alternatively, tyrosine ammonia-lyase (TAL) can be used to directly synthesize *p*-coumaric acid from tyrosine (Fig. 1), thus averting the rate-limiting hydroxylation step. Wang et al. have successfully expressed codon-optimized *TAL* from *Rhodopseudomonas sphaeroides* in yeast to obtain 1.90 mg L^{-1} resveratrol, when supplemented with 12 mg L^{-1} tyrosine, and 1.06 mg L^{-1} resveratrol without supplementation but in complex medium, which contained tyrosine (Wang et al., 2011). In another case, Shin et al. used a tyrosine/phenylalanine ammonia-lyase from *Rhodosporidium toruloides* to produce 5.8 mg L^{-1} resveratrol in complex medium supplemented with 2.17 g L^{-1} tyrosine (Shin et al., 2012). The highest resveratrol titer reported in yeast from the literature so far is 391 mg L^{-1}, obtained by supplementing complex medium with 2.46 g L^{-1} *p*-coumaric acid and using a genetically engineered industrial Brazilian *S. cerevisiae* strain that overexpressed *4CL1* and *STS* (stilbene synthase) genes (Sydor et al., 2010).

In the present study, we aimed to achieve *de novo* biosynthesis of resveratrol from cheap carbon sources, glucose or ethanol, without supplementation of aromatic precursors. We chose to apply *S. cerevisiae* as the host, due to its safe use status in pharmaceutical biotechnology and food industry, and due to its high amenability to genetic manipulations. Here we describe step-wise metabolic engineered efforts towards obtaining an efficient cell factory for resveratrol production.

2. Materials and methods

2.1. Strains and growth conditions

The *Escherichia coli* strain DH5α was used for all the cloning work. The *E. coli* transformants were selected and maintained on Luria-Bertani (LB) plates containing 100 μg mL^{-1} ampicillin.

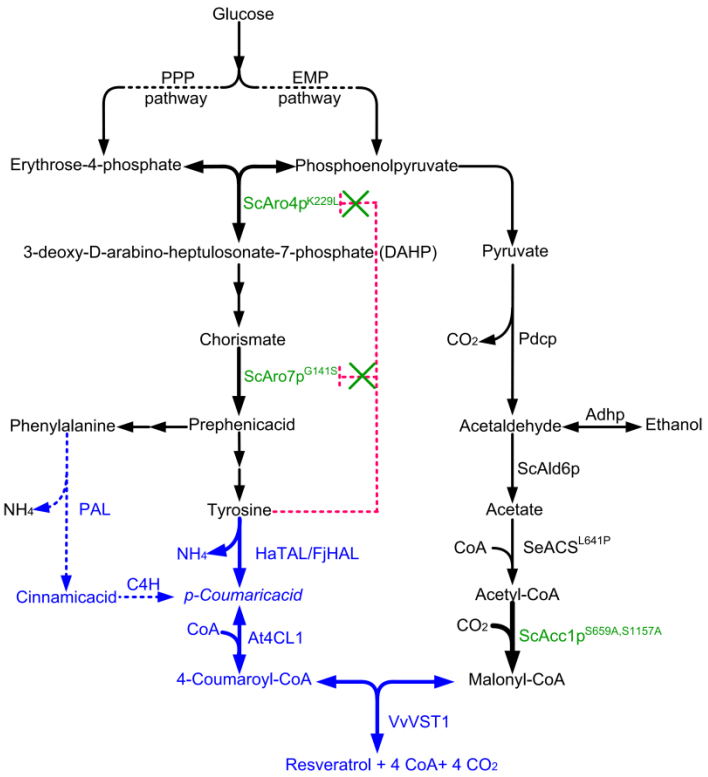

Fig. 1. Biosynthesis pathways towards resveratrol in engineered yeast. ScAro4p: DAHP synthase; ScAro7p: chorismate mutase; PAL: phenylalanine ammonia-lyase; C4H: cinnamate-4-hydroxylase; HaTAL/FjTAL: tyrosine ammonia-lyase from *H. aurantiacus/Flavobacterium johnsoniae*; At4CL1: 4-coumarate-CoA ligase; VST1: resveratrol synthase; Pdcp: pyruvate decarboxylase; Adhp: alcohol dehydrogenase; ScAld6p: aldehyde dehydrogenase; SeACS1: acetyl-CoA synthetase; ScAcc1p: acetyl-CoA carboxylase. Native reactions and intermediates are shown in black, heterologous in blue. The enzymes over-expressed in the described resveratrol-producing strain are highlighted in bold. The dash arrows mark the reactions that were not used in this study. Double arrows represent multiple enzymatic steps.

Table 1
List of yeast strains used in the study.

Strains	Parent strains	Integrative plasmids	Genotype	Reference
CEN.PK102-5B			MAT*a ura*3-52 *his*3Δ1 *leu*2-3/112 *MAL*2-8^{c} *SUC*2	Entian and Kötte (2000)
ST4120	CEN.PK102-5B	pCfB388, pCfB872	P_{TEF1}- > *HaTAL*, ura-	This study
ST4121	CEN.PK102-5B	pCfB854, pCfB872	P_{TEF1}- > *HaTAL*, P_{PGK1}- > *At4CL1*, P_{TEF1}- > *VvVST1*, ura-	This study
ST4122	CEN.PK102-5B	pCfB1020, pCfB872	P_{TEF1}- > *HaTAL*, P_{TEF1}- > *At4CL1*, P_{PGK1}- > *VvVST1*, ura-	This study
ST4123	CEN.PK102-5B	pCfB856, pCfB872	P_{TEF1}- > *HaTAL*, P_{TEF1}- > *4CL1::VST1*, ura-	This study
ST4124	CEN.PK102-5B	pCfB855, pCfB872	P_{TEF1}- > *HaTAL*, P_{PGK1}- > *At4CL2*, P_{TEF1}- > *VvVST1*, ura-	This study
ST4125	CEN.PK102-5B	pCfB1021, pCfB872	P_{TEF1}- > *HaTAL*, P_{TEF1}- > *At4CL2*, P_{PGK1}- > *VvVST1*, ura-	This study
ST4126	CEN.PK102-5B	pCfB857, pCfB872	P_{TEF1}- > *HaTAL*, P_{TEF1}- > *4CL2::VST1*, ura-	This study
ST4127	CEN.PK102-5B	pCfB388, pCfB873	P_{TEF1}- > *FjTAL*, ura-	This study
ST4128	CEN.PK102-5B	pCfB854, pCfB873	P_{TEF1}- > *FjTAL*, P_{PGK1}- > *At4CL1*, P_{TEF1}- > *VvVST1*, ura-	This study
ST4129	CEN.PK102-5B	pCfB1020, pCfB873	P_{TEF1}- > *FjTAL*, P_{TEF1}- > *At4CL1*, P_{PGK1}- > *VvVST1*, ura-	This study
ST4130	CEN.PK102-5B	pCfB856, pCfB873	P_{TEF1}- > *FjTAL*, P_{TEF1}- > *4CL1::VST1*, ura-	This study
ST4131	CEN.PK102-5B	pCfB855, pCfB873	P_{TEF1}- > *FjTAL*, P_{PGK1}- > *At4CL2*, P_{TEF1}- > *VvVST1*, ura-	This study
ST4132	CEN.PK102-5B	pCfB1021, pCfB873	P_{TEF1}- > *FjTAL*, P_{TEF1}- > *At4CL2*, P_{PGK1}- > *VvVST1*, ura-	This study
ST4133	CEN.PK102-5B	pCfB857, pCfB873	P_{TEF1}- > *FjTAL*, P_{TEF1}- > *4CL2::VST1*, ura-	This study
ST4158	ST4121		his-, leu-, ura-	This study
ST4135	ST4158	pCfB255, pCfB257, pCfB258	P_{TEF1}- > *HaTAL*, P_{PGK1}- > *At4CL1*, P_{TEF1}- > *VvVST1*	This study
ST4136	ST4158	pCfB255, pCfB257, pCfB826	P_{TEF1}- > *HaTAL*, P_{PGK1}- > *At4CL1*, P_{TEF1}- > *VvVST1*, P_{TEF1}- > *ScARO7*^{G141S}, P_{PGK1}- > *ScARO4* ^{K229L}	This study
ST4137	ST4158	pCfB1175, pCfB257, pCfB258	P_{TEF1}- > *HaTAL*, P_{PGK1}- > *At4CL1*, P_{TEF1}- > *VvVST1*, P_{TEF1}- > *ScACC1*$^{S659A,\ S1157A}$	This study
ST4140	ST4158	pCfB1175, pCfB257, pCfB826	P_{TEF1}- > *HaTAL*, P_{PGK1}- > *At4CL1*, P_{TEF1}- > *VvVST1*, P_{TEF1}- > *ScARO7*^{G141S}, P_{PGK1}- > *ScARO4* $^{K229\ L}$, P_{TEF1}- > *ScACC1*$^{S659A,\ S1157A}$	This study
ST4159	ST4121	pCfB1175	P_{TEF1}- > *HaTAL*, P_{PGK1}- > *At4CL1*, P_{TEF1}- > *VvVST1*, P_{TEF1}- > *ScACC1*$^{S659A,\ S1157A}$	This study
ST4160	ST4159		P_{TEF1}- > *HaTAL*, P_{PGK1}- > *At4CL1*, P_{TEF1}- > *VvVST1*, P_{TEF1}- > *ScACC1*$^{S659A,\ S1157A}$, his-, leu-, ura-	This study
ST4171	ST4160	pCfB257, pCfB826	P_{TEF1}- > *HaTAL*, P_{PGK1}- > *At4CL1*, P_{TEF1}- > *VvVST1*, P_{TEF1}- > *ScARO7*^{G141S}, P_{PGK1}- > *ScARO4* $^{K229\ L}$, P_{TEF1}- > *ScACC1*$^{S659A,\ S1157A}$, ura-	This study
ST4152	ST4171	pCfB2068	Ty-(P_{TEF1}- > *HaTAL*, P_{PGK1}- > *At4CL1*, P_{TEF1}- > *VvVST1*), P_{TEF1}- > *ScARO7*^{G141S}, P_{PGK1}- > *ScARO4* $^{K229\ L}$, P_{TEF1}- > *ScACC1*$^{S659A,\ S1157A}$	This study

S. cerevisiae CEN.PK102-5B (MAT*a ura*3-52 *his*3Δ1 *leu*2-3/112 *MAL*2-8^{c} *SUC*2) (Entian and Kötter, 2007) was used for construction of resveratrol-producing strains. All the yeast strains used in this study are listed in Table 1. Yeast cells transformed with integrative plasmids were selected on synthetic complete (SC) drop-out media.

LB and SC drop-out media were made using pre-mixed powders from Sigma-Aldrich. The defined minimal medium used for fermentation in microtiter plates was described as before (Jensen et al., 2014b).

2.2. Genes and biobricks

Two genes, encoding tyrosine ammonia-lyase from *H. aurantiacus (HaTAL)* and from *Flavobacterium johnsoniae* (*FjTAL*), were described in a previous study (Jendresen et al., 2015). The genes, encoding 4-coumarate:CoA ligases from *A. thaliana* (*At4CL*1 and *At4CL*2) and stilbene synthase from *V. vinifera* (*VvVST*1) were synthesized by GeneArt (Life Technologies) in codon-optimized versions for *S. cerevisiae*. The feedback-inhibition-insensitive alleles of *ScARO4*^{K229L} (3-deoxy-D-arabino-heptulosonate-7-phosphate (DAHP) synthase) and *ScARO7*^{G141S} (chorismate mutase) were described in the previous study (Rodriguez et al., 2015). Acetyl-CoA synthase from *Salmonella enterica* (*SeACS*^{L641P}), aldehyde dehydrogenase from *S. cerevisiae* (*ScALD*6) were described in (Shiba et al., 2007). Inactivation-resistant acetyl-CoA carboxylase from *S. cerevisiae ScACC*1^{S659A,S1157A} was described in Shi et al. (2014). All the biobricks were PCR-amplified using Phu X7 polymerase (Norholm, 2010). The biobricks generated in this study are listed in Table 2 along with the template DNA and primers that were used for PCR amplification.

2.3. Plasmid and strain construction

The primers used in the study are summarized in Table 3 and the plasmids in Table 4. All the biobricks were assembled into integrative EasyClone vectors using USER cloning (Jensen et al., 2014b). The multiple integrative plasmid pCfB2068 was constructed in a different way: plasmid pCfB322 was amplified by PCR using primers Open_fw and Open_rv. Then biobricks BB293 (< -*At4CL*1), BB302 (< -P_{PGK1}-P_{TEF1}- >), and BB295 (*VvVST*1- >) were cloned into the opened pCfB322 vector following USER protocol, resulting in plasmid pCfB2067. Thereafter the plasmid pCfB2067 was PCR-amplified again by the same primers and biobricks BB429 ($T_{<\text{-}NAT5}$), BB379 (< -*HaTAL*), and BB530 ($P_{<\text{-}TDH3}$) were inserted in the same way to generate plasmid pCfB2068.

Colony PCR and sequencing was performed to confirm the correct cloning. Yeast transformations were carried out following lithium acetate protocol (Gietz and Woods, 2002). The correct genomic insertions were verified by yeast colony PCR using the primers listed in Table 3.

ST4158 and ST4160 were generated by removal of the selection markers in ST4122 and ST4159 respectively. It was performed by introducing plasmid pSH65, expressing *creA* gene under control of the P_{GAL10} promoter (Gueldener et al., 2002). Strains harboring pSH65 were grown in yeast peptone galactose medium for 12–16 h for induction and then plated on yeast peptone dextrose (YPD) agar plates. The colonies were replica-plated on SC drop-out plates to select for the colonies that have lost the markers. The loss of markers was verified by yeast colony PCR.

2.4. Determination of gene copy number by qPCR

The design of qPCR primers was conducted using the online PrimerQuest® Tool at https://eu.idtdna.com/Primerquest/Home/Index. All the primers used for qPCR in this study are listed in Supplementary Table 1.

Genomic DNA of ST4140 and ST4152 were extracted using the ZR Fungal/Bacterial DNA MiniPrep™ kit (Zymo Research) following the manufacturer's manual. The SYBR® Green qPCR MasterMix from Life Technologies was used to test for the copy number of *HaTAL*, *At4CL*1 and *VvVST*1. The housekeeping gene *ALG*9 was used as the reference. Reactions were performed in a 20 µl volume with 10 µl 2 × SYBR Green QPCR master mix, 1 µl of each upstream and downstream primer, 0.3 µl diluted reference dye and 7.7 µl gDNA containing serially diluted gDNA template (62.5–1000 pg). A no-template control reaction (NTC) for each gene was made by replacement of gDNA with nuclease-free PCR-grade water.

qPCR runs were performed in Stratagene Mx3005P instrument using the thermocycler program as follows: 10 min of pre-incubation at 95 °C followed by 40 amplification cycles of denaturation at 95 °C for 20 s, annealing and elongation at 60 °C for 22 s; and a single final cycle of 95 °C for 1 min, 55 °C for 30 s and 95 °C for 30 s.

2.5. Microtiter plate cultivation of yeast strains

Three biological transformants of each strain were inoculated in 0.5 mL SC drop-out liquid medium without histidine and leucine supplemented with 2% glucose in a 96-deep well microtiter plate with air-penetrable lid (EnzyScree, NL). The cultures were incubated at 30 °C with 250 rpm agitation for 24 h. 50 µl of the

Table 2
List of biobricks used in the study.

Biobricks	Description	Templates	Forward primers	Reverse primers
BB008	Promoter, $<\text{-}P_{TEF1}$	pCfB826	$P_{<\text{-}TEF1}$_fw	$P_{<\text{-}TEF1}$_rv
BB010	Bidirectional promoter, $<\text{-}P_{TEF1}\text{-}P_{PGK1}\text{-}>$	pCfB826	$P_{<\text{-}TEF1}$_fw	$P_{PGK1\text{-}>}$_rv
BB302	Bidirectional promoter, $<\text{-}P_{PGK1}\text{-}P_{TEF1}\text{-}>$	pCfB826	$P_{<\text{-}PGK1}$_fw	$P_{TEF1\text{-}>}$_rv
BB379	*HaTAL* from *Herpetosiphon aurantiacus*	pCBJ279	< -*HaTAL*_fw	< -*HaTAL*_rv
BB380	*FjTAL* from *Flavobacterium johnsoniae*	pCBJ280	< -*FjTAL*_fw	< -*FjTAL*_rv
BB293	*At4CL*1 from *Arabidopsis thaliana*	pCfB757	< -*At4CL*1_fw	< -*At4CL*1_rv
BB294	*At4CL*2 from *Arabidopsis thaliana*	pCfB758	< -*At4CL*2_fw	< -*At4CL*2_rv
BB295	*VvVST*1 from *Vitis vinifera*	pCfB759	*VvVST*1- > _fw	*VvVST*1- > _rv
BB304	The front part of *4CL*1::*VST*1 fusion	pCfB757	< -*At4CL*1_fw	< -*4CL*1-*VST*1_rv
BB305	The latter part of *4CL*1::*VST*1 fusion	pCfB759	< -*4CL*1-*VST*1_fw	*VvVST*1 < -_rv
BB306	The front part of *4CL*2::*VST*1 fusion	pCfB758	< -*At4CL*2_fw	*4CL*2-*VST*1 < -_rv
BB307	The latter part of *4CL*2::*VST*1 fusion	pCfB759	< -*4CL*2-*VST*1_fw	*VvVST*1 < -_rv
BB364	*ScARO4*^{K229L} from *S. cerevisiae*	pCfB826	*ScARO4*- > _fw	*ScARO4*- > _rv
BB361	*ScARO7*^{G141S} from *S. cerevisiae*	pCfB826	< -*ScARO7*_fw	< -*ScARO7*_rv
BB012	*ScACC1*$^{S659A,\ S1157A}$ from *S. cerevisiae*	p474	< -*ScACC*1_ fw	< -*ScACC*1_rv
BB530	Promoter, $<\text{-}P_{TDH3}$	Genomic DNA of CEN.PK102-5B	$P_{<\text{-}TDH3}$_fw	$P_{<\text{-}TDH3}$_rv
BB429	Terminator, $T_{<\text{-}NAT5}$	Genomic DNA of CEN.PK102-5B	$T_{<\text{-}NAT5}$_fw	$T_{<\text{-}NAT5}$_rv

seed cultures were inoculated into 0.5 mL minimal medium containing 5 mM tyrosine in a new 96-deep well plate. The minimal medium (pH 6.0) was described in (Jensen et al., 2014b). After 72 h cultivation at 30 °C with 250 rpm agitation, OD_{600} was measured with a 20 times dilution in microplate reader BioTek Synergy MX (BioTek). The remaining cultures were mixed with equal volume of absolute ethanol and centrifuged at 2272 g for 30 min. The supernatants were used to analyze resveratrol concentration by HPLC.

2.6. Batch and fed-batch fermentation of yeast strains in controlled reactors

Inoculum for bioreactors was prepared as following. Yeast strains from −80 °C glycerol stock were inoculated into 5 mL of defined minimal medium with 2% glucose as above, and incubated in 13 mL tubes at 30 °C with shaking at 250 rpm for 18 h. The whole culture volume was consequently transferred into 50 mL of fresh defined minimal medium in a 500 ml baffled shake flask and incubated at 30 °C with shaking at 250 rpm for 12 h. The culture OD_{600} was measured and reactors were inoculated with such a volume of inoculum that an initial OD_{600} of 0.02–0.05 was obtained.

Batch and fed-batch fermentations were performed in 1 L-DasGip stirrerpro® bioreactors (DasGip, Julich, Germany) with a starting volume of 0.5 L. Batch medium and medium for batch phase of fed-batch fermentation contained per 1L:30 g (batch fermentation)/40 g (fed-batch fermentation) glucose, 5 g $(NH4)_2SO_4$, 3 g KH_2PO_4, 0.5 g $MgSO_4 \cdot 7H_2O$, 2 mL trace metals solution, and 1 mL vitamin solution, where the composition of trace metals and vitamin solutions was the same as in (Jensen et al., 2014b). The medium was adjusted to pH 5.0 before autoclaving in reactors at 121 °C for 20 min. Filter-sterilized glucose, trace metal and vitamins solutions were added to the medium after autoclavation. Fed-batch medium contained 10-fold higher concentration of all the nutrients in the batch phase, except for carbon source which was replaced by 200 g L^{-1} glucose or 150 g L^{-1} ethanol in the fed-batch medium, but was otherwise prepared in the same way. The feed was started only after residual ethanol produced from the glucose phase was completely depleted. A volumetric growth rate constant-dependent feed strategy (Villadsen et al., 2011) was adopted as described in (Scalcinati et al., 2012). The fermentations were performed at 30 °C; pH was maintained at 5.0 with automatic addition of 2 M KOH or 2 M HCl. The agitation rate was kept at 800 rpm and the air flow was set to 0.5 L per min. The dissolved oxygen concentration was above 30%

Table 3
List of primers used in the study.

Name	Sequence (5′–3′)
P < -*TEF1*_fw (ID005)	ACCTGCACU TTGTAATTAAAACTTAG
P < -*TEF1*_rv (ID006)	CACGCGAU GCACACACCATAGCTTC
P*PGK1*- > _rv (ID008)	ATGACAGAU TTGTTTTATATTTGTTG
P < -*PGK1*_fw (ID1562)	ACCTGCACU TTGTTTTATATTTGTTG
P*TEF1*- > _rv (ID1565)	ATGACAGAU TTGTAATTAAAACTTAG
< -*HaTAL*_fw (ID1689)	AGTGCAGGU AAAACAATGAGCACCACCCTGATTCTG
< -*HaTAL*_rv (ID1690)	CGTGCGAU TTAGCGAAACAGAATAAT
< -*FjTAL*_fw (ID1691)	AGTGCAGGU AAAACAATGAACACCATCAACGAATATCTGAGC
< -*FjTAL*_rv (ID1692)	CGTGCGAU TTAATTGTTAATCAGGTG
< -*At4CL1*_fw (ID1548)	AGTGCAGGU AAAACAATGGCTCCACAAGAACAAGCTGTTTCC
< -*At4CL1*_rv (ID1549)	CGTGCGAU TCACAAACCGTTAGCCAA
< -*At4CL2*_fw (ID1550)	AGTGCAGGU AAAACAATGACTACCCAAGATGTTA
< -*At4CL2*_rv (ID1551)	CGTGCGAU TCAGTTCATCAAACCGTT
***VvVST1*- > _fw (ID1552)**	ATCTGTCAU AAAACAATGGCTTCCGTTGAAGAA
***VvVST1*- > _rv (ID1553)**	CACGCGAU TCAATTGGTAACGGTTGG
< -*4CL1-VST1*_rv (ID1588)	AAACCGTU AGCCAACTTGGCTC
< -*4CL1-VST1*_fw (ID1589)	AACGGTTU GGTTCTGGTGCTTCCGTTGAAGAATTCAGAAACGC
< -*VvVST1*_rv (ID1590)	CGTGCGAU TCAATTGGTAACGGTTGG
< -*4CL2-VST1*_rv (ID1591)	AGAACCGTU CATCAAACCGTTAGCC
< -*4CL2-VST1*_fw (ID1592)	AACGGTTCU GGTGCTTCCGTTGAAGAATTCAG
***ScARO4*- > _fw (ID1396)**	ATCTGTCAU AAAACA ATGAGTGAATCTCCAATGTTCG
***ScARO4*- > _rv (ID1397)**	CACGCGAU TCATTTCTTGTTAACTTCTCTTCTTTG
< -*ScARO7*_fw (ID1398)	AGTGCAGGU AAAACA ATGGATTTCACAAAACCAGAAAC
< -*ScARO7*_rv (ID1399)	CGTGCGAU TCACTCTTCCAACCTTCTTAGCAAG
< -*ScACC1*_fw (ID053)	CGTGCGAU TCATTTCAAAGTCTTCAACAATTT
< -*ScACC1*_rv (ID054)	AGTGCAGGU AAAACAATGAGCGAAGAAAGCTTA
< -*SeACS* _fw (ID1644)	AGTGCAGGU AAAACAATGTCACAAACACAC
< -*SeACS* _rv (ID1645)	CGTGCGAU TCATGATGGCATAGCAATAG
***ScALD6*- > _fw (ID738)**	ATCTGTCAU AAAACA ATGACTAAGCTACACTTTGACAC
***ScALD6*- > _rv (ID739)**	CACGCGAU TCACAACTTAATTCTGACAGCTTTTAC
Open_fw (ID1858)	AGCTGAAGCU TCGTACGCTG
Open_rv (ID2167)	ACGCGATCU TCGAGCGTCC
< -T*NAT5*_fw (ID2164)	ATCGCACGAU TTCTTAACAGATGGCTG
< -T*NAT5*_rv (ID2168)	AGATCGCGU TCGGGACCATAAAAATTC
P < -*TDH3*_fw (ID2141)	AGCTTCAGCU ATAAAAAACACGCTTTTTCAG
P < -*TDH3*_rv (ID1853)	ACCTGCACU TTTGTTTGTTTATGTGTGTTTATTC
ColPCR_DW_fw (ID2220)	CCTGCAGGACTAGTGCTGAG
Loopout_DW_fw (ID400)	ATCGCGTCAGCTGAAGCTTCGTACGC
X-2_DW_rv (ID902)	GAGAACGAGAGGACCCAACAT
X-3_DW_rv (ID904)	CCGTGCAATACCAAAATCG
X-4_DW_rv (ID906)	GACGGTACGTTGACCAGAG
XI-1_DW _rv (ID908)	GAAGACCCATGGTTCCAAGGA
XI-5_DW_rv (ID2157)	CCCAAAAGCAATCCAGGAAAAACC

Note: Underlined sequences represent overhangs used in USER cloning.

Table 4
List of plasmids used in the study.

Name	Parent plasmids	Properties	Reference
pCBJ279		*HaTAL*, Amp (ampicillin resistance)	Jendresen et al. (2015)
pCBJ280		*FjTAL*, Amp (ampicillin resistance)	Jendresen et al. (2015)
pCfB757		*At4CL1*[a], Amp (ampicillin resistance)	This study
pCfB758		*At4CL2*[a], Amp (ampicillin resistance)	This study
pCfB759		*VvVST1*[a], Amp (ampicillin resistance)	This study
p474		*ScACC1*$^{S659A,\ S1157A}$, *CaMCR*, *KlURA3*	Jensen et al. (2014a)
pSH65		P_{GAL1}-*creA*; *bleR* (phleomycin resistant)	Gueldener et al. (2002)
pCfB255		Integrative plasmid, X-2-loxP, *KlURA3*	Jensen et al. (2014b)
pCfB257		Integrative plasmid, X-3-loxP, *KlLEU2*	Jensen et al. (2014b)
pCfB258		Integrative plasmid, X-4-loxP, *SpHIS5*	Jensen et al. (2014b)
pCfB388		Integrative plasmid, XI-1-LoxP, *KlLEU2*	Jensen et al. (2014b)
pCfB391		Integrative plasmid, XI-5-LoxP, *SpHIS5*	Jensen et al. (2014b)
pCfB322		Multiple integrative plasmid, Ty4, *KlURA3*	(Maury et al., submitted for publication)
pCfB826	pCfB258	Integrative plasmid, X-4-LoxP, *SpHIS5*, BB0364(< -*ScARO7*^{G141S}), BB010(< -P_{TEF1}-P_{PGK1}- >), BB0361(*ScARO4* $^{K229\ L}$- >)	(Prado et al., submitted for publication)
pCfB854	pCfB388	Integrative plasmid, XI-1, LoxP, *KlLEU2*, BB293(< -*At4CL1*), BB302(< -P_{PGK1}-P_{TEF1}- >), BB295(*VvVST1*- >)	This study
pCfB855	pCfB388	Integrative plasmid, XI-1, LoxP, *KlLEU2*, BB294(< -*At4CL2*), BB302(< -P_{PGK1}-P_{TEF1}- >), BB295(*VvVST1*- >)	This study
pCfB856	pCfB388	Integrative plasmid, XI-1, LoxP, *KlLEU2*, BB304 ± BB305(< -*4CL1*::*VST1*), BB008(< -P_{TEF1})	This study
pCfB857	pCfB388	Integrative plasmid, XI-1, LoxP, *KlLEU2*, BB306 ± BB307(< -*4CL2*::*VST1*), BB008(< -P_{TEF1})	This study
pCfB872	pCfB391	Integrative plasmid, XI-5-LoxP, *SpHIS5*, BB379(< -*HaTAL*), BB008(< -P_{TEF1})	This study
pCfB873	pCfB391	Integrative plasmid, XI-5-LoxP, *SpHIS5*, BB380(< -*FjTAL*), BB008(< -P_{TEF1})	This study
pCfB1020	pCfB388	Integrative plasmid, XI-1-LoxP, *KlLEU2*, BB293(< -*At4CL1*), BB010(< -P_{TEF1}-P_{PGK1}- >), BB295(*VvVST1*- >)	This study
pCfB1021	pCfB388	Integrative plasmid, XI-1-LoxP, *KlLEU2*, BB294(< -*At4CL2*), BB010(< -P_{TEF1}-P_{PGK1}- >), BB295(*VvVST1*- >)	This study
pCfB1175	pCfB255	Integrative plasmid, X-2-LoxP, *KlLURA3*, BB012(< -*ScACC1*$^{S659A,\ S1157A}$), BB008(< -P_{TEF1})	This study
p380	pCfB257	Integrative plasmid, X-3-loxP, *KlLEU2*, BB119(< -*SeACS* ^{L641P}), BB010(< -P_{TEF1}-P_{PGK1}- >), BB158(*ScALD6*- >)	Jensen et al. (2014a)
pCfB1176	pCfB322	Multiple integrative plasmid, Ty4, *KlURA3*, BB379(< -*HaTAL*), BB008(< -P_{TEF1})	This study
pCfB2067	pCfB1176	Multiple integrative plasmid, Ty4, *KlURA3*, BB293(< -*At4CL1*), BB302(< -P_{PGK1}-P_{TEF1}- >), BB295(*VvVST1*- >)	This study
pCfB2068	pCfB2067	Multiple integrative plasmid, Ty4, *KlURA3*, BB429($T_{<-NAT5}$), BB379(< -*HaTAL*), BB530 ($P_{<-TDH3}$)	This study

[a] Codon optimized for *S.cerevisiae* and synthesized from GeneArt (Life Technologies).

throughout the cultivation. The DASGIP fedbatch pro® gas analysis system, equipped with gas analyzer 1 GA4 based on zirconium dioxide and two-beam infrared sensor (DASGIP), was employed for monitoring oxygen and carbon dioxide concentration. Samples were taken at regular intervals to measure OD_{600}. Supernatants were stored at −20 °C until HPLC analysis for organic acids, glycerol, ethanol, and residual glucose. Another portion of sample was mixed with an equal volume of absolute ethanol and centrifuged at 12,000 rpm for 2 min. The supernatant was stored at −20 °C until HPLC analysis for resveratrol and *p*-coumaric acid.

2.7. Analytical methods

The OD_{600} was measured on a Genesys 20 Spectrophotometer (Thermo Scientific). The HPLC quantification of glucose, glycerol, ethanol, succinate, and pyruvate was performed as before (Ostergaard et al., 2000). Resveratrol and *p*-coumaric acid were quantified on HPLC (Thermo) equipped with a Discovery HS F5 150 mm × 2.1 mm column (particle size 3 μm). The eluent flow rate was 1.5 mL min^{-1}. Linear gradient from 5% to 60% of solvent A over 0.5–9.5 min was used. Solvent A was 10 mM ammonium formate (pH 3.0, adjusted by formic acid). Solvent B was acetonitrile. Resveratrol was detected by absorbance at 304 nm with a retention time of 6.4 min and *p*-coumaric acid at 277 nm of 4.7 min. Resveratrol and *p*-coumaric acids concentrations were calculated from the standard curves, and both resveratrol and *p*-coumaric acid standards were purchased from Sigma-Aldrich.

3. Results

3.1. Reconstruction of resveratrol biosynthetic pathway from tyrosine precursor

Our previous study showed that tyrosine ammonia-lyases from *H. aurantiacus* and *Flavobacterium johnsoniae* have high activity in yeast (Jendresen et al., 2015). By over-expressing *HaTAL* (ST4121) and *FjTAL* (ST4128) in *S. cerevisiae*, we obtained respectively 7.04 ± 2.03 and 13.71 ± 2.14 mg L^{-1} of *p*-coumaric acid in minimal medium supplemented with 5 mM tyrosine (Fig. 2A and B). Two versions of 4-coumarate:CoA ligase from *A. thaliana* (*At4CL1* and *At4CL2*) and stilbene synthase from *V. vinifera* (*VvVST1*) were then introduced under control of strong constitutive promoters in order to convert *p*-coumaric acid into resveratrol. Contrarily to *p*-coumaric acid results, the highest titers were obtained in the strains carrying *HaTAL*. *At4CL1* consistently resulted in slightly higher resveratrol titers than *At4CL2*. The highest titer of 11.66 ± 0.57 mg L^{-1} resveratrol was obtained in ST4122, over-expressing *HaTAL and VvVST1* under P_{TEF1} promoters and *At4CL1* under P_{PGK1} promoter. When the direction of the double promoter was reversed, so that *At4CL1* was under control of the P_{TEF1} promoter and *VvVST1* under control of P_{PGK1} promoter, resveratrol titer dropped to 4.48 ± 0.22 to mg L^{-1} (ST4123). This result underlines the importance of balancing gene expression in the pathway. To reduce loss of pathway intermediates and improve turnover rates due to higher local substrate concentration, fusing related enzymes is a promising strategy (Li and Borodina, 2015). Fusion of two enzymes, At4CL1 and VvVST1, was previously reported to improve resveratrol production due to metabolic channeling

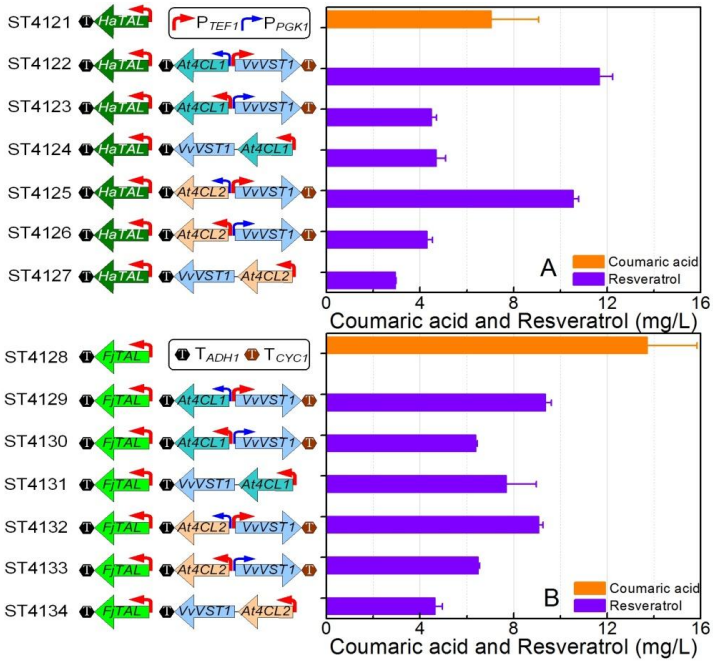

Fig. 2. Microbial production of resveratrol from tyrosine. Strains carrying *HaTAL* from *H. aurantiacus* (A) and *FjTAL* from *F. johnsoniae* (B) together with different combinations of *At4CL1* and *VvVST1* were grown in minimal medium with 20 g L^{-1} glucose and 5 mM tyrosine and the cultures were sampled at 72 h of cultivation. Strains ST4124, ST4127, ST4131, and ST4134 over-express fusions of *At4CL1* and *VvVST* genes. The displayed average values ± standard deviations were calculated from three biological replicates.

(Zhang et al., 2006). We also attempted expressing the fusion of the two proteins, linked by Gly–Ser–Gly linker, in ST4124. This however led to a lower resveratrol titer of 4.69 ± 0.39 mg L^{-1} so we did not pursue this strategy further.

3.2. *De novo* biosynthesis of resveratrol from glucose

It was observed that *p*-coumaric acid production continued in batch cultures after the supplemented tyrosine had been consumed, thus indicating that at least a fraction of *p*-coumaric acid was produced *de novo* from glucose or ethanol (Jendresen et al., 2015). To investigate if resveratrol also can be produced directly from glucose and also to test the effect of precursor improvement, we cultivated the strain ST4135 (analogous to ST4122) with the resveratrol pathway (*HaTAL*, *At4CL1* and *VvVST1*) in a minimal medium with glucose as the only carbon source. Fermentation of ST4135 resulted in 2.73 ± 0.05 mg L^{-1} resveratrol from 30 g L^{-1} glucose (Fig. 3A). Interestingly, resveratrol was primarily produced during the ethanol consumption phase, which indicates that during growth on glucose the fluxes towards resveratrol precursors, tyrosine and malonyl-CoA, were low.

The aromatic amino acids are the least abundant amino acids in the *S. cerevisiae* cell, with intracellular concentrations of tyrosine and phenylalanine being as low as 0.5 and 0.6 mM, respectively (Braus, 1991). The biosynthesis of aromatic amino acid is strongly regulated, both at the transcriptional and posttranscriptional levels. In order to improve the flux towards tyrosine, we over-expressed feedback-inhibition resistant versions of DAHP synthase ScAro4p^{K229L} and chorismate mutase ScAro7p^{G141S}. This resulted in a 78%-improvement of resveratrol titer in batch cultures compared with that of the strain ST4135 harboring only the resveratrol pathway, i.e. 4.85 ± 0.31 mg L^{-1} resveratrol was obtained (Fig. 3B).

Another precursor for resveratrol biosynthesis is malonyl-CoA. Thus, 3 molecules of malonyl-CoA are necessary for biosynthesis of 1 molecule of resveratrol. In *S. cerevisiae*, malonyl-CoA is synthesized in the cytosol by acetyl-CoA carboxylase (ScAcc1p). The acetyl-CoA carboxylase can be phosphorylated by the sucrose non-fermenting protein 1 (Snf1p) and thus targeted for degradation, which leads to decreased activity of this enzyme in the cell (Shirra et al., 2001). A double mutation of Acc1p protein at Ser659 and Ser1157 positions could abolish the phosphorylation (Shi et al., 2014). We over-expressed the inactivation-resistant version of acetyl-CoA carboxylase (ScAcc1p$^{S659A,\ S1157A}$) in resveratrol-producing yeast, which gave 3.57 ± 0.18 mg L^{-1} resveratrol, corresponding to a 31% improvement in comparison with ST4135 (Fig. 3C). Finally, we combined over-expression of *ScARO4*^{K229L}, *ScARO7*^{G141S}, and *ScACC1*$^{S659A,\ S1157A}$ genes in strain ST4140, which improved resveratrol titer by 234% to 6.39 ± 0.03 mg L^{-1} (Fig. 3D).

In order to further improve the flux towards acetyl-CoA, we also attempted over-expression of acetyl-CoA synthase (SeACS^{L641P}) from *Salmonella enterica* and aldehyde dehydrogenase ScAld6, in various combinations with ScAro4p^{K229L} and ScAro7p^{G141S} or ScAcc1p$^{S659A,\ S1157A}$. Surprisingly no improvement was obtained (Supplementary Fig. S1). Further investigation is needed to determine the reason for the negative effect of this modification (Fig. 4)

3.3. Increasing resveratrol production via integration of multiple copies of resveratrol pathway

We hypothesized that the low activity of the resveratrol biosynthetic pathway may be limiting resveratrol biosynthesis. We therefore introduced multiple copies of the genes *HaTAL*, *At4CL1* and *VvVST1* into a strain, over-expressing *ScARO4*^{K229L}, *ScARO7*^{G141S}, and *ScACC1*$^{S659A,\ S1157A}$. The multicopy integration was achieved by using

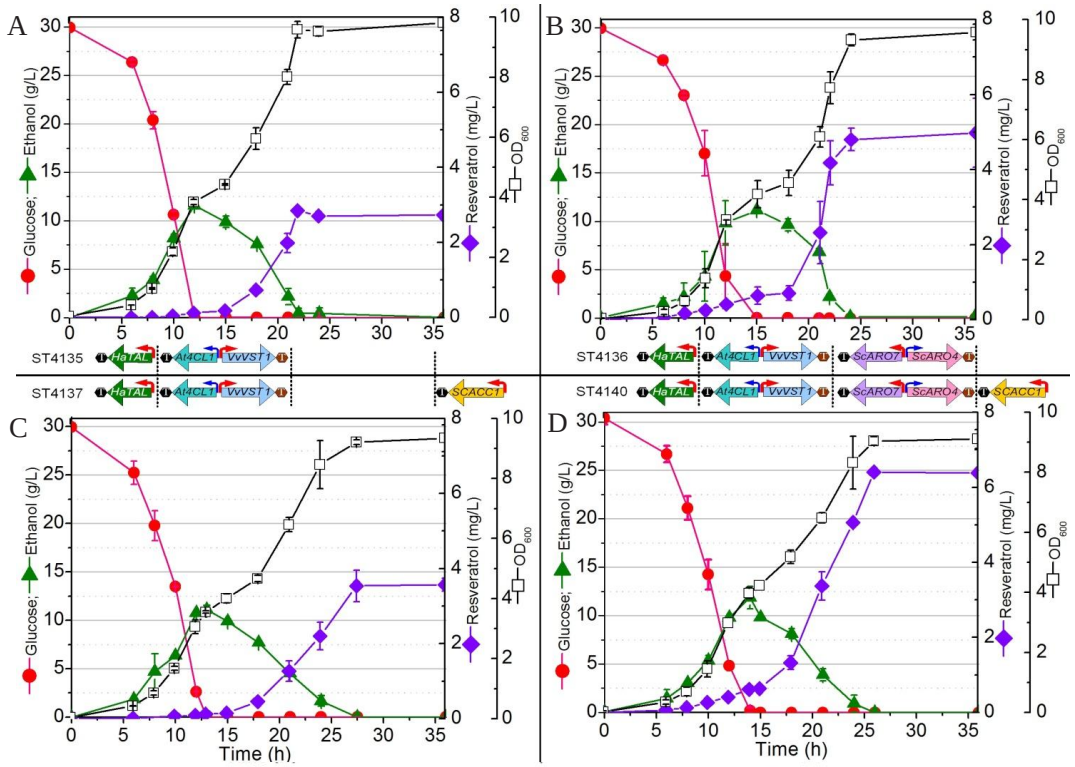

Fig. 3. Microbial production of resveratrol from glucose. The strains were cultivated on minimal medium with 30 g L^{-1} glucose in bioreactors. (A) ST4135, the reference strain expressing *HaTAL*, *At4CL*1 and *VvVST*1; (B) ST4136, over-expressing $ScARO4^{K229L}$ and $ScARO7^{G141S}$. (C) ST41222, over-expressing $ScACC1^{S659A,\ S1157A}$, (D) ST4140, over-expressing $ScARO4^{K229L}$, $ScARO7^{G141S}$ and $ScACC1^{S659A,\ S1157A}$. The displayed average values ± standard deviations were calculated from two biological replicates.

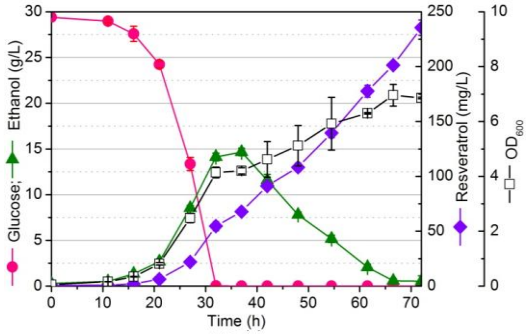

Fig. 4. Optimization of resveratrol pathway by multiple integrations of genes. Multiple integrative plasmid p2068 carrying *HaTAL*, *At4CL*1, and *VvVST*1 was integrated onto Ty4 elements of $ScARO4^{K229L}$, $ScARO7^{G141S}$ and $ScACC1^{S659A,\ S1157A}$ over-expressing strain. The strain was grown on defined minimal medium with 30 g L^{-1} glucose in batch bioreactors. The displayed average values ± standard deviations were calculated from two biological replicates.

an integrative vector that targets Ty4 retrotransposons (Maury et al., submitted for publication). As the transformants were expected to integrate different copy numbers of the expression vector, we randomly screened 8 transformants to select the best producer, named ST4152. The copy number of the genes in the strain ST4152 was identified to be 8.43 ± 0.85 for *HaTAL*, 8.64 ± 1.60 for *At4CL*1, and 11.16 ± 1.23 for *VvVST*1 respectively by qPCR.

The strain ST4152 had a longer lag phase and lower biomass accumulation than the strain ST4140 in batch fermentation. However, the resveratrol titer in both the glucose and ethanol phases was greatly improved (Table 5). The final titer was 235.57 ± 7.00 mg L^{-1}, 36-fold higher than in the parent strain ST4140.

3.4. Resveratrol production in fed-batch fermentation

As resveratrol primarily accumulated after glucose depletion in batch cultivations, we carried out fed-batch cultivations with feeding of glucose or ethanol. The batch phase was on 40 g L^{-1} glucose, once all carbon sources were consumed, the carbon-limited feeding of glucose or ethanol was initiated. The strain ST4152 produced around 200 mg L^{-1} in the batch phase. In the glucose feeding phase, 222.08 mg L^{-1} additional resveratrol was accumulated on the feeding of 15.93 g L^{-1} glucose (Fig. 5) and resulted in a final titer of 415.65 mg L^{-1} resveratrol. In the ethanol feeding phase, 333.57 mg L^{-1} resveratrol was additionally produced from 16.63 g L^{-1} ethanol resulting in a final titer of 531.41 mg L^{-1} resveratrol. Small amounts of acetate and glycerol and no other by-products, such as *p*-coumaric acid or succinate were detected during the fed-batch process.

Table 5
Comparison of resveratrol titers and kinetic parameters obtained from different resveratrol producing strains in batch cultivations.

		ST4135	ST4136	ST41222	ST4140	ST4152
μ_{max} (h^{-1})	Glucose phase	0.40 ± 0.01	0.35 ± 0.03	0.36 ± 0.01	0.33 ± 0.04	0.15 ± 0.02
	Ethanol phase	0.10 ± 0.00	0.09 ± 0.01	0.08 ± 0.01	0.07 ± 0.02	0.018 ± 0.00
Production (mg L^{-1})	Glucose phase	0.11 ± 0.00	0.64 ± 0.23	0.13 ± 0.02	0.62 ± 0.00	61.69 ± 8.72
	Ethanol phase	2.73 ± 0.11	4.34 ± 0.68	3.41 ± 0.40	6.01 ± 0.44	172.04 ± 13.12
Yield (mg g^{-1}glucose)	Glucose phase	0.00 ± 0.00	0.02 ± 0.01	0.00 ± 0.00	0.02 ± 0.00	2.10 ± 0.30
(mg g^{-1}ethanol)	Ethanol phase	0.25 ± 0.00	0.39 ± 0.06	0.31 ± 0.05	0.51 ± 0.01	12.14 ± 1.02
Productivity (mg (L^{-1} h^{-1}))	Glucose phase	0.01 ± 0.00	0.05 ± 0.01	0.01 ± 0.00	0.04 ± 0.00	1.67 ± 0.24
	Ethanol phase	0.27 ± 0.01	0.39 ± 0.06	0.24 ± 0.03	0.25 ± 0.02	4.92 ± 0.37

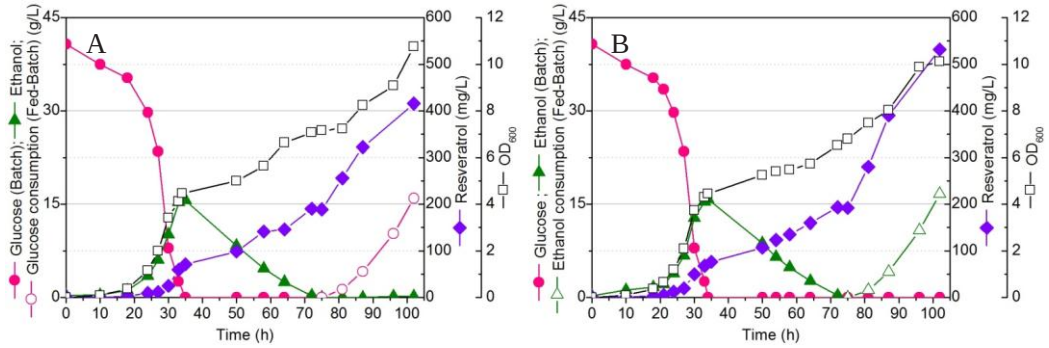

Fig. 5. Fed-batch fermentation of the optimized resveratrol-producing strain ST4152. Aerobic fed-batch fermentations were carried out by feeding glucose (A) or ethanol (B) respectively following carbon source-limited feeding strategy. The cultivations were performed in duplicates (Supplementary Fig. S2); here representative graphs are shown.

4. Discussion

In the previous studies resveratrol production was achieved by supplementing *p*-coumaric acid (Becker et al., 2003; Beekwilder et al., 2006; Shin et al., 2011; Sydor et al., 2010; Wang and Yu, 2012), which is an expensive precursor. Besides, tyrosine or phenylalanine were also used as the substrates for resveratrol production (Trantas et al., 2009; Zhang et al., 2006). Also several previous studies described resveratrol production without supplementation of precursor, but in SC-dropout (Wang et al., 2011) or Yeast extract-Peptone-Galactose (Shin et al., 2012) media, which contain tyrosine and phenylalanine. This study, for the first time, demonstrates *de novo* microbial production of resveratrol from cheap carbon source (glucose or ethanol) in a minimal medium. We chose *TAL* instead of *PAL* for the first step of resveratrol biosynthesis pathway (deamination from tyrosine or phenylalanine), thus by-passing the P450-dependent step. Although previous studies failed in producing resveratrol via the TAL-dependent pathway in yeast (Zhang et al., 2006), our study shows that it is possible to construct a high-level resveratrol producing yeast based on the TAL route. The resveratrol production of 530 mg L^{-1} obtained in this study, to our knowledge, is the highest level reported in yeast.

This study adopted a push and pull strategy by increasing precursor supply and multiple integration of resveratrol pathway to improve resveratrol production. Aromatic amino acids were shown to have feedback inhibition on the shikimate pathway (Koopman et al., 2012; Luttik et al., 2008). Deregulation of feedback inhibition is a general way to improve production of aromatic amino acids derivatives. This has been corroborated by overexpression of aromatic amino acids-insensitive *ARO*4 and *ARO*7 alleles in several studies. Koopman et al. overexpressed feedback-insensitive allele of *ARO*4 (*ARO*4^{G226S}), which led to 2-fold increase of naringenin in *S. cerevisiae* (Koopman et al., 2012). Another study by Curran *et al.* improved muconic acid production by 50%, when overexpressing tyrosine insensitive *ARO*4 allele (*ARO*4^{K229L}) in *S. cerevisiae* (Curran et al., 2013). By combining overexpression of the feedback insensitive alleles of *ARO*4 and *ARO*7 (*ARO*4^{K229L} and *ARO*7^{G141S}), Luttik et al. obtained 200-fold increase of the extracellular aromatic amino acids concentration (Luttik et al., 2008). Thus, the 78% increase of resveratrol we observed upon overexpression of *ARO*4^{K229L} and *ARO*7^{G141S} is consistent with these studies. Supply of the other precursor, malonyl-CoA, catalyzed by Acc1p was a well-known limiting step in the fatty acids biosynthesis pathway due to posttranslational regulation by Snf1 protein kinase (Tehlivets et al., 2007). Shi et al. found that the phosphorylation of Acc1p by Snf1 could be diminished by site-directed mutagenesis at Ser659 and Ser1157 positions (Shi et al., 2014). Overexpression of *ACC*1^{S659A,S1157A} in engineered *S. cerevisiae* resulted in 3-fold increase of fatty acid ethyl esters production and more than 3.5-fold improvement of 3-hydroxypropionic acid titer (Shi et al., 2014). The 31% improvement was obtained in this study, when we overexpressed *ACC*1^{S659A,S1157A} in the engineered strain. However, it was surprising that further overexpressing *ALD*6 and *SeACS*^{L641P}, which was previously shown to enhance acetyl-CoA flux (Shiba et al., 2007), decreased resveratrol production. We suppose that in the strain with a single copy of resveratrol biosynthesis pathway the flux control resided mainly with the downstream of the pathway and therefore the push strategies had only a limited effect. In case of *ALD*6 and *SeACS*^{L641P} overexpression, the negative result was possibly due to the effect of acetyl-CoA overproduction, which exhibits genome-wide regulatory effects (Shi and Tu, 2013; Zhang et al., 2013) and may also divert to other products than resveratrol especially in glucose consuming phase. In future studies it would be interesting to

investigate the effect of increased acetyl-CoA supply in a strain carrying multiple copies of resveratrol biosynthesis.

High level-expression of the flux controlling enzymes in the pathway is a common solution to a low enzymatic activity problem. We chose to integrate multiple copies of the resveratrol biosynthetic genes into yeast chromosomes as a pull strategy. In comparison to the high-copy number episomal vectors, e.g., 2μ-based vectors, integration results in better strain stability. A 36-fold improvement in titer was achieved in this study when three genes, *HaTAL*, *At4CL*1 and *VvVST*1, were integrated in multiple copies. This finding highlights that indeed the resveratrol flux was limited by the activity of the biosynthetic enzymes. At the same time, the strain fitness decreased, manifested by a longer lag phase, lower maximum specific growth rate and lower biomass yield on glucose. This could be expected as multiple integration of several genes likely resulted in high metabolic burden for the cell. A solution to the problem could be replacement of constitutive promoters with regulated ones for control of the resveratrol biosynthesis pathway, e.g., one could use a glucose-repressed P_{HXT7} promoter, so the resveratrol biosynthesis is first turned on in the fed-batch phase after sufficient biomass has been accumulated in the batch phase. Moreover, the observation that resveratrol primarily accumulated in the ethanol phase of batch fermentation inspired us to use ethanol feed for fed-batch fermentation. An ethanol pulse feed strategy was also successfully applied earlier for amorphadiene production (Westfall et al., 2012).

Developing a high-producing microbial strain for industrial production of resveratrol is a serious metabolic engineering challenge. In our study, we implemented the push strategies first, followed by the pull strategy. Retrospectively, it would be better to do it the other way around. Future development of the cell factory may include optimization of activities of the resveratrol biosynthetic genes (via enzyme engineering, protein scaffolding or expression level balancing), further improvement of precursor supply, improvement of reducing co-factor (NADPH) supply, eliminating product degradation (Koopman et al., 2012), decoupling of growth and production phases, and other rational designs. Additionally genome-scale modeling or –omic data can be used to predict non-intuitive metabolic engineering strategies (Curran et al., 2013; Gold et al., 2015).

5. Conclusions

There is an increasing demand for resveratrol in the pharmaceutical, food and cosmetic industries. Production of resveratrol from a cheap carbon source by microbial fermentation is attractive due to short process time, reduction of production costs, reliable supply and high purity, when compared to the extraction from plant materials. In this study we constructed the resveratrol pathway via tyrosine intermediate in *S. cerevisiae* and for the first time demonstrated the possibility of *de novo* resveratrol biosynthesis from glucose. By step-wise metabolic engineering, targeted towards improvement of precursor supply and increased expression of the biosynthetic genes, we obtained an optimized strain, which produced around 0.5 g L^{-1} resveratrol in fed-batch fermentation on a minimal medium. This strain represents a good basis for development of microbial resveratrol production process.

Author contributions

M.L., I.B. and J.N. conceived the study. M.L., K.R.K. and I.B designed the experiments. M.L. performed most of the experimental work and A.R. performed parts of the experimental work. M.L., Y.C., I.B., and J.N. analyzed the results. M.L., I.B., and J.N. wrote the manuscript.

Competing financial interests

The authors declare no competing financial interests.

Acknowledgments

This work was financed by the Novo Nordisk Foundation. We thank Dr. Christian Bille Jendresen for providing the *TAL* genes and Mette Kristensen and Julia Karlsson for assistance with HPLC analysis.

Appendix A. Supplementary material

Supplementary data associated with this article can be found in the online version at http://dx.doi.org/10.1016/j.ymben.2015.08.007.

References

Becker, J.V., Armstrong, G.O., van der Merwe, M.J., Lambrechts, M.G., Vivier, M.A., Pretorius, I.S., 2003. Metabolic engineering of *Saccharomyces cerevisiae* for the synthesis of the wine-related antioxidant resveratrol. FEMS Yeast Res. 4, 79–85.
Beekwilder, J., Wolswinkel, R., Jonker, H., Hall, R., de Vos, C.H., Bovy, A., 2006. Production of resveratrol in recombinant microorganisms. Appl. Environ. Microbiol. 72, 5670–5672.
Blount, J.W., Korth, K.L., Masoud, S.A., Rasmussen, S., Lamb, C., Dixon, R.A., 2000. Altering expression of cinnamic acid 4-hydroxylase in transgenic plants provides evidence for a feedback loop at the entry point into the phenylpropanoid pathway. Plant Physiol. 122, 107–116.
Bolwell, G.P., Mavandad, M., Millar, D.J., Edwards, K.J., Schuch, W., Dixon, R.A., 1988. Inhibition of mRNA levels and activities by *trans*-cinnamic acid in elicitor-induced bean cells. Phytochemistry 27, 2109–2117.
Borodina, I., Nielsen, J., 2014. Advances in metabolic engineering of yeast *Saccharomyces cerevisiae* for production of chemicals. Biotechnol. J. 9, 609–620.
Braus, G.H., 1991. Aromatic amino acid biosynthesis in the yeast *Saccharomyces cerevisiae*: a model system for the regulation of a eukaryotic biosynthetic pathway. Microbiol. Rev. 55, 349–370.
Curran, K.A., Leavitt, J.M., Karim, A.S., Alper, H.S., 2013. Metabolic engineering of muconic acid production in *Saccharomyces cerevisiae*. Metab. Eng. 15, 55–66.
Entian, K.-D., Kötter, P., 2007. 25 Yeast genetic strain and plasmid collections. Method Microbiol. 36, 629–666.
Gietz, R.D., Woods, R.A., 2002. Transformation of yeast by lithium acetate/single-stranded carrier DNA/polyethylene glycol method. Methods Enzymol. 350, 87–96.
Gold, N.D., Gowen, C.M., Lussier, F.X., Cautha, S.C., Mahadevan, R., Martin, V.J., 2015. Metabolic engineering of a tyrosine-overproducing yeast platform using targeted metabolomics. Microb. Cell Fact. 14, 73.
Gueldener, U., Heinisch, J., Koehler, G.J., Voss, D., Hegemann, J.H., 2002. A second set of loxP marker cassettes for Cre-mediated multiple gene knockouts in budding yeast. Nucleic Acids Res. 30, e23.
Jeandet, P., Delaunois, B., Aziz, A., Donnez, D., Vasserot, Y., Cordelier, S., Courot, E., 2012. Metabolic engineering of yeast and plants for the production of the biologically active hydroxystilbene, resveratrol. J. Biomed. Biotechnol. 2012, 579089.
Jendresen, C.B., Stahlhut, S.G., Li, M., Gaspar, P., Siedler, S., Forster, J., Maury, J., Borodina, I., Nielsen, A.T., 2015. Novel highly active and specific tyrosine ammonia-lyases from diverse origins enable enhanced production of aromatic compounds in bacteria and yeast. Appl. Environ. Microbiol. 81, 4458–4476.
Jensen N.B., Borodina I., Chen Y., Maury J., Kildegaard, K.R., Förster J. and Nielsen J., Microbial Production of 3-Hydroxypropionic Acid, (Patent number WO 2014/198831 A1) 2014, https://www.lens.org/lens/patent/WO_2014_198831_A1.
Jensen, N.B., Strucko, T., Kildegaard, K.R., David, F., Maury, J., Mortensen, U.H., Forster, J., Nielsen, J., Borodina, I., 2014b. EasyClone: method for iterative chromosomal integration of multiple genes in *Saccharomyces cerevisiae*. FEMS Yeast Res. 14, 238–248.
Koopman, F., Beekwilder, J., Crimi, B., van Houwelingen, A., Hall, R.D., Bosch, D., van Maris, A.J., Pronk, J.T., Daran, J.M., 2012. De novo production of the flavonoid naringenin in engineered *Saccharomyces cerevisiae*. Microb. Cell Fact. 11, 155.

Kumar, S., Omer, S., Chitransh, S., Khan, B.M., 2012. Cinnamate 4-hydroxylase downregulation in transgenic tobacco alters transcript level of other phenylpropanoid pathway genes. Int. J. Adv. Biotechnol. Res. 3, 545–557.
Li, M., Borodina, I., 2015. Application of synthetic biology for production of chemicals in yeast *Saccharomyces cerevisiae*. FEMS Yeast Res. 14, 1–5.
Luttik, M.A., Vuralhan, Z., Suir, E., Braus, G.H., Pronk, J.T., Daran, J.M., 2008. Alleviation of feedback inhibition in *Saccharomyces cerevisiae* aromatic amino acid biosynthesis: quantification of metabolic impact. Metab. Eng. 10, 141–153.
Mei, Y.Z., Liu, R.X., Wang, D.P., Wang, X., Dai, C.C., 2015. Biocatalysis and biotransformation of resveratrol in microorganisms. Biotechnol. Lett. 37, 9–18.
Norholm, M.H., 2010. A mutant Pfu DNA polymerase designed for advanced uracil-excision DNA engineering. BMC Biotechnol. 10, 21.
Ostergaard, S., Olsson, L., Nielsen, J., 2000. Metabolic engineering of *Saccharomyces cerevisiae*. Microbiol. Mol. Biol. Rev. 64, 34–50.
Poulsen, M.M., Jorgensen, J.O., Jessen, N., Richelsen, B., Pedersen, S.B., 2013. Resveratrol in metabolic health: an overview of the current evidence and perspectives. Ann. N.Y. Acad. Sci. 1290, 74–82.
Rodriguez, A., Kildegaard, K.R., Li, M., Borodina, I., Nielsen, J., 2015. Establishment of a yeast platform strain for production of p-coumaric acid through metabolic engineering of aromatic amino acid biosynthesis. Metab. Eng. 31, 181–188.
Scalcinati, G., Knuf, C., Partow, S., Chen, Y., Maury, J., Schalk, M., Daviet, L., Nielsen, J., Siewers, V., 2012. Dynamic control of gene expression in *Saccharomyces cerevisiae* engineered for the production of plant sesquitepene alpha-santalene in a fed-batch mode. Metab. Eng. 14, 91–103.
Shi, L., Tu, B.P., 2013. Acetyl-CoA induces transcription of the key G1 cyclin CLN3 to promote entry into the cell division cycle in *Saccharomyces cerevisiae*. Proc. Natl. Acad. Sci. USA 110, 7318–7323.
Shi, S., Chen, Y., Siewers, V., Nielsen, J., 2014. Improving production of malonyl coenzyme A-derived metabolites by abolishing Snf1-dependent regulation of Acc1. MBio 5, e01130-14.
Shiba, Y., Paradise, E.M., Kirby, J., Ro, D.K., Keasling, J.D., 2007. Engineering of the pyruvate dehydrogenase bypass in *Saccharomyces cerevisiae* for high-level production of isoprenoids. Metab. Eng. 9, 160–168.
Shin, S.Y., Han, N.S., Park, Y.C., Kim, M.D., Seo, J.H., 2011. Production of resveratrol from p-coumaric acid in recombinant *Saccharomyces cerevisiae* expressing 4-coumarate:coenzyme A ligase and stilbene synthase genes. Enzy. Microb. Technol. 48, 48–53.
Shin, S.Y., Jung, S.M., Kim, M.D., Han, N.S., Seo, J.H., 2012. Production of resveratrol from tyrosine in metabolically engineered *Saccharomyces cerevisiae*. Enzy. Microb. Technol. 51, 211–216.
Shirra, M.K., Patton-Vogt, J., Ulrich, A., Liuta-Tehlivets, O., Kohlwein, S.D., Henry, S.A., Arndt, K.M., 2001. Inhibition of acetyl coenzyme A carboxylase activity restores expression of the INO1 gene in a snf1 mutant strain of *Saccharomyces cerevisiae*. Mol. Cell Biol. 21, 5710–5722.
Srinivas, G., Babykutty, S., Sathiadevan, P.P., Srinivas, P., 2007. Molecular mechanism of emodin action: transition from laxative ingredient to an antitumor agent. Med. Res. Rev. 27, 591–608.
Sydor, T., Schaffer, S., Boles, E., 2010. Considerable increase in resveratrol production by recombinant industrial yeast strains with use of rich medium. Appl. Environ. Microbiol. 76, 3361–3363.
Tehlivets, O., Scheuringer, K., Kohlwein, S.D., 2007. Fatty acid synthesis and elongation in yeast. Biochim. Biophys. Acta 1771, 255–270.
Trantas, E., Panopoulos, N., Ververidis, F., 2009. Metabolic engineering of the complete pathway leading to heterologous biosynthesis of various flavonoids and stilbenoids in *Saccharomyces cerevisiae*. Metab. Eng. 11, 355–366.
Villadsen J., Nielsen J. and Lidén G., Bioreaction Engineering Principles, 2011, Springer, New York, Dordrecht, Heidelberg, London, Library of Congress Control Number: 2011931856 Springer Science+Business Media, LLC 2011, http://dx.doi.org/10.1007/978-1-4419-9688-6.
Wang, Y., Halls, C., Zhang, J., Matsuno, M., Zhang, Y., Yu, O., 2011. Stepwise increase of resveratrol biosynthesis in yeast *Saccharomyces cerevisiae* by metabolic engineering. Metab. Eng. 13, 455–463.
Wang, Y., Yu, O., 2012. Synthetic scaffolds increased resveratrol biosynthesis in engineered yeast cells. J. Biotechnol. 157, 258–260.
Westfall, P.J., Pitera, D.J., Lenihan, J.R., Eng, D., Woolard, F.X., Regentin, R., Horning, T., Tsuruta, H., Melis, D.J., Owens, A., Fickes, S., Diola, D., Benjamin, K.R., Keasling, J.D., Leavell, M.D., McPhee, D.J., Renninger, N.S., Newman, J.D., Paddon, C.J., 2012. Production of amorphadiene in yeast, and its conversion to dihydroartemisinic acid, precursor to the antimalarial agent artemisinin. Proc. Natl. Acad. Sci. USA 109, E111–E118.
Yan, Y., Kohli, A., Koffas, M.A., 2005. Biosynthesis of natural flavanones in *Saccharomyces cerevisiae*. Appl. Environ. Microbiol. 71, 5610–5613.
Zhang, M., Galdieri, L., Vancura, A., 2013. The yeast AMPK homolog SNF1 regulates acetyl coenzyme A homeostasis and histone acetylation. Mol. Cell Biol. 33, 4701–4717.
Zhang, Y., Li, S.Z., Li, J., Pan, X., Cahoon, R.E., Jaworski, J.G., Wang, X., Jez, J.M., Chen, F., Yu, O., 2006. Using unnatural protein fusions to engineer resveratrol biosynthesis in yeast and Mammalian cells. J. Am. Chem. Soc. 128, 13030–13031.

Supplementary information

Supplementary Table 1. Primers for qPCR

Name	Sequence (5' to 3')
*ALG9*_fw (ID434)	CACGGATAGTGGCTTTGGTGAACAATTAC
*ALG9*_rv (ID435)	TATGATTATCTGGCAGCAGGAAAGAACTTGGG
*HaTAL*_fw (ID 13219)	GCAGTTTCTGGGTCCGATTAT
*HaTAL*_rv (ID 13220)	CGGTATCAATCAGCGGGTTATC
*At4CL1*_fw (ID 13209)	GTACTTCCACTCCGATGATGTC
*At4CL1*_rv (ID 13210)	AGCAGCACCAACTCTCAAA
*VvVST1*_fw (ID 13213)	CGAAGTTCCAAGATTGGGTAGA
*VvVST1*_rv (ID 13214)	CAACACCAGAGGTAGTACAGAAA

Supplementary Figure 1. Microbial production of resveratrol from tyrosine. Strains with different gene over-expression combinations were grown in 0.5 mL minimal medium with 20 g L^{-1} glucose in 96-deep well microtiter plates and the cultures were sampled at 72 h of cultivation. The displayed average values ± standard deviations were calculated from three biological replicates.

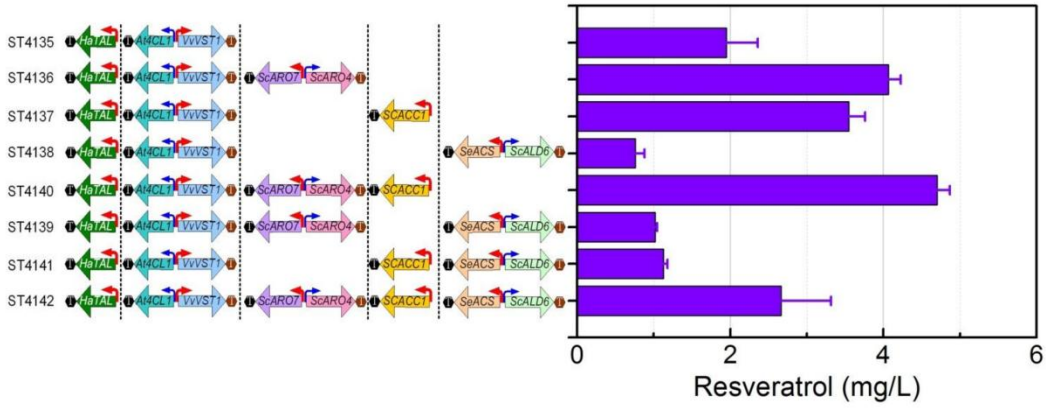

Supplementary Figure 2. A replicate of fed-batch fermentation of the optimized resveratrol-producing strain ST4152. Aerobic fed-batch fermentations were carried out by feeding glucose (A) or ethanol (B) respectively following carbon source-limited feeding strategy. The cultivations were performed in duplicates; here the replicates of fermentations from Figure 5 are shown.

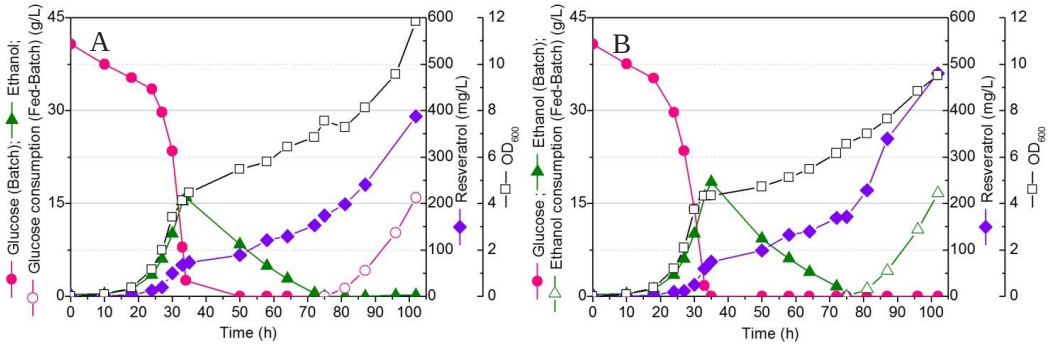

CHAPTER 5 Engineering yeast for high-level production of stilbenoid antioxidants

Mingji Li[1], Konstantin Schneider[1], Mette Kristensen[1], Irina Borodina[1] & Jens Nielsen[1,2,3*]

ABSTRACT

Stilbenoids, including resveratrol and its methylated derivatives, are natural potent antioxidants, produced by some plants in trace amounts as defense compounds. Extraction of stilbenoids from natural sources is costly due to their low abundance and often limited availability of the plant. Here we engineered the yeast *Saccharomyces cerevisiae* for production of stilbenoids on a simple mineral medium typically used for industrial production. We applied a pull-push-block strain engineering strategy that included overexpression of the resveratrol biosynthesis pathway, optimization of the electron transfer to the cytochrome P450 monooxygenase, increase of the precursors supply, and decrease of the pathway intermediates degradation. Fed-batch fermentation of the final strain resulted in a final titer of 800 mg l^{-1} resveratrol, which is by far the highest titer reported to date for production of resveratrol from glucose. We further integrated heterologous methyltransferases into the resveratrol platform strain and hereby demonstrated for the first time *de novo* biosynthesis of pinostilbene and pterostilbene, which have better stability and uptake in the human body, from glucose.

Key words: resveratrol; phenylalanine; metabolic engineering; pinostilbene; pterostilbene; *Saccharomyces cerevisiae*

---

[1] The Novo Nordisk Foundation Center for Biosustainability, Technical University of Denmark, DK-2970 Hørsholm, Denmark

[2] Department of Biology and Biological Engineering, Chalmers University of Technology, SE-41296 Gothenburg, Sweden

[3] The Novo Nordisk Foundation Center for Biosustainability, Chalmers University of Technology, SE-41296 Gothenburg, Sweden

*email: nielsenj@chalmers.se

INTRODUCTION

Resveratrol (3, 5, 4'-trihydroxystilbene) is a natural plant defense compound with strong antioxidant activity. The therapeutical effects of resveratrol in humans are not documented in terms of mode of action and molecular target, but there are several reports on its efficacy for treatment of cardiovascular diseases (Catalgol *et al.*, 2012; Kopp, 1998; Vidavalur *et al.*, 2006), cancer (Benitez *et al.*, 2009; Roy *et al.*, 2009) and aging (Baur *et al.*, 2006) in mice. This makes resveratrol a promising compound for applications as dietary supplement, functional food ingredient, cosmetics ingredient, and even as a therapeutic. Several derivatives of resveratrol have been created, where the methylated derivatives pinostilbene and pterostilbene showed better stability and uptake (Sarpietro *et al.*, 2007). The market for resveratrol and its derivatives is expected to grow further in the future. Currently, resveratrol is predominantly extracted from Japanese knotweed *Polygonum cuspidatum*; however the process is dependent on the variable harvest, has low extraction yield and results in a low-purity product (Palma *et al.*, 2013). Production of resveratrol by microbial fermentation presents an alternative process circumventing the mentioned disadvantages of extraction from plants. Recombinant production of resveratrol was first shown in *S. cerevisiae* in 2003 (Becker *et al.*, 2003). Several groups subsequently improved the production of resveratrol and its derivatives in yeast and *Escherichia coli*. However, all of these studies applied feeding of expensive precursors, such as *p*-coumaric acid (Beekwilder *et al.*, 2006; Jeong *et al.*, 2015; Sydor *et al.*, 2010b; Wang *et al.*, 2015; Wang and Yu, 2012; Zhang *et al.*, 2006a), tyrosine (Shin *et al.*, 2012; Wang *et al.*, 2011a; Zhang *et al.*, 2006a) or phenylalanine (Trantas *et al.*, 2009). The highest reported titer of resveratrol was 2.3 g l^{-1}, when 2.5 g l^{-1} *p*-coumaric acid was fed to engineered *E. coli* (Lim *et al.*, 2011). We previously described the biosynthesis of resveratrol directly from glucose and ethanol, via the tyrosine pathway in yeast,

which resulted in production of up to 531 mg l^{-1} resveratrol in fed-batch fermentation (Li *et al.*, 2015). Here, we describe the development of a *S. cerevisiae* platform strain for production of resveratrol via phenylalanine pathway. The platform strain was obtained through extensive metabolic engineering of both the resveratrol pathway and pathways forming precursors for its biosynthesis, and it demonstrates clearly that for efficient production of plant chemicals by microbial fermentation it is necessary to combine pathway reconstruction with engineering of the endogenous metabolism(Nielsen and Keasling, 2016). We evaluated the platform strain for high-level production of resveratrol and also demonstrated its use for production of resveratrol derivatives.

RESULTS

Reconstruction of resveratrol biosynthetic pathway in *S. cerevisiae*

The resveratrol biosynthesis pathway (**Fig. 1a**) was reconstructed in yeast by introducing phenylalanine ammonia lyase (*AtPAL2*), cinnamic acid hydroxylase (*AtC4H*), *p*-coumaryl-CoA ligase (*At4CL2*) from *Arabidopsis thaliana* and resveratrol synthase (*VvVST1*) from *Vitis vinifera*. Two strong constitute promoters, pTEF1 and pPGK1, were employed to control gene expression in different combinations. Engineered cells were cultivated on mineral medium supplemented with 5 mM phenylalanine for 72 hours to obtain 20-33 mg l^{-1} of resveratrol (**Fig. 1b**). No by-products (cinnamic acid or *p*-coumaric acid) were detected in the medium. The highest titer of 32.32 ± 0.37 mg l^{-1} was obtained for the strain ST4978, which had *AtPAL2* and *VvVST1* genes under control of pTEF1 promoter, and the other two genes under control of the pPGK1 promoter. Considering that the pTEF1 promoter is somewhat stronger than pPGK1 (Partow *et al.*, 2010), the results imply that *AtPAL2* and *VvVST1* may be rate limiting. This would also explain the absence of accumulation of pathway intermediates.

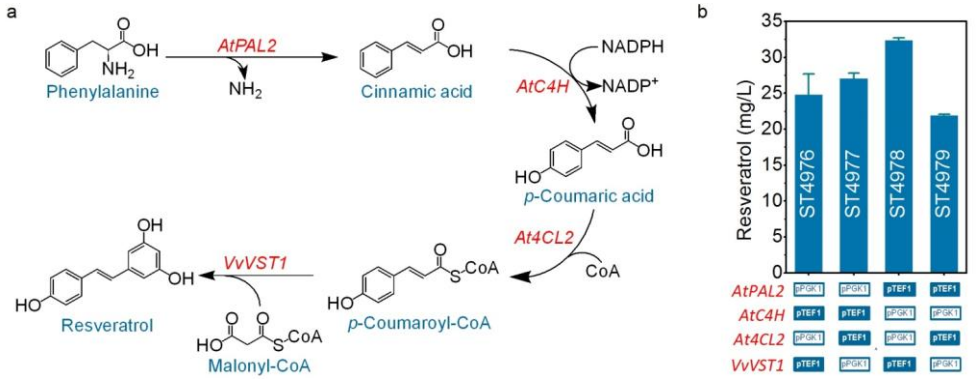

Figure 1 (a) The resveratrol biosynthetic pathway. *AtPAL2*, phenylalanine ammonia lyase from *A. thaliana*; *AtC4H*, cinnamic acid hydroxylase from *A. thaliana*; *At4CL2*, *p*-coumaryl-CoA ligase from *A. thaliana*; *VvVST1*, resveratrol synthase from *V. vinifera*. (b) Resveratrol production by engineered strains expressing the four biosynthetic genes from different promoters. The resveratrol concentration in the broth was measured after the cells were cultivated on mineral medium with 2% glucose and 5 mM phenylalanine for 72 hours in 96-deep-well plates. The displayed average values and standard deviations were calculated from biological triplicates.

Enhancement of P450 activity

Many cytochrome P450 monooxygenases present a challenge, when expressed in a heterologous host, due to their notorious low activity, limited stability, NAD(P)H-dependence, and auxiliary of electron carrier proteins (Urlacher *et al.*, 2004). As C4H used in resveratrol pathway is a membrane-associated plant-derived P450 enzyme, which requires an electron carrier for optimal activity, we hypothesized that C4H activity may be limiting resveratrol production. Plant-derived P450s have previously been reported to poorly accept electrons directly from yeast endogenous electron carriers (Guengerich *et al.*, 1993). Thus, we upgraded the strain ST4978 (basic resveratrol pathway) with overexpression of cytochrome P450 reductase (*AtATR2*) from *A. thaliana* or cytochrome B5 (*CYB5*)

from *S. cerevisiae* or both (**Fig. 2**). Overexpression of *CYB5* did not improve resveratrol production on mineral medium with 5 mM phenylalanine supplementation (**Fig. 2b**, ST4980), possibly due to inability to directly donate electrons to C4H and due to induction of membrane proliferation (Vergeres *et al.*, 1993). On the other hand, resveratrol titer increased from 32.32±0.37 to 40.75±1.60 mg l^{-1} when *AtATR2* was introduced (**Fig. 2b**, ST4981), and further increased to 77.19±0.84 mg l^{-1} when *CYB5* was subsequently overexpressed (**Fig. 2b**, ST4982), which corresponds to 26% and 139% improvement in relation to the reference strain ST4978. Trace amount of *p*-coumaric acid was also detected during the cultivation process (at 24 h) of the strain ST4982, but not in the other strains. Thus, the activity of C4H was clearly enhanced when ATR2 and Cyb5p were overexpressed.

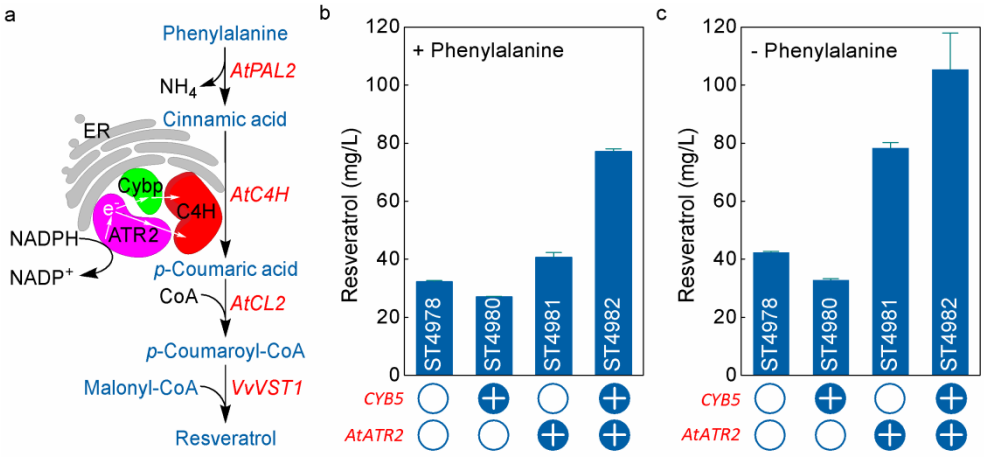

Figure 2 (a) Cytochrome P450 reductase (CPR)-mediated electron transfer from NADPH to cinnamic acid hydroxylase (*AtC4H*) and effects of functional expression of CPR (*AtATR2*) and cytochrome B5 (*CYB5*) on resveratrol production on mineral medium with (b) and without (c) 5 mM phenylalanine in 96-deep-well plates. The displayed average values and standard deviations were calculated from three biological replicates.

We then tested resveratrol production from glucose by the engineered strains on mineral medium without supplementation of phenylalanine. Interestingly, higher resveratrol production was obtained for all the strains without phenylalanine supplementation (**Fig. 2c**). This shows that resveratrol can be *de novo* synthesized from glucose via the phenylalanine pathway and that adding phenylalanine to the medium inhibits resveratrol production. The inhibition effect of phenylalanine was more obvious when *AtATR2* was expressed (**Fig. 2b, c**). ST4981 and ST4982 resulted in 78.30±1.93 mg l^{-1} and 105.31±12.59 mg l^{-1} resveratrol respectively on mineral medium without phenylalanine, which was 92% and 36% higher than resveratrol production with phenylalanine supplementation. We also observed that, with the increase of phenylalanine concentration from 0 to 5 mM, the biomass accumulation increased (**Supplementary Fig. 1**).

Increasing copy number of the resveratrol pathway genes

We have previously shown that for tyrosine-mediated resveratrol biosynthesis the production of resveratrol could be increased 36-fold by integration of multiple copies of the biosynthetic genes (Li *et al.*, 2015). We therefore tested whether the same pull-strategy would work for the phenylalanine-mediated pathway. The basic resveratrol biosynthesis pathway genes (*AtPAL2*, *AtC4H*, *At4CL2* and *VvVST1*) were integrated onto Ty-elements in the *AtATR2* and *CYB5* overexpression strain. The weakened *URA3* marker ensures multiple integrations of the expression cassette (Maury *et al.*, 2016). 12 isolates were screened to identify the highest producing strain ST4984, which had 2 copies of the resveratrol pathway genes when checked by qPCR. When the strain ST4984 was cultivated on mineral medium with 2% glucose in shake flasks, 169.04±2.42 mg l^{-1} resveratrol was obtained (**Fig. 3a**). In contrast, only 108.31±4.68 mg l^{-1} resveratrol was obtained with strain ST4982 carrying a single copy of the resveratrol pathway. Resveratrol

production was growth associated (**Fig. 3b**, **c**). About 17% and 26% of the total resveratrol were produced during the growth on glucose for ST4982 and ST4984 respectively, while the majority of resveratrol was produced during growth on ethanol for both strains (**Fig. 3a**). This is consistent with the results we have obtained in our previous study (Li *et al.*, 2015). The effect of the multicopy gene integration was however mostly pronounced in the glucose phase, where 2.4-fold more resveratrol was produced in ST4984 than in ST4982. For the ethanol phase the relative increase was smaller, namely 1.4-fold. Interestingly the multicopy strain ST4984 had a lower biomass yield on ethanol than ST4982, while the biomass yields on glucose were similar (**Fig. 3b**). The final OD_{600} of ST4984 was 30% lower than that of ST4982 (**Fig. 3c**) probably due to the metabolic burden brought by the high-level expression of the resveratrol pathway enzymes.

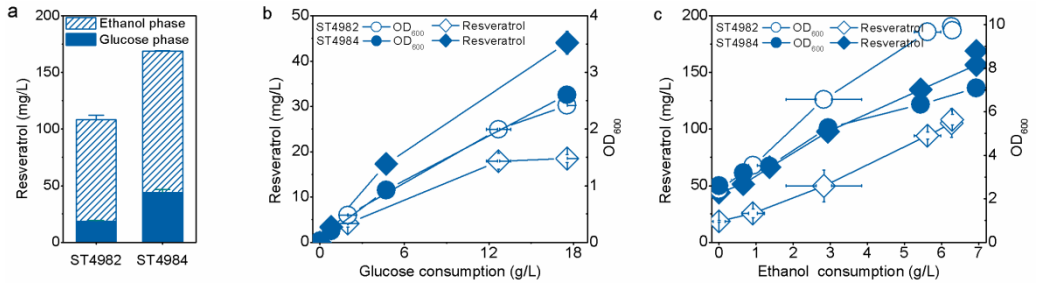

Figure 3 (a) Resveratrol production from glucose by strains carrying single and multiple copies of resveratrol pathway. Resveratrol titer in relation to substrate consumption in glucose phase (b) and ethanol phase (c) by the engineered strains. The strains were cultivated on mineral medium with 20 g l^{-1} glucose in shake flasks. The displayed average values and standard deviations were calculated from three biological replicates.

Precursor supply

To further improve resveratrol production we applied a push-and-block strategy, where we overexpressed the upstream pathways and eliminated competing

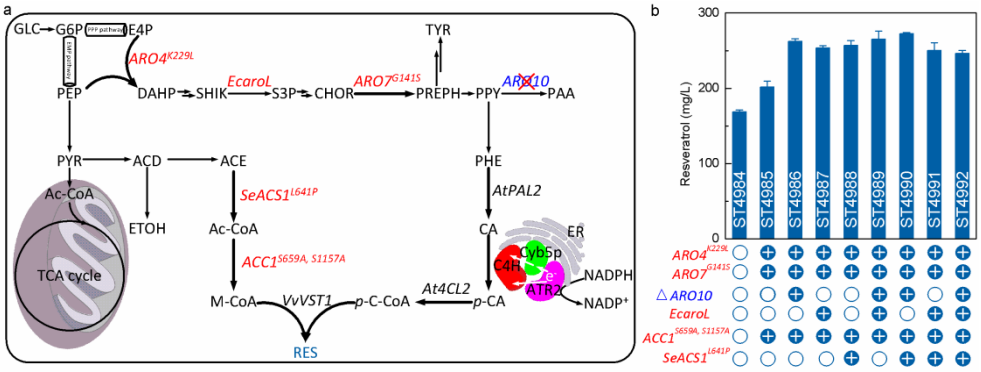

Figure 4 (a) Schematic overview of resveratrol biosynthesis in engineered yeast *S. cerevisiae* and the main engineering targets implemented in this study. Single arrows represent single reaction steps, while two arrows represent multiple reaction steps. The modified targets are shown in red, while the gene *ARO10* subjected to deletion is shown in blue. Arrows shown in bold indicate that the genes were overexpressed. GLC, glucose; G6P, glucose 6-phosphate; E4P, erythrose 4-phosphate; DAHP, 3-deoxy-D-arabino-heptulosonic acid 7-phosphate, SHIK, shikimate; S3P, shikimate 3-phosphate; CHOR, chorismate; PREPH, prephenate; TYR, tyrosine; PPY, phenylpyruvate; PAA, phenylacetaldehyde; PHE, phenylalanine; CA, cinnamic acid; *p*-CA, *p*-coumaric acid; *p*-C-CoA, *p*-coumaroyl-CoA; RES, resveratrol; M-CoA, malonyl-CoA; Ac-CoA, acetyl-CoA; ACE, acetate; ACD, acetaldehyde; ETOH, ethanol; PYR, pyruvate; PEP, phosphoenolpyruvate; *ARO4*^{K229L}, feedback-inhibition resistant version of DAHP synthase; *ARO7*^{G141S}, feedback-inhibition resistant version of chorismate mutase; *EcaroL*, *E. coli* shikimate kinase II; *ARO10*, phenylpyruvate decarboxylase, *AtPAL2*, phenylalanine ammonia lyase; *AtC4H*, cinnamate-4-hydroxylase; *At4CL2*, 4-coumarate-CoA ligase; *VvVST1*, resveratrol synthase; *SeACS*^{L641P}, post-translationally de-regulated variant of acetyl-CoA synthetase; *ACC1*$^{S659A, S1157A}$, acetyl-CoA carboxylase devoid of *SNF1*-phosphorylation sites. (b) Microbial production of resveratrol from glucose by strains with different genetic modifications. The strains were cultivated on mineral medium with 20 g l^{-1} glucose in shake flasks. The displayed average values and standard deviations were calculated from three biological replicates.

pathways for the precursor phenylalanine. To increase precursors supply, the feedback-inhibition resistant versions of DAHP synthase (*ARO4*^{K229L}) and chorismate mutase (*ARO7*^{G141S}) (Luttik *et al.*, 2008) and a de-regulated variant of acetyl-CoA carboxylase (*ACC1*$^{S659A, S1157A}$) (Shi *et al.*, 2014) were overexpressed in ST4984 to generate ST4985. The strain ST4985 resulted in a 19% improvement of resveratrol production to 201.72±7.91 mg l^{-1} (**Fig. 4b**), which is supported by our previous study(Li *et al.*, 2015). The strain ST4985 was further modified by the following strategies and combinations thereof in order to increase the push by overproduction of precursors: (i) deletion of phenylpyruvate decarboxylase (*ARO10*), (ii) overexpression of a heterologous shikimate kinase (*aroL*) from *E. coli*, (iii) overexpression of a post-translationally non-regulated version of acetyl-CoA synthase (*SeACS*^{L641P}) from *Salmonella enteric* (Shiba *et al.*, 2007). While each of the tested strategies individually resulted in 26-30% increase of resveratrol titer, their effects was not additive upon combination (**Fig. 4b**). No by-products, such as *p*-coumaric acid or cinnamic acid, were observed at the end of cultivation process in any of the strains. The highest production of resveratrol (272.64±1.34 mg l^{-1}) was obtained in strain ST4990, in which *ARO10* was deleted and *SeACS*^{L641P} was overexpressed.

Fed-batch fermentation

Fed-batch fermentation of the engineered strain ST4990 was performed in controlled bioreactors on mineral medium with glucose (**Fig. 5a**) or ethanol (**Fig. 5b**) feed in the feeding phase. The batch phase was on 40 g l^{-1} glucose, once the glucose was consumed, the constant feeding of glucose or ethanol was initiated. A long lag phase of 40 h was observed followed by a fast growing log phase with the rapid consumption of glucose (**Fig. 5**). Resveratrol accumulation was growth-associated and reached 268.70 mg l^{-1} with a yield of 11.35 mg g^{-1} glucose when

glucose was depleted. A nearly linear increase in OD_{600} over time was observed while glucose or ethanol was being fed. The OD_{600} increase and resveratrol accumulation corresponded well with the substrate consumption (**Fig. 5a, b**). At the end of the glucose fed-batch fermentation, 812 mg l^{-1} resveratrol and 22 g l^{-1} dry weight (DW) biomass was obtained from feeding 88 g l^{-1} glucose. In the ethanol fed-batch fermentation, where 79 g l^{-1} ethanol was fed, the final concentrations of DW biomass (19 g l^{-1}) and resveratrol (755 mg l^{-1}) were similar to the reactors with glucose feeding strategy.

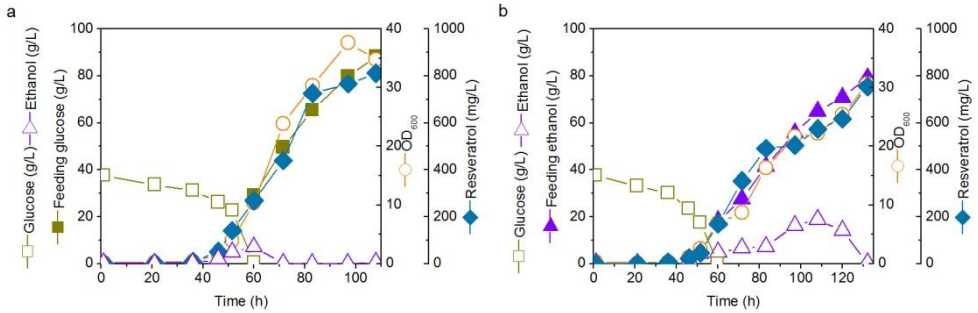

Figure 5 Fed-batch fermentation of the strain ST4990. Aerobic fed-batch fermentations were carried out by feeding glucose (a) or ethanol (b) respectively with a constant feeding rate of 5 g h^{-1} or 10 g h^{-1}.

Production of resveratrol derivatives

The instability of resveratrol, which is sensitive to light and oxygen, limits the bioavailability and bioactivity of the compound (Walle *et al.*, 2004). The bioactivity and bioavailability of resveratrol can be enhanced by substitution of hydroxyl groups with methoxy groups (Lee *et al.*, 2003; Remsberg *et al.*, 2008). Two resveratrol O-methyltransferases from *Sorghum bicolor* (*SbROMT*) and *Vitis vinifera* (*VvROMT*) were shown to methylate resveratrol to pinostilbene and pterostilbene, respectively (**Fig. 6a**) (Jeong *et al.*, 2015; Wang *et al.*, 2015). We expressed the two enzymes in the resveratrol producing strain ST4990 to generate

strains ST4993 and ST4994. Growing the strains ST4993 and ST4994 on mineral medium with 20 g l^{-1} glucose resulted in 1.38±0.06 mg l^{-1} pinostilbene and 5.52±2.84 mg l^{-1} pterostilbene, respectively (**Fig. 6b**). When grown on feed-in-time (FIT) medium, the strain ST4993 accumulated 5.52±2.84 mg l^{-1} pinostilbene and strain ST4994 accumulated 34.93 ±8.53 mg l^{-1} pterostilbene (**Fig. 6c**). Interestingly, 1.96±0.42 mg l^{-1} pinostilbene was also observed in ST4994 culture (**Fig. 6c**), which indicates that the two methylation groups are introduced sequentially, as also proposed before by Wang *et al* (Wang *et al.*, 2015). Although only small amounts of resveratrol derivatives were detected, it demonstrates for the first time the feasibility of *de novo* biosynthesis of the two resveratrol derivatives from glucose.

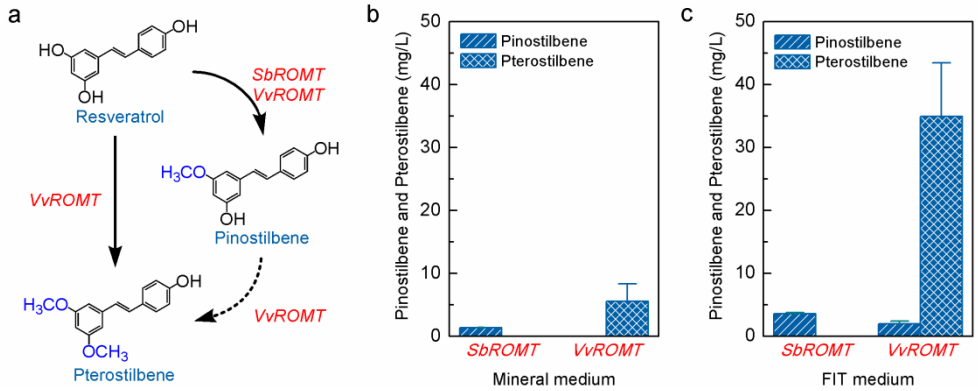

Figure 6 (a) Methylation of resveratrol to produce its derivatives, pinostilbene and pterostilbene, by strains ST4993 and ST4994 carrying *SbROMT* and *VvROMT* respectively. The strains were cultivated on mineral medium with 20 g l^{-1} glucose (b) or on FIT medium (c) in shake flasks. The displayed average values and standard deviations were calculated from duplicates.

DISCUSSION

We have applied a pull-push-block strategy to improve resveratrol production. The “pull” was improved by optimizing the resveratrol pathway expression and P450 function, the “push” was achieved by increasing the supply of precursors phenylalanine and malonyl-CoA, and finally the “block” was realized by reducing the degradation of the pathway intermediates.

In earlier reports on resveratrol production via phenylalanine, the cultures were supplemented with phenylalanine. For example, Trantas *et al.* have reported a yeast strain that produced 0.29 mg l^{-1} resveratrol when 10 mM phenylalanine was fed to the medium (Trantas *et al.*, 2009). We found that supplementation of the medium with as little as 0.25 mM phenylalanine decreased resveratrol titer. This phenomena could be explained by the inhibitory effect of phenylalanine on C4H (Ro and Douglas, 2004).

We previously succeeded in inserting up to 8 copies of the resveratrol pathway (TAL) onto yeast genome (Li *et al.*, 2015). However, here where we produce resveratrol via phenylalanine we managed to integrate only 2 copies of the genes encoding the resveratrol pathway enzymes. The failure to obtain integration of more copies of the genes may result from heavy stress response, such as ER membrane proliferation (Sandig *et al.*, 1999) or ER morphology variation (Trenchard and Smolke, 2015), when the P450 enzyme is highly expressed. Another plausible explanation might be that the yeast host would incur too much metabolic burden if the copy number of resveratrol pathway integrated onto the genome were very high and this causes a major shift in protein allocation, which has recently been shown to have significant impact on yeast metabolism (Nilsson and Nielsen, 2016). The decreased yield of biomass on glucose that was observed in the multicopy strain is consistent with this hypothesis. In addition, we also

observed that accumulation of resveratrol was strongly related to growth, which is also supported by recently published study on requirement of ATP for resveratrol production (Vos *et al.*, 2015).

Overexpression of feedback-inhibition resistant versions of DAHP synthase (*ARO4*^{K229L}) and chorismate mutase (*ARO7*^{G141S}) together with constitutively active acetyl-CoA carboxylase (*ACC1*$^{S659A, S1157A}$) gave a 19% improvement in resveratrol titer, which is similar to the increase we observed in the previous study for TAL pathway (Li *et al.*, 2015). We further improved phenylalanine supply by inactivating phenylpyruvate decarboxylase. Two broad-substrate-specificity decarboxylases, Aro10p and Pdc5p, were reported to catalyze decarboxylation of phenylpyruvate to phenylacetaldehyde, i.e., the first degradation step (Hazelwood *et al.*, 2008). Although a previous study showed that double deletion of *ARO10* and *PDC5* improved *p*-coumaric acid production (Rodriguez *et al.*, 2015), no further improvement of resveratrol production was obtained when *PDC5* was knocked out in addition to *ARO10* (**Supplementary Fig. 2**). This is consistent with publication by Vuralhan *et al*., who found that Aro10p had higher activity than Pdc5p towards phenylpyruvate (Vuralhan *et al.*, 2003). In addition, the supply of malonyl-CoA, another key precursor for resveratrol, would be attenuated when *PDC5* was knocked out as Pdc5p is also responsible for pyruvate decarboxylation. We have previously obtained negative results upon combined overexpression of *ScACS*^{L641P} and *ALD6* (Li *et al.*, 2015). On the other hand, overexpression of *ALD6* may lead to reduction of phenylalanine supply through the Ehrlich pathway (Hazelwood *et al.*, 2008). Consequently, in this study we chose to overexpress *SeACS*^{L641P} alone, which resulted in improvement of resveratrol production. Further strategies for increasing malonyl-CoA supply could be envisioned, such as down-regulation of the competing pathway towards fatty acid biosynthesis (Lim *et al.*, 2011).

While the final strain harbored a dozen of genetic modifications, the resveratrol yield (0.007 mol mol^{-1} glucose) was still far lower than the maximum theoretical yield of 0.28 mol mol^{-1} glucose (Vos *et al.*, 2015), which shows that there is a lot of potential to further improve the strain. One of the strategies that would be interesting to test could be optimization of the energetics of cytosolic acetyl-CoA generation by overexpression of bacterial pyruvate dehydrogenase complex in the cytosol as recently reported by Kozak *et al* (Kozak *et al.*, 2014). Besides, strong correlation between resveratrol biosynthesis and biomass indicates that low biomass is another issue to be solved for improving resveratrol production. Therefore, decoupling growth and production as illustrated recently using a biosensor for malonyl-CoA (David *et al.*, 2016) could possibly further increase the production of resveratrol.

ACKNOWLEDGMENTS

We thank Yun Chen and Kanchana R. Kildegaard for helpful discussions. We are grateful to Tadas Jakočiūnas, Mathew M. J. Fabre and Jie Zhang for sharing plasmids used in CRISPR/Cas9-mediated strains construction. We also acknowledge the support with fermentation from Inger Rosenstand. This work was supported by the Novo Nordisk Foundation.

AUTHOR CONTRIBUTIONS

M.L., I.B. and J.N. conceived of the project and wrote the manuscript. M.L. and I.B. designed the experiments and analyzed the results. M.L. carried out most of the experimental work. M.L. and K.S. designed the fed-batch fermentation. M.L. and M.K. performed LC-MS assay of resveratrol derivatives.

COMPETING FINANCIAL INTERESTS STATEMENT

The authors declare no competing financial interests.

MATERIALS AND METHODS

Strains and plasmids

All the engineered yeast strains (**Table 1**) were constructed from CEN.PK102-5B (MATa *ura*3-52 *his*3Δ1 *leu*2-3/112 *MAL2*-8^{c} *SUC*2)(Entian and Kötter, 2007a). Genetic engineering was carried out using either integrative EasyClone vectors with auxotrophic selection markers(Jensen *et al.*, 2014b) or using EasyClone-MarkerFree vectors with CRISPR/Cas9 system (Jessop-Fabre *et al.*, submitted). Details on the cloning and strain construction are provided in Supplementary Methods. All the oligos used for genetic modifications are listed in **Supplementary Table 1**. All the biobricks and plasmids used in the study are summarized in **Supplementary Tables 2** and **3** respectively.

Media and cultivations

Seed cultures were prepared by cultivating yeast in SC Drop-out (SD) liquid medium without histidine, leucine and uracil at 30 ℃ with 250 rpm agitation for 24 h. The inoculation size of 10% (v/v) for 96-deep well plate cultivation or initial OD_{600} of 0.02 for shake flask cultivation was used. The mineral medium (pH 6.0) with 2% glucose or feed-in-time (FIT) medium (m2p-labs, Inc.) and cultivation conditions for resveratrol and its derivatives production was described in(Li *et al.*, 2015). Samples were taken at regular intervals or at the end of cultivation. OD was measured at a wavelength of 600 nm using a Genesys 20 spectrophotometer (Thermo Scientific). The dry cell weight was measured by filtrating 3 ml of the cultures through membrane filters and drying at 105 ℃ to a constant weight. Part of the sample was centrifuged at 12,000 rpm for 2 min and the supernatant was used for analysis of general secreted metabolites. Another part of the sample was mixed with an equal volume of ethanol (99.9%), centrifuged at 12,000 rpm for 2 min and the supernatant was used for resveratrol quantification.

HPLC and LC-MS measurements

Glucose and ethanol concentrations were quantified by HPLC (Thermo Fisher Scientific, CA) equipped with an Aminex HPX-87H ion-exchange column (Bio-Rad, Hercules, CA) and a UV and RI detector. 5 mM H_2SO_4 was used as the mobile phase and the column was kept at 45 ℃ with a flow rate of 0.6 ml min^{-1}. The HPLC detection was carried out with 10 mM ammonium formate (pH 3.0) and acetonitrile as the eluents at a linear gradient flow rate of acetonitrile from 5% to 60% with a Discovery HS F5 150 mm×2.1 mm column (particle size 3 mm) as described in(Li *et al.*, 2015). The analyses of pinostilbene and pterostilbene were performed by LC-MS (Thermo Fisher Scientific, CA). Confirmation of the identity of pinostilbene and pterostilbene was done by comparing the retention time and accurate mass spectrum with the standards purchased from Sigma-Aldrich. The details on LC-MS analysis are provided in Supplementary materials and methods.

Fed-batch fermentation

Fermentation was carried out in Sartorius bioreactors equipped with an acoustic gas analyzer (model number 1311, Brüel & Kjær). An initial OD_{600} of 0.2 was used for inoculation of seed culture into 0.4 l mineral medium containing 4% glucose. During the fermentation the temperature was maintained at 30 ℃, pH at 6.0 with NH_4OH, agitation rate at 800 rpm, and air flow at 1 l min^{-1}. The detailed setup for batch and fed-batch fermentation is described in Supplementary Methods.

REFERENCES

1. Catalgol, B., Batirel, S., Taga, Y. & Ozer, N.K. Resveratrol: French paradox revisited. *Front Pharmacol* **3**, 141 (2012).
2. Kopp, P. Resveratrol, a phytoestrogen found in red wine. A possible explanation for the conundrum of the 'French paradox'? *Eur J Endocrinol* **138**, 619-20 (1998).
3. Vidavalur, R., Otani, H., Singal, P.K. & Maulik, N. Significance of wine and resveratrol in cardiovascular disease: French paradox revisited. *Exp Clin Cardiol* **11**, 217-25 (2006).
4. Benitez, D.A., Hermoso, M.A., Pozo-Guisado, E., Fernandez-Salguero, P.M. & Castellon, E.A. Regulation of cell survival by resveratrol involves inhibition of NF kappa B-regulated gene expression in prostate cancer cells. *Prostate* **69**, 1045-54 (2009).
5. Roy, P., Madan, E., Kalra, N., Nigam, N., George, J. *et al*. Resveratrol enhances ultraviolet B-induced cell death through nuclear factor-kappaB pathway in human epidermoid carcinoma A431 cells. *Biochem Biophys Res Commun* **384**, 215-20 (2009).
6. Baur, J.A., Pearson, K.J., Price, N.L., Jamieson, H.A., Lerin, C. *et al*. Resveratrol improves health and survival of mice on a high-calorie diet. *Nature* **444**, 337-42 (2006).
7. Sarpietro, M.G., Spatafora, C., Tringali, C., Micieli, D. & Castelli, F. Interaction of resveratrol and its trimethyl and triacetyl derivatives with biomembrane models studied by differential scanning calorimetry. *J Agric Food Chem* **55**, 3720-8 (2007).
8. Palma, M., Barbero, G., Piñeiro, Z., Liazid, A., Barroso, C. *et al*. Extraction of natural products: Principles and fundamental aspects. *Natural Product Extraction: Principles and Applications. Londres: RSC Publishing*, 58-88 (2013).
9. Becker, J.V., Armstrong, G.O., van der Merwe, M.J., Lambrechts, M.G., Vivier, M.A. *et al*. Metabolic engineering of *Saccharomyces cerevisiae* for the synthesis of the wine-related antioxidant resveratrol. *FEMS Yeast Res* **4**, 79-85 (2003).
10. Beekwilder, J., Wolswinkel, R., Jonker, H., Hall, R., de Vos, C.H. *et al*. Production of resveratrol in recombinant microorganisms. *Appl Environ Microbiol* **72**, 5670-2 (2006).
11. Jeong, Y.J., Woo, S.G., An, C.H., Jeong, H.J., Hong, Y.S. *et al*. Metabolic engineering for resveratrol derivative biosynthesis in *Escherichia coli*. *Mol Cells* **38**, 318-26 (2015).
12. Sydor, T., Schaffer, S. & Boles, E. Considerable increase in resveratrol production by recombinant industrial yeast strains with use of rich medium. *Applied and environmental microbiology* **76**, 3361-3363 (2010).

13. Wang, Y., Bhuiya, M.W., Zhou, R. & Yu, O. Pterostilbene production by microorganisms expressing resveratrol O-methyltransferase. *Annals of Microbiology* **65**, 817-826 (2015).
14. Wang, Y. & Yu, O. Synthetic scaffolds increased resveratrol biosynthesis in engineered yeast cells. *J Biotechnol* **157**, 258-60 (2012).
15. Zhang, Y., Li, S.-Z., Li, J., Pan, X., Cahoon, R.E. *et al*. Using unnatural protein fusions to engineer resveratrol biosynthesis in yeast and mammalian cells. *Journal of the American Chemical Society* **128**, 13030-13031 (2006).
16. Shin, S.Y., Jung, S.M., Kim, M.D., Han, N.S. & Seo, J.H. Production of resveratrol from tyrosine in metabolically engineered *Saccharomyces cerevisiae*. *Enzyme Microb Technol* **51**, 211-6 (2012).
17. Wang, Y., Halls, C., Zhang, J., Matsuno, M., Zhang, Y. *et al*. Stepwise increase of resveratrol biosynthesis in yeast *Saccharomyces cerevisiae* by metabolic engineering. *Metab Eng* **13**, 455-63 (2011).
18. Trantas, E., Panopoulos, N. & Ververidis, F. Metabolic engineering of the complete pathway leading to heterologous biosynthesis of various flavonoids and stilbenoids in *Saccharomyces cerevisiae*. *Metab Eng* **11**, 355-66 (2009).
19. Lim, C.G., Fowler, Z.L., Hueller, T., Schaffer, S. & Koffas, M.A. High-yield resveratrol production in engineered *Escherichia coli*. *Appl Environ Microbiol* **77**, 3451-60 (2011).
20. Li, M., Kildegaard, K.R., Chen, Y., Rodriguez, A., Borodina, I. *et al*. *De novo* production of resveratrol from glucose or ethanol by engineered *Saccharomyces cerevisiae*. *Metab Eng* **32**, 1-11 (2015).
21. Nielsen, J. & Keasling, J.D. Engineering Cellular Metabolism. *Cell* **164**, 1185-97 (2016).
22. Partow, S., Siewers, V., Bjorn, S., Nielsen, J. & Maury, J. Characterization of different promoters for designing a new expression vector in *Saccharomyces cerevisiae*. *Yeast* **27**, 955-64 (2010).
23. Urlacher, V.B., Lutz-Wahl, S. & Schmid, R.D. Microbial P450 enzymes in biotechnology. *Appl Microbiol Biotechnol* **64**, 317-25 (2004).
24. Guengerich, F.P., Gillam, E.M., Ohmori, S., Sandhu, P., Brian, W.R. *et al*. Expression of human cytochrome P450 enzymes in yeast and bacteria and relevance to studies on catalytic specificity. *Toxicology* **82**, 21-37 (1993).
25. Vergeres, G., Yen, T.S., Aggeler, J., Lausier, J. & Waskell, L. A model system for studying membrane biogenesis. Overexpression of cytochrome b5 in yeast results in marked proliferation of the intracellular membrane. *J Cell Sci* **106 (Pt 1)**, 249-59 (1993).
26. Maury, J., Germann, S.M., Baallal Jacobsen, S.A., Jensen, N.B., Kildegaard, K.R. *et al*. EasyCloneMulti: A Set of Vectors for Simultaneous and Multiple

Genomic Integrations in Saccharomyces cerevisiae. *PLoS One* **11**, e0150394 (2016).
27. Luttik, M.A., Vuralhan, Z., Suir, E., Braus, G.H., Pronk, J.T. *et al*. Alleviation of feedback inhibition in Saccharomyces cerevisiae aromatic amino acid biosynthesis: quantification of metabolic impact. *Metab Eng* **10**, 141-53 (2008).
28. Shi, S., Chen, Y., Siewers, V. & Nielsen, J. Improving production of malonyl coenzyme A-derived metabolites by abolishing Snf1-dependent regulation of Acc1. *MBio* **5**, e01130-14 (2014).
29. Shiba, Y., Paradise, E.M., Kirby, J., Ro, D.K. & Keasling, J.D. Engineering of the pyruvate dehydrogenase bypass in *Saccharomyces cerevisiae* for high-level production of isoprenoids. *Metab Eng* **9**, 160-8 (2007).
30. Walle, T., Hsieh, F., DeLegge, M.H., Oatis, J.E. & Walle, U.K. High absorption but very low bioavailability of oral resveratrol in humans. *Drug metabolism and disposition* **32**, 1377-1382 (2004).
31. Lee, S.K., Nam, K.A., Hoe, Y.H., Min, H.Y., Kim, E.Y. *et al*. Synthesis and evaluation of cytotoxicity of stilbene analogues. *Arch Pharm Res* **26**, 253-7 (2003).
32. Remsberg, C.M., Yanez, J.A., Ohgami, Y., Vega-Villa, K.R., Rimando, A.M. *et al*. Pharmacometrics of pterostilbene: preclinical pharmacokinetics and metabolism, anticancer, antiinflammatory, antioxidant and analgesic activity. *Phytother Res* **22**, 169-79 (2008).
33. Ro, D.-K. & Douglas, C.J. Reconstitution of the entry point of plant phenylpropanoid metabolism in yeast (*Saccharomyces cerevisiae*): implications for control of metabolic flux into the phenylpropanoid pathway. *Journal of Biological Chemistry* **279**, 2600-2607 (2004).
34. Sandig, G., Kargel, E., Menzel, R., Vogel, F., Zimmer, T. *et al*. Regulation of endoplasmic reticulum biogenesis in response to cytochrome P450 overproduction. *Drug Metab Rev* **31**, 393-410 (1999).
35. Trenchard, I.J. & Smolke, C.D. Engineering strategies for the fermentative production of plant alkaloids in yeast. *Metab Eng* **30**, 96-104 (2015).
36. Nilsson, A. & Nielsen, J. Metabolic Trade-offs in Yeast are Caused by F1F0-ATP synthase. *Sci Rep* **6**, 22264 (2016).
37. Vos, T., de la Torre Cortes, P., van Gulik, W.M., Pronk, J.T. & Daran-Lapujade, P. Growth-rate dependency of de novo resveratrol production in chemostat cultures of an engineered *Saccharomyces cerevisiae* strain. *Microb Cell Fact* **14**, 133 (2015).
38. Hazelwood, L.A., Daran, J.M., van Maris, A.J., Pronk, J.T. & Dickinson, J.R. The Ehrlich pathway for fusel alcohol production: a century of research on *Saccharomyces cerevisiae* metabolism. *Appl Environ Microbiol* **74**, 2259-66 (2008).

39. Rodriguez, A., Kildegaard, K.R., Li, M., Borodina, I. & Nielsen, J. Establishment of a yeast platform strain for production of *p*-coumaric acid through metabolic engineering of aromatic amino acid biosynthesis. *Metabolic engineering* **31**, 181-188 (2015).
40. Vuralhan, Z., Morais, M.A., Tai, S.L., Piper, M.D. & Pronk, J.T. Identification and characterization of phenylpyruvate decarboxylase genes in *Saccharomyces cerevisiae*. *Appl Environ Microbiol* **69**, 4534-41 (2003).
41. Kozak, B.U., van Rossum, H.M., Luttik, M.A., Akeroyd, M., Benjamin, K.R. *et al*. Engineering acetyl coenzyme A supply: functional expression of a bacterial pyruvate dehydrogenase complex in the cytosol of *Saccharomyces cerevisiae*. *MBio* **5**, e01696-14 (2014).
42. David, F., Nielsen, J. & Siewers, V. Flux control at the malonyl-CoA node through hierarchical dynamic pathway regulation in Saccharomyces cerevisiae. *ACS synthetic biology* (2016).
43. Entian, K.-D. & Kötter, P. 25 Yeast genetic strain and plasmid collections. *Method Microbiol* **36**, 629-666 (2007).
44. Jensen, N.B., Strucko, T., Kildegaard, K.R., David, F., Maury, J. *et al*. EasyClone: method for iterative chromosomal integration of multiple genes in *Saccharomyces cerevisiae*. *FEMS Yeast Res* **14**, 238-48 (2014).

Table 1. List of yeast strains used in the study.

Strains	Genotype	Reference
ST4976	P_{PGK1}->*AtPAL2*, P_{TEF1}->*AtC4H*, P_{PGK1}->*At4CL2*, P_{TEF1}->*VvVST1*	This study
ST4977	P_{PGK1}->*AtPAL2*, P_{TEF1}->*AtC4H*, P_{TEF1}->*At4CL2*, P_{PGK1}->*VvVST1*	This study
ST4978	P_{TEF1}->*AtPAL2*, P_{PGK1}->*AtC4H*, P_{PGK1}->*At4CL2*, P_{TEF1}->*VvVST1*	This study
ST4979	P_{TEF1}->*AtPAL2*, P_{PGK1}->*AtC4H*, P_{TEF1}->*At4CL2*, P_{PGK1}->*VvVST1*	This study
ST4980	P_{TEF1}->*AtPAL2*, P_{PGK1}->*AtC4H*, P_{PGK1}->*At4CL2*, P_{TEF1}->*VvVST1*, P_{TEF1}->*CYB5*	This study
ST4981	P_{TEF1}->*AtPAL2*, P_{PGK1}->*AtC4H*, P_{PGK1}->*At4CL2*, P_{TEF1}->*VvVST1*, P_{TEF1}->*AtATR2*	This study
ST4982	P_{TEF1}->*AtPAL2*, P_{PGK1}->*AtC4H*, P_{PGK1}->*At4CL2*, P_{TEF1}->*VvVST1*, P_{TEF1}->*AtATR2*, P_{PGK1}->*CYB5*	This study
ST4984	P_{TEF1}->*AtATR2*, P_{PGK1}->*CYB5*, Ty-(P_{TDH3}->*AtPAL2*, P_{FBA1}->*AtC4H*, P_{PGK1}->*At4CL2*, P_{TEF1}->*VvVST1*)	This study
ST4985	P_{TEF1}->*AtATR2*, P_{PGK1}->*CYB5*, Ty-(P_{TDH3}->*AtPAL2*, P_{FBA1}->*AtC4H*, P_{PGK1}->*At4CL2*, P_{TEF1}->*VvVST1*), P_{TEF1}->$ACC1^{S659A,\ S1157A}$, P_{TEF1}->$ARO7^{G141S}$, P_{PGK1}->$ARO4^{K229\ L}$	This study
ST691	MAT*a ura3-52 his3Δ1 leu2-3/112 MAL2-8^{c} SUC2, ΔARO10, ΔPDC5*	(Rodriguez *et al.*, 2015)
ST4986	P_{TEF1}->*AtATR2*, P_{PGK1}->*CYB5*, Ty-(P_{TDH3}->*AtPAL2*, P_{FBA1}->*AtC4H*, P_{PGK1}->*At4CL2*, P_{TEF1}->*VvVST1*), P_{TEF1}->$ACC1^{S659A,\ S1157A}$, P_{TEF1}->$ARO7^{G141S}$, P_{PGK1}->$ARO4^{K229\ L}$, *ΔARO10*	This study
ST4995	P_{TEF1}->*AtATR2*, P_{PGK1}->*CYB5*, Ty-(P_{TDH3}->*AtPAL2*, P_{FBA1}->*AtC4H*, P_{PGK1}->*At4CL2*, P_{TEF1}->*VvVST1*), P_{TEF1}->$ACC1^{S659A,\ S1157A}$, P_{TEF1}->$ARO7^{G141S}$, P_{PGK1}->$ARO4^{K229\ L}$, *ΔARO10*, *ΔPDC5*	This study
ST4987	P_{TEF1}->*AtATR2*, P_{PGK1}->*CYB5*, Ty-(P_{TDH3}->*AtPAL2*, P_{FBA1}->*AtC4H*, P_{PGK1}->*At4CL2*, P_{TEF1}->*VvVST1*), P_{TEF1}->$ACC1^{S659A,\ S1157A}$, P_{TEF1}->$ARO7^{G141S}$, P_{PGK1}->$ARO4^{K229\ L}$, P_{TEF1}->*EcaroL*	This study
ST4988	P_{TEF1}->*AtATR2*, P_{PGK1}->*CYB5*, Ty-(P_{TDH3}->*AtPAL2*, P_{FBA1}->*AtC4H*, P_{PGK1}->*At4CL2*, P_{TEF1}->*VvVST1*), P_{TEF1}->$ACC1^{S659A,\ S1157A}$, P_{TEF1}->$ARO7^{G141S}$, P_{PGK1}->$ARO4^{K229\ L}$, P_{TDH3}->$SeACS^{L641P}$	This study

ST4989	P_{TEF1}->*AtATR2*, P_{PGK1}->*CYB5*, Ty-(P_{TDH3}->*AtPAL2*, P_{FBA1}->*AtC4H*, P_{PGK1}->*At4CL2*, P_{TEF1}->*VvVST1*), P_{TEF1}->*ACC1*$^{S659A,\ S1157A}$, P_{TEF1}->*ARO7*^{G141S}, P_{PGK1}->*ARO4* $^{K229\ L}$, *ΔARO10*, P_{TEF1}->*EcaroL*	This study
ST4990	P_{TEF1}->*AtATR2*, P_{PGK1}->*CYB5*, Ty-(P_{TDH3}->*AtPAL2*, P_{FBA1}->*AtC4H*, P_{PGK1}->*At4CL2*, P_{TEF1}->*VvVST1*), P_{TEF1}->*ACC1*$^{S659A,\ S1157A}$, P_{TEF1}->*ARO7*^{G141S}, P_{PGK1}->*ARO4* $^{K229\ L}$, *ΔARO10*, P_{TDH3}->*SeACS*^{L641P}	This study
ST4991	P_{TEF1}->*AtATR2*, P_{PGK1}->*CYB5*, Ty-(P_{TDH3}->*AtPAL2*, P_{FBA1}->*AtC4H*, P_{PGK1}->*At4CL2*, P_{TEF1}->*VvVST1*), P_{TEF1}->*ACC1*$^{S659A,\ S1157A}$, P_{TEF1}->*ARO7*^{G141S}, P_{PGK1}->*ARO4* $^{K229\ L}$, P_{TEF1}->*EcaroL*, P_{TDH3}->*SeACS*^{L641P}	This study
ST4992	P_{TEF1}->*AtATR2*, P_{PGK1}->*CYB5*, Ty-(P_{TDH3}->*AtPAL2*, P_{FBA1}->*AtC4H*, P_{PGK1}->*At4CL2*, P_{TEF1}->*VvVST1*), P_{TEF1}->*ACC1*$^{S659A,\ S1157A}$, P_{TEF1}->*ARO7*^{G141S}, P_{PGK1}->*ARO4* $^{K229\ L}$, *ΔARO10*, P_{TEF1}->*EcaroL*, P_{TDH3}->*SeACS*^{L641P}	This study
ST4993	P_{TEF1}->*AtATR2*, P_{PGK1}->*CYB5*, Ty-(P_{TDH3}->*AtPAL2*, P_{FBA1}->*AtC4H*, P_{PGK1}->*At4CL2*, P_{TEF1}->*VvVST1*), P_{TEF1}->*ACC1*$^{S659A,\ S1157A}$, P_{TEF1}->*ARO7*^{G141S}, P_{PGK1}->*ARO4* $^{K229\ L}$, *ΔARO10*, P_{TDH3}->*SeACS*^{L641P}, P_{TDH3}->*SbROMT*	This study
ST4994	P_{TEF1}->*AtATR2*, P_{PGK1}->*CYB5*, Ty-(P_{TDH3}->*AtPAL2*, P_{FBA1}->*AtC4H*, P_{PGK1}->*At4CL2*, P_{TEF1}->*VvVST1*), P_{TEF1}->*ACC1*$^{S659A,\ S1157A}$, P_{TEF1}->*ARO7*^{G141S}, P_{PGK1}->*ARO4* $^{K229\ L}$, *ΔARO10*, P_{TDH3}->*SeACS*^{L641P}, P_{TDH3}->*VvROMT*	This study

Supplementary materials and methods

Biobricks and plasmids construction

All the plasmids were constructed by following the described USER cloning procedure(Jensen *et al.*, 2014b). All the biobricks (**Supplementary Table 2**) were amplified using corresponding templates and primers, which are summarized in Supplementary Table 2 and Table 1, respectively. The PCR reactions were performed in PCR instrument (Bio-Rad) using Phu X7 polymerase(Norholm, 2010). The generated biobricks were assembled into either EasyClone vectors(Jensen *et al.*, 2014b) or EasyClone-MarkerFree vectors (Jessop-Fabre *et al*. submitted) to construct integrative plasmids for gene overexpression. The plasmid pCfB4286 was generated by assembling BB599 (*hph*MXsyn) into opened plasmid pCfB2312 with primers Open_2_fw and Open_2_rv. The constructed plasmids were sequenced by Eurofins Scientific to confirm the correct cloning.

Strain construction

The resveratrol- and its derivatives-producing strains were engineered by transforming corresponding integrative plasmids into the given parent strains (**Supplementary Table 4**). Yeast transformations were performed following lithium acetate protocol(Gietz and Woods, 2002). When antibiotic selection was used the transformed strains were incubated 30℃ for 2 hours prior to plating on selective medium. For CRISPR/Cas9 mediated gene insertions/deletions, the strains were first transformed with Cas9-expressing plasmid pCfB4286 and selected on hygromycin B plates. The resulting Cas9-expressing strains were transformed with appropriate DNA target fragments together with the corresponding gRNA plasmids. The correct genetic modifications were verified by yeast colony PCR using the primers summarized in Supplementary Table 1.

LC-MS measurements

LC-MS measurements were carried out on a Dionex UltiMate 3000 UHPLC (Thermo Fisher Scientific, San Jose, CA) connected to an Orbitrap Fusion Mass Spectrometer (Thermo Fisher Scientific, San Jose, CA). The UHPLC used a Hypersil GOLD PFP, 15 cm x 2.1 mm, 3 μm column. Temperature was 35°C and flow rate was 1 mL/min with a mobile phase of 100% formic acid (0.1%) for 1 min followed by a linear gradient of 100% formic acid (0.1%)/0% acetonitrile (0.1%) to 5% formic acid (0.1%)/95% acetonitrile (0.1%) over 14 minutes. This gradient was held for 2 minute after which it was changed immediately to 100% formic acid (0.1%) and 0% acetonitrile (0.1%) and held for 4 minutes. The sample was passed on to the MS equipped with a heated electrospray ionization source (HESI) in positive-ion mode with nitrogen as nebulizer gas (45 a.u.). The cone and probe temperature were 342 ℃ and 358 ℃, respectively. Probe gas flow was 13 a.u. and spray voltage was 3500 V. Scan range was 100 to 1000 Da and time between scans was 100 ms.

Fed-batch fermentation of yeast strains in controlled reactors

Four seed pre-cultures were prepared by inoculating fresh colonies from agar plate into 5 ml SC (ura^-, his^-, leu^-) medium and cultivating at 30 ℃ for 24 hours in an orbital shaker (250 rpm). The pre-cultures were then inoculated to an initial OD_{600} of 0.02 into 50 ml minimal medium (pH 6.0), as described in(Gietz and Woods, 2002) in 250 ml flasks. The start OD_{600} of 0.2 in bioreactors was prepared by inoculating seed culture into 400 ml fermentation medium in four bioreactors. The composition of the fermentation medium was as following: 15.0 g l^{-1} $(NH_4)_2SO_4$, 6.0 g l^{-1} KH_2PO_4, 1.0 g l^{-1} MgSO4 ·7H_2O, 2 ml l^{-1} trace metals solution, 2 ml l^{-1} vitamins solution, 0.5 ml l^{-1} antifoam A (Sigma-Aldrich), and 40 g l^{-1} glucose, where the composition of trace metal solution and vitamin solution was as

described in(Jensen *et al.*, 2014b). The medium without vitamins, trace metals and glucose was autoclaved at 121 ℃ for 20 min. Glucose was autoclaved separately using the same conditions. Vitamins solution and trace metals solution were added to the sterilized medium by filtration. The fermentation was performed at 30 ℃ with the agitation rate of 800 rpm and the air flow of 1 l per min. The pH was automatically maintained at 6.0 with NH_4 H_2O. Once the glucose was depleted, which was judged by the sharp decline of exhaust CO_2, the feed was initialed at a constant feeding rate of 5 g h^{-1} or 10 g h^{-1} for ethanol and glucose feeds respectively. The feed medium contained 45 g l^{-1} $(NH_4)_2SO_4$, 18 g l^{-1} KH_2PO_4, 3 g l^{-1} $MgSO_4$ $7H_2O$, 12 ml L^{-1} trace metals solution, 6 ml L^{-1} vitamins solution, 0.6 ml L^{-1} antifoam A, and 160 g l^{-1} of glucose or ethanol. Glucose, vitamins, and trace metals were added to the feed solution in the same way as to the batch fermentation medium. Samples were taken at regular intervals and used for measurements of biomass and metabolites concentration.

Supplementary Figure 1. Final concentrations of resveratrol and OD_{600} of ST4982, cultivated on minimal medium with 2% glucose and 0 to 5 mM phenylalanine. The strains were grown in 96-deep well plates for 72 hours. The displayed average values and standard deviations were calculated from three biological replicates.

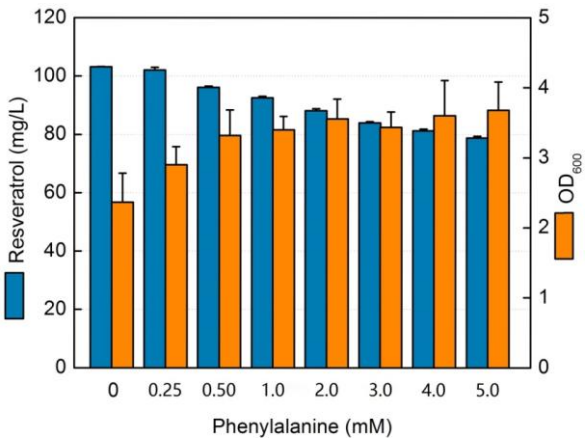

Supplementary Figure 2. Resveratrol production by the strains ST4986 and ST4995 on minimal medium with 2% glucose in shake flasks. The displayed average values and standard deviations were calculated from three biological replicates.

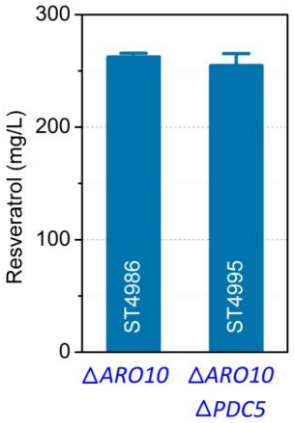

Supplementary Table 1. List of primers used in the study.

Name	Sequence (5' to 3')
$P_{<-TEF1}$_fw	ACCTGCACU TTGTAATTAAAACTTAG
$P_{<-TEF1}$_rv	CACGCGAU GCACACACCATAGCTTC
$P_{PGK1->}$_rv	ATGACAGAU TTGTTTTATATTTGTTG
$P_{<-PGK1}$_fw	ACCTGCACU TTGTTTTATATTTGTTG
$P_{TEF1->}$_fw	CGTGCGAU GCACACACCATAGCTTC
$P_{TEF1->}$_rv	ATGACAGAU TTGTAATTAAAACTTAG
<-*AtPAL2*_fw	AGTGCAGGU AAAACAATGGATCAAATC
<-*AtPAL2*_rv	CGTGCGAU TCAGCAGATAGGAATAGG
*AtC4H->*_fw	ATCTGTCAU AAAACAATGGACTTGTTGTTGTTG
*AtC4H->*_rv	CACGCGAU TCAACAGTTTCTTGGCTT
<-*CYB5*_fw	AGTGCAGGU AAAACA ATGCCTAAAGTTTACAGTTACC
<-*CYB5*_rv	CGTGCGAU TCA TTCGTTCAACAAATAATAAGC
*AtATR2->*_fw	ATCTGTCAU AAAACAATGTCCTCCTCTTCTTCATCATCCACC
*AtATR2->*_rv	CACGCGAU TCACCAGACATCTCTCAA
<-*At4CL2*_fw	AGTGCAGGU AAAACAATGACTACCCAAGATGTTA
<-*At4CL2*_rv	CGTGCGAU TCAGTTCATCAAACCGTT
*VvVST1->*_fw	ATCTGTCAU AAAACAATGGCTTCCGTTGAAGAA
*VvVST1->*_rv	CACGCGAU TCAATTGGTAACGGTTGG
Open_1_fw	AGCTGAAGCU TCGTACGCTG
Open_1_rv	ACGCGATCU TCGAGCGTCC
<-*ACC1*_fw	CGTGCGAU TCATTTCAAAGTCTTCAACAATTT
<-*ACC1*_rv	AGTGCAGGU AAAACAATGAGCGAAGAAAGCTTA
USER_fw	ATTGGGU GCATAGGCCACTAGTGGATCTG
USER_rv	ATCGCGU CAGCTGAAGCTTCGTACGC
Open_2_fw	ACGCGAU CTCGTGATACGCCTATTTT
Open_2_rv	ACCCAAU ATCAGTTATTACCCTATGCG
TJOS-62 (P1F)	CGTGCGAU AGGGAACAAAAGCTGGAGCT
TJOS-65 (P1R)	CACGCGAU TAACTAATTACATGACTCGA
TJOS-64 (P3F)	ATCTGTCAU AGGGAACAAAAGCTGGAGCT
TJOS-67(P3F)	ATGACAGAU TAACTAATTACATGACTCGA
*PDC5*_KO_fw	CGTAAACCTGCATTAAG

*PDC5*_KO_rv	CTAAGATCATAGCTAAAGG
*ARO10*_KO_fw	GGATAGCCGTCATTTAC
*ARO10*_KO_rv	CGATAGGAATGACAGAA
EcaroL->_fw	ATCTGTCAU AAAACAATGACACAACCTCTTTTTCTGA
EcaroL->_rv	CACGCGAU TCAACAATTGATCGTCTGTGC
<-*SeACS*_fw	AGTGCAGGU AAAACAATGTCACAAACACAC
<-*SeACS*_rv	CGTGCGAU TCATGATGGCATAGCAATAG
<-T_{NAT5}_fw	ATCGCACGAU TTCTTAACAGATGGCTG
<-T_{NAT5}_rv	AGATCGCGU TCGGGACCATAAAAATTC
$P_{<-TDH3}$_fw	AGCTTCAGCU ATAAAAAACACGCTTTTTCAG
$P_{<-TDH3}$_rv	ACCTGCACU TTTGTTTGTTTATGTGTGTTTATTC
P_{FBA1}->_fw	GCGTGTTU TTTATATAACAATACTGACAGTACT
P_{FBA1}->_rv	ATGACAGAU TTTGAATATGTATTACTTGG
*SbROMT*_fw	ATCTGTCAU AAAACAATGGTCTTGATCTCCGAAGATTCC AGAGAATTATTG
*SbROMT*_rv	CACGCGAU TCATGGGTATAATTCGATGAT
*VvROMT*_fw	ATCTGTCAU AAAACAATGGATTTGGCCAAC
*VvROMT*_rv	CACGCGAU TCATGGGTAAACTTCGATCAA
ColPCR_DW_fw	CCTGCAGGACTAGTGCTGAG
X-3_DW_rv	CCGTGCAATACCAAAATCG
X-4_DW_rv	GACGGTACGTTGACCAGAG
XI-1_DW _rv	GAAGACCCATGGTTCCAAGGA
XI-2_DW_rv	GAGACAAGATGGGGCAAGAC
XI-5_DW_rv	CCCAAAAGCAATCCAGGAAAAACC
XII-1_DW_rv	GGACGACAACTACGGAGGAT
*PDC5*_chk_fw	AAAGCCTCCATATCCAAAG
*PDC5*_chk_rv	AGGTATGGTTAAAGATCACAC
*ARO10*_chk_fw	ACCGAAATTTAAAAAAGCAG
*ARO10*_chk_rv	GTTTTCGGATAAAACTTCTTC

Note: Underlined sequences represent overhangs used for USER cloning.

Supplementary Table 2. List of biobricks used in the study.

Biobrick	Description	Template	Forward primer	Reverse Primer
BB008	Promoter, <-P_{TEF1}	pCfB826	$P_{<\text{-}TEF1}$_fw	$P_{<\text{-}TEF1}$_rv
BB301	Promoter, $P_{TEF1\text{->}}$	pCfB826	$P_{TEF1\text{->}}$_fw	$P_{TEF1\text{->}}$_rv
BB010	Bidirectional promoter, <-P_{TEF1}-P_{PGK1}->	pCfB826	$P_{<\text{-}TEF1}$_fw	$P_{PGK1\text{->}}$_rv
BB302	Bidirectional promoter, <-P_{PGK1}-P_{TEF1}->	pCfB826	$P_{<\text{-}PGK1}$_fw	$P_{TEF1\text{->}}$_rv
BB291	*PAL2* from *A. thaliana*	pCfB756	<-*AtPAL2*_fw	<-*AtPAL2*_rv
BB292	*C4H* from *A. thaliana*	pCfB754	*AtC4H*->_fw	*AtC4H*->_rv
BB290	*CYB5* from *S. cerevisiae*	gDNA of CEN.PK102-5B	<-*CYB5*_fw	<-*CYB5*_rv
BB296	*ATR2* from *A. thaliana*	pCfB755	*AtATR2*->_fw	*AtATR2*->_rv
BB294	*4CL2* from *A. thaliana*	pCfB758	<-*At4CL2*_fw	<-*At4CL2*_rv
BB295	*VST1* from *V. vinifera*	pCfB759	*VvVST1*->_fw	*VvVST1*->_rv
BB580	*KanMXpm*	pCfB2055	USER_fw	USER_rv
BB530	Promoter, <-P_{TDH3}	gDNA of CEN.PK102-5B	$P_{<\text{-}TDH3}$_fw	$P_{<\text{-}TDH3}$_rv
BB705	Promoter, $P_{FBA1\text{->}}$	gDNA of CEN.PK102-5B	$P_{FBA1\text{->}}$_fw	$P_{FBA1\text{->}}$_rv
BB713	Promoter, <-P_{TDH3}-P_{FBA1}->	BB530 + BB705	$P_{<\text{-}TDH3}$_fw	$P_{FBA1\text{->}}$_rv
BB429	Terminator, $T_{<\text{-}NAT5}$	gDNA of CEN.PK102-5B	$T_{<\text{-}NAT5}$_fw	$T_{<\text{-}NAT5}$_rv
BB1655	Linearized pCfB1178	pCfB1178	Open_1_fw	Open_1_rv
BB599	*hph*MXsyn	pCfB2513	USER_fw	USER_rv
BB364	$ARO4^{K229L}$ from *S. cerevisiae*	pCfB826	*ScARO4*->_fw	*ScARO4*->_rv
BB361	$ARO7^{G141S}$ from *S. cerevisiae*	pCfB826	<-*ScARO7*_fw	<-*ScARO7*_rv
BB012	$ACC1^{S659A, S1157A}$ from *S. cerevisiae*	pCfB1175	<-*ACC1*_fw	<-*ACC1*_rv
BB1268	gBlock of *PDC5*		TJOS-62	TJOS-67
BB1269	gBlock of *ARO10*		TJOS-64	TJOS-65
BB1623	Knockout fragment of *ARO10*	gDNA of ST691	*ARO10*KO_fw	*ARO10*KO_rv

BB1644	Knockout fragment of *PDC5*	gDNA of ST691	*PDC5*_KO_fw	*PDC5*_KO_rv
BB501	*aroL* from *E. coli*	pCfB2747	*EcaroL*->_fw	*EcaroL*->_rv
BB119	ACS^{L641P} from *S. enterica*	pCfB324	<-*SeACS*_fw	<-*SeACS*_rv
BB1309	*ROMT* from *S. bicolor*	pCfB4659	*SbROMT*->_fw	*SbROMT*->_rv
BB1310	*ROMT* from *V. vinifera*	pCfB4660	*VvROMT*->_fw	*VvROMT*->_rv

Supplementary Table 3. List of plasmids used in the study.

Name	Parent plasmid	Biobricks	Properties	Reference
pCfB756			*AtPAL2*[a], *KanMX*	This study
pCfB754			*AtC4H*[a], *KanMX*	This study
pCfB755			*AtATR2*[a], *KanMX*	This study
pCfB758			*At4CL2*[a], *KanMX*	(Li *et al.*, 2015)
pCfB759			*VvVST1*[a], *KanMX*	(Li *et al.*, 2015)
pCfB4659			*SbROMT*[a], *KanMX*	This study
pCfB4660			*VvROMT*[a], *KanMX*	This study
pCfB388			Integrative plasmid, XI-1-LoxP, *KlLEU2*	(Jensen *et al.*, 2014b)
pCfB389			Integrative plasmid, XI-2-LoxP, *KlURA3*	(Jensen *et al.*, 2014b)
pCfB391			Integrative plasmid, XI-5-LoxP, *SpHIS5*	(Jensen *et al.*, 2014b)
pCfB844	pCfB391	BB291, BB302, BB292	Integrative plasmid, XI-5, LoxP, P_{PGK1}-*AtPAL2*, P_{TEF1}-*AtC4H*, *SpHIS5*	This study
pCfB855	pCfB388	BB294, BB302, BB295	Integrative plasmid, XI-1, LoxP, P_{PGK1}-*At4CL2*, P_{TEF1}-*VvVST1*, *KlLEU2*	This study
pCfB846	pCfB389	BB290, BB008,	Integrative plasmid, XI-2, LoxP, P_{TEF1}-*CYB5*, *KlURA3*	This study
pCfB847	pCfB389	IBB301, BB296	Integrative plasmid, XI-2, LoxP, P_{TEF1}-*AtATR2*, *KlURA3*	This study
pCfB848	pCfB389	BB290, BB302,	Integrative plasmid, XI-2, LoxP, P_{PGK1}-*CYB5*, P_{TEF1}-*AtATR2*,	This study

		BB296	*KlURA3*	
pCfB1018	pCfB391	BB291, BB010, BB292	Integrative plasmid, XI-5, LoxP, P_{TEF1}-*AtPAL2*, P_{PGK1}-*AtC4H*, *SpHIS5*	This study
pCfB1021	pCfB388	BB294, BB010, BB295	Integrative plasmid, XI-1, LoxP, P_{TEF1}-*At4CL2*, P_{PGK1}-*VvVST1*, *KlLEU2*	This study
pCfB2224			Integrative plasmid, XI-2, LoxP, *KanMX*	(Stovicek *et al.*, 2015b)
pCfB2767	pCfB2224	BB290, BB302, BB296	Integrative plasmid, XI-2, LoxP, P_{PGK1}-*CYB5*, P_{TEF1}-*AtATR2*, *KanMX*	This study
pCfB826			Integrative plasmid, X-4,LoxP, P_{TEF1}-*ScARO7*^{G141S}, P_{PGK1}-*ScARO4*^{K229L}, *SpHIS*5	(Rodriguez *et al.*, 2015)
pCfB257			Integrative plasmid, *X-3*, *LoxP*, *KlLEU2*	(Jensen *et al.*, 2014b)
pCfB2582	pCfB257	BB012, BB008	Integrative plasmid, *X-3*, *LoxP*, P_{TEF1}-*ScACC1*$^{S659A, S1157A}$, *KlLEU2*	This study
pCfB322			Multiple integrative plasmid, Ty4, *KlURA3*	(Maury *et al.*, 2016)
pCfB1178	pCfB322	BB294, BB302, BB295	Multiple integrative plasmid, Ty4, P_{PGK1}-*At4CL2*, P_{TEF1}-*VvVST1*, *KlURA3*	This study
pCfB2584	pCfB1178	BB429, BB291, BB713, BB292	Multiple integrative plasmid, Ty4, P_{TDH3}-*AtPAL2*, P_{FBA1}-*AtC4H*, P_{PGK1}-*At4CL2*, P_{TEF1}-*VvVST1*, *KlURA3*	This study
pCfB2312			Centromeric plasmid, P_{TEF1}-*CAS9*, *KanMX*.	(Stovicek *et al.*, 2015b)
pCfB4286	pCfB2312	BB599	Centromeric plasmid, P_{TEF1}-*CAS9*, *hph*MXsyn	This study
pTAJAK-71			2 µ plasmid, *NatMX*	(Ronda *et al.*, 2015)
pCfB4156	pCfB2926	BB1268, BB1269	2 µ plasmid, P_{SNR52}-gBlock_*PDC5*-gBlock_*ARO10*-T_{SUP}, *NatMX*	This study
pCfB3041	pCfB2926	BB1324	2 µ plasmid, P_{SNR52}-gBlock_X-3-T_{SUP}, *NatMX*	(Jessop-Fabre *et al.*, submitted)

pCfB3034			Integrative plasmid, X-3, MarkerFree	(Jessop-Fabre *et al*., submitted)
pCfB2747	pCfB3034		Integrative plasmid, X-3, P_{PGK1}-*EcaroL*, *KlLEU2*	(Rodriguez *et al.*, 2015)
pCfB4289	pCfB3034	BB301, BB501	Integrative plasmid, X-3, P_{TEF1}-*EcaroL*, MarkerFree	This study
pCfB3047	pCfB2926		2 µ plasmid, P_{SNR52}-gBlock_XII-1-T_{SUP}, *NatMX*	(Jessop-Fabre *et al*., submitted)
pCfB3038			Integrative plasmid, XII-1, MarkerFree	(Jessop-Fabre *et al*., submitted)
pCfB4655	pCfB3048	BB704, BB119	Integrative plasmid, XII-1, P_{TDH3}-$SeACS^{L641P}$, MarkerFree	This study
			Integrative plasmid, XII-2, MarkerFree	(Jessop-Fabre *et al*., submitted)
pCfB4290		BB704, BB1309	Integrative plasmid, XII-2, P_{TDH3}-*SbROMT*, MarkerFree	This study
pCfB4292		BB704, BB1310	Integrative plasmid, XII-2, P_{TDH3}-*VvROMT*, MarkerFree	This study

[a] The genes were codon-optimized for *S.cerevisiae* and synthesized by GeneArt (Life Technologies). The DNA sequences are provided at the end of the Supplementary materials and methods.

Supplementary Table 4. The strains engineered in this study.

Strains	Parent strain	Transformed integrative plasmids
ST4976	CEN.PK102-5B	pCfB844, pCfB855, pCfB389
ST4977	CEN.PK102-5B	pCfB844, pCfB1021, pCfB389
ST4978	CEN.PK102-5B	pCfB1018, pCfB855, pCfB389
ST4979	CEN.PK102-5B	pCfB1018, pCfB1021, pCfB389
ST4980	CEN.PK102-5B	pCfB1018, pCfB855, pCfB846
ST4981	CEN.PK102-5B	pCfB1018, pCfB855, pCfB847
ST4982	CEN.PK102-5B	pCfB1018, pCfB855, pCfB848
ST4984	CEN.PK102-5B	pCfB2767, pCfB2584, pCfB257, pCfB258
ST4985	CEN.PK102-5B	pCfB2767, pCfB2584, pCfB826, pCfB2582
ST4986	ST4985	*ΔARO10*
ST4987	ST4985	pCfB4289
ST4988	ST4985	pCfB4655
ST4989	ST4986	pCfB4289
ST4990	ST4986	pCfB4655
ST4991	ST4985	pCfB4289, pCfB4655
ST4992	ST4986	pCfB4289, pCfB4655
ST4993	ST4990	pCfB4290
ST4994	ST4990	pCfB4292
ST4995	ST4985	*ΔARO10*, *ΔPDC5*

DNA sequence of *AtPAL2* codon-optimized for *S. cerevisiae* by GeneArt (Life Technologies)

ATGGATCAAATCGAAGCTATGTTGTGTGGTGGTGGTGAAAAAACAAAA
GTTGCTGTTACTACTAAGACCTTGGCCGATCCATTGAATTGGGGTTTGG
CTGCTGATCAAATGAAGGGTTCTCATTTGGATGAAGTCAAGAAGATGGT
CGAAGAATACAGAAGACCAGTTGTTAATTTGGGTGGTGAAACTTTGACT
ATTGGTCAAGTTGCTGCTATTTCTACTGTTGGTGGTTCTGTTAAGGTTGA
ATTGGCTGAAACTTCTAGAGCTGGTGTTAAGGCTTCTTCTGATTGGGTT
ATGGAATCTATGAACAAGGGTACTGATTCTTACGGTGTTACTACAGGTT
TTGGTGCTACTTCTCATAGAAGAACTAAGAATGGTACTGCCTTGCAAAC
CGAATTGATCAGATTTTTGAACGCCGGTATTTTCGGTAACACCAAAGAA
ACTTGTCATACCTTGCCACAATCTGCTACTAGAGCTGCTATGTTGGTTA
GAGTTAACACTTTGTTGCAAGGTTACTCCGGTATCAGATTCGAAATTTT
GGAAGCTATCACCTCCTTGTTGAACCATAACATTTCTCCATCTTTGCCAT
TGAGAGGTACTATTACTGCTTCTGGTGATTTGGTTCCATTGTCTTATATT
GCTGGTTTGTTGACTGGTAGACCAAACTCTAAAGCTACTGGTCCAGATG
GTGAATCATTGACTGCTAAAGAAGCTTTTGAAAAGGCTGGTATCTCTAC
TGGTTTTTTCGACTTGCAACCTAAAGAAGGTTTGGCTTTGGTTAATGGT
ACAGCTGTTGGTTCTGGTATGGCTTCTATGGTTTTGTTTGAAGCTAACGT
TCAAGCTGTTTTGGCCGAAGTTTTGTCTGCTATTTTTGCTGAAGTTATGT
CCGGTAAGCCAGAATTCACTGATCATTTGACCCATAGATTGAAACATCA
CCCAGGTCAAATTGAAGCTGCTGCAATTATGGAACATATCTTGGATGGT
TCCTCTTACATGAAGTTGGCTCAAAAAGTTCACGAAATGGACCCATTGC
AAAAGCCAAAACAAGATAGATACGCTTTGAGAACTTCTCCACAATGGT
TGGGTCCACAAATAGAAGTTATTAGACAAGCCACCAAGTCCATCGAAA
GAGAAATCAATTCTGTTAACGACAACCCATTGATCGACGTCAGTAGAA
ACAAAGCTATTCATGGTGGTAACTTCCAAGGTACTCCAATTGGTGTTTC
TATGGACAACACTAGATTGGCTATTGCTGCCATTGGTAAATTGATGTTC
GCTCAATTCTCCGAATTGGTCAACGATTTTTACAACAACGGTTTGCCTTC
TAACTTGACCGCTTCTTCTAATCCATCATTGGATTACGGTTTTAAGGGTG
CTGAAATTGCTATGGCTTCATACTGTTCTGAATTGCAATACTTGGCTAA
CCCAGTTACCTCTCATGTTCAATCTGCTGAACAACACAATCAAGACGTT
AACTCCTTGGGTTTGATCTCTTCTAGAAAGACTTCTGAAGCCGTTGACA
TCTTGAAGTTGATGTCTACTACATTCTTGGTCGGTATTTGCCAAGCTGTT
GATTTGAGACATTTGGAAGAAAACTTGAGACAAACCGTCAAGAACACC
GTTTCACAAGTTGCTAAGAAAGTTTTGACCACCGGTATTAACGGTGAAT
TGCATCCATCTAGATTCTGCGAAAAGGATTTGTTGAAGGTCGTTGATAG
AGAACAAGTTTTCACCTACGTTGATGATCCATGTTCTGCTACTTATCCAT
TGATGCAAAGATTGAGACAAGTCATCGTTGATCATGCTTTGTCTAATGG

TGAAACCGAAAAGAACGCTGTTACCTCCATTTTCCAAAAGATTGGTGCT
TTCGAAGAAGAATTGAAGGCCGTTTTGCCAAAAGAAGTTGAAGCAGCT
AGAGCAGCTTACGGTAACGGTACTGCTCCAATTCCAAATAGAATCAAA
GAATGCAGATCCTACCCATTATACAGATTCGTTAGAGAAGAATTAGGTA
CTAAGTTGTTGACCGGTGAAAAGGTTGTTTCTCCAGGTGAAGAATTCGA
TAAGGTTTTCACTGCTATGTGCGAAGGTAAATTGATCGATCCATTGATG
GACTGCTTGAAAGAATGGAATGGTGCTCCTATTCCTATCTGCTGA

DNA sequence of *AtC4H* codon-optimized for *S. cerevisiae* by GeneArt (Life Technologies)

ATGGACTTGTTGTTGTTGGAAAAGTCCTTGATTGCTGTTTTCGTTGCTGT
TATTTTGGCCACCGTTATCTCTAAATTGAGAGGTAAGAAATTGAAGTTG
CCACCAGGTCCAATTCCAATCCCAATTTTTGGTAATTGGTTGCAAGTTG
GTGATGACTTGAACCACAGAAACTTGGTTGATTACGCTAAAAAGTTCGG
TGATTTGTTCTTGTTGAGAATGGGTCAAAGAAATTTGGTCGTTGTTTCCT
CACCAGACTTGACCAAAGAAGTTTTGTTGACTCAAGGTGTCGAATTCGG
TTCCAGAACTAGAAATGTTGTTTTCGATATCTTCACCGGTAAGGGTCAA
GATATGGTTTTTACTGTTTACGGTGAACATTGGAGAAAGATGAGAAGA
ATTATGACCGTTCCATTCTTCACCAACAAGGTTGTCCAACAAAACAGAG
AAGGTTGGGAATTTGAAGCTGCTTCTGTTGTTGAAGATGTCAAGAAGAA
TCCAGATTCTGCTACTAAGGGTATCGTTTTGAGAAAAAGATTGCAATTG
ATGATGTACAACAACATGTTCAGAATCATGTTCGACAGAAGATTTGAAT
CCGAAGATGACCCTTTGTTTTTGAGATTGAAGGCTTTGAACGGTGAAAG
ATCTAGATTGGCTCAATCCTTCGAATACAACTACGGTGATTTCATCCCA
ATCTTAAGACCATTCTTGAGAGGTTACTTGAAGATCTGCCAAGATGTTA
AGGATAGAAGAATCGCCTTGTTCAAAAAGTACTTCGTTGACGAAAGAA
AGCAAATCGCTTCTTCTAAACCTACTGGTTCTGAAGGTTTGAAGTGCGC
CATTGATCATATTTTGGAAGCTGAACAAAAGGGTGAAATCAACGAAGA
TAACGTCTTGTACATCGTCGAAAACATTAACGTTGCTGCTATTGAAACT
ACCTTGTGGTCTATTGAATGGGGTATTGCTGAATTGGTTAATCACCCAG
AAATCCAATCCAAGTTGAGAAACGAATTGGATACTGTTTTGGGTCCAGG
TGTTCAAGTTACTGAACCTGACTTGCATAAGTTGCCATACTTGCAAGCT
GTTGTAAAAGAAACCTTGAGATTAAGAATGGCCATCCCTTTGTTGGTTC
CACATATGAACTTGCATGATGCTAAATTGGCCGGTTATGATATTCCAGC
CGAATCCAAGATTTTGGTTAATGCTTGGTGGTTGGCTAACAATCCAAAT
TCTTGGAAAAAGCCAGAAGAATTCAGACCAGAAAGATTTTTCGAAGAA
GAAAGTCACGTTGAAGCCAACGGTAATGATTTTAGATACGTTCCATTTG
GTGTTGGTAGAAGATCTTGTCCAGGTATTATCTTGGCTTTGCCAATTTTG
GGTATTACCATCGGTAGAATGGTCCAAAACTTCGAATTATTGCCACCAC

CTGGTCAATCTAAGGTTGATACTTCTGAAAAGGGTGGTCAATTCTCCTT
GCATATTTTGAACCACTCCATCATCGTTATGAAGCCAAGAAACTGTTGA

DNA sequence of *AtATR2* codon-optimized for *S. cerevisiae* by GeneArt (Life Technologies)

ATGTCCTCCTCTTCTTCATCATCCACCTCTATGATTGATTTGATGGCCGC
TATTATCAAGGGTGAACCAGTTATAGTTTCTGATCCAGCTAATGCTTCT
GCCTATGAATCTGTTGCTGCTGAATTATCCTCCATGTTGATCGAAAACA
GACAATTCGCTATGATCGTCACTACCTCTATTGCTGTTTTGATTGGTTGC
ATCGTTATGTTGGTTTGGAGAAGATCTGGTTCTGGTAACTCTAAAAGAG
TCGAACCATTGAAGCCATTGGTTATCAAACCTAGAGAAGAAGAAATTG
ACGACGGTAGAAAGAAGGTTACCATTTTCTTTGGTACTCAAACCGGTAC
TGCTGAAGGTTTTGCTAAAGCTTTGGGTGAAGAAGCTAAAGCCAGATA
CGAAAAGACTAGATTCAAGATCGTTGACTTGGATGATTACGCTGCAGAT
GATGATGAATACGAAGAAAAGTTGAAGAAAGAAGATGTCGCCTTTTTC
TTCTTGGCTACTTATGGTGATGGTGAACCTACTGATAATGCTGCTAGAT
TTTACAAGTGGTTCACCGAAGGTAATGATAGAGGTGAATGGTTGAAAA
ACTTGAAGTACGGTGTTTTCGGTTTGGGTAATAGACAATACGAACACTT
CAACAAGGTTGCCAAGGTTGTTGATGATATCTTGGTTGAACAAGGTGCC
CAAAGATTGGTTCAAGTTGGTTTAGGTGATGATGACCAATGCATCGAAG
ATGATTTTACTGCTTGGAGAGAAGCTTTGTGGCCAGAATTGGATACAAT
CTTGAGAGAAGAAGGTGATACTGCTGTTGCTACTCCATATACTGCTGCT
GTTTTAGAATACAGAGTTTCCATCCACGATTCCGAAGATGCTAAGTTCA
ACGATATTAACATGGCTAACGGTAACGGTTACACCGTTTTTGATGCTCA
ACATCCATACAAGGCTAACGTTGCTGTTAAGAGAGAATTGCATACTCCA
GAATCTGACAGATCCTGCATTCATTTGGAATTCGATATTGCTGGTTCCG
GTTTGACTTACGAAACTGGTGATCATGTTGGTGTTTTGTGCGATAACTT
GTCTGAAACTGTTGATGAAGCCTTGAGATTATTGGATATGTCTCCAGAT
ACCTACTTCTCCTTGCATGCCGAAAAAGAAGATGGTACTCCAATCTCTT
CATCTTTGCCACCACCATTTCCACCATGTAATTTGAGAACTGCTTTGACC
AGATACGCTTGCTTGTTGTCATCTCCAAAAAAGTCTGCTTTGGTTGCTTT
GGCTGCTCATGCTTCAGATCCAACTGAAGCTGAAAGATTGAAACATTTG
GCTTCTCCAGCTGGTAAGGATGAATATTCTAAATGGGTTGTTGAATCCC
AAAGATCCTTGTTGGAAGTTATGGCTGAATTTCCATCTGCTAAACCACC
ATTGGGTGTTTTTTTTGCTGGTGTTGCTCCAAGATTGCAACCTAGATTCT
ACTCTATTTCCTCCTCCCCAAAAATTGCCGAAACCAGAATTCATGTTAC
TTGCGCTTTGGTCTACGAAAAAATGCCAACTGGTAGAATCCATAAGGGT
GTTTGTTCTACCTGGATGAAGAATGCTGTTCCTTACGAAAAGTCCGAAA
ACTGTTCTTCTGCTCCAATCTTCGTTAGACAATCCAATTTCAAGTTGCCA

TCCGATTCTAAGGTTCCAATTATCATGATTGGTCCAGGTACTGGTTTGG
CTCCTTTTAGAGGTTTTTTACAAGAAAGATTGGCCTTGGTCGAATCCGG
TGTTGAATTGGGTCCATCTGTTTTGTTTTTCGGTTGCAGAAACAGAAGA
ATGGACTTCATCTACGAAGAAGAATTACAAAGATTCGTCGAATCAGGT
GCTTTGGCAGAATTGTCAGTTGCTTTTTCTAGAGAAGGTCCAACAAAAG
AATACGTCCAACACAAGATGATGGATAAGGCTTCTGATATCTGGAACA
TGATTTCTCAAGGTGCCTACTTGTATGTTTGTGGTGATGCTAAAGGTAT
GGCCAGAGATGTTCATAGATCCTTGCATACAATTGCCCAAGAACAAGG
TTCTATGGACTCTACAAAAGCAGAAGGTTTCGTCAAGAACTTGCAAACT
TCTGGTAGATACTTGAGAGATGTCTGGTGA

DNA sequence of *At4CL2* codon-optimized for *S. cerevisiae* by GeneArt (Life Technologies)

ATGACTACCCAAGATGTTATCGTCAACGATCAAAACGACCAAAAGCAA
TGTTCCAACGATGTCATCTTCAGATCTAGATTGCCAGATATCTACATCC
CAAACCATTTGCCATTGCACGATTACATCTTCGAAAACATTTCTGAATT
CGCTGCTAAGCCATGCTTGATTAACGGTCCAACTGGTGAAGTTTACACT
TACGCTGATGTTCATGTTACCTCTAGAAAATTGGCTGCTGGTTTACACA
ATTTGGGTGTTAAGCAACACGATGTCGTTATGATTTTGTTGCCAAACTC
TCCAGAAGTTGTCTTGACTTTTTTGGCTGCTTCTTTCATTGGTGCTATTA
CTACTTCTGCTAACCCATTTTTTACCCCAGCCGAAATTTCTAAACAAGCT
AAAGCTTCTGCTGCCAAGTTGATCGTTACTCAATCAAGATACGTTGACA
AGATCAAGAACTTGCAAAACGATGGTGTTTTGATTGTCACCACTGATTC
TGATGCTATTCCAGAAAACTGCTTGAGATTCTCTGAATTGACCCAATCT
GAAGAACCTAGAGTTGATTCCATCCCAGAAAAGATTTCACCAGAAGAT
GTTGTTGCTTTGCCATTCTCTTCAGGTACTACTGGTTTGCCAAAAGGTGT
TATGTTGACTCATAAGGGTTTGGTTACATCCGTTGCTCAACAAGTTGAT
GGTGAAAATCCAAACTTGTACTTCAACAGAGATGACGTTATCTTGTGCG
TTTTGCCAATGTTTCATATCTACGCCTTGAACTCCATCATGTTGTGTTCT
TTGAGAGTTGGTGCCACCATTTTGATTATGCCAAAGTTCGAAATCACCT
TGTTGTTGGAACAAATCCAAAGATGCAAGGTTACCGTTGCTATGGTTGT
TCCACCAATAGTTTTGGCTATTGCTAAGTCTCCAGAAACCGAAAAGTAC
GATTTGTCCTCTGTTAGAATGGTTAAGTCTGGTGCTGCTCCATTGGGTA
AAGAATTGGAAGATGCTATTTCTGCTAAGTTCCCAAATGCTAAGTTGGG
TCAAGGTTATGGTATGACTGAAGCTGGTCCAGTTTTAGCTATGTCTTTG
GGTTTTGCTAAAGAACCATTCCCAGTAAAATCTGGTGCTTGTGGTACTG
TTGTTAGAAACGCTGAAATGAAGATTTTGGACCCAGATACTGGTGATTC
TTTGCCAAGAAACAAACCAGGTGAAATATGCATCAGAGGTAATCAAAT
CATGAAGGGTTACTTGAACGATCCATTGGCTACTGCTTCTACCATTGAT

AAGGATGGTTGGTTGCATACAGGTGATGTTGGTTTCATAGATGATGACG
ACGAATTATTCATCGTTGATAGATTGAAAGAATTGATCAAGTACAAGG
GTTTCCAAGTTGCTCCAGCTGAATTGGAATCTTTGTTGATTGGTCATCCA
GAAATCAACGACGTTGCTGTTGTTGCAATGAAGGAAGAAGATGCCGGT
GAAGTTCCAGTTGCTTTCGTTGTTAGATCCAAGGATTCTAACATCTCCG
AAGACGAAATCAAGCAATTCGTTTCTAAGCAAGTCGTTTTCTACAAGAG
AATCAACAAGGTTTTCTTCACCGACTCTATTCCAAAAGCTCCATCTGGT
AAGATCTTGAGAAAGGATTTGAGAGCTAGATTGGCTAACGGTTTGATG
AACTGA

DNA sequence of *VvVST1* codon-optimized for *S. cerevisiae* by GeneArt (Life Technologies)

ATGGCTTCCGTTGAAGAATTCAGAAACGCTCAAAGAGCTAAAGGTCCA
GCTACTATTTTGGCTATTGGTACTGCTACTCCAGATCATTGTGTTTACCA
ATCTGATTACGCCGACTACTACTTCAGAGTTACTAAGTCTGAACACATG
ACCGAATTGAAGAAAAAGTTCAACAGAATCTGCGACAAGTCCATGATC
AAGAAGAGATATATCCACTTGACCGAAGAAATGTTGGAAGAACATCCA
AACATTGGTGCTTATATGGCTCCATCCTTGAACATCAGACAAGAAATTA
TCACTGCCGAAGTTCCAAGATTGGGTAGAGATGCTGCTTTGAAGGCTTT
GAAAGAATGGGGTCAACCTAAGTCTAAGATCACCCATTTGGTTTTCTGT
ACTACCTCTGGTGTTGAAATGCCAGGTGCTGATTACAAATTGGCTAACT
TGTTGGGTTTGGAAACCTCCGTTAGAAGAGTTATGTTGTACCATCAAGG
TTGTTATGCTGGTGGTACTGTTTTGAGAACTGCTAAAGATTTGGCTGAA
AACAATGCTGGTGCTAGAGTTTTGGTTGTTTGCTCTGAAATTACCGTTGT
TACTTTCAGAGGTCCATCTGAAGATGCTTTGGATTCTTTGGTTGGTCAA
GCTTTGTTTGGTGATGGTTCTTCTGCTGTTATAGTTGGTTCTGATCCAGA
TGTCTCTATCGAAAGACCTTTGTTCCAATTGGTTTCTGCTGCTCAAACTT
TCATTCCAAATTCTGCTGGTGCAATTGCTGGTAACTTGAGAGAAGTTGG
TTTGACTTTTCATTTGTGGCCAAACGTTCCAACTTTGATCTCCGAAAACA
TTGAAAAGTGTTTGACCCAAGCTTTCGATCCATTGGGTATTTCTGATTG
GAATTCCTTGTTCTGGATTGCTCATCCAGGTGGTCCAGCAATTTTGGAT
GCTGTTGAAGCTAAATTGAACTTGGAAAAGAAGAAGTTGGAAGCCACC
AGACATGTTTTGTCTGAATACGGTAATATGTCCTCTGCTTGCGTTTTGTT
CATTTTGGACGAAATGAGAAAAAAGTCCTTGAAGGGTGAAAAGGCTAC
TACTGGTGAAGGTTTGGATTGGGGTGTTTTGTTCGGTTTTGGTCCAGGTT
TGACTATTGAAACTGTTGTCTTGCATTCTGTTCCAACCGTTACCAATTGA

DNA sequence of *SbROMT* codon-optimized for *S. cerevisiae* by GeneArt (Life Technologies)

ATGGTCTTGATCTCCGAAGATTCCAGAGAATTATTGCAAGCCCATGTCG
AATTGTGGAATCAAACTTACTCTTTCATGAAGTCCGTTGCTTTGGCTGTT
GCTTTAGACTTGCATATTGCTGATGCCATTCATAGAAGAGGTGGTGCTG
CTACTTTGTCTCAAATTTTGGGTGAAATTGGTGTCAGACCATGTAAATT
GCCAGGTTTACACAGAATCATGAGAGTCTTGACTGTTTCTGGTACTTTC
ACTATCGTTCAACCATCTGCTGAAACCATGTCATCTGAATCTGATGGTA
GAGAACCAGTTTACAAGTTGACTACTGCTTCCTCTTTGTTGGTTTCCTCT
GAATCTTCTGCTACAGCTTCTTTGTCTCCAATGTTGAACCATGTTTTGTC
CCCATTCAGAGATTCTCCATTGTCTATGGGTTTGACTGCTTGGTTTAGAC
ACGATGAAGATGAACAAGCTCCAGGTATGTGTCCTTTTACTTTGATGTA
TGGTACTACCTTGTGGGAAGTCTGTAGAAGAGATGATGCTATTAACGCC
TTGTTCAACAATGCTATGGCTGCTGATTCTAACTTCTTGATGCAAATCTT
GTTGAAAGAATTCTCCGAAGTTTTCTTGGGTATCGACTCTTTGGTTGATG
TTGCTGGTGGTGTTGGTGGTGCTACTATGGCTATTGCTGCTGCTTTTCCA
TGTTTGAAGTGTACCGTTTTGGATTTGCCACATGTTGTTGCTAAAGCTCC
ATCTTCTTCTATCGGTAACGTTCAATTTGTCGGTGGTGATATGTTCGAAT
CTATTCCACCAGCTAACGTCGTTTTGTTGAAATGGATTTTACACGACTG
GTCCAACGATGAATGCATTAAGATTTTGAAGAACTGCAAGCAAGCCAT
CCCATCTAGAGATGCCGGTGGTAAGATTATTATCATCGATGTTGTTGTC
GGTTCCGATTCTTCTGATACAAAGTTGTTGGAAACCCAAGTCATCTACG
ACTTGCATTTGATGAAGATTGGTGGTGTCGAAAGAGATGAACAAGAAT
GGAAGAAGATTTTCTTGGAAGCCGGTTTCAAGGACTACAAGATTATGCC
AATTTTAGGTTTGAGATCCATCATCGAATTATACCCATGA

DNA sequence of *VvROMT* codon-optimized for *S. cerevisiae* by GeneArt (Life Technologies)

ATGGATTTGGCCAACGGTGTTATTTCCGCTGAATTATTGCATGCTCAAG
CTCATGTTTGGAACCACATTTTCAACTTCATCAAGTCCATGTCTTTGAAG
TGCGCTATTCAATTGGGTATCCCAGATATCATTCATAACCATGGTAAGC
CAATGACCTTGCCAGAATTGGTTGCTAAATTGCCAGTTCACCCAAAAAG
ATCTCAATGCGTTTACAGATTGATGAGAATCTTGGTCCATTCTGGTTTTT
TGGCTGCTCAAAGAGTTCAACAAGGTAAAGAAGAAGAAGGTTACGTTT
TGACCGATGCCTCTAGATTGTTGTTGATGGATGATTCCTTGTCCATCAG
ACCATTGGTTTTGGCTATGTTGGATCCTATTTTGACTAAGCCATGGCATT
ATTTGTCCGCCTGGTTTCAAAATGATGACCCAACTCCATTTCATACCGCT
CACGAAAGATCATTTTGGGATTATGCTGGTCATGAACCACAATTGAACA

ACTCATTCAATGAAGCTATGGCTTCCGATGCTAGATTATTGACTTCCGT
CTTGTTGAAAGAAGGTCAAGGTGTTTTTGCTGGTTTGAACTCATTGGTT
GATGTTGGTGGTGGTACTGGTAAAGTTGCTAAAGCTATTGCTAATGCCT
TCCCACATTTGAACTGTACCGTTTTGGATTTGCCACATGTTGTTGCAGGT
TTACAAGGTTCTAAGAACTTGAATTACTTCGCCGGTGATATGTTCGAAG
CTATTCCACCAGCTGATGCTATTTTGTTGAAATGGATATTGCACGACTG
GTCCGATGAAGAATGTGTTAAGATTTTGAAGAGATGCAGAGAAGCCAT
CCCATCTAAAGAAAATGGTGGTAAGGTTATCATCATCGACATGATTATG
ATGAAGAATCAAGGTGACTACAAGTCCACTGAAACCCAATTATTCTTCG
ACATGACCATGATGATTTTCGCTCCAGGTAGAGAAAGAGATGAAAACG
AATGGGAAAAGTTGTTCTTGGATGCTGGTTTCTCCCATTACAAGATTAC
TCCAATTTTGGGTTTGAGATCCTTGATCGAAGTTTACCCATGA

References

1. Jensen, N.B. *et al*. EasyClone: method for iterative chromosomal integration of multiple genes in *Saccharomyces cerevisiae*. *FEMS Yeast Res* **14**, 238-48 (2014).
2. Norholm, M.H. A mutant Pfu DNA polymerase designed for advanced uracil-excision DNA engineering. *BMC Biotechnol* **10**, 21 (2010).
3. Gietz, R.D. & Woods, R.A. Transformation of yeast by lithium acetate/single-stranded carrier DNA/polyethylene glycol method. *Methods Enzymol* **350**, 87-96 (2002).
4. Li, M. *et al*. *De novo* production of resveratrol from glucose or ethanol by engineered *Saccharomyces cerevisiae*. *Metab Eng* **32**, 1-11 (2015).
5. Stovicek, V., Borodina, I. & Forster, J. CRISPR–Cas system enables fast and simple genome editing of industrial *Saccharomyces cerevisiae* strains. *Metabolic Engineering Communications* **2**, 13-22 (2015).
6. Rodriguez, A., Kildegaard, K.R., Li, M., Borodina, I. & Nielsen, J. Establishment of a yeast platform strain for production of *p*-coumaric acid through metabolic engineering of aromatic amino acid biosynthesis. *Metabolic engineering* **31**, 181-188 (2015).
7. Maury, J. *et al*. EasyCloneMulti: A Set of Vectors for Simultaneous and Multiple Genomic Integrations in *Saccharomyces cerevisiae*. *PLoS One* **11**, e0150394 (2016).
8. Ronda, C. *et al*. CrEdit: CRISPR mediated multi-loci gene integration in *Saccharomyces cerevisiae*. *Microb Cell Fact* **14**, 97 (2015).

CHAPTER 6 Conclusions and perspective

The work presented in this thesis describes effords of engineering *S. cerevisiae* for production of resveratrol and its derivatives. The detailed strategies used in this study to explore resveratrol biosynthesis in yeast include screening for enzymes with highest activity and specificity, enhancement of P450 enzymatic activity, overexpression of resveratrol pathway genes, improvement of precursors supply and elimination of precursors degradation.

Taken together, the presented work shows the great potential of industrial application of the engineered yeast for resveratrol production. On the other hand, the obtained yield of resveratrol is still far lower than the maximum theoretical yield of 0.28 mol mol^{-1} glucose (Vos *et al.*, 2015), which indicates that there is a lot of potential to further optimize the strains. Based on the above summarised results and findings, we have advanced understanding of resveratrol biosynthesis in *S. cerevisiae*, and therefore propose the following strategies to further improve resveratrol production.

1. Decouple resveratrol production from growth

Resveratrol biosynthesis is a growth-dependent process, which means that high accumulation of biomass is required to obtain high resveratrol production. However, slow growth rate was observed in engineered strains producing high amounts of resveratrol, which indicates a metabolic burden. A feasible solution to the problem could be decoupling resveratrol accumulation from the growth by designing switches to dynamically control

resveratrol synthesis. As example, first gene encoding TAL/PAL, which is the first step of the resveratrol pathway, could be controlled by a glucose-repressed pHXT7 promoter, so that resveratrol biosynthesis is first triggered in the glucose-limited fed-batch phase after sufficient biomass has been accumulated in the batch phase.

2. Ethanol fed-batch

Resveratrol was observed to be primarily accumulated in the ethanol phase of batch fermentation, but yeast grows faster in the glucose phase. A suggestion for fermentation process optimization could be mixed feed strategy, where a mix of glucose and ethanol is used, or ethanol pulse feed strategy, which had been successfully applied previously for amorphadiene production (Westfall *et al.*, 2012).

3. Increase cytosolic acetyl-CoA supply

As malonyl-CoA is a key precursor for resveratrol biosynthesis as well as for fatty acids biosynthesis, Lim *et al*. obtained 2-fold improvement of resveratrol titre when they added cerulenin to the medium to limit the carbon flux to fatty acids synthesis from malonyl-CoA in *E. coli* (Lim *et al.*, 2011). Significant improvements of different flavanones production were also obtained in *E. coli* in the same way (Leonard *et al.*, 2008). An alternative strategy would be down-regulating the promoter of *FAS1*, which is the first gene for fatty acids synthesis. As malonyl-CoA is generated from cytosolic acetyl-CoA, a possible solution to improve malonyl-CoA supply may be optimizing the acetyl-CoA supply in the cytosol. Kozak *et al.* proved that the cytosolic acetyl-CoA can be generated by ATP-independent

pyruvate dehydrogenase (*PDH*) from *Enterococcus faecalis* instead of the native *ACS*-dependent pathway in *S. cerevisiae* without affecting the cellular physiology (Kozak *et al.*, 2014).

4. Compartmentalisation of resveratrol biosynthetic genes

C4H is attached to the endoplasmic reticulum with its N-terminal, while PAL2 is generally recognised as a cytosolic enzyme (Achnine *et al.*, 2004; Rasmussen and Dixon, 1999). The C4H in tobacco, *Nicotiana tabacum*, can mediate the movement of PAL2 from cytosol to endoplasmic reticulum, thus forming a complex of PAL2 and C4H to channel cinnamic acid (Achnine *et al.*, 2004) probably due to some specific mechanism existing in plants. This strategy may reduce the losses in the transportation due to diffusion, degradation and competing pathways (Li and Borodina, 2014). Therefore, compartmentalisation of the two enzymes, PAL and C4H, in the form of fusion protein or scaffold might be a way to improve resveratrol production.

ACKNOWLEDGEMENTS

First of all, I would like to sincerely thank my supervisor, Jens Nielsen, for offering me the opportunity to take on the fantastic project and giving me enough freedom on it. You have been always supportive, open-minded and enthusiastic. Your knowledgeable guidance, insightful inspiration and positive attitude motivated me along the way.

My great gratitude also goes to my co-supervisor, Irina Borodina, who is always patient and tolerant to me. Your scientific attitude, professional instructions and constructive discussions are crucial to my accomplishment of this thesis. I also thank you for that you spent much valuable time on correcting my manuscripts and thesis.

I also want to thank Kanchana R. Kildegaard and Yun Chen for introducing me into the 'yeast world'. You are always there when I need help and your great expertise and suggestions make me move faster on the way to science.

I would like to acknowledge my collaborators, Christian B. Jendresen, Steen G. Stahlhut, Angelica Rodriguez, Björn Hallström, Sakda Khoomrung, Konstantin Schneider and Mette Kristensen for your productive contributions to the projects and your great comments on the manuscripts.

I would like to thank Carina Holkenbrink, Jie Zhang, Vratislav Stovicek, Mathew M. J. Fabre, Tadas Jakociunas, Arun S. Rajkumar, Gheorghe M. B. Zamfir, Tomas Strucko, Jerome Maury, Michael K. Jensen, Jochen Förster and all my collegues in the yeast group at CfB and Chalmers for your

assistance, constructive discussions, sharing information and experimental materials. Specifically, I want to thank Anne Lykke for helping translation of my thesis abstract into Danish.

I would like to thank my close Chinese friends in the Systems and Synthetic Biology group (Sys2Bio) at Chalmers, Guodong Liu, Mingtao Huang, Jiufu Qin, Yongjin Zhou, Yongjun Wei, Jichen Bao, Boyang Ji, Zongjie Dai, Yating Hu, Zheng Wang, Zhiwei Zhu, Ruifei Wang, Xin Chen, Yiming Zhang, Cheng Zhang and Lei Shi for your accompany when I stayed in Chalmers.

I am also very appreaciate of all the administrative support from Julia Karlsson, Inger Rosenstand, Martina Butorac, Marie Nordqvist, Ximena Sevilla, Emma Ribbenhed, Andreas Hellström and Mads Christensen. Your professional assistance in the lab and office made me work efficiently. Thank all of you for your help!

I would also like to thank my friends in Denmark, Zhihao Wang, Shengjun Wang, Yun Kong, Yaojun Tong, Songyuan Li, Xiaochen Yang, Hao Luo, Lei Yang, Tian Zhang, Xiaoyong Pan, Chenying Zhang and Xinglin Jiang for your accompany during the leisure time and for your very practical suggestions on my job searching.

Finally, I own my deepest gratitude to my parents for your forever and unconditional love and support. The special goes to my wife, Yingying Guo. Thank you so much for your selfless love and your endless support!

Reference

Achnine, L., Blancaflor, E. B., Rasmussen, S., Dixon, R. A., 2004. Colocalization of L-phenylalanine ammonia-lyase and cinnamate 4-hydroxylase for metabolic channeling in phenylpropanoid biosynthesis. Plant Cell. 16, 3098-109.

Afonso, M. S., Ferreira, S., Domingues, F. C., Silva, F., 2015. Resveratrol production in bioreactor: Assessment of cell physiological states and plasmid segregational stability. Biotechnology Reports. 5, 7-13.

Aggarwal, B. B., Bhardwaj, A., Aggarwal, R. S., Seeram, N. P., Shishodia, S., Takada, Y., 2004. Role of resveratrol in prevention and therapy of cancer: preclinical and clinical studies. Anticancer Res. 24, 2783-840.

Alper, H., Fischer, C., Nevoigt, E., Stephanopoulos, G., 2005. Tuning genetic control through promoter engineering. Proceedings of the National Academy of Sciences of the United States of America. 102, 12678-12683.

Apfeld, J., O'Connor, G., McDonagh, T., DiStefano, P. S., Curtis, R., 2004. The AMP-activated protein kinase AAK-2 links energy levels and insulin-like signals to lifespan in *C. elegans*. Genes Dev. 18, 3004-9.

Arichi, H., Kimura, Y., Okuda, H., Baba, K., Kozawa, M., Arichi, S., 1982. Effects of stilbene components of the roots of *Polygonum cuspidatum* Sieb. et Zucc. on lipid metabolism. Chem Pharm Bull (Tokyo). 30, 1766-70.

Arthur, P. G., Niu, X., Rigby, P., Steer, J. H., Jeffrey, G. P., 2008. Oxidative stress causes a decline in lysosomal integrity during hypothermic incubation of rat hepatocytes. Free Radic Biol Med. 44, 24-33.

Avalos, J. L., Fink, G. R., Stephanopoulos, G., 2013. Compartmentalization of metabolic pathways in yeast mitochondria improves the production of branched-chain alcohols. Nat Biotechnol. 31, 335-41.

Bauer, J. H., Goupil, S., Garber, G. B., Helfand, S. L., 2004. An accelerated assay for the identification of lifespan-extending interventions in *Drosophila melanogaster*. Proc Natl Acad Sci U S A. 101, 12980-5.

Baur, J. A., Pearson, K. J., Price, N. L., Jamieson, H. A., Lerin, C., Kalra, A., Prabhu, V. V., Allard, J. S., Lopez-Lluch, G., Lewis, K., Pistell, P. J., Poosala, S., Becker, K. G., Boss, O., Gwinn, D., Wang, M., Ramaswamy, S., Fishbein, K. W., Spencer, R. G., Lakatta, E. G., Le Couteur, D., Shaw, R. J., Navas, P., Puigserver, P., Ingram, D. K., de Cabo, R., Sinclair, D. A., 2006. Resveratrol improves health and survival of mice on a high-calorie diet. Nature. 444, 337-42.

Baur, J. A., Sinclair, D. A., 2006. Therapeutic potential of resveratrol: the in vivo evidence. Nat Rev Drug Discov. 5, 493-506.

Becker, J. V., Armstrong, G. O., van der Merwe, M. J., Lambrechts, M. G., Vivier, M. A., Pretorius, I. S., 2003. Metabolic engineering of *Saccharomyces cerevisiae* for the synthesis of the wine-related antioxidant resveratrol. FEMS Yeast Res. 4, 79-85.

Beekwilder, J., Wolswinkel, R., Jonker, H., Hall, R., de Vos, C. H., Bovy, A., 2006. Production of resveratrol in recombinant microorganisms. Appl Environ Microbiol. 72, 5670-2.

Benitez, D. A., Hermoso, M. A., Pozo-Guisado, E., Fernandez-Salguero, P. M., Castellon, E. A., 2009. Regulation of cell survival by resveratrol involves inhibition of NF kappa B-regulated gene expression in prostate cancer cells. Prostate. 69, 1045-54.

Bergman, L. W., 2001. Growth and maintenance of yeast. Methods Mol Biol. 177, 9-14.

Borodina, I., Kildegaard, K. R., Jensen, N. B., Blicher, T. H., Maury, J., Sherstyk, S., Schneider, K., Lamosa, P., Herrgard, M. J., Rosenstand, I., Oberg, F., Forster, J., Nielsen, J., 2015. Establishing a synthetic pathway for high-level production of 3-hydroxypropionic acid in *Saccharomyces cerevisiae* via beta-alanine. Metab Eng. 27, 57-64.

Borra, M. T., Smith, B. C., Denu, J. M., 2005. Mechanism of human SIRT1 activation by resveratrol. J Biol Chem. 280, 17187-95.

Brochado, A. R., Matos, C., Moller, B. L., Hansen, J., Mortensen, U. H., Patil, K. R., 2010. Improved vanillin production in baker's yeast through in silico design. Microb Cell Fact. 9, 84.

Burgard, A. P., Pharkya, P., Maranas, C. D., 2003. Optknock: a bilevel programming framework for identifying gene knockout strategies for microbial strain optimization. Biotechnol Bioeng. 84, 647-57.

Burkhardt, S., Reiter, R. J., Tan, D.-X., Hardeland, R., Cabrera, J., Karbownik, M., 2001. DNA oxidatively damaged by chromium (III) and H_2O_2 is protected by the antioxidants melatonin, N1-acetyl-N2-formyl-5-methoxykynuramine, resveratrol and uric acid. The international journal of biochemistry & cell biology. 33, 775-783.

Camont, L., Cottart, C. H., Rhayem, Y., Nivet-Antoine, V., Djelidi, R., Collin, F., Beaudeux, J. L., Bonnefont-Rousselot, D., 2009. Simple spectrophotometric assessment of the *trans*-/*cis*-resveratrol ratio in aqueous solutions. Anal Chim Acta. 634, 121-8.

Canelas, A. B., Ras, C., Pierick, A. T., Dam, J. C. V., Heijnen, J. J., Gulik, W. M. V., 2008. Leakage-free rapid quenching technique for yeast metabolomics. Metabolomics. 4, 226-239.

Canto, C., Gerhart-Hines, Z., Feige, J. N., Lagouge, M., Noriega, L., Milne, J. C., Elliott, P. J., Puigserver, P., Auwerx, J., 2009. AMPK regulates energy

expenditure by modulating NAD+ metabolism and SIRT1 activity. Nature. 458, 1056-60.
Carling, D., Zammit, V. A., Hardie, D. G., 1987. A common bicyclic protein kinase cascade inactivates the regulatory enzymes of fatty acid and cholesterol biosynthesis. FEBS Lett. 223, 217-22.
Castello, L., Tessitore, L., 2005. Resveratrol inhibits cell cycle progression in U937 cells. Oncol Rep. 13, 133-7.
Catalgol, B., Batirel, S., Taga, Y., Ozer, N. K., 2012. Resveratrol: French paradox revisited. Front Pharmacol. 3, 141.
Chandramouli, K., Qian, P. Y., 2009. Proteomics: challenges, techniques and possibilities to overcome biological sample complexity. Hum Genomics Proteomics. 2009.
Chao, J., Li, H., Cheng, K.-W., Yu, M.-S., Chang, R. C.-C., Wang, M., 2010. Protective effects of pinostilbene, a resveratrol methylated derivative, against 6-hydroxydopamine-induced neurotoxicity in SH-SY5Y cells. The Journal of nutritional biochemistry. 21, 482-489.
Chen, Y., Bao, J., Kim, I. K., Siewers, V., Nielsen, J., 2014. Coupled incremental precursor and co-factor supply improves 3-hydroxypropionic acid production in *Saccharomyces cerevisiae*. Metab Eng. 22, 104-9.
Chen, Y., Zhang, Y., Siewers, V., Nielsen, J., 2015. Ach1 is involved in shuttling mitochondrial acetyl units for cytosolic C2 provision in *Saccharomyces cerevisiae* lacking pyruvate decarboxylase. FEMS Yeast Res. 15.
Cherry, J. M., Adler, C., Ball, C., Chervitz, S. A., Dwight, S. S., Hester, E. T., Jia, Y., Juvik, G., Roe, T., Schroeder, M., Weng, S., Botstein, D., 1998. SGD: *Saccharomyces* Genome Database. Nucleic Acids Res. 26, 73-9.
Chung, I. M., Kim, J. J., Lim, J. D., Yu, C. Y., Kim, S. H., Hahn, S. J., 2006. Comparison of resveratrol, SOD activity, phenolic compounds and free amino acids in *Rehmannia glutinosa* under temperature and water stress. Environmental and experimental botany. 56, 44-53.
Clark, T. A., Sugnet, C. W., Ares, M., Jr., 2002. Genomewide analysis of mRNA processing in yeast using splicing-specific microarrays. Science. 296, 907-10.
Cottart, C. H., Nivet-Antoine, V., Laguillier-Morizot, C., Beaudeux, J. L., 2010. Resveratrol bioavailability and toxicity in humans. Mol Nutr Food Res. 54, 7-16.
Crabtree, H. G., 1929. Observations on the carbohydrate metabolism of tumours. Biochemical journal. 23, 536.
Curran, K. A., Leavitt, J. M., Karim, A. S., Alper, H. S., 2013. Metabolic engineering of muconic acid production in *Saccharomyces cerevisiae*. Metab Eng. 15, 55-66.

Curran, K. A., Morse, N. J., Markham, K. A., Wagman, A. M., Gupta, A., Alper, H. S., 2015. Short Synthetic Terminators for Improved Heterologous Gene Expression in Yeast. ACS Synth Biol. 4, 824-32.

David, F., Nielsen, J., Siewers, V., 2016. Flux control at the malonyl-CoA node through hierarchical dynamic pathway regulation in Saccharomyces cerevisiae. ACS synthetic biology.

Demoulin, B., Hermant, M., Castrogiovanni, C., Staudt, C., Dumont, P., 2015. Resveratrol induces DNA damage in colon cancer cells by poisoning topoisomerase II and activates the ATM kinase to trigger p53-dependent apoptosis. Toxicol In Vitro. 29, 1156-65.

DiCarlo, J. E., Norville, J. E., Mali, P., Rios, X., Aach, J., Church, G. M., 2013. Genome engineering in *Saccharomyces cerevisiae* using CRISPR-Cas systems. Nucleic Acids Res. 41, 4336-43.

Ding, X. Z., Adrian, T. E., 2002. Resveratrol inhibits proliferation and induces apoptosis in human pancreatic cancer cells. Pancreas. 25, e71-6.

Drinnenberg, I. A., Weinberg, D. E., Xie, K. T., Mower, J. P., Wolfe, K. H., Fink, G. R., Bartel, D. P., 2009. RNAi in budding yeast. Science. 326, 544-50.

Dunn, W. B., Winder, C. L., 2011. Chapter fifteen–Sample Preparation Related to the Intracellular Metabolome of Yeast : Methods for Quenching, Extraction, and Metabolite Quantitation. Methods in Enzymology. 500, 277-297.

Entian, K.-D., Kötter, P., 2007a. 25 Yeast genetic strain and plasmid collections. Method Microbiol. 36, 629-666.

Entian, K.-D., Kötter, P., 2007b. 25 Yeast genetic strain and plasmid collections. Methods in microbiology. 36, 629-666.

Fan, E., Zhang, K., Zhu, M., Wang, Q., 2010. Obtaining resveratrol: from chemical synthesis to biotechnological production. Mini-Reviews in Organic Chemistry. 7, 272-281.

Fare, T. L., Coffey, E. M., Dai, H., He, Y. D., Kessler, D. A., Kilian, K. A., Koch, J. E., LeProust, E., Marton, M. J., Meyer, M. R., Stoughton, R. B., Tokiwa, G. Y., Wang, Y., 2003. Effects of atmospheric ozone on microarray data quality. Anal Chem. 75, 4672-5.

Feng, X., Zhao, H., 2013. Investigating host dependence of xylose utilization in recombinant *Saccharomyces cerevisiae* strains using RNA-seq analysis. Biotechnol Biofuels. 6, 96.

Feng, Y., De Franceschi, G., Kahraman, A., Soste, M., Melnik, A., Boersema, P. J., de Laureto, P. P., Nikolaev, Y., Oliveira, A. P., Picotti, P., 2014. Global analysis of protein structural changes in complex proteomes. Nat Biotechnol. 32, 1036-44.

Fernandez-Mar, M., Mateos, R., Garcia-Parrilla, M., Puertas, B., Cantos-Villar, E., 2012. Bioactive compounds in wine: resveratrol, hydroxytyrosol and melatonin: a review. Food Chemistry. 130, 797-813.

Flikweert, M. T., van Dijken, J. P., Pronk, J. T., 1997. Metabolic responses of pyruvate decarboxylase-negative *Saccharomyces cerevisiae* to glucose excess. Appl Environ Microbiol. 63, 3399-404.

Forster, J., Famili, I., Fu, P., Palsson, B. O., Nielsen, J., 2003. Genome-scale reconstruction of the *Saccharomyces cerevisiae* metabolic network. Genome Res. 13, 244-53.

Frankel, E. N., Waterhouse, A. L., Kinsella, J. E., 1993. Inhibition of human LDL oxidation by resveratrol. Lancet. 341, 1103-4.

Fulda, S., 2010. Resveratrol and derivatives for the prevention and treatment of cancer. Drug Discov Today. 15, 757-65.

Galanie, S., Thodey, K., Trenchard, I. J., Filsinger Interrante, M., Smolke, C. D., 2015. Complete biosynthesis of opioids in yeast. Science. 349, 1095-100.

Giaever, G., Chu, A. M., Ni, L., Connelly, C., Riles, L., Veronneau, S., Dow, S., Lucau-Danila, A., Anderson, K., Andre, B., Arkin, A. P., Astromoff, A., El-Bakkoury, M., Bangham, R., Benito, R., Brachat, S., Campanaro, S., Curtiss, M., Davis, K., Deutschbauer, A., Entian, K. D., Flaherty, P., Foury, F., Garfinkel, D. J., Gerstein, M., Gotte, D., Guldener, U., Hegemann, J. H., Hempel, S., Herman, Z., Jaramillo, D. F., Kelly, D. E., Kelly, S. L., Kotter, P., LaBonte, D., Lamb, D. C., Lan, N., Liang, H., Liao, H., Liu, L., Luo, C., Lussier, M., Mao, R., Menard, P., Ooi, S. L., Revuelta, J. L., Roberts, C. J., Rose, M., Ross-Macdonald, P., Scherens, B., Schimmack, G., Shafer, B., Shoemaker, D. D., Sookhai-Mahadeo, S., Storms, R. K., Strathern, J. N., Valle, G., Voet, M., Volckaert, G., Wang, C. Y., Ward, T. R., Wilhelmy, J., Winzeler, E. A., Yang, Y., Yen, G., Youngman, E., Yu, K., Bussey, H., Boeke, J. D., Snyder, M., Philippsen, P., Davis, R. W., Johnston, M., 2002. Functional profiling of the *Saccharomyces cerevisiae* genome. Nature. 418, 387-91.

Gietz, R. D., Woods, R. A., 2002. Transformation of yeast by lithium acetate/single-stranded carrier DNA/polyethylene glycol method. Methods Enzymol. 350, 87-96.

Goffeau, A., Barrell, B. G., Bussey, H., Davis, R. W., Dujon, B., Feldmann, H., Galibert, F., Hoheisel, J. D., Jacq, C., Johnston, M., Louis, E. J., Mewes, H. W., Murakami, Y., Philippsen, P., Tettelin, H., Oliver, S. G., 1996. Life with 6000 genes. Science. 274, 546, 563-7.

Gresele, P., Pignatelli, P., Guglielmini, G., Carnevale, R., Mezzasoma, A. M., Ghiselli, A., Momi, S., Violi, F., 2008. Resveratrol, at concentrations

attainable with moderate wine consumption, stimulates human platelet nitric oxide production. J Nutr. 138, 1602-8.

Guengerich, F. P., Gillam, E. M., Ohmori, S., Sandhu, P., Brian, W. R., Sari, M. A., Iwasaki, M., 1993. Expression of human cytochrome P450 enzymes in yeast and bacteria and relevance to studies on catalytic specificity. Toxicology. 82, 21-37.

Harikumar, K. B., Aggarwal, B. B., 2008. Resveratrol: a multitargeted agent for age-associated chronic diseases. Cell Cycle. 7, 1020-35.

Hasunuma, T., Sanda, T., Yamada, R., Yoshimura, K., Ishii, J., Kondo, A., 2011. Metabolic pathway engineering based on metabolomics confers acetic and formic acid tolerance to a recombinant xylose-fermenting strain of *Saccharomyces cerevisiae*. Microb Cell Fact. 10, 2.

Hawkins, K. M., Smolke, C. D., 2008. Production of benzylisoquinoline alkaloids in *Saccharomyces cerevisiae*. Nat Chem Biol. 4, 564-73.

Hawley, S. A., Ross, F. A., Chevtzoff, C., Green, K. A., Evans, A., Fogarty, S., Towler, M. C., Brown, L. J., Ogunbayo, O. A., Evans, A. M., Hardie, D. G., 2010. Use of cells expressing gamma subunit variants to identify diverse mechanisms of AMPK activation. Cell Metab. 11, 554-65.

Hazelwood, L. A., Daran, J. M., van Maris, A. J., Pronk, J. T., Dickinson, J. R., 2008. The Ehrlich pathway for fusel alcohol production: a century of research on *Saccharomyces cerevisiae* metabolism. Appl Environ Microbiol. 74, 2259-66.

Holvoet, P., 2004. Oxidized LDL and coronary heart disease. Acta Cardiol. 59, 479-84.

Howitz, K. T., Bitterman, K. J., Cohen, H. Y., Lamming, D. W., Lavu, S., Wood, J. G., Zipkin, R. E., Chung, P., Kisielewski, A., Zhang, L. L., Scherer, B., Sinclair, D. A., 2003. Small molecule activators of sirtuins extend *Saccharomyces cerevisiae* lifespan. Nature. 425, 191-6.

Husnik, J. I., Volschenk, H., Bauer, J., Colavizza, D., Luo, Z., van Vuuren, H. J., 2006. Metabolic engineering of malolactic wine yeast. Metab Eng. 8, 315-23.

Ibanez, A. J., Fagerer, S. R., Schmidt, A. M., Urban, P. L., Jefimovs, K., Geiger, P., Dechant, R., Heinemann, M., Zenobi, R., 2013. Mass spectrometry-based metabolomics of single yeast cells. Proc Natl Acad Sci U S A. 110, 8790-4.

Ideker, T., Thorsson, V., Ranish, J. A., Christmas, R., Buhler, J., Eng, J. K., Bumgarner, R., Goodlett, D. R., Aebersold, R., Hood, L., 2001. Integrated genomic and proteomic analyses of a systematically perturbed metabolic network. Science. 292, 929-34.

Irizarry, R. A., Warren, D., Spencer, F., Kim, I. F., Biswal, S., Frank, B. C., Gabrielson, E., Garcia, J. G., Geoghegan, J., Germino, G., Griffin, C.,

Hilmer, S. C., Hoffman, E., Jedlicka, A. E., Kawasaki, E., Martinez-Murillo, F., Morsberger, L., Lee, H., Petersen, D., Quackenbush, J., Scott, A., Wilson, M., Yang, Y., Ye, S. Q., Yu, W., 2005. Multiple-laboratory comparison of microarray platforms. Nat Methods. 2, 345-50.

Ishida, N., Saitoh, S., Ohnishi, T., Tokuhiro, K., Nagamori, E., Kitamoto, K., Takahashi, H., 2006. Metabolic engineering of *Saccharomyces cerevisiae* for efficient production of pure L-(+)-lactic acid. Appl Biochem Biotechnol. 129-132, 795-807.

Ito, Y., Yamanishi, M., Ikeuchi, A., Imamura, C., Tokuhiro, K., Kitagawa, T., Matsuyama, T., 2013. Characterization of five terminator regions that increase the protein yield of a transgene in *Saccharomyces cerevisiae*. Journal of biotechnology. 168, 486-492.

Ivanov, V. N., Partridge, M. A., Johnson, G. E., Huang, S. X., Zhou, H., Hei, T. K., 2008. Resveratrol sensitizes melanomas to TRAIL through modulation of antiapoptotic gene expression. Exp Cell Res. 314, 1163-76.

Jakociunas, T., Bonde, I., Herrgard, M., Harrison, S. J., Kristensen, M., Pedersen, L. E., Jensen, M. K., Keasling, J. D., 2015a. Multiplex metabolic pathway engineering using CRISPR/Cas9 in *Saccharomyces cerevisiae*. Metab Eng. 28, 213-22.

Jakociunas, T., Rajkumar, A. S., Zhang, J., Arsovska, D., Rodriguez, A., Jendresen, C. B., Skjodt, M. L., Nielsen, A. T., Borodina, I., Jensen, M. K., Keasling, J. D., 2015b. CasEMBLR: Cas9-Facilitated Multiloci Genomic Integration of in Vivo Assembled DNA Parts in *Saccharomyces cerevisiae*. ACS Synth Biol. 4, 1226-34.

Jang, M., Cai, L., Udeani, G. O., Slowing, K. V., Thomas, C. F., Beecher, C. W., Fong, H. H., Farnsworth, N. R., Kinghorn, A. D., Mehta, R. G., Moon, R. C., Pezzuto, J. M., 1997. Cancer chemopreventive activity of resveratrol, a natural product derived from grapes. Science. 275, 218-20.

Jendresen, C. B., Stahlhut, S. G., Li, M., Gaspar, P., Siedler, S., Forster, J., Maury, J., Borodina, I., Nielsen, A. T., 2015. Highly Active and Specific Tyrosine Ammonia-Lyases from Diverse Origins Enable Enhanced Production of Aromatic Compounds in Bacteria and *Saccharomyces cerevisiae*. Appl Environ Microbiol. 81, 4458-76.

Jensen, N., Borodina, I., Chen, Y., Maury, J., Kildegaard, K., Forster, J., Nielsen, J., 2014a. Microbial production of 3-hydroxypropionic acid. WO Patent Application. 198831, A1.

Jensen, N. B., Strucko, T., Kildegaard, K. R., David, F., Maury, J., Mortensen, U. H., Forster, J., Nielsen, J., Borodina, I., 2014b. EasyClone: method for iterative chromosomal integration of multiple genes in *Saccharomyces cerevisiae*. FEMS Yeast Res. 14, 238-48.

Jeong, Y. J., An, C. H., Woo, S. G., Jeong, H. J., Kim, Y. M., Park, S. J., Yoon, B. D., Kim, C. Y., 2014. Production of pinostilbene compounds by the expression of resveratrol *O*-methyltransferase genes in Escherichia coli. Enzyme Microb Technol. 54, 8-14.

Jeong, Y. J., Woo, S. G., An, C. H., Jeong, H. J., Hong, Y. S., Kim, Y. M., Ryu, Y. B., Rho, M. C., Lee, W. S., Kim, C. Y., 2015. Metabolic engineering for resveratrol derivative biosynthesis in *Escherichia coli*. Mol Cells. 38, 318-26.

Jeppsson, M., Johansson, B., Jensen, P. R., Hahn-Hagerdal, B., Gorwa-Grauslund, M. F., 2003. The level of glucose-6-phosphate dehydrogenase activity strongly influences xylose fermentation and inhibitor sensitivity in recombinant *Saccharomyces cerevisiae* strains. Yeast. 20, 1263-72.

Jiang, H., Wood, K. V., Morgan, J. A., 2005. Metabolic engineering of the phenylpropanoid pathway in *Saccharomyces cerevisiae*. Appl Environ Microbiol. 71, 2962-9.

Joe, A. K., Liu, H., Suzui, M., Vural, M. E., Xiao, D., Weinstein, I. B., 2002. Resveratrol induces growth inhibition, S-phase arrest, apoptosis, and changes in biomarker expression in several human cancer cell lines. Clin Cancer Res. 8, 893-903.

Kaeberlein, M., McDonagh, T., Heltweg, B., Hixon, J., Westman, E. A., Caldwell, S. D., Napper, A., Curtis, R., DiStefano, P. S., Fields, S., Bedalov, A., Kennedy, B. K., 2005. Substrate-specific activation of sirtuins by resveratrol. J Biol Chem. 280, 17038-45.

Kapetanovic, I. M., Muzzio, M., Huang, Z., Thompson, T. N., McCormick, D. L., 2011. Pharmacokinetics, oral bioavailability, and metabolic profile of resveratrol and its dimethylether analog, pterostilbene, in rats. Cancer chemotherapy and pharmacology. 68, 593-601.

Karacabey, E., Mazza, G., 2008. Optimization of solid-liquid extraction of resveratrol and other phenolic compounds from milled grape canes (*Vitis vinifera*). J Agric Food Chem. 56, 6318-25.

Katsuyama, Y., Funa, N., Horinouchi, S., 2007. Precursor-directed biosynthesis of stilbene methyl ethers in *Escherichia coli*. Biotechnol J. 2, 1286-93.

Katz, M. P., Durhuus, T., Smits, H. P., Forster, J., Production of Metabolites. Google Patents, 2011.

Kildegaard, K. R., Jensen, N. B., Schneider, K., Czarnotta, E., Ozdemir, E., Klein, T., Maury, J., Ebert, B. E., Christensen, H. B., Chen, Y., Kim, I. K., Herrgard, M. J., Blank, L. M., Forster, J., Nielsen, J., Borodina, I., 2016. Engineering and systems-level analysis of *Saccharomyces cerevisiae* for production of 3-hydroxypropionic acid via malonyl-CoA reductase-dependent pathway. Microb Cell Fact. 15, 53.

Kim, S. K., Jin, Y. S., Choi, I. G., Park, Y. C., Seo, J. H., 2015. Enhanced tolerance of *Saccharomyces cerevisiae* to multiple lignocellulose-derived inhibitors through modulation of spermidine contents. Metab Eng. 29, 46-55.

Kim, Y. S., Sull, J. W., Sung, H. J., 2012. Suppressing effect of resveratrol on the migration and invasion of human metastatic lung and cervical cancer cells. Mol Biol Rep. 39, 8709-16.

Kimura, Y., Ohminami, H., Okuda, H., Baba, K., Kozawa, M., Arichi, S., 1983. Effects of stilbene components of roots of *Polygonum* ssp. on liver injury in peroxidized oil-fed rats. Planta Med. 49, 51-4.

King, R. E., Bomser, J. A., Min, D. B., 2006. Bioactivity of resveratrol. Comprehensive Reviews in Food Science and Food Safety. 5, 65-70.

Kirby, J., Keasling, J. D., 2008. Metabolic engineering of microorganisms for isoprenoid production. Nat Prod Rep. 25, 656-61.

Kopp, P., 1998. Resveratrol, a phytoestrogen found in red wine. A possible explanation for the conundrum of the 'French paradox'? Eur J Endocrinol. 138, 619-20.

Kovanen, P. T., Pentikainen, M. O., 2003. Circulating lipoproteins as proinflammatory and anti-inflammatory particles in atherogenesis. Curr Opin Lipidol. 14, 411-9.

Kozak, B. U., van Rossum, H. M., Luttik, M. A., Akeroyd, M., Benjamin, K. R., Wu, L., de Vries, S., Daran, J. M., Pronk, J. T., van Maris, A. J., 2014. Engineering acetyl coenzyme A supply: functional expression of a bacterial pyruvate dehydrogenase complex in the cytosol of *Saccharomyces cerevisiae*. MBio. 5, e01696-14.

Kumar, A., Kaundal, R. K., Iyer, S., Sharma, S. S., 2007. Effects of resveratrol on nerve functions, oxidative stress and DNA fragmentation in experimental diabetic neuropathy. Life Sci. 80, 1236-44.

Laden, B. P., Porter, T. D., 2001. Resveratrol inhibits human squalene monooxygenase. Nutrition Research. 21, 747-753.

Langcake, P., Pryce, R., 1976. The production of resveratrol by *Vitis vinifera* and other members of the Vitaceae as a response to infection or injury. Physiological Plant Pathology. 9, 77-86.

Lee, F. W., Da Silva, N. A., 1997. Improved efficiency and stability of multiple cloned gene insertions at the delta sequences of *Saccharomyces cerevisiae*. Appl Microbiol Biotechnol. 48, 339-45.

Lee, S. H., Seo, D. I., Kim, H. S., Park, S. Y., Park, O. J., Kim, Y. M., 2012. Regulation of TNF-a, Akt and COX-2 by Resveratrol in MCF-7 Breast Cancer Cells. Cancer prevention research. 17, 121-127.

Lee, S. K., Nam, K. A., Hoe, Y. H., Min, H. Y., Kim, E. Y., Ko, H., Song, S., Lee, T., Kim, S., 2003. Synthesis and evaluation of cytotoxicity of stilbene analogues. Arch Pharm Res. 26, 253-7.

Leonard, E., Yan, Y., Fowler, Z. L., Li, Z., Lim, C. G., Lim, K. H., Koffas, M. A., 2008. Strain improvement of recombinant *Escherichia coli* for efficient production of plant flavonoids. Mol Pharm. 5, 257-65.

Li, M., Borodina, I., 2014. Application of synthetic biology for production of chemicals in yeast *Saccharomyces cerevisiae*. FEMS Yeast Res.

Li, M., Kildegaard, K. R., Chen, Y., Rodriguez, A., Borodina, I., Nielsen, J., 2015. *De novo* production of resveratrol from glucose or ethanol by engineered *Saccharomyces cerevisiae*. Metab Eng. 32, 1-11.

Lies, D., Porter-Scheinman, S., Kelly, J., Dundon, C. A., Aristidou, A., Hawkins, A., Reduced by-product accumulation for improved production of isobutanol. Google Patents, 2012.

Lim, C. G., Fowler, Z. L., Hueller, T., Schaffer, S., Koffas, M. A., 2011. High-yield resveratrol production in engineered *Escherichia coli*. Appl Environ Microbiol. 77, 3451-60.

Lin, F. M., Qiao, B., Yuan, Y. J., 2009. Comparative proteomic analysis of tolerance and adaptation of ethanologenic *Saccharomyces cerevisiae* to furfural, a lignocellulosic inhibitory compound. Appl Environ Microbiol. 75, 3765-76.

Lou, Z., Wang, H., Rao, S., Sun, J., Ma, C., Li, J., 2012. *p*-Coumaric acid kills bacteria through dual damage mechanisms. Food Control. 25, 550-554.

Luttik, M. A., Vuralhan, Z., Suir, E., Braus, G. H., Pronk, J. T., Daran, J. M., 2008. Alleviation of feedback inhibition in *Saccharomyces cerevisiae* aromatic amino acid biosynthesis: quantification of metabolic impact. Metab Eng. 10, 141-53.

Malone, J. H., Oliver, B., 2011. Microarrays, deep sequencing and the true measure of the transcriptome. BMC Biol. 9, 34.

Maury, J., Germann, S. M., Baallal Jacobsen, S. A., Jensen, N. B., Kildegaard, K. R., Herrgard, M. J., Schneider, K., Koza, A., Forster, J., Nielsen, J., Borodina, I., 2016. EasyCloneMulti: A Set of Vectors for Simultaneous and Multiple Genomic Integrations in *Saccharomyces cerevisiae*. PLoS One. 11, e0150394.

Mei, Y. Z., Liu, R. X., Wang, D. P., Wang, X., Dai, C. C., 2015. Biocatalysis and biotransformation of resveratrol in microorganisms. Biotechnol Lett. 37, 9-18.

Mizutani, K., Ikeda, K., Yamori, Y., 2000. Resveratrol inhibits AGEs-induced proliferation and collagen synthesis activity in vascular smooth muscle

cells from stroke-prone spontaneously hypertensive rats. Biochem Biophys Res Commun. 274, 61-7.
Mutka, S. C., Bondi, S. M., Carney, J. R., Da Silva, N. A., Kealey, J. T., 2006. Metabolic pathway engineering for complex polyketide biosynthesis in *Saccharomyces cerevisiae*. FEMS Yeast Res. 6, 40-7.
Nagalakshmi, U., Wang, Z., Waern, K., Shou, C., Raha, D., Gerstein, M., Snyder, M., 2008. The transcriptional landscape of the yeast genome defined by RNA sequencing. Science. 320, 1344-9.
Nakayashiki, H., Kadotani, N., Mayama, S., 2006. Evolution and diversification of RNA silencing proteins in fungi. J Mol Evol. 63, 127-35.
Naz, S., Vallejo, M., Garcia, A., Barbas, C., 2014. Method validation strategies involved in non-targeted metabolomics. J Chromatogr A. 1353, 99-105.
Nielsen, J., Keasling, J. D., 2016. Engineering Cellular Metabolism. Cell. 164, 1185-97.
Nikolova, V., 2007. Resveratrol: a crossroad of enology and biomedicine. Biomedical Reviews. 18, 89-101.
Nilsson, A., Nielsen, J., 2016. Metabolic Trade-offs in Yeast are Caused by F1F0-ATP synthase. Sci Rep. 6, 22264.
Nonomura, S., Kanagawa, H., Makimoto, A., 1963. Chemical Constituents of Polygonaceous Plants. I. Studies on the Components of Ko-J O-Kon. (*Polygonum cuspidatum* Sieb. Et Zucc.). Yakugaku Zasshi. 83, 988-90.
Norholm, M. H., 2010. A mutant Pfu DNA polymerase designed for advanced uracil-excision DNA engineering. BMC Biotechnol. 10, 21.
Olas, B., Nowak, P., Kolodziejczyk, J., Ponczek, M., Wachowicz, B., 2006. Protective effects of resveratrol against oxidative/nitrative modifications of plasma proteins and lipids exposed to peroxynitrite. J Nutr Biochem. 17, 96-102.
Olas, B., Nowak, P., Wachowicz, B., 2004. Resveratrol protects against peroxynitrite-induced thiol oxidation in blood platelets. Cell Mol Biol Lett. 9, 577-87.
Olas, B., Saluk-Juszczak, J., Wachowicz, B., 2008. D-glucaro 1,4-lactone and resveratrol as antioxidants in blood platelets. Cell Biol Toxicol. 24, 189-99.
Ondov, B. D., Varadarajan, A., Passalacqua, K. D., Bergman, N. H., 2008. Efficient mapping of Applied Biosystems SOLiD sequence data to a reference genome for functional genomic applications. Bioinformatics. 24, 2776-7.
Otero, J. M., Cimini, D., Patil, K. R., Poulsen, S. G., Olsson, L., Nielsen, J., 2013. Industrial systems biology of *Saccharomyces cerevisiae* enables novel succinic acid cell factory. PLoS One. 8, e54144.

Oud, B., Flores, C. L., Gancedo, C., Zhang, X., Trueheart, J., Daran, J. M., Pronk, J. T., van Maris, A. J., 2012. An internal deletion in MTH1 enables growth on glucose of pyruvate-decarboxylase negative, non-fermentative Saccharomyces cerevisiae. Microb Cell Fact. 11, 131.

Pacholec, M., Bleasdale, J. E., Chrunyk, B., Cunningham, D., Flynn, D., Garofalo, R. S., Griffith, D., Griffor, M., Loulakis, P., Pabst, B., 2010. SRT1720, SRT2183, SRT1460, and resveratrol are not direct activators of SIRT1. Journal of Biological Chemistry. 285, 8340-8351.

Paddon, C. J., Westfall, P. J., Pitera, D. J., Benjamin, K., Fisher, K., McPhee, D., Leavell, M. D., Tai, A., Main, A., Eng, D., Polichuk, D. R., Teoh, K. H., Reed, D. W., Treynor, T., Lenihan, J., Fleck, M., Bajad, S., Dang, G., Dengrove, D., Diola, D., Dorin, G., Ellens, K. W., Fickes, S., Galazzo, J., Gaucher, S. P., Geistlinger, T., Henry, R., Hepp, M., Horning, T., Iqbal, T., Jiang, H., Kizer, L., Lieu, B., Melis, D., Moss, N., Regentin, R., Secrest, S., Tsuruta, H., Vazquez, R., Westblade, L. F., Xu, L., Yu, M., Zhang, Y., Zhao, L., Lievense, J., Covello, P. S., Keasling, J. D., Reiling, K. K., Renninger, N. S., Newman, J. D., 2013. High-level semi-synthetic production of the potent antimalarial artemisinin. Nature. 496, 528-32.

Palma, M., Barbero, G., Piñeiro, Z., Liazid, A., Barroso, C., Rostagno, M., Prado, J., Meireles, M., 2013. Extraction of natural products: Principles and fundamental aspects. Natural Product Extraction: Principles and Applications. Londres: RSC Publishing. 58-88.

Parekh, R. N., Shaw, M. R., Wittrup, K. D., 1996. An integrating vector for tunable, high copy, stable integration into the dispersed Ty delta sites of *Saccharomyces cerevisiae*. Biotechnol Prog. 12, 16-21.

Park, S. R., Yoon, J. A., Paik, J. H., Park, J. W., Jung, W. S., Ban, Y. H., Kim, E. J., Yoo, Y. J., Han, A. R., Yoon, Y. J., 2009. Engineering of plant-specific phenylpropanoids biosynthesis in *Streptomyces venezuelae*. J Biotechnol. 141, 181-8.

Parkhurst, J. R., Hodgins, D. S., 1971. Phenylalanine and tyrosine ammonia-lyase activity in *Sporobolomyces pararoseus*. Phytochemistry. 10, 2997-3000.

Partow, S., Siewers, V., Bjorn, S., Nielsen, J., Maury, J., 2010. Characterization of different promoters for designing a new expression vector in *Saccharomyces cerevisiae*. Yeast. 27, 955-64.

Patel, K. R., Scott, E., Brown, V. A., Gescher, A. J., Steward, W. P., Brown, K., 2011. Clinical trials of resveratrol. Ann N Y Acad Sci. 1215, 161-9.

Patil, K. R., Rocha, I., Forster, J., Nielsen, J., 2005. Evolutionary programming as a platform for in silico metabolic engineering. BMC Bioinformatics. 6, 308.

Peng, B., Williams, T. C., Henry, M., Nielsen, L. K., Vickers, C. E., 2015. Controlling heterologous gene expression in yeast cell factories on

different carbon substrates and across the diauxic shift: a comparison of yeast promoter activities. Microb Cell Fact. 14, 91.
Peralta-Yahya, P. P., Ouellet, M., Chan, R., Mukhopadhyay, A., Keasling, J. D., Lee, T. S., 2011. Identification and microbial production of a terpene-based advanced biofuel. Nat Commun. 2, 483.
Pervaiz, S., Holme, A. L., 2009. Resveratrol: its biologic targets and functional activity. Antioxid Redox Signal. 11, 2851-97.
Petes, T. D., Malone, R. E., Symington, L. S., 1991. 8 Recombination in Yeast. Cold Spring Harbor Monograph Archive. 21, 407-521.
Pharkya, P., Burgard, A. P., Maranas, C. D., 2004. OptStrain: a computational framework for redesign of microbial production systems. Genome Res. 14, 2367-76.
Potter, G. A., Patterson, L. H., Wanogho, E., Perry, P. J., Butler, P. C., Ijaz, T., Ruparelia, K. C., Lamb, J. H., Farmer, P. B., Stanley, L. A., Burke, M. D., 2002. The cancer preventative agent resveratrol is converted to the anticancer agent piceatannol by the cytochrome P450 enzyme CYP1B1. Br J Cancer. 86, 774-8.
Rasmussen, S., Dixon, R. A., 1999. Transgene-mediated and elicitor-induced perturbation of metabolic channeling at the entry point into the phenylpropanoid pathway. Plant Cell. 11, 1537-1552.
Redden, H., Alper, H. S., 2015. The development and characterization of synthetic minimal yeast promoters. Nat Commun. 6, 7810.
Remsberg, C. M., Yanez, J. A., Ohgami, Y., Vega-Villa, K. R., Rimando, A. M., Davies, N. M., 2008. Pharmacometrics of pterostilbene: preclinical pharmacokinetics and metabolism, anticancer, antiinflammatory, antioxidant and analgesic activity. Phytother Res. 22, 169-79.
Renaud, S., de Lorgeril, M., 1992. Wine, alcohol, platelets, and the French paradox for coronary heart disease. Lancet. 339, 1523-6.
Rimando, A. M., Cuendet, M., Desmarchelier, C., Mehta, R. G., Pezzuto, J. M., Duke, S. O., 2002. Cancer chemopreventive and antioxidant activities of pterostilbene, a naturally occurring analogue of resveratrol. J Agric Food Chem. 50, 3453-7.
Ro, D.-K., Douglas, C. J., 2004. Reconstitution of the entry point of plant phenylpropanoid metabolism in yeast (*Saccharomyces cerevisiae*): implications for control of metabolic flux into the phenylpropanoid pathway. Journal of Biological Chemistry. 279, 2600-2607.
Ro, D. K., Paradise, E. M., Ouellet, M., Fisher, K. J., Newman, K. L., Ndungu, J. M., Ho, K. A., Eachus, R. A., Ham, T. S., Kirby, J., Chang, M. C., Withers, S. T., Shiba, Y., Sarpong, R., Keasling, J. D., 2006. Production of the

antimalarial drug precursor artemisinic acid in engineered yeast. Nature. 440, 940-3.
Rodriguez, A., Kildegaard, K. R., Li, M., Borodina, I., Nielsen, J., 2015. Establishment of a yeast platform strain for production of *p*-coumaric acid through metabolic engineering of aromatic amino acid biosynthesis. Metabolic engineering. 31, 181-188.
Ronda, C., Maury, J., Jakociunas, T., Jacobsen, S. A., Germann, S. M., Harrison, S. J., Borodina, I., Keasling, J. D., Jensen, M. K., Nielsen, A. T., 2015. CrEdit: CRISPR mediated multi-loci gene integration in *Saccharomyces cerevisiae*. Microb Cell Fact. 14, 97.
Rosler, J., ., Krekel, F., ., Amrhein, N., ., Schmid, J., . 1997. Maize phenylalanine ammonia-lyase has tyrosine ammonia-lyase activity. Plant Physiology. 113, 175-179.
Roy, P., Madan, E., Kalra, N., Nigam, N., George, J., Ray, R. S., Hans, R. K., Prasad, S., Shukla, Y., 2009. Resveratrol enhances ultraviolet B-induced cell death through nuclear factor-kappaB pathway in human epidermoid carcinoma A431 cells. Biochem Biophys Res Commun. 384, 215-20.
Sander, J. D., Joung, J. K., 2014. CRISPR-Cas systems for editing, regulating and targeting genomes. Nat Biotechnol. 32, 347-55.
Sandig, G., Kargel, E., Menzel, R., Vogel, F., Zimmer, T., Schunck, W. H., 1999. Regulation of endoplasmic reticulum biogenesis in response to cytochrome P450 overproduction. Drug Metab Rev. 31, 393-410.
Sarpietro, M. G., Spatafora, C., Tringali, C., Micieli, D., Castelli, F., 2007. Interaction of resveratrol and its trimethyl and triacetyl derivatives with biomembrane models studied by differential scanning calorimetry. J Agric Food Chem. 55, 3720-8.
Sawada, S., Kumagai, H., Yamada, H., Hill, R. K., Mugibayashi, Y., Ogata, K., 1973. Stereochemistry of ammonia elimination from L-tyrosine with L-phenylalanine ammonia-lyase. Biochim Biophys Acta. 315, 204-7.
Schena, M., Shalon, D., Davis, R. W., Brown, P. O., 1995. Quantitative monitoring of gene expression patterns with a complementary DNA microarray. Science. 270, 467-70.
Sengottuvelan, M., Viswanathan, P., Nalini, N., 2006. Chemopreventive effect of trans-resveratrol--a phytoalexin against colonic aberrant crypt foci and cell proliferation in 1,2-dimethylhydrazine induced colon carcinogenesis. Carcinogenesis. 27, 1038-46.
Shakibaei, M., Harikumar, K. B., Aggarwal, B. B., 2009. Resveratrol addiction: to die or not to die. Molecular nutrition & food research. 53, 115-128.
Shi, J., Zeng, Q., Liu, Y., Pan, Z., 2012. *Alternaria* sp. MG1, a resveratrol-producing fungus: isolation, identification, and optimal cultivation

conditions for resveratrol production. Appl Microbiol Biotechnol. 95, 369-79.

Shi, S., Chen, Y., Siewers, V., Nielsen, J., 2014. Improving production of malonyl coenzyme A-derived metabolites by abolishing Snf1-dependent regulation of Acc1. MBio. 5, e01130-14.

Shiba, Y., Paradise, E. M., Kirby, J., Ro, D. K., Keasling, J. D., 2007. Engineering of the pyruvate dehydrogenase bypass in *Saccharomyces cerevisiae* for high-level production of isoprenoids. Metab Eng. 9, 160-8.

Shin, S. Y., Han, N. S., Park, Y. C., Kim, M. D., Seo, J. H., 2011. Production of resveratrol from *p*-coumaric acid in recombinant *Saccharomyces cerevisiae* expressing 4-coumarate:coenzyme A ligase and stilbene synthase genes. Enzyme Microb Technol. 48, 48-53.

Shin, S. Y., Jung, S. M., Kim, M. D., Han, N. S., Seo, J. H., 2012. Production of resveratrol from tyrosine in metabolically engineered *Saccharomyces cerevisiae*. Enzyme Microb Technol. 51, 211-6.

Si, T., Luo, Y., Bao, Z., Zhao, H., 2015. RNAi-assisted genome evolution in *Saccharomyces cerevisiae* for complex phenotype engineering. ACS Synth Biol. 4, 283-91.

Siemann, E., Creasy, L., 1992. Concentration of the phytoalexin resveratrol in wine. American Journal of Enology and Viticulture. 43, 49-52.

Song, J. H., Kim, S., Kim, K. H., 2015. Cold Methanol Quenching vs. Fast Filtration for the Global Metabolite Profiling of *Saccharomyces cerevisiae*. Journal of Applied Physics. 101, 013112 - 013112-9.

Srinivas, G., Babykutty, S., Sathiadevan, P. P., Srinivas, P., 2007. Molecular mechanism of emodin action: transition from laxative ingredient to an antitumor agent. Med Res Rev. 27, 591-608.

Stovicek, V., Borja, G. M., Forster, J., Borodina, I., 2015a. EasyClone 2.0: expanded toolkit of integrative vectors for stable gene expression in industrial *Saccharomyces cerevisiae* strains. J Ind Microbiol Biotechnol. 42, 1519-31.

Stovicek, V., Borodina, I., Forster, J., 2015b. CRISPR–Cas system enables fast and simple genome editing of industrial *Saccharomyces cerevisiae* strains. Metabolic Engineering Communications. 2, 13-22.

Sun, P., Liang, J. L., Kang, L. Z., Huang, X. Y., Huang, J. J., Ye, Z. W., Guo, L. Q., Lin, J. F., 2015. Increased resveratrol production in wines using engineered wine strains *Saccharomyces cerevisiae* EC1118 and relaxed antibiotic or auxotrophic selection. Biotechnol Prog. 31, 650-5.

Sydor, T., Schaffer, S., Boles, E., 2010a. Considerable increase in resveratrol production by recombinant industrial yeast strains with use of rich medium. Appl Environ Microbiol. 76, 3361-3.

Sydor, T., Schaffer, S., Boles, E., 2010b. Considerable increase in resveratrol production by recombinant industrial yeast strains with use of rich medium. Applied and environmental microbiology. 76, 3361-3363.

Takaoka, M., 1939. Resveratrol, a new phenolic compound, from *Veratrum grandiflorum*. Nippon Kagaku Kaishi. 60, 1090–1100.

Tan, P. K., Downey, T. J., Spitznagel, E. L., Jr., Xu, P., Fu, D., Dimitrov, D. S., Lempicki, R. A., Raaka, B. M., Cam, M. C., 2003. Evaluation of gene expression measurements from commercial microarray platforms. Nucleic Acids Res. 31, 5676-84.

Tissenbaum, H. A., Guarente, L., 2001. Increased dosage of a sir-2 gene extends lifespan in *Caenorhabditis elegans*. Nature. 410, 227-30.

Torre, L. A., Bray, F., Siegel, R. L., Ferlay, J., Lortet-Tieulent, J., Jemal, A., 2015. Global cancer statistics, 2012. CA Cancer J Clin. 65, 87-108.

Trantas, E., Panopoulos, N., Ververidis, F., 2009. Metabolic engineering of the complete pathway leading to heterologous biosynthesis of various flavonoids and stilbenoids in *Saccharomyces cerevisiae*. Metab Eng. 11, 355-66.

Trela, B. C., Waterhouse, A. L., 1996. Resveratrol: isomeric molar absorptivities and stability. Journal of Agricultural and Food Chemistry. 44, 1253-1257.

Trenchard, I. J., Smolke, C. D., 2015. Engineering strategies for the fermentative production of plant alkaloids in yeast. Metab Eng. 30, 96-104.

Urlacher, V. B., Lutz-Wahl, S., Schmid, R. D., 2004. Microbial P450 enzymes in biotechnology. Appl Microbiol Biotechnol. 64, 317-25.

van Maris, A. J., Geertman, J. M., Vermeulen, A., Groothuizen, M. K., Winkler, A. A., Piper, M. D., van Dijken, J. P., Pronk, J. T., 2004. Directed evolution of pyruvate decarboxylase-negative *Saccharomyces cerevisiae*, yielding a C2-independent, glucose-tolerant, and pyruvate-hyperproducing yeast. Appl Environ Microbiol. 70, 159-66.

Vang, O., 2013. What is new for resveratrol?: Is a new set of recommendations necessary? New York Academy of Sciences. Annals.

Vera, J. C., Wheat, C. W., Fescemyer, H. W., Frilander, M. J., Crawford, D. L., Hanski, I., Marden, J. H., 2008. Rapid transcriptome characterization for a nonmodel organism using 454 pyrosequencing. Mol Ecol. 17, 1636-47.

Vergeres, G., Yen, T. S., Aggeler, J., Lausier, J., Waskell, L., 1993. A model system for studying membrane biogenesis. Overexpression of cytochrome b5 in yeast results in marked proliferation of the intracellular membrane. J Cell Sci. 106 (Pt 1), 249-59.

Verstrepen, K. J., Chambers, P. J., Pretorius, I. S., 2006. The development of superior yeast strains for the food and beverage industries: challenges,

opportunities and potential benefits. Yeasts in Food and Beverages. Springer, pp. 399-444.
Vidavalur, R., Otani, H., Singal, P. K., Maulik, N., 2006. Significance of wine and resveratrol in cardiovascular disease: French paradox revisited. Exp Clin Cardiol. 11, 217-25.
Villas-Boas, S. G., Mas, S., Akesson, M., Smedsgaard, J., Nielsen, J., 2005. Mass spectrometry in metabolome analysis. Mass Spectrom Rev. 24, 613-46.
Viswanathan, M., Kim, S. K., Berdichevsky, A., Guarente, L., 2005. A role for SIR-2.1 regulation of ER stress response genes in determining *C. elegans* life span. Dev Cell. 9, 605-15.
Vos, T., de la Torre Cortes, P., van Gulik, W. M., Pronk, J. T., Daran-Lapujade, P., 2015. Growth-rate dependency of de novo resveratrol production in chemostat cultures of an engineered *Saccharomyces cerevisiae* strain. Microb Cell Fact. 14, 133.
Vuralhan, Z., Morais, M. A., Tai, S. L., Piper, M. D., Pronk, J. T., 2003. Identification and characterization of phenylpyruvate decarboxylase genes in *Saccharomyces cerevisiae*. Appl Environ Microbiol. 69, 4534-41.
Walker, G. M., 1998. Yeast physiology and biotechnology. John Wiley & Sons.
Walle, T., Hsieh, F., DeLegge, M. H., Oatis, J. E., Walle, U. K., 2004. High absorption but very low bioavailability of oral resveratrol in humans. Drug metabolism and disposition. 32, 1377-1382.
Wallerath, T., Deckert, G., Ternes, T., Anderson, H., Li, H., Witte, K., Forstermann, U., 2002. Resveratrol, a polyphenolic phytoalexin present in red wine, enhances expression and activity of endothelial nitric oxide synthase. Circulation. 106, 1652-8.
Wang, H., Liu, L., Guo, Y. X., Dong, Y. S., Zhang, D. J., Xiu, Z. L., 2007. Biotransformation of piceid in Polygonum cuspidatum to resveratrol by *Aspergillus oryzae*. Appl Microbiol Biotechnol. 75, 763-8.
Wang, X., Wang, Z., Da Silva, N. A., 1996. G418 Selection and stability of cloned genes integrated at chromosomal delta sequences of *Saccharomyces cerevisiae*. Biotechnol Bioeng. 49, 45-51.
Wang, Y., Bhuiya, M. W., Zhou, R., Yu, O., 2015. Pterostilbene production by microorganisms expressing resveratrol O-methyltransferase. Annals of Microbiology. 65, 817-826.
Wang, Y., Halls, C., Zhang, J., Matsuno, M., Zhang, Y., Yu, O., 2011a. Stepwise increase of resveratrol biosynthesis in yeast *Saccharomyces cerevisiae* by metabolic engineering. Metab Eng. 13, 455-63.
Wang, Y., Yi, H., Wang, M., Yu, O., Jez, J. M., 2011b. Structural and kinetic analysis of the unnatural fusion protein 4-coumaroyl-CoA ligase::stilbene synthase. J Am Chem Soc. 133, 20684-7.

Wang, Y., Yu, O., 2012. Synthetic scaffolds increased resveratrol biosynthesis in engineered yeast cells. J Biotechnol. 157, 258-60.

Wang, Z., Gerstein, M., Snyder, M., 2009. RNA-Seq: a revolutionary tool for transcriptomics. Nat Rev Genet. 10, 57-63.

Wang, Z., Huang, Y., Zou, J., Cao, K., Xu, Y., Wu, J. M., 2002. Effects of red wine and wine polyphenol resveratrol on platelet aggregation *in vivo* and *in vitro*. Int J Mol Med. 9, 77-9.

Watanabe, S. K., Hernandez-Velazco, G., Iturbe-Chiñas, F., Lopez-Munguia, A., 1992. Phenylalanine ammonia lyase from *Sporidiobolus pararoseus* and *Rhodosporidium toruloides* : Application for phenylalanine and tyrosine deamination. World Journal of Microbiology & Biotechnology. 8, 406-410.

Watts, K. T., Lee, P. C., Schmidt-Dannert, C., 2006. Biosynthesis of plant-specific stilbene polyketides in metabolically engineered *Escherichia coli*. BMC Biotechnol. 6, 22.

Weber, C., Bruckner, C., Weinreb, S., Lehr, C., Essl, C., Boles, E., 2012. Biosynthesis of *cis,cis*-muconic acid and its aromatic precursors, catechol and protocatechuic acid, from renewable feedstocks by *Saccharomyces cerevisiae*. Appl Environ Microbiol. 78, 8421-30.

Wei, R., Li, G., Seymour, A. B., 2010. High-throughput and multiplexed LC/MS/MRM method for targeted metabolomics. Anal Chem. 82, 5527-33.

Wenzel, E., Soldo, T., Erbersdobler, H., Somoza, V., 2005. Bioactivity and metabolism of trans-resveratrol orally administered to Wistar rats. Mol Nutr Food Res. 49, 482-94.

Westfall, P. J., Pitera, D. J., Lenihan, J. R., Eng, D., Woolard, F. X., Regentin, R., Horning, T., Tsuruta, H., Melis, D. J., Owens, A., Fickes, S., Diola, D., Benjamin, K. R., Keasling, J. D., Leavell, M. D., McPhee, D. J., Renninger, N. S., Newman, J. D., Paddon, C. J., 2012. Production of amorphadiene in yeast, and its conversion to dihydroartemisinic acid, precursor to the antimalarial agent artemisinin. Proc Natl Acad Sci U S A. 109, E111-8.

Wu, J., Liu, P., Fan, Y., Bao, H., Du, G., Zhou, J., Chen, J., 2013. Multivariate modular metabolic engineering of *Escherichia coli* to produce resveratrol from L-tyrosine. J Biotechnol. 167, 404-11.

Xiao, B., Sanders, M. J., Underwood, E., Heath, R., Mayer, F. V., Carmena, D., Jing, C., Walker, P. A., Eccleston, J. F., Haire, L. F., Saiu, P., Howell, S. A., Aasland, R., Martin, S. R., Carling, D., Gamblin, S. J., 2011. Structure of mammalian AMPK and its regulation by ADP. Nature. 472, 230-3.

Xu, G., Chen, X., Liu, L., Jiang, L., 2013. Fumaric acid production in *Saccharomyces cerevisiae* by simultaneous use of oxidative and reductive routes. Bioresour Technol. 148, 91-6.

Yamanishi, M., Ito, Y., Kintaka, R., Imamura, C., Katahira, S., Ikeuchi, A., Moriya, H., Matsuyama, T., 2013. A genome-wide activity assessment of terminator regions in *Saccharomyces cerevisiae* provides a "terminatome" toolbox. ACS Synth Biol. 2, 337-47.

Zampar, G. G., Kummel, A., Ewald, J., Jol, S., Niebel, B., Picotti, P., Aebersold, R., Sauer, U., Zamboni, N., Heinemann, M., 2013. Temporal system-level organization of the switch from glycolytic to gluconeogenic operation in yeast. Mol Syst Biol. 9, 651.

Zelle, R. M., de Hulster, E., van Winden, W. A., de Waard, P., Dijkema, C., Winkler, A. A., Geertman, J. M., van Dijken, J. P., Pronk, J. T., van Maris, A. J., 2008. Malic acid production by *Saccharomyces cerevisiae*: engineering of pyruvate carboxylation, oxaloacetate reduction, and malate export. Appl Environ Microbiol. 74, 2766-77.

Zhang, J., Shi, J., Liu, Y., 2013a. Bioconversion of resveratrol using resting cells of non-genetically modified *Alternaria* sp. Biotechnol Appl Biochem. 60, 236-43.

Zhang, J., Shi, J., Liu, Y., 2013b. Substrates and enzyme activities related to biotransformation of resveratrol from phenylalanine by *Alternaria* sp. MG1. Appl Microbiol Biotechnol. 97, 9941-54.

Zhang, Y., Li, S.-Z., Li, J., Pan, X., Cahoon, R. E., Jaworski, J. G., Wang, X., Jez, J. M., Chen, F., Yu, O., 2006a. Using unnatural protein fusions to engineer resveratrol biosynthesis in yeast and mammalian cells. Journal of the American Chemical Society. 128, 13030-13031.

Zhang, Y., Li, S. Z., Li, J., Pan, X., Cahoon, R. E., Jaworski, J. G., Wang, X., Jez, J. M., Chen, F., Yu, O., 2006b. Using unnatural protein fusions to engineer resveratrol biosynthesis in yeast and Mammalian cells. J Am Chem Soc. 128, 13030-1.

Zou, J., Huang, Y., Cao, K., Yang, G., Yin, H., Len, J., Hsieh, T. C., Wu, J. M., 2000. Effect of resveratrol on intimal hyperplasia after endothelial denudation in an experimental rabbit model. Life Sci. 68, 153-63.